Arzneimittelrückstände in der Umwelt – Identifizierung prioritärer Stoffe für die Beurteilung von Umwelt- und Gesundheitswirkungen

Der Fakultät Nachhaltigkeit

der Leuphana Universität Lüneburg

zur Erlangung des Grades

Doktor der Naturwissenschaften

- Dr. rer. nat. -

vorgelegte Dissertation von

Jakob Menz

geb. 06.03.1986 in Merdingen

Eingereicht am: 31. Mai 2017

Betreuer und Gutachter: Prof. Dr. Klaus Kümmerer
(Leuphana Universität Lüneburg)

Gutachterin: Prof. Dr. Carolin Floeter
(Hochschule für Angewandte Wissenschaften Hamburg)

Gutachter: Prof. Dr. Gerd Hamscher
(Justus-Liebig-Universität Gießen)

Tag der Disputation: 20. Februar 2018

“The human race is challenged more than ever before to demonstrate our mastery, not over nature but of ourselves.”

- **Rachel Carson, *Silent Spring*, 1962**

Kurzfassung

Das ubiquitäre Vorkommen von Arzneimittelrückständen ist eng mit möglichen Risiken für Mensch und Umwelt verbunden. Das übergeordnete Ziel dieser Forschungsarbeit ist die Weiterentwicklung methodischer Ansätze für die Identifizierung prioritärer Arzneimittelrückstände vor dem Hintergrund bestehender Wissens- und Regulierungslücken. Unter diesem Gesichtspunkt wurden drei aktuelle Problemfelder aus dem Themenkomplex „Arzneimittel in der Umwelt“ ausgewählt und anhand konkreter Fallbeispiele betrachtet.

Tierarzneimittel werden häufig mit der Ausbringung von Wirtschaftsdünger in landwirtschaftlich genutzte Böden eingetragen. Gegenstand der ersten Publikation ist die Frage, inwiefern Anwendungsschemata aus der Nutztierhaltung für die retrospektive Identifizierung prioritärer Tierarzneimittelrückstände genutzt werden können. Hierzu wurde eine spezielle Herangehensweise entwickelt und am Beispiel von Antibiotika erprobt. Die durchgeführte Eintragsabschätzung ermöglichte erstmalig eine umfassende Einschätzung der potenziellen Antibiotikabelastung in Wirtschaftsdünger und landwirtschaftlich genutzten Böden im nordwestdeutschen Raum. Die Ergebnisse deuten auf erhebliche Umwelteinträge hin, die eine Neubewertung bestehender Wirkstoffzulassungen notwendig erscheinen lassen. Die vorgestellte Methodik zur Eintragsabschätzung kann ein effizientes Werkzeug für die Auswahl prioritärer Wirkstoffe im Hinblick auf eine solche Neubewertung darstellen.

Das kommunale Abwasser beinhaltet komplexe Mischungen von Arzneistoffen, die mikrobielle Lebensgemeinschaften in Kläranlagen und in der aquatischen Umwelt auf vielfältige Weise beeinträchtigen können. In der zweiten Publikation wurden am Beispiel einer Mischung aus 18 Arzneistoffen verschiedene Bewertungsansätze verfolgt, um das Risiko einer kombinierten antimikrobiellen Wirkung genauer zu charakterisieren und prioritäre Mischungsbestandteile zu identifizieren. Das Risiko einer antimikrobiellen Wirkung wurde sowohl durch eine experimentelle Prüfung der Mischung als auch durch einen komponentenbasierten Berechnungsansatz bestätigt. Der komponentenbasierte Ansatz verdeutlichte zudem die besondere Relevanz der in der Mischung enthaltenen Fluorchinolon-Antibiotika. Die notwendige Grundlage für eine belastbare Abschätzung von Kombinationseffekten sind jedoch harmonisierte Einzelstoffdaten, die bisher nicht im benötigten Umfang zur Verfügung stehen. Deshalb sollte speziell für Antibiotika eine systematische Prüfung der Wirkung auf Umweltmikroorganismen durchgeführt werden. Dieser Lösungsansatz zur Beurteilung von Kombinationseffekten kann mit hoher Wahrscheinlichkeit auch auf andere problematische Wirkstoffgruppen übertragen werden, was generell für eine stärkere Berücksichtigung des pharmakologischen Wirkmechanismus in der ökotoxikologischen Prüfung von Arzneimittelwirkstoffen spricht.

Arzneistoffe können entlang ihres Lebenszyklus verschiedene biotische und abiotische Transformationsprozesse durchlaufen, die oft zur Bildung von unvollständig charakterisierten Transformationsprodukten (TPs) führen. Die Publikationen 3-7 leisten einen allgemeinen Beitrag zur Einschätzung des möglichen Gefahrenpotenzials von pharmazeutischen TPs im Wasserkreislauf und generieren neue methodische Erkenntnisse vor dem Hintergrund einer vorausschauenden Identifizierung von prioritären Abbauprodukten. Die durchgeführten Fallstudien bestätigten, dass photochemische Transformationsprozesse nicht nur zur Abschwächung bereits vorhandener, sondern im Gegenteil auch zur Entstehung gänzlich neuer Gefahrenpotenziale beitragen können. Es ist somit stark in Frage zu stellen, ob die alleinige Fokussierung auf bekannte Aktivitäten der Muttersubstanz für eine sichere Bewertung von TPs ausreicht. Die aktuell größten Herausforderungen auf diesem Gebiet sind das Etablieren einheitlicher Standards und die strategische Ausrichtung zukünftiger Forschungsaktivitäten. Langfristig sollte das gesammelte Wissen in die Weiterentwicklung von geeigneten *in silico* Methoden einfließen, um die Identifizierung prioritärer TPs vergleichbarer und effizienter zu gestalten.

Abstract

The ubiquitous occurrence of pharmaceutical residues is closely linked to possible risks for humans and the environment. The overall objective of this research work was the further development of methodological approaches for the prioritization of pharmaceutical residues with regard to possible gaps in knowledge and legislation. With this in mind, three current problems related to "Pharmaceuticals in the Environment" were discussed on the basis of specific case studies.

Veterinary medicinal products are frequently released into agricultural soils with the application of livestock manure. The first publication dealt with the question how usage patterns from livestock farming could be applied to the retrospective prioritization of veterinary drugs. For this purpose, a special approach was developed and assessed by the example of antibiotic agents. This resulted in a first comprehensive picture of the potential antibiotic load in manure and agricultural soils in the region of northwestern Germany. The obtained findings suggested a significant environmental contamination, showing the need for a re-evaluation of existing active substance approvals. With regard to this possible re-evaluation, the presented methodology could represent an efficient tool for the selection of high priority substances.

Municipal wastewater contains multi-component mixtures of active pharmaceutical ingredients that can potentially shape microbial communities in sewage treatment plants and the aquatic environment. In the second publication, different assessment approaches were applied to an exemplary mixture of 18 pharmaceuticals in order to characterize the risk of a combined antimicrobial effect more precisely and to identify priority mixture components. The risk of an antimicrobial effect was confirmed by both the experimental testing of the whole mixture and a component-based calculation approach. The component-based approach also demonstrated the particular relevance of the fluorchinolone antibiotics in the mixture. However, the necessary basis for a reliable estimation of combination effects are harmonized individual substance data, which are currently not available to the extent required. This argues for a more sophisticated bacterial toxicity assessment of environmentally relevant pharmaceuticals, especially for antibiotics. This approach to the assessment of combination effects is highly likely to be applicable to other problematic pharmaceutical groups as well, which generally argues in favor of a stronger consideration of the pharmacological mode of action in the ecotoxicological testing of pharmaceuticals.

Pharmaceuticals can undergo various biotic and abiotic transformation processes along their life cycle, which often lead to the formation of incompletely characterized transformation products (TPs). Publications 3-7 pursued the evaluation of potential hazards of pharmaceutical TPs in the water cycle and the generation of new methodological findings with regard to a proactive identification of hazardous degradation products. The performed case studies con-

firmed that photochemical transformation processes can contribute not only to the mitigation of existing, but also to the creation of completely new hazard potentials. Therefore, it must be questioned whether the sole focus on known activities of the parent substance is sufficient for a reliable evaluation of TPs. The current major challenges in this area are the establishment of uniform standards and the strategic orientation of future research activities. In the long term, the accumulated knowledge should be incorporated into the further development of *in silico* methods, to make the identification of priority TPs more comparable and efficient.

Beiträge zur Veröffentlichung

Veröffentlichungen in Fachzeitschriften

Publikation 1: Menz, J., Schneider, M., Kümmerer, K. (2015). Usage pattern-based exposure screening as a simple tool for the regional priority-setting in environmental risk assessment of veterinary antibiotics: A case study of northwestern Germany. *Chemosphere* 127, 42-48.

Publikation 2: Menz, J., Baginska, E., Arrhenius, A., Haiβ, A., Backhaus, T., Kümmerer, K. (2017). Antimicrobial activity of pharmaceutical cocktails in sewage treatment plant effluent - An experimental and predictive approach to mixture risk assessment. *Environmental Pollution* 231, 1507-1517.

Publikation 3: Herrmann, M., Menz, J., Olsson, O., Kümmerer, K. (2015). Identification of phototransformation products of the antiepileptic drug gabapentin: Biodegradability and initial assessment of toxicity. *Water Research* 85, 11-21.

Publikation 4: Herrmann, M., Menz, J., Gassmann, M., Olsson, O., Kümmerer, K. (2016). Experimental and in silico assessment of fate and effects of the antipsychotic drug quetiapine and its bio- and phototransformation products in aquatic environments. *Environmental Pollution* 218, 66-76.

Publikation 5: Wilde, M. L., Menz, J., Trautwein, C., Leder, C., Kümmerer, K. (2016). Environmental fate and effect assessment of thioridazine and its transformation products formed by photodegradation. *Environmental Pollution* 213, 658-670.

Publikation 6: Toolaram, A., Menz, J., Rastogi, T., Leder, C., Schneider, M., Kümmerer, K. (2017). Hazard screening of photo-transformation products from pharmaceuticals: application to selective β1-blockers Atenolol and Metoprolol. *Science of The Total Environment* 571, 1769-1780.

Publikation 7: Menz, J., Toolaram, A., Leder, C., Olsson, O., Kümmerer, K., Schneider, M. (2017). Transformation products in the water cycle and the unsolved problem of their proactive assessment: a combined in vitro/in silico approach. *Environment International* 98, 171-180.

Konferenzbeiträge

Menz, J., Rastogi, T., Leder, C., Schneider, M., Kümmerer, K. (2013). First-time application of a modified luminescent bacteria test for the initial ecotoxicity assessment of beta-blockers after phototransformation. *SETAC North America 34th Annual Meeting*. 17.–21. November 2013, Nashville, Tennessee.

Menz, J., Trautwein, C., Wilde, M.L., Schneider, M., Kümmerer, K. (2014). Initial microbial ecotoxicity assessment of Thioridazine, Thioridazine 5-Sulfoxide and photolytic mixtures of Thioridazine. *SETAC Europe 24th Annual Meeting*. 11.–15. Mai 2014, Basel.

Schneider, M., Toolaram, A., Menz, J., Rastogi, T., Kümmerer, K. (2014). Genotoxicity and ecotoxicity screening of photolytic mixtures from the selective β1-receptor blockers Atenolol and Metoprolol. *SETAC Europe 24th Annual Meeting*. 11.–15. Mai 2014, Basel.

Menz, J., Müller, J., Munck, M., Gottschalk, S., Kümmerer, K. (2015). Prioritization of veterinary antibiotics for environmental analysis using a simple screening approach. *SETAC Europe 25th Annual Meeting*, 3.–7. Mai 2015, Barcelona.

Menz, J., Schneider, M., Olsson, O., Kümmerer K. (2015). Veterinärantibiotika in der Umwelt - Abschätzung von Eintragsmengen auf der Basis von Verbrauchsdaten. *BfR-Symposium Antibiotikaresistenz in der Lebensmittelkette*, 2.–3. November 2015, Berlin.

Inhaltsverzeichnis

1 Arzneimittelrückstände in der Umwelt

Die weltweiten Ausgaben für Medikamente betrugen im Jahr 2014 etwa 1 Billion US Dollar und werden bis 2018 aufgrund von Bevölkerungswachstum, steigender Lebenserwartung und verbessertem Zugang zu Arzneimitteln in Schwellenländern auf etwa 1,3 Billionen US Dollar ansteigen [1,2]. In Deutschland, als Beispiel für einen stark entwickelten Arzneimittelmarkt, wurden im Jahr 2014 innerhalb der gesetzlichen Krankenversicherung über alle Arzneimittel hinweg etwa 1,5 definierte Tagesdosen pro Mitglied und Tag verordnet [3]. Arzneimittel sind demnach für viele Menschen ein fester Bestandteil des alltäglichen Lebens und leisten dadurch einen wichtigen Beitrag zur Verbesserung des allgemeinen Gesundheitszustands. Die biologisch hoch aktiven Wirkstoffe gelangen jedoch auch in die Umwelt, wo sie gleichermaßen eine Wirkung auf Organismen entfalten können. Der steigende Verbrauch von Arzneimitteln ist somit eng mit möglicherweise zunehmenden Risiken für Mensch und Umwelt verbunden, deren Bewertung aktuell noch mit vielen Unsicherheiten behaftet ist [4,5]. Die überwältigende Anzahl von potenziell umweltrelevanten Verbindungen und deren vielfältige Wirkungsweisen stellen in dieser Hinsicht bedeutende Faktoren dar. Deshalb liegt es im allgemeinen Interesse prioritäre Stoffe und Stoffwirkungen zu identifizieren, um die notwendige Voraussetzung für eine zielgerichtete Schließung bestehender Wissens- und Regulierungslücken zu schaffen.

1.1 Eintragswege und Umweltverhalten

In der Humanmedizin werden allein in Deutschland pro Jahr etwa 8 100 t potenziell umweltrelevante Arzneimittelwirkstoffe eingesetzt, die insgesamt etwa 1 200 verschiedene Wirkstoffe umfassen [6]. Darüber hinaus werden auch in der Tiermedizin erhebliche Wirkstoffmengen verabreicht. So sind im Jahr 2015 allein 805 t Antibiotika von pharmazeutischen Unternehmen und Großhändlern an Tierärzte in Deutschland abgegeben worden [7].

Die meisten Arzneistoffe werden nach der Verabreichung vom menschlichen oder tierischen Körper wieder ausgeschieden und können anschließend in die Umwelt gelangen. Vom Menschen ausgeschiedene bzw. unsachgemäß entsorgte Arzneimittelwirkstoffe werden mit dem kommunalen Abwasser in Oberflächengewässer eingeleitet, sofern nicht vorher im Zuge der Abwasserreinigung eine Eliminierung stattfindet. Arzneimittelrückstände, die hierbei sorptiv an den Belebtschlamm gebunden werden, können durch eine Verwendung des Klärschlamms als Dünger in der Landwirtschaft ebenfalls in die Umwelt eingetragen werden. Der in Kläranlagen erreichte Wirkungsgrad hängt sowohl von anlagenspezifischen als auch von stoffspezifischen Faktoren ab und kann deshalb bei vergleichender Betrachtung stark variieren [8,9]. In herkömmlichen Kläranlagen werden jedoch nur die wenigsten Wirkstoffe vollständig aus dem Abwasser entfernt, weshalb eine kontinuierliche Einleitung von Arzneimittelrückständen in

die aquatische Umwelt erfolgt [10–13]. Im Gegensatz zu Humanarzneimitteln, die vorwiegend über Punktquellen freigesetzt werden, gelangen Tierarzneimittel auf diffusen Wegen in die terrestrische und aquatische Umwelt. Hier spielt insbesondere die Ausbringung von Wirtschaftsdünger in landwirtschaftlich genutzte Böden eine wichtige Rolle, aber auch der direkte Umwelteintrag in Folge der Behandlung von Weidetieren oder des Einsatzes von Arzneimitteln in Aquakulturen sind bekannte Eintragspfade für Wirkstoffe aus der Veterinärmedizin [14,15].

Entlang ihres Lebenszyklus sind Arzneimittelwirkstoffe unterschiedlichen biotischen und abiotischen Einflüssen ausgesetzt, die oftmals zur Entstehung von stabilen Abbauprodukten führen. Bereits im behandelten Organismus werden viele Wirkstoffe in ihrer chemischen Struktur verändert, sodass nicht nur die ursprünglich eingenommenen Muttersubstanzen, sondern auch die im Körper gebildeten Abbauprodukte (Metabolite) ausgeschieden werden [15]. In der Umwelt, bzw. auf dem Weg dorthin, können anschließend weitere Umwandlungsprozesse stattfinden, wobei die außerhalb des menschlichen oder tierischen Körpers entstehenden Abbauprodukte nicht mehr als Metabolite, sondern im Sinne einer klaren begrifflichen Abgrenzung als Transformationsprodukte bezeichnet werden [16]. Im Wasserkreislauf entstehen Transformationsprodukte u.a. durch mikrobiologische oder abiotisch-chemische Prozesse in der Kläranlage und im Oberflächengewässer [15–17]. Des Weiteren können auch bestimmte Verfahren der technischen Abwasser- oder Trinkwasserbehandlung die Entstehung von Transformationsprodukten begünstigen [18].

Die zuvor beschriebenen Vorgänge haben zur Folge, dass Böden, Oberflächengewässer, sowie in geringerem Umfang auch Grund- und Trinkwasser, nachweislich durch eine Vielzahl von Substanzen pharmazeutischen Ursprungs belastet werden [19–23]. Die nachgewiesenen Maximalkonzentrationen für Arzneimittelrückstände im europäischen Raum liegen im µg/l-Bereich für Oberflächen- und Grundwasser und im ng/l-Bereich für Trinkwasser [24]. Die Maximalbefunde für Arzneimittelrückstände im Boden liegen überwiegend im Bereich von 100 µg/kg bis 1 mg/kg, in Einzelfällen aber auch darüber [24]. Weltweit wurden bisher mindestens 631 verschiedene pharmazeutische Verbindungen in unterschiedlichen Umweltmedien nachgewiesen [25].

1.2 Umwelt- und Gesundheitswirkungen

Es gibt eine steigende Anzahl von Studien, die belegen, dass bestimmte Arzneimittelrückstände bereits in umweltrelevanten Konzentrationen ökotoxische Effekte ausüben können [25]. Diese Erkenntnisse haben auch dazu geführt, dass Arzneimittel von den zuständigen Aufsichtsbehörden und der Europäischen Kommission als zunehmendes Umweltproblem wahrgenommen werden [26]. Mögliche Auswirkungen auf die menschliche Gesundheit sind im Vergleich zu Umweltwirkungen weitaus weniger eindeutig beschrieben. Die Unbedenklichkeit der Anwendung muss im Rahmen der Arzneimittelzulassung für klinisch relevante

Patientengruppen und Behandlungszeiträume nachgewiesen werden. Es steht jedoch die Frage im Raum, inwiefern eine lebenslange Exposition der Gesamtpopulation, z.B. über Rückstände im Trinkwasser oder in Nahrungsmitteln, gesundheitliche Folgen haben kann [27,28]. Eine akute Gefährdung der menschlichen Gesundheit durch Pharmakarückstände im Trinkwasser ist jedoch nach derzeitigem Kenntnisstand nicht zu erwarten [29]. Von aktuell großer Bedeutung ist zudem die Frage, ob Antibiotikarückstände in der Umwelt zur Selektion und Verbreitung von Antibiotikaresistenzen beitragen [30,31].

In der aquatischen Umwelt treten Arzneimittelrückstände üblicherweise als Bestandteil von zufällig entstehenden, komplexen Stoffgemischen in Erscheinung [12,32]. Die aktuellen regulatorischen Ansätze für die Bewertung von Umwelt- und Gesundheitsrisiken basieren jedoch in der Regel auf der Beurteilung von Einzelstoffen, wodurch die ernstzunehmende Gefahr einer Unterschätzung des Risikos gegeben ist [33,34]. Die grundsätzliche Relevanz der Mischungstoxizität und die Eignung verschiedener Modelle zur Vorhersage einer additiven Wirkung wurden in der Vergangenheit hinreichend belegt [34]. Demnach übersteigt das ökotoxikologische Risiko von Arzneistoffgemischen regelmäßig das individuelle Risiko der einzelnen Bestandteile und es sind auch dann ökotoxische Wirkungen möglich, wenn alle Bestandteile nur in geringen Konzentrationen vorhanden sind [35]. Die Vielzahl der möglichen Einflussfaktoren und die hohen Anforderungen an die Datenverfügbarkeit erschweren jedoch momentan noch die präzise Vorhersage von möglichen Kombinationseffekten in der Umwelt [35,36].

Die möglichen ökologischen und gesundheitlichen Probleme, die sich aus der Anwesenheit von Transformationsprodukten im Wasserkreislauf ergeben, sind ebenfalls unzureichend erforscht [37,38]. Bisher wurde vermutlich erst ein Bruchteil der umweltrelevanten Transformationsprodukte identifiziert, weshalb es momentan auch nicht möglich ist diese Verbindungen umfassend umweltanalytisch zu beobachten oder gar zufriedenstellend toxikologisch zu bewerten. Es ist jedoch bekannt, dass sich Transformationsprodukte in der Umwelt häufig anders verhalten als ihre Ausgangsverbindungen und dass manche Umwandlungsprozesse neue schädliche Stoffeigenschaften hervorbringen können [39–41]. Darüber hinaus können Transformationsprodukte pharmazeutischen Ursprungs eine ähnliche pharmakologische Aktivität wie die Muttersubstanz besitzen [42,43] und in manchen Fällen sogar höhere Konzentrationen als ihre Ausgangsverbindungen im Oberflächen- und Grundwasser erreichen [20–22].

2 Zielstellung und Beitrag der Arbeit

Das übergeordnete Ziel dieser Dissertation war die Weiterentwicklung methodischer Ansätze für die Identifizierung prioritärer Arzneimittelrückstände vor dem Hintergrund bestehender Wissens- und Regulierungslücken. Hierbei sollte es weniger darum gehen, gänzlich neue Entwürfe als Alternative zu bereits vorhandenen Konzepten zu etablieren, sondern vielmehr darum, realistische Handlungsempfehlungen zur punktuellen Verbesserung bestehender Ansätze zu entwickeln. Unter diesem Gesichtspunkt wurden drei aktuelle Problemfelder aus dem Themenkomplex „Arzneimittel in der Umwelt“ ausgewählt und jeweils anhand konkreter Fallbeispiele analysiert:

(i) Priorisierung von Tierarzneimitteln für die retrospektive Neubewertung am Beispiel des Antibiotikaeinsatzes in der Nutztierhaltung.

(ii) Identifizierung prioritärer Bestandteile in umweltrelevanten Arzneistoffgemischen am Beispiel der antimikrobiellen Aktivität in Kläranlagenablauf.

(iii) Identifizierung prioritärer Transformationsprodukte am Beispiel ausgewählter Wirkstoffe und Prozesse.

Es muss an dieser Stelle angemerkt werden, dass im engen Rahmen dieser Arbeit keine erschöpfende Auseinandersetzung mit dem Thema angestrebt wurde, sondern vielmehr eine besonders detaillierte und praxisnahe Sichtweise, die in einer umfassenden Übersichtsarbeit nicht erreichbar gewesen wäre. Zu jedem ausgewählten Problemfeld wurden eigene wissenschaftliche Studien durchgeführt und die Ergebnisse in führenden internationalen Fachzeitschriften mit Review-System publiziert. Auf diese Weise sollten aktuelle Probleme aufgezeigt werden und die speziell entwickelten Lösungsansätze unmittelbar in den aktuellen wissenschaftlichen Diskurs einfließen. Im Idealfall soll mit dieser Arbeit ein schlaglichtartiger Beitrag zur Entwicklung einer ganzheitlichen Lösungsstrategie geleistet werden.

3 Priorisierung von Tierarzneimitteln für die retrospektive Neubewertung

3.1 Problemstellung

Im europäischen Zulassungsverfahren für Tierarzneimittel werden in der abschließenden Nutzen-Risiko-Abwägung auch Umweltrisiken berücksichtigt [4]. Der entsprechende Leitfaden zur Durchführung der Umweltrisikobewertung sieht zunächst eine Abschätzung des potenziellen Umwelteintrags anhand des erwartungsgemäßen Anwendungsschemas vor [44]. Ergibt diese Expositionsabschätzung eine initiale Umweltkonzentration von >1 µg/l (aquatische Umwelt) bzw. >100 µg/kg (Boden), dann ist eine vertiefte Umweltprüfung durchzuführen [44]. Bei einem Großteil der momentan eingesetzten Tierarzneimittel handelt es sich jedoch um Wirkstoffe, die bereits vor dem in Kraft treten der aktuellen Vorschriften zugelassen wurden und für die häufig noch keine entsprechende Umweltrisikobewertung vorliegt [45–47]. Ein aktueller Verordnungsvorschlag der Europäischen Kommission sieht jedoch vor, dass die Mitgliedstaaten oder die Europäische Kommission eine Neubewertung von auf dem Markt verfügbaren Tierarzneimitteln verlangen können, wenn sie der Ansicht sind, dass von ihnen ein Risiko für die Gesundheit von Mensch oder Tier bzw. für die Umwelt ausgeht [48]. Die retrospektive Abschätzung des tatsächlichen Umwelteintrags auf der Basis von Verbrauchsdaten könnte wichtige Informationen für die Identifizierung prioritärer Wirkstoffe im Hinblick auf eine solche Neubewertung liefern.

Es gibt in Deutschland keine umfassende Überwachung des Tierarzneimitteleinsatzes, weshalb die wirkstoffspezifischen Verbrauchsmengen und Anwendungsschemata nicht genau bekannt sind. Es wird jedoch angenommen, dass die landwirtschaftliche Tiermast für den Hauptanteil des Tierarzneimittelverbrauchs verantwortlich ist [49]. Zwei unabhängige Schätzungen des tiermedizinischen Arzneimittelverbrauchs aus den Jahren 2000/2001 und 2003 deuten zudem darauf hin, dass über 90 % der insgesamt verbrauchten Wirkstoffmenge auf die Gruppe der Antibiotika (Antiinfektiva) zurückzuführen ist [50,51]. Antibiotika und bestimmte Hormone stellen gleichzeitig die einzigen Wirkstoffe dar, deren Abgabemengen seit 2011 kontinuierlich über das Tierarzneimittel-Abgabemengen-Register (TAR) erfasst werden [52]. Die mittlerweile bekannt gewordenen Antibiotikaabgaben werden jedoch nur teilweise durch die Anzahl der in Böden nachgewiesenen Wirkstoffe abgebildet. So ergab eine Zusammenstellung von europaweit erhobenen Monitoringdaten aus dem Jahr 2011, dass lediglich Wirkstoffe aus vier verschiedenen Antibiotikaklassen in Bodenproben analytisch nachweisbar waren [24]. Demgegenüber stehen mindestens 18 Wirkstoffklassen, die nachweislich aktuell in Deutschland abgegeben werden [7].

Die Abschätzung des potenziellen Umwelteintrags von Tierarzneimitteln erfolgt üblicherweise anhand der Häufigkeit der Verabreichung und der zugehörigen Dosierung [44]. Somit sind neben absoluten Abgabemengen auch anwendungsbezogene Daten zum Tierarzneimitteleinsatz von essentieller Bedeutung. Seit Inkrafttreten der 16. AMG-Novelle im April 2014 sind nach AMG § 58a–d alle Betriebe, die Rinder, Schweine, Hühner oder Puten zur Mast berufs- oder gewerbsmäßig halten, zur Mitteilung des Antibiotikaeinsatzes an die zuständige Behörde verpflichtet [53]. Die erfassten Daten sind jedoch für die Öffentlichkeit nicht unmittelbar zugänglich, sondern dürfen nach AMG § 58f ausschließlich für die Ermittlung und Überwachung von abstrahierten Kennzahlen zur Therapiehäufigkeit genutzt werden. Darüber hinaus gilt die Meldepflicht nur für Fleisch erzeugende Agrarbetriebe, nicht aber für Milchviehhaltungen, obwohl auch in solchen Betrieben vergleichsweise häufig Antibiotika eingesetzt werden [54]. Im nordwestdeutschen Raum wurden jedoch bereits vor Einführung der Mitteilungspflicht Erhebungen zum Antibiotikaeinsatz durch ausgewählte Betriebe und Tierärzte durchgeführt und öffentlich gemacht [55–57]. Somit standen erstmalig in begrenztem Umfang anwendungsbezogene Daten für die Einschätzung des potenziellen Umwelteintrags von Veterinärantibiotika in Deutschland zur Verfügung.

In der ersten Publikation wurde am Beispiel der verfügbaren Antibiotikaverbrauchsdaten untersucht, inwiefern Anwendungsschemata aus der Nutztierhaltung für die retrospektive Identifizierung prioritärer Tierarzneimittel genutzt werden können. Darüber hinaus sollten in erster Annäherung Wirkstoffe identifiziert werden, die im Zeitraum der zugrundeliegenden Erhebungen möglicherweise durch ein expositionsseitiges Risikopotential gekennzeichnet waren.

3.2 Methodisches Vorgehen

Basierend auf den öffentlich verfügbaren Daten aus der VetCAb-Machbarkeitsstudie [55,56] wurde zunächst für alle dort erfassten Wirkstoffe mit dokumentierter, oraler Verabreichung die relative Anwendungshäufigkeit und die durchschnittliche Dosierung für die Tierarten Schwein, Rind und Geflügel als sogenanntes „Anwendungsmuster“ definiert. In einem zweiten Schritt wurde für jede Tierart eine repräsentative Nutztierkategorie ausgewählt (Schwein: Mastschwein, Rind: Kalb, Geflügel: Masthuhn) und die durchschnittliche Therapiehäufigkeit (Durchschnittsszenario) bzw. die maximale Therapiehäufigkeit (Worst-Case-Szenario) unter Berücksichtigung einer weiteren Erhebung zum Antibiotikaeinsatz [57] abgeschätzt. Mithilfe dieser Variablen war es nun möglich in Anlehnung an den Leitfaden der Europäischen Arzneimittelagentur [44] für jeden Wirkstoff und jede ausgewählte Tierart die theoretisch mögliche Rückstandskonzentration für Dünger und Boden zu berechnen. Dabei wurde zunächst ein Gesamtrückstandsansatz („total residue approach“) verfolgt, d.h. Metabolisierungs- und Transformationsprozesse wurden nicht berücksichtigt.

3.3 Ergebnisse

Aus der VetCAb-Machbarkeitsstudie geht hervor, dass im Rahmen der Erhebung 45 aktive Wirkstoffe aus 12 verschiedenen Klassen in signifikanten Mengen oral verabreicht wurden. Die vorhergesagten Rückstandskonzentrationen dieser Wirkstoffe im Wirtschaftsdünger lagen in Konzentrationsbereichen von ng/kg Trockengewicht (TG) bis g/kg TG, in Abhängigkeit vom jeweils betrachteten Szenario (Publikation 1, Tabellen S6-S7). Im Durchschnittsszenario wurde die höchste Rückstandskonzentration mit 0,67 g/kg TG für den Wirkstoff Chlortetracyclin in Rindergülle prognostiziert. Die Anwendung des Worst-Case-Szenarios ergab eine maximale Konzentration von 1,8 g/kg TG für den Wirkstoff Tetracyclin in Schweinegülle.

Zur Überprüfung der Plausibilität wurden die berechneten Konzentrationen im Dünger mit gemessenen Maximalwerten aus der Literatur verglichen. Im Durchschnittsszenario wurde in 11 von 17 betrachteten Fällen der maximale Literaturwert unterschritten, wobei jedoch in 13 von 17 Fällen die vorhergesagte und die gemessene Konzentration in derselben Größenordnung lagen (Publikation 1, Abbildung 1). Im Worst-Case-Szenario wurde in 4 von 17 betrachteten Fällen der maximale Literaturwert um weniger als eine Größenordnung unterschritten. Darüber hinaus war die höchste gemessene Konzentration in 6 von 17 Fällen um mehr als eine Größenordnung niedriger als der vorhergesagte Wert (Publikation 1, Abbildung 1).

Die vorhergesagten initialen Rückstandskonzentrationen im Boden lagen in Konzentrationsbereichen von pg/kg TG bis mg/kg TG mit einem Spitzenwert im Worst-Case-Szenario von 4,4 mg/kg TG für Tetracyclin (Publikation 1, Tabellen S6-S7). Im Durchschnittsszenario erreichte Chlortetracyclin eine maximale initiale Rückstandskonzentrationen im Boden von bis zu 1,1 mg/kg TG. Darüber hinaus erreichten im Worst-Case-Szenario die Wirkstoffe Amoxicillin und Sulfadiazin theoretische Rückstandskonzentrationen im Boden oberhalb von 1,0 mg/kg TG. Insgesamt überschritten 14 Wirkstoffe aus 10 verschiedenen Klassen eine initiale Rückstandskonzentrationen im Boden von 100 µg/kg TG (Publikation 1, Abbildung 2). Die vorhergesagte Rückstandskonzentration des vergleichsweise niedrig dosierten Wirkstoffs Enrofloxacin lag unterhalb dieses Schwellenwertes, obwohl eine überdurchschnittlich hohe Anwendungshäufigkeit vorgelegen hat.

3.4 Diskussion

Die durchgeführte Eintragsabschätzung ermöglichte erstmalig eine umfassende Einschätzung der potenziellen Antibiotikabelastung in Wirtschaftsdünger und landwirtschaftlich genutzten Böden im nordwestdeutschen Raum. Die vorhergesagten Rückstandskonzentrationen im Dünger erscheinen im Vergleich zu gemessenen Spitzenwerten bis auf wenige Ausnahmen plausibel. Die Abschätzung des Umwelteintrags mithilfe von Anwendungsmustern aus der Nutztierhaltung ermöglicht somit auch eine erste Einschätzung für Wirkstoffe, die bisher umweltanalytisch kaum in Erscheinung getreten sind.

Selbst unter Annahme einer durchschnittlichen Therapiehäufigkeit könnten gleich mehrere Wirkstoffe den aus regulatorischer Sicht kritischen Schwellenwert von >100 µg/kg im Boden erreichen (Publikation 1, Abbildung 2). Es sollte jedoch angemerkt werden, dass die berechneten Werte mögliche Gesamtrückstände abbilden, sodass eine fundierte Risikobewertung erst im Zuge einer erweiterten Umweltprüfung unter Berücksichtigung von Umwandlungs- und Abbauprozessen erfolgen kann. Diese Erkenntnisse unterstreichen die Notwendigkeit einer Neubewertung bestehender Zulassungen unter Berücksichtigung der tatsächlichen Anwendungsschemata in den Betrieben. Dabei sollte die Identifizierung prioritärer Stoffe nicht nur auf Grundlage der vorhergesagten Umweltkonzentration erfolgen, sondern insbesondere bei niedrigdosierten Wirkstoffen auch die Häufigkeit der Anwendung eine Berücksichtigung finden.

Die Datenverfügbarkeit zum Tierarzneimitteleinsatz in Deutschland ist noch immer als unzureichend einzuschätzen. Die wenigen öffentlich zugänglichen Daten sind von mangelnder Aktualität und regional begrenzt bzw. unvollständig oder nicht ausreichend detailliert, sodass eine unabhängige Bewertung der aktuellen Gesamtsituation auf überregionaler und lokaler Ebene kaum möglich ist. Zwar konnte in den letzten Jahren insgesamt ein deutlicher Rückgang der Antibiotikaabgabemengen beobachtet werden [52], es ist jedoch unklar, wie sich dieser Trend auf die Anwendungsschemata einzelner Wirkstoffe ausgewirkt hat. Darüber hinaus gibt es kaum öffentliche Daten über die Verbräuche und Anwendungsschemata von Antiparasitika und Hormonen, obwohl von diesen Wirkstoffgruppen ebenfalls ein erhöhtes Umweltrisiko ausgeht [58,59].

4 Identifizierung prioritärer Bestandteile in umweltrelevanten Arzneistoffgemischen

4.1 Problemstellung

Das kommunale Abwasser beinhaltet komplexe Mischungen von Arzneistoffen, die im Zuge der Abwasserreinigung nur unzureichend abgebaut werden [23,60,61] und mikrobielle Lebensgemeinschaften in Kläranlagen und in der aquatischen Umwelt auf vielfältige Weise beeinträchtigen könnten [62–68]. In diesem Zusammenhang sind Antibiotika aufgrund ihrer beabsichtigten antimikrobiellen Aktivität von besonderem Interesse [69]. Darüber hinaus könnten Antibiotika die Selektion und Ausbreitung von Antibiotikaresistenzen in Kläranlagen fördern [70,71] und die kombinierte Einleitung von Antibiotika und resistenten Keimen zur Verbreitung von Antibiotikaresistenzen in der aquatischen Umwelt beitragen [72].

Die Notwendigkeit einer stärkeren Berücksichtigung von Effekten auf Mikroorganismen in der Umweltrisikobewertung von Chemikalien wurde erst kürzlich hervorgehoben [73]. Die Umweltverträglichkeitsprüfung im Zulassungsverfahren für Humanarzneimittel erfordert jedoch nicht grundsätzlich eine Beurteilung von antimikrobiellen Effekten. Die Prüfung einer solchen Wirkung wird ausdrücklich nur für Arzneistoffe empfohlen, die antimikrobiell wirksam sind und deren prognostizierte Umweltkonzentration 0,01 µg/l überschreitet [74]. Darüber hinaus spielen mögliche Kombinationseffekte von unbeabsichtigt entstehenden Wirkstoffgemischen bisher keine Rolle im europäischen Zulassungsverfahren [33]. Als möglicher Lösungsansatz für dieses Problem wurde von Backhaus und Faust ein mehrstufiges Verfahren für die Risikobewertung von komplexen Stoffgemischen vorgeschlagen [75]. Der Ansatz basiert auf dem Konzept der Konzentrationsadditivität (engl. concentration addition, CA) und wurde bereits am Beispiel der aquatischen Ökotoxizität von Arzneistoffgemischen in Kläranlagenabläufen erfolgreich erprobt [76]. In diesem Zusammenhang wurde für mehrere Expositionsszenarien ein erhebliches Risiko identifiziert, welches vor allem auf die spezifische Wirkung von Antibiotika gegenüber Cyanobakterien zurückzuführen war [76].

In Publikation 2 wurden am Beispiel einer Mischung aus 18 Arzneistoffen verschiedene Bewertungsansätze verfolgt, um das zuvor beschriebene Risiko einer kombinierten antimikrobiellen Wirkung genauer zu charakterisieren und prioritäre Mischungsbestandteile zu identifizieren.

4.2 Methodisches Vorgehen

Auf der Grundlage von gemessenen Konzentrationen im Ablauf einer kommunalen Kläranlage [12] wurde eine Stammlösung aus 18 verschiedenen Arzneimittelwirkstoffen hergestellt

(Publikation 2, Tabelle 1). Die Wirkstoffkonzentrationen in dieser Stammlösung entsprachen ungefähr dem 40.000-fachen der gemessenen Ablaufkonzentrationen (engl. measured effluent concentration, MEC). Die hemmende Wirkung der Stammlösung auf ein Misch-Inokulum aus dem Ablauf einer kommunalen Kläranlagen wurde anhand des biologischen Sauerstoffbedarfs (engl. biochemical oxygen demand, BOD) und der Anzahl koloniebildender Einheiten (engl. colony forming units, CFU) untersucht. Darüber hinaus wurde im Anschluss an die Exposition mittels Biolog EcoPlate™ das physiologische Profil der Mikrobengemeinschaft analysiert. Als Endpunkte wurden hierbei die durchschnittliche Farbentwicklung (engl. average well color development, AWCD), der Shannon-Diversitätsindex (H′) und das Muster der Substratnutzung betrachtet. Die spezifische Toxizität der Stammlösung gegenüber Bakterien wurde anhand von Hemmtests mit *Pseudomonas putida* und *Vibrio fischeri* bestimmt. Zusätzlich wurden Daten zur Bakterientoxizität der einzelnen Mischungskomponenten aus der Literatur zusammengetragen. Im Anschluss erfolgte eine Risikocharakterisierung in Hinblick auf antimikrobielle Effekte in kommunalen Kläranlagen und in der aquatischen Umwelt. Das Risiko für mikrobielle Lebensgemeinschaften in Kläranlagen wurde anhand des Quotienten aus der gemessenen Ablaufkonzentration (MEC) und der vorhergesagten Konzentration, bei der keine Wirkung auftritt (predicted no effect concentration, PNEC), bestimmt. Ein MEC/PNEC-Verhältnis von >1 wurde hierbei als Hinweis für ein hohes Risiko gewertet [74]. Die Charakterisierung des Risikos für die aquatische Umwelt erfolgte semiquantitativ anhand von Toxic Units (TU), d.h. dem Verhältnis aus MEC und halbmaximaler Effektkonzentration (EC_{50}) im Bakterienhemmtest. Die gemeinsame Toxizität der einzelnen Mischungskomponenten wurde zusätzlich aus den Literaturdaten anhand der Summe der TU (STU) abgeschätzt.

4.3 Ergebnisse

Gegenüber den Expositionskulturen mit Kläranlagenablauf rief das Arzneistoffgemisch bei allen betrachteten Endpunkten deutliche Effekte hervor. Der Endpunkt BOD zeigte nach 24 h und einer Behandlungskonzentration von 100 MEC eine deutlich erkennbare Respirationshemmung. Mit zunehmender Inkubationsdauer wurde jedoch in allen Testansätzen eine Angleichung des BOD beobachtet (Publikation 2, Abbildung 1). Die Anzahl der kultivierbaren Mikroorganismen (CFU) wurde nach 24h ausgehend von 1 000 MEC und nach 48h bei 4 000 MEC signifikant beeinträchtigt (Publikation 2, Abbildung 2A). Die Gesamtstoffwechselaktivität (AWCD) wurde nach 24 h Exposition gegenüber 100 MEC und nach 48 h Exposition gegenüber 1 MEC leicht abgesenkt (Publikation 2, Abbildung 2B). Die Substratdiversität (H‘) wurde nach 24 h Exposition gegenüber 1 000 MEC und nach 48h Exposition gegenüber 4 000 MEC signifikant beeinträchtigt (Publikation 2, Abbildung 2C). Die vertiefende Analyse des Substratverwertungsmusters offenbarte einen zeitabhängigen Anpassungsprozess, der ab einer Behandlungskonzentration von 10 MEC mit zunehmender Deutlichkeit auftrat (Publikation 2, Abbildung 3).

Die experimentelle Testung der spezifischen Wirkung auf Bakterien lieferte Belege für eine hohe antibakterielle Aktivität der Mischung mit EC_{50}-Werten für die Wachstumshemmung in *P. putida* und *V. fischeri* von 41,5 bzw. 12,9 MEC (Publikation 2, Tabelle S4, Abbildung 5A). Der EC_{50}-Wert für die Langzeit-Leuchthemmung in *V. fischeri* lag mit 9,2 MEC in einem ähnlichen Bereich wie der EC_{50}-Wert für die Wachstumshemmung, wohingegen der EC_{50}-Wert für die Kurzzeit-Leuchthemmung mit ca. 12 000 MEC mehrere Größenordnungen darüber lag (Publikation 2, Tabelle S4, Abbildung 5B).

Die Literaturrecherche zur antibakteriellen Aktivität der einzelnen Mischungskomponenten ergab 89 Effektkonzentrationen für 12 verschiedene Bakterienspezies und 16 Wirkstoffe (Publikation 2, Tabelle S6). Im Falle der β-Blocker Acebutolol und Oxprenolol waren keine Daten zur Bakterientoxizität verfügbar. Die niedrigsten Effektkonzentrationen der in der Mischung enthaltenen Antibiotika lagen zwischen 15-150 nmol/l, während der effektive Bereich der nicht antibiotisch wirksamen Substanzen 0,9-190 µmol/l betrug.

Die abschließende Risikocharakterisierung ergab für die getestete Mischung ein maximales PEC/PNEC-Verhältnis von 0,64 für Mikroorganismen in Kläranlagen (Publikation 2, Tabelle 2). Darüber hinaus wurden für die aquatische Umwelt experimentelle TU-Werte von 0,024-0,11 (Publikation 2, Tabelle 3) und ein literaturbasierter STU-Wert von 0,1 ermittelt (Publikation 2, Tabelle 4). Hierbei waren 98 % der prognostizierten Mischungstoxizität (STU) auf die Wirkstoffe mit bekannter antibiotischer Wirksamkeit zurückzuführen. Die ermittelten TU- bzw. STU-Werte belegen, dass die Mischungskonzentration der untersuchten Arzneistoffe im Kläranlagenablauf nur etwa zehnmal niedriger war als diejenige Konzentration, welche eine Hemmwirkung von 50 % gegenüber Umweltbakterien hervorrufen könnte.

4.4 Diskussion

Die betrachtete Mischung enthielt nur diejenigen Arzneistoffe, die im Rahmen des Monitorings erfasst wurden. Hierbei wurden auch keinerlei Metabolite oder Transformationsprodukte berücksichtigt. Infolgedessen muss davon ausgegangen werden, dass in dieser Studie das tatsächliche Risiko von Arzneistoffgemischen in der Umwelt systematisch unterschätzt wurde. Trotzdem konnte mithilfe einer Kombination aus experimentellen und prädiktiven Methoden ein mögliches Risiko für Mikroorganismen in Kläranlagen und in der aquatischen Umwelt identifiziert werden. Diese Ergebnisse unterstreichen die Notwendigkeit einer stärkeren Berücksichtigung von Kombinationswirkungen auf mikrobielle Lebensgemeinschaften in der Umweltrisikobewertung von Arzneistoffen.

Ein wesentliches Problem in der Risikobewertung von Umweltgemischen ist die hohe räumliche und zeitliche Variabilität, welche eindeutig für einen komponentenbasierten Modellierungsansatz und gegen die experimentelle Prüfung von ganzen Mischungen spricht. Die Ergebnisse der vorliegenden Studie deuten darauf hin, dass eine zuverlässige Abschätzung der kombinierten bakterientoxischen Wirkung in komplexen Arzneistoffgemischen auf der Basis

von Einzelstoffdaten prinzipiell möglich ist. Eine solche Abschätzung der Mischungstoxizität kann jedoch auch mit hohen Unsicherheiten behaftet sein, beispielweise wenn der Standardisierungsgrad der zugrundeliegenden Einzelstoffdaten zu gering ist und/oder die verwendeten Daten auf vergleichsweise unempfindlichen Bakterienstämmen beruhen. Daher ist es besonders wichtig, harmonisierte Datensätze auf Grundlage von standardisierten Testverfahren zu generieren. Diese Prüfung sollte ein klar definiertes Spektrum repräsentativer Bakterienstämme umfassen, um Speziesunterschiede ausreichend zu berücksichtigen und eine Vielzahl von funktionellen Merkmalen einzuschließen. Unter diesen Gesichtspunkten können mikrotierbasierte Multispezies-Tests, beispielsweise nach dem Vorbild des MARA-Assays [77], als vielversprechender Lösungsansatz betrachtet werden. Einmal verfügbar, könnten solche Daten für die retrospektive Abschätzung von ortsspezifischen Kombinationseffekten verwendet werden, um den relativen Einfluss jeder Mischungskomponente auf verschiedene Bakterienspezies und deren assoziierte Ökosystemfunktionen zu bestimmen.

5 Identifizierung prioritärer Transformationsprodukte

5.1 Problemstellung

Aufgrund ihres ubiquitären Vorkommens im Wasserkreislauf können Arzneistoffe entlang ihres Lebenszyklus verschiedene biotische und abiotische Transformationsprozesse durchlaufen, die oft zur Bildung von unvollständig charakterisierten Transformationsprodukten (TPs) führen. Tatsächlich wurde bereits für verschiedene Arzneistoffe ein gemeinsames Vorkommen von Muttersubstanzen und TPs in Oberflächenwasser und Grundwasser beschrieben [20,21]. Die chemische Identität der meisten TPs im Wasserkreislauf ist jedoch gänzlich unbekannt, weshalb das aktuell vorhandene Risiko nicht zufriedenstellend beurteilt werden kann [37,78,79]. Als Reaktion auf dieses Problem wurde eine vorausschauende Bewertung von TPs, d.h. deren toxikologische Beurteilung vor dem Inverkehrbringen der Ausgangsverbindung, bereits von verschiedenen Stellen gefordert [80,81]. Im europäischen Zulassungsverfahren für Arzneimittel wird eine toxikologische Bewertung von Abbauprodukten, die erst in der Umwelt entstehen, bisher jedoch nicht verlangt [74].

In der Vergangenheit wurden verschiedene Strategien zur Identifizierung potenziell gefährlicher TPs vorgeschlagen und erprobt. Eine ganzheitliche Einschätzung des Risikos ist jedoch aufgrund einer mangelnden Vergleichbarkeit und strategischen Ausrichtung zurückliegender Forschungsaktivitäten bisher kaum möglich [38,40,82]. Die vorhandenen Bewertungskonzepte lassen sich überwiegend als expositions- oder wirkungsorientiert beschreiben und wurden bereits an anderer Stelle tiefergehend erörtert [38,40,82,83]. Bisher gelang es nur in wenigen Fällen potenziell toxische TPs eindeutig zu identifizieren [38,40], wobei erste Erfolge durch die Kopplung von simulierten Abbauprozessen mit aufwändiger wirkungsgeleiteter Analytik (engl. effect-directed analysis, EDA) erzielt wurden [41,84]. Die Korrelation der Konzentrationen einzelner Mischungsbestandteile mit der insgesamt messbaren biologischen Aktivität einer Mischung im zeitlichen Verlauf („virtuelle EDA“) stellt eine deutlich vereinfachte Variante des wirkungsorientierten Ansatzes dar und wurde in der Vergangenheit ebenfalls erfolgreich zur Identifizierung toxischer TPs eingesetzt [81, 85]. TPs, die auf diesen oder auch auf anderen Wegen als potenziell gefährlich identifiziert werden, sind häufig nicht in isolierter Form für eine bestätigende Toxizitätsprüfung verfügbar. Aus diesem Grund werden (Quantitative) Struktur-Wirkungs-Beziehungen [engl. (quantitative) structure-activity relationships), (Q)SARs] zunehmend als Mittel für die Charakterisierung nicht experimentell zugänglicher TPs betrachtet [82,86].

Die Publikationen 3-7 wurden mit den Zielen verfasst (i) einen allgemeinen Beitrag zur Einschätzung des möglichen Gefahrenpotenzials von pharmazeutischen TPs im Wasserkreislauf

zu leisten und (ii) neue methodische Erkenntnisse vor dem Hintergrund einer vorausschauenden Identifizierung von prioritären TPs zu generieren.

5.2 Methodisches Vorgehen

Die betrachteten Wirkstoffe (Tabelle 1) wurden aufgrund einer besonderen Umweltrelevanz, eines photochemischen Modellcharakters und/oder vorhandener Anknüpfungspunkte aus vorhergehenden Studien ausgewählt. Eine wässrige Lösung des untersuchten Wirkstoffs wurde in einem Batch-Reaktor mittels Quecksilber-Mitteldrucktauchlampe (TQ 150) oder Xenon-Mitteldrucktauchlampe (TXE 150) polychromatisch bestrahlt. Die Auswahl der Lichtquelle erfolgte hierbei stets unter Berücksichtigung der spezifischen Absorptionscharakteristika der Modellsubstanz. Während der Behandlung wurden zu definierten Zeitpunkten Proben aus dem Reaktor entnommen und direkt im Anschluss die Parameter pH-Wert, Temperatur und Peroxid-Gehalt bestimmt. Darüber hinaus wurde der gelöste organische Kohlenstoff (engl. dissolved organic carbon, DOC) bzw. der nicht ausblasbare organische Kohlenstoff (engl. non-purgeable organic carbon, NPOC) bestimmt und mittels HPLC und LC-MS die Primärelimination und die Bildung von TPs untersucht. Zusätzlich wurden MS^n-Fragmentierungen für die Identifizierung und Strukturaufklärung von TPs mittels LC-MS bzw. LC-HRMS analysiert. Die Toxizität der Photolysegemische gegenüber Bakterien wurde mit einem modifizierten Leuchtbakterientest untersucht. In ausgewählten Photolysegemischen wurde zusätzlich mittels Umu-Test, Ames-Fluktuationstest und *in vitro* Mikrokerntest die Genotoxizität analysiert. Des Weiteren wurden in ausgewählten Fällen Strukturvorschläge für neu entstandene TPs abgeleitet und eine ergänzende Gefährdungsbeurteilung mit verschiedenen (Q)SAR-Modellen durchgeführt.

Tabelle 1: Wirkstoffe, Versuchsbedingungen und eingesetzte Analysemethoden.

Wirkstoff	Konzentration (mg/l)	Lichtquelle	Analysemethoden	Publikation
Gabapentin	100, 20, 5, 1, 0,1	TQ 150 200-600 nm	LC-MS LC-HRMS Leuchtbakterientest Umu-Test	Publikation 3
Quetiapin-Hemifumarat	100, 20, 5, 1	TQ 150 200-600 nm	LC-MS LC-HRMS Leuchtbakterientest Umu-Test	Publikation 4
Thioridazin-Hydrochlorid	50, 0,5	TXE 150 300-800 nm	LC-MS LC-HRMS Leuchtbakterientest QSAR	Publikation 5
Atenolol	100	TQ 150 200-600 nm	LC-MS Leuchtbakterientest Umu-Test Ames-Fluktuationstest *In vitro* Mikrokerntest QSAR	Publikation 6
Metoprolol-Tartrat	400	TQ 150 200-600 nm	LC-MS Leuchtbakterientest Umu-Test Ames-Fluktuationstest *In vitro* Mikrokerntest QSAR	Publikation 6
Propranolol-Hydrochlorid	100, 1	TQ 150 200-600 nm	LC-MS Leuchtbakterientest Umu-Test Ames-Fluktuationstest *In vitro* Mikrokerntest QSAR	Publikation 7

5.3 Ergebnisse

Gabapentin (GAB) zeigte bei einer Startkonzentration von 100 mg/l nach 128 min UV-Bestrahlung eine Primärelimination von 80 %, wohingegen die Kohlenstoffelimination lediglich einen Endwert von 9 % erreichte (Publikation 3, Abbildung 1). Insgesamt wurden 27 TPs im Photolysegemisch identifiziert (Publikation 3, Tabelle 1, Abbildung 3). Vor der Behandlung zeigte GAB im Leuchtbakterientest keine signifikante Wirkung. Zum Ende der Behandlung wurde jedoch ein deutlicher Anstieg der Bakterientoxizität beobachtet (Publikation 3, Abbildung 5). Der Umu-Test lieferte zu keinem der untersuchten Behandlungszeitpunkte einen Hinweis auf das Vorhandensein genotoxischer Abbauprodukte.

Quetiapin (QUT) zeigte bei einer Startkonzentration von 100 mg/l nach 128 min UV-Bestrahlung eine Primärelimination von 60 % und eine Kohlenstoffelimination von 1 % (Publikation 4, Abbildung 1). Insgesamt wurden 7 TPs im Photolysegemisch identifiziert (Publikation 4, Tabelle 3). Im Leuchtbakterientest induzierte QUT bereits ohne Bestrahlung einen deutlichen Effekt, der erst zum Ende der Behandlung leicht zurückging. Die residuale Wirkung des Reaktionsgemisches überstieg jedoch die prognostizierte alleinige Wirkung der

Muttersubstanz (Publikation 4, Abbildung 3). Der Umu-Test lieferte zu keinem der untersuchten Behandlungszeitpunkte einen Hinweis auf das Vorhandensein genotoxischer Abbauprodukte.

Thioridazin (THI) zeigte bei einer Startkonzentration von 50 mg/l nach 256 min Bestrahlung mittels Xenon-Lampe eine Primärelimination von 97 % und eine Kohlenstoffelimination von 11 % (Publikation 5, Abbildung 1). Insgesamt wurden 21 TPs im Photolysegemisch identifiziert (Publikation 5, Abbildung 2). Im Leuchtbakterientest zeigte THI bereits ohne Bestrahlung eine deutliche Wirkung, welche im Laufe der Behandlung kontinuierlich abnahm (Publikation 5, Abbildung 5A). Die kommerziell erhältlichen TPs THI-2-SO und THI-5-SO zeigten im Vergleich zu THI eine deutlich geringere Toxizität im Leuchtbakterientest und der residuale Effekt des Reaktionsgemisches zeigte eine gute Übereinstimmung mit dem prognostizierten Kombinationseffekt von THI und THI-2-SO. Die (Q)SAR-Vorhersagen für Mutagenität in Bakterien lieferten Hinweise für eine vorhandene Aktivität im Fall von TP 355 und TP 339 (Publikation 5, Tabelle 2).

Atenolol (ATL) zeigte bei einer Startkonzentration von 100 mg/l nach 256 min UV-Bestrahlung eine Primärelimination von 98 % und eine Kohlenstoffelimination von 7 % (Publikation 6, Abbildung 1). Insgesamt wurden 54 TPs im Photolysegemisch identifiziert (Publikation 6, Tabelle S6.1). Vor der Behandlung zeigte ATL im Leuchtbakterientest keine signifikante Hemmwirkung. Im Laufe der Behandlung wurde jedoch ein deutlicher Anstieg der Bakterientoxizität beobachtet (Publikation 6, Abbildung 3). Im Ames-Fluktuationstest, im Umu-Test und im *in vitro* Mikrokerntest rief ATL weder vor noch nach Bestrahlung eine signifikante Antwort hervor (Publikation 6, Tabelle 2). Die (Q)SAR-Vorhersagen signalisierten jedoch für mehrere TPs ein genotoxisches Potenzial (Publikation 6, Tabelle 1).

Metoprolol (MTL) zeigte bei einer Startkonzentration von 400 mg/l nach 256 min UV-Bestrahlung eine Primärelimination von 61 % und eine Kohlenstoffelimination von 5 % (Publikation 6, Abbildung 2). Insgesamt wurden 15 TPs im Photolysegemisch identifiziert (Publikation 6, Tabelle S6.2). Vor der Behandlung zeigte MTL im Leuchtbakterientest nur eine geringe Hemmwirkung. Im Laufe der Behandlung wurde jedoch ein deutlicher Anstieg der Bakterientoxizität beobachtet (Publikation 6, Abbildung 3). Im Ames-Fluktuationstest, im Umu-Test und im *in vitro* Mikrokerntest rief MTL weder vor noch nach Bestrahlung eine signifikante Antwort hervor (Publikation 6, Tabelle 3). Es wurde jedoch im Verlauf des *in vitro* Mikrokerntests nach 16 und 256 min Bestrahlung ein deutlicher Anstieg der Zytotoxizität festgestellt. Die (Q)SAR-Vorhersagen signalisierten zudem für mehrere TPs ein genotoxisches Potenzial (Publikation 6, Tabelle 1).

Propranolol (PPL) zeigte bei einer Startkonzentration von 100 mg/l nach 256 min UV-Bestrahlung eine Primärelimination von nahezu 100 % und eine Kohlenstoffelimination von 30 % (Publikation 7, Abbildung 1). Insgesamt wurden 115 TPs im Photolysegemisch detektiert (Publikation 7, Tabelle S4.1, Abbildung 2). PPL zeigte vor der Behandlung im Leucht-

bakterientest nur eine geringe Hemmwirkung (Publikation 7, Abbildung 3B). Das Reaktionsgemisch nach 4 min Bestrahlung war jedoch durch einen deutlichen Anstieg der Hemmung geprägt. Im Ames-Fluktuationstest wurde im Laufe der Behandlung ebenfalls eine deutliche Zunahme der Aktivität beobachtet, wobei die Probe nach 128 min Bestrahlung den Höhepunkt markierte (Publikation 7, Abbildung 3A). Im Umu-Test und im *in vitro* Mikrokerntest induzierte PPL weder vor noch nach Behandlung eine signifikante Antwort. Das Auftreten von zytotoxischen und mutagenen Effekten in Bakterien war mit dem Auftreten bestimmter TPs korreliert (Publikation 7, Abbildung 4 und 6). Die anschließende Analyse von Struktur-Wirkungs-Beziehungen dieser TPs ergab, dass die neu entstandene Toxizität vermutlich auf eine oxidative Öffnung des Naphtylrings im Molekül von PPL zurückzuführen war (Publikation 7, Abbildungen 5 und 7). Darüber hinaus konnte im Experiment gezeigt werden, dass die Hydroxylierung von PPL an der C4-Position des Naphtylrings mit einer bis zu 70-fachen Verstärkung der Toxizität gegenüber Bakterien einherging (Publikation 7, Tabelle 1).

5.4 Diskussion

Obwohl alle durchgeführten Studien auf einem ähnlichen Untersuchungsdesign basierten, traten im Laufe der betrachteten Transformationsprozesse deutlich voneinander abweichende Aktivitätsverläufe auf. Diese Beobachtung kann nur bedingt auf die unterschiedliche Substanzklassenzugehörigkeit der ausgewählten Modellsubstanzen zurückgeführt werden, da auch die eng verwandten ß-Blocker ATL, MTL und PPL mitunter deutliche Unterschiede aufwiesen. Diese Ergebnisse verdeutlichen einmal mehr, dass keine allgemeingültige Antwort auf die Frage nach der toxikologischen Relevanz von TPs existiert. Es kann aber davon ausgegangen werden, dass die Wahrscheinlichkeit einer Aktivitätsabnahme hoch ist, wenn die Muttersubstanz selbst eine vergleichsweise hohe Aktivität besitzt. An dieser Stelle muss jedoch dringend festgehalten werden, dass eine Aktivitätsabnahme auf Mischungsebene allein nicht ausreicht, um eine geringe Relevanz der entstandenen TPs zu belegen. Vielmehr kann erst von einem vernachlässigbaren Beitrag zur Gesamtwirkung ausgegangen werden, wenn die residuale Aktivität der Mischung nicht die prognostizierte alleinige Aktivität der Muttersubstanz überschreitet. Die gute Praxistauglichkeit dieses Bewertungskonzepts konnte an den Fallbeispielen QUT und THI hinreichend demonstriert werden. Es ist demnach mit relativ geringem Aufwand möglich, eine Abschwächung des Risikos für bekannte Aktivitäten der Muttersubstanz nachzuweisen. Am Beispiel von THI wurde aber ebenfalls deutlich, dass die Abschwächung einer bekannten Aktivität mit der Entstehung neuer Aktivitäten einhergehen könnte. Es ist somit stark in Frage zu stellen, ob die alleinige Fokussierung auf bekannte Aktivitäten der Muttersubstanz für eine sichere Bewertung von TPs ausreicht. Vielmehr sollte bei der Beurteilung von Transformationsprozessen immer mit der Entstehung neuer Gefahrenpotenziale gerechnet werden.

Die Simulation von Transformationsprozessen im Labor in Verbindung mit chemisch-analytischen und wirkungsbasierten Untersuchungsmethoden ist ein vielversprechender Ansatz für die Identifizierung von potenziell gefährlichen TPs. Mit geeigneten Biotestverfahren ist es mit geringem Aufwand möglich, die im Laufe des Transformationsprozesses entstandene Mischung hinsichtlich einer bestimmten Wirkung zu prüfen. Die Beispiele GAB, MTL, ATL und PPL zeigten, dass zur Verfügung stehende Biotestverfahren durchaus geeignet sind, um auch neu entstandene Aktivitäten auf Mischungsebene sichtbar zu machen. Ein obligatorisches Screening, welches eine repräsentative Auswahl der wichtigsten Aktivitäten abdeckt, könnte somit einen pragmatischen Ansatz für die Früherkennung neuer Gefahrenpotenziale darstellen. Die Simulation des Transformationsprozesses sollte hierfür idealerweise unter möglichst realistischen Bedingungen erfolgen, z.B. durch Verwendung von umweltnahen Matrices und Behandlungskonzentrationen. Es muss jedoch bei der Festlegung der Startkonzentration die limitierte Sensitivität der eingesetzten Biotestverfahren berücksichtigt werden, um falsch negative Untersuchungsergebnisse zu vermeiden. An den Beispielen GAB, QUET, THI und PPL konnte demonstriert werden, dass mit deutlich erhöhten Startkonzentrationen im Bereich von 50-100 mg/l auch ohne Anreicherungsschritt aussagekräftige Ergebnisse erzielt werden können, sofern ergänzende Daten zur Bestätigung der Konzentrationsunabhängigkeit zentraler Abbauwege vorliegen. Bei einer positiven Antwort im Biotest erscheint zudem eine nachgeschaltete Identifizierung von prioritären TPs sinnvoll. Dies kann in der Praxis jedoch häufig nur mit extrem hohem Aufwand realisiert werden. Die statistische Auswertung von Zeitverläufen („virtuelle EDA“) könnte in dieser Hinsicht einen vielversprechenden Lösungsansatz darstellen, dessen Potenzial es weiter zu erforschen gilt.

Die Strukturaufklärung mit anschließender Analyse von Struktur-Wirkungs-Beziehungen kann zusätzliche Hinweise für die Identifizierung prioritärer TPs liefern und ermöglicht das Knüpfen einer Verbindung zwischen den neu entstandenen Aktivitäten eines Reaktionsgemisches und den strukturellen Merkmalen darin enthaltener TPs. Es muss jedoch auch daran erinnert werden, dass die massenspektrometrische Strukturaufklärung häufig noch mit großen Unsicherheiten behaftet ist, wodurch die Anwendbarkeit strukturbasierter Vorhersagemodelle momentan noch stark eingeschränkt wird. Dennoch sollte mehr in die Entwicklung und Validierung von strukturbasierten Bewertungskonzepten investiert werden, um die Identifizierung prioritärer TPs vergleichbarer und effizienter zu gestalten. Langfristig könnte sogar der intelligente Einsatz von *in silico* Methoden, beispielsweise durch Kopplung von regelbasierten Modellen zur Vorhersage von Abbaupfaden und –produkten (z.B. EAWAG-BBD oder Meta-PC) mit toxikologischen Vorhersagemodellen, ein vorausschauendes Screening gänzlich ohne experimentelle Prüfungen ermöglichen.

6 Schlussfolgerungen und Ausblick

Die Präsenz von Arzneimittelrückständen in der Umwelt ist mit potenziellen Risiken für Mensch und Umwelt verknüpft, die in den aktuellen Regulierungsansätzen häufig nur unvollständige Berücksichtigung finden. Die Identifizierung prioritärer Arzneimittelrückstände ist eine wichtige Voraussetzung für die systematische Schließung bestehender Wissens- und Regulierungslücken. Im Folgenden sollen nochmals mögliche Lösungswege und darüber hinausgehende Erkenntnisse der zuvor beschriebenen Fallstudien zusammengefasst werden.

Die wenigen öffentlich zugänglichen Daten zum Arzneimitteleinsatz in der Nutztierhaltung deuten auf erhebliche Umwelteinträge hin, die eine Neubewertung bestehender Wirkstoffzulassungen notwendig erscheinen lassen. Der aktuelle Verordnungsvorschlag über Tierarzneimittel der Europäischen Kommission sieht unter bestimmten Voraussetzungen die Möglichkeit einer Neubewertung bestehender Zulassungen vor [48]. In diesem Zusammenhang könnte die vorgestellte Methodik zur retrospektiven Eintragsabschätzung ein effizientes Werkzeug für die Auswahl prioritärer Wirkstoffe darstellen, mit dessen Hilfe eine systematische Schließung bestehender Wissenslücken deutlich vereinfacht werden könnte. Gleichzeitig muss jedoch auch ein eklatanter Mangel an Transparenz im Umgang mit Verbrauchsdaten im tiermedizinischen Sektor bescheinigt werden, wodurch eine unabhängige Bewertung aktueller Risiken durch außenstehende Akteure nahezu unmöglich wird.

Arzneistoffgemische, die Antibiotika enthalten, könnten mikrobielle Lebensgemeinschaften in Kläranlagen und in der aquatischen Umwelt nachhaltig beeinflussen und damit auch zur Verbreitung von Antibiotikaresistenzen beitragen. Der komponentenbasierte Bewertungsansatz ermöglicht eine ausreichend präzise Abschätzung der kombinierten bakterientoxischen Wirkung und kann zudem wichtige Hinweise für die Identifizierung prioritärer Mischungsbestandteile liefern. So konnte am Beispiel der untersuchten Mischung gezeigt werden, dass die beobachtete Gesamtwirkung mit hoher Wahrscheinlichkeit auf nur wenige Vertreter der Fluorchinolon-Antibiotika zurückzuführen war. Die notwendige Grundlage für eine belastbare Einschätzung von Kombinationseffekten sind jedoch harmonisierte Einzelstoffdaten, die bisher leider nicht im benötigten Umfang zur Verfügung stehen. Deshalb sollte speziell für Antibiotika eine systematische Prüfung der Wirkung auf Umweltmikroorganismen durchgeführt werden. Dieser Lösungsansatz zur Beurteilung von Kombinationseffekten kann mit hoher Wahrscheinlichkeit auch auf andere problematische Wirkstoffgruppen übertragen werden, was generell für eine stärkere Berücksichtigung des pharmakologischen Wirkmechanismus in der ökotoxikologischen Prüfung von Arzneimittelwirkstoffen spricht.

Es existiert keine allgemeingültige Antwort auf die Frage nach der toxikologischen Relevanz von Transformationsprodukten. Die Ergebnisse der durchgeführten Fallstudien belegen aber eindeutig, dass photochemische Transformationsprozesse nicht nur zur Abschwächung bereits

vorhandener, sondern auch zur Entstehung gänzlich neuer Gefahrenpotenziale beitragen können. Es ist somit stark in Frage zu stellen, ob die alleinige Fokussierung auf bekannte Aktivitäten der Muttersubstanz für eine sichere Bewertung von TPs ausreicht. Diese Erkenntnis sollte Anlass genug sein, weiter an verbesserten Methoden zur vorausschauenden Identifizierung prioritärer TPs zu forschen. Die aktuell größten Herausforderungen auf diesem Gebiet sind das Etablieren einheitlicher Standards und die strategische Ausrichtung zukünftiger Forschungsaktivitäten. Langfristig sollte das gesammelte Wissen in die Weiterentwicklung von geeigneten *in silico* Methoden einfließen, um die Identifizierung prioritärer TPs vergleichbarer und effizienter zu gestalten.

Referenzen

[1] Rickwood, S., Kleinrock, M., Núñez-Gaviria, M. (2013). The global use of medicines: Outlook through 2017. IMS Institute for Healthcare Informatics, Parsippany.

[2] Aitken, M., Kleinrock, M., Lyle, M., Nass, D., Caskey, L. (2014). The global use of medicines: Outlook through 2018. IMS Institute for Healthcare Informatics, Parsippany.

[3] Schwabe, U., Paffrath, D. (Hrsg.) (2015). Arzneiverordnungs-Report 2015. Aktuelle Daten, Kosten, Trends und Kommentare. Springer, Berlin, Heidelberg.

[4] Mudgal, S., Toni, A. de, Lockwood, S., Salès, K., Backhaus, T., Halling-Sørensen, B. (2013). Study on the environmental risks of medicinal products. Final Report prepared for Executive Agency for Health and Consumers. BIO Intelligence Service, Paris.

[5] Tarazona, J. V., Escher, B. I., Giltrow, E., Sumpter, J., Knacker, T. (2010). Targeting the environmental risk assessment of pharmaceuticals: facts and fantasies. Integrated Environmental Assessment and Management 6 Suppl, 603–613.

[6] Ebert, I., Conradi, S., Hein, A., Amato, R. (2014). Arzneimittel in der Umwelt – vermeiden, reduzieren, überwachen. Umweltbundesamt, Dessau-Roßlau.

[7] Bundesamt für Verbraucherschutz und Lebensmittelsicherheit (2016). Menge der abgegebenen Antibiotika in der Tiermedizin halbiert. https://www.bvl.bund.de/DE/08_PresseInfothek/01_FuerJournalisten/01_Presse_und_Hintergrundinformationen/05_Tierarzneimittel/2016/2016_08_03_pi_Antibiotikaabgabemenge2015.html (letzter Zugriff am 22.1.2017).

[8] Jelic, A., Gros, M., Ginebreda, A., Cespedes-Sánchez, R., Ventura, F., Petrovic, M., Barcelo, D. (2011). Occurrence, partition and removal of pharmaceuticals in sewage water and sludge during wastewater treatment. Water Research 45, 1165–1176.

[9] Gros, M., Petrović, M., Ginebreda, A., Barceló, D. (2010). Removal of pharmaceuticals during wastewater treatment and environmental risk assessment using hazard indexes. Environment International 36, 15–26.

[10] Verlicchi, P., Al Aukidy, M., Zambello, E. (2012). Occurrence of pharmaceutical compounds in urban wastewater: removal, mass load and environmental risk after a secondary treatment – a review. Science of The Total Environment 429, 123–155.

[11] Daughton, C. G., Ternes, T. A. (1999). Pharmaceuticals and personal care products in the environment: agents of subtle change? Environmental Health Perspectives 107 Suppl 6, 907–938.

[12] Andreozzi, R., Raffaele, M., Nicklas, P. (2003). Pharmaceuticals in STP effluents and their solar photodegradation in aquatic environment. Chemosphere 50, 1319–1330.

[13] Ternes, T. A. (1998). Occurrence of drugs in German sewage treatment plants and rivers. Water Research 32, 3245–3260.

[14] Thiele-Bruhn, S. (2003). Pharmaceutical antibiotic compounds in soils – a review. Journal of Plant Nutrition and Soil Science 166, 145–167.

[15] Kümmerer, K. (2008). Pharmaceuticals in the Environment – A Brief Summary. In: Pharmaceuticals in the Environment: Sources, Fate, Effects and Risks. Kümmerer, K. (Hrsg.). Springer, Berlin, Heidelberg, 3–21.

[16] Längin, A., Schuster, A., Kümmerer, K. (2008). Chemicals in the environment – the need for a clear nomenclature: parent compounds, metabolites, transformation products and their elimination. CLEAN – Soil, Air, Water 36, 349–350.

[17] Packer, J. L., Werner, J. J., Latch, D. E., McNeill, K., Arnold, W. A. (2003). Photochemical fate of pharmaceuticals in the environment: naproxen, diclofenac, clofibric acid, and ibuprofen. Aquatic Sciences 65, 342–351.

[18] Kümmerer, K., Dionysiou, D. D., Fatta-Kassinos, D. (2016). Long-term strategies for tackling micropollutants. In: Advanced treatment technologies for urban wastewater reuse. Fatta-Kassinos, D., Dionysiou, D. D., Kümmerer, K. (Hrsg.). Springer International Publishing, Cham, 291–299.

[19] Trautwein, C., Berset, J.-D., Wolschke, H., Kümmerer, K. (2014). Occurrence of the antidiabetic drug Metformin and its ultimate transformation product Guanylurea in several compartments of the aquatic cycle. Environment International 70, 203–212.

[20] López-Serna, R., Petrović, M., Barceló, D. (2012). Occurrence and distribution of multi-class pharmaceuticals and their active metabolites and transformation products in the Ebro River basin (NE Spain). Science of The Total Environment 440, 280–289.

[21] López-Serna, R., Jurado, A., Vázquez-Suñé, E., Carrera, J., Petrović, M., Barceló, D. (2013). Occurrence of 95 pharmaceuticals and transformation products in urban groundwaters underlying the metropolis of Barcelona, Spain. Environmental Pollution 174, 305–315.

[22] Jongh, C. M. de, Kooij, P. J., Voogt, P. de, ter Laak, T. L. (2012). Screening and human health risk assessment of pharmaceuticals and their transformation products in Dutch surface waters and drinking water. Science of The Total Environment 427-428, 70–77.

[23] Heberer, T. (2002). Occurrence, fate, and removal of pharmaceutical residues in the aquatic environment: a review of recent research data. Toxicology Letters 131, 5–17.

[24] Bergmann, A., Fohrmann, R., Weber, F. (2011). Zusammenstellung von Monitoringdaten zu Umweltkonzentrationen von Arzneimitteln. Umweltbundesamt, Dessau-Roßlau.

[25] Aus der Beek, Tim, Weber, F.-A., Bergmann, A., Hickmann, S., Ebert, I., Hein, A., Küster, A. (2016). Pharmaceuticals in the environment – Global occurrences and perspectives. Environmental Toxicology and Chemistry 35, 823–835.

[26] Küster, A., Adler, N. (2014). Pharmaceuticals in the environment: scientific evidence of risks and its regulation. Philosophical Transactions of the Royal Society B: Biological Sciences 369, 20130587.

[27] Brooks, B. W., Huggett, D. B., Boxall, A. B. (2009). Pharmaceuticals and personal care products: research needs for the next decade. Environmental Toxicology and Chemistry 28, 2469–2472.

[28] Paltiel, O., Fedorova, G., Tadmor, G., Kleinstern, G., Maor, Y., Chefetz, B. (2016). Human exposure to wastewater-derived pharmaceuticals in fresh produce: a randomized controlled trial focusing on carbamazepine. Environmental Science & Technology 50, 4476–4482.

[29] World Health Organization (2012). Pharmaceuticals in drinking-water. World Health Organization, Genf.

[30] Martinez, J. L. (2008). Antibiotics and antibiotic resistance genes in natural environments. Science 321, 365–367.

[31] Bengtsson-Palme, J., Larsson, D. J. (2016). Concentrations of antibiotics predicted to select for resistant bacteria: proposed limits for environmental regulation. Environment International 86, 140–149.

[32] Kostich, M. S., Batt, A. L., Lazorchak, J. M. (2014). Concentrations of prioritized pharmaceuticals in effluents from 50 large wastewater treatment plants in the US and implications for risk estimation. Environmental Pollution 184, 354–359.

[33] Vasquez, M., Lambrianides, A., Schneider, M., Kümmerer, K., Fatta-Kassinos, D. (2014). Environmental side effects of pharmaceutical cocktails: What we know and what we should know. Journal of Hazardous Materials 279, 169–189.

[34] Kortenkamp, A., Backhaus, T., Faust, M. (2009). State of the art report on mixture toxicity. Final Report. Study Contract Number 070307/2007/485103/ETU/D.1. University of London.

[35] Backhaus, T. (2016). Environmental risk assessment of pharmaceutical mixtures: demands, gaps, and possible bridges. AAPS Journal 18, 804–813.

[36] Heys, K. A., Shore, R. F., Pereira, M. G., Jones, K. C., Martin, F. L. (2016). Risk assessment of environmental mixture effects. RSC Advances 6, 47844–47857.

[37] Evgenidou, E. N., Konstantinou, I. K., Lambropoulou, D. A. (2015). Occurrence and removal of transformation products of PPCPs and illicit drugs in wastewaters: a review. Science of The Total Environment 505, 905–926.

[38] Fatta-Kassinos, D., Vasquez, M., Kümmerer, K. (2011). Transformation products of pharmaceuticals in surface waters and wastewater formed during photolysis and advanced oxidation processes – degradation, elucidation of byproducts and assessment of their biological potency. Chemosphere 85, 693–709.

[39] DellaGreca, M., Brigante, M., Isidori, M., Nardelli, A., Previtera, L., Rubino, M., Temussi, F. (2003). Phototransformation and ecotoxicity of the drug Naproxen-Na. Environmental Chemistry Letters 1, 237–241.

[40] Escher, B. I., Fenner, K. (2011). Recent Advances in Environmental Risk Assessment of Transformation Products. Environmental Science & Technology 45, 3835–3847.

[41] Schulze, T., Weiss, S., Schymanski, E., von der Ohe, P., Schmitt-Jansen, M., Altenburger, R., Streck, G., Brack, W. (2010). Identification of a phytotoxic photo-transformation product of diclofenac using effect-directed analysis. Environmental pollution 158, 1461–1466.

[42] Halling-Sørensen, B., Sengeløv, G., Tjørnelund, J. (2002). Toxicity of tetracyclines and tetracycline degradation products to environmentally relevant bacteria, including selected tetracycline-resistant bacteria. Archives of environmental contamination and toxicology 42, 263–271.

[43] Rastogi, T., Leder, C., Kummerer, K. (2015). Re-designing of existing pharmaceuticals for environmental biodegradability: a tiered approach with beta-blocker propranolol as an example. Environmental Science & Technology 49, 11756–11763.

[44] European Medicines Agency (2008). Revised Guideline on Environmental Impact Assessment for Veterinary Medicinal Products. EMEA/CVMP/ERA/418282/2005-Rev.1.

[45] Winckler, C., Grafe, A. (2001). Use of veterinary drugs in intensive animal production. Journal of Soils and Sediments 1, 66–70.

[46] Kools, Stefan A E, Boxall, A., Moltmann, J. F., Bryning, G., Koschorreck, J., Knacker, T. (2008). A ranking of European veterinary medicines based on environmental risks. Integrated environmental assessment and management 4, 399–408.

[47] Haffmans, S. (2012). Tierarzneimittel und Umweltschutz. Pestizid Aktions-Netzwerk (PAN) e. V., Hamburg.

[48] Europäische Kommission (2014). Vorschlag für eine Verordnung des Europäischen Parlaments und des Rates über Tierarzneimittel, 2014/0257 (COD).

[49] Bund/Länderausschuss für Chemikaliensicherheit (2003). Arzneimittel in der Umwelt. Auswertung der Untersuchungsergebnisse, Hamburg.

[50] Schneidereit, M. (2004). Aktuelle Studie: Verbrauchsmengen von Tierarzneimitteln. UBA-Symposium – Arzneimittel in der Umwelt, 29.–30.09.2004, Berlin. http://www.bft-online.de/schwerpunktthemen/aktuelle-studie-verbrauchsmengen-von-tierarzneimitteln (letzter Zugriff am 22.1.2017).

[51] Klein-Goedicke, J. (2005). Arzneimitteleinsatz in der intensiven Tierhaltung. In: Arzneimittel in der Umwelt - Zu Risiken und Nebenwirkungen fragen Sie das Umweltbundesamt. Umweltbundesamt, Dessau-Roßlau.

[52] BVL (Bundesamt für Verbraucherschutz und Lebensmittelsicherheit). Tierarzneimittel-Abgabemengen-Register. http://www.bvl.bund.de/DE/05_Tierarzneimittel/01_Aufgaben/04_UeberwachungBetreuung/06_tam_TAM_Abgabemengen_Register/tam_TAM_Abgabemengen_Register_node.html (letzter Zugriff am 22.1.2017).

[53] Schneichel, R. (2014). Antibiotika im Visier. Veterinär Spiegel 24, 27–29.

[54] Benning, R. (2016). Reserveantibiotika in der Milcherzeugung in Deutschland. Weniger Hochleistung - eine Gesundheit für Alle. Germanwatch e.V., Bonn.

[55] Robanus, M. (2011). Antibiotika-Verbrauchsmengenerfassung bei landwirtschaftlichen Nutztieren in ausgewählten Betrieben und Tierarztpraxen in Niedersachsen und Nordrhein-Westfalen unter Berücksichtigung pharmakologischer Parameter. Inaugural-Dissertation. Universität Leipzig.

[56] Merle, R., Hajek, P., Kasbohrer, A., Hegger-Gravenhorst, C., Mollenhauer, Y., Robanus, M., Ungemach, F.-R., Kreienbrock, L. (2012). Monitoring of antibiotic consumption in livestock: a german feasibility study. Preventive Veterinary Medicine 104, 34–43.

[57] Niedersächsisches Landesamt für Verbraucherschutz und Lebensmittelsicherheit (2011). Bericht über den Antibiotikaeinsatz in der landwirtschaftlichen Nutztierhaltung in Niedersachsen. Niedersächsisches Ministerium für Ernährung, Landwirtschaft und Verbraucherschutz, Hannover.

[58] Bundschuh, M., Hahn, T., Ehrlich, B., Höltge, S., Kreuzig, R., Schulz, R. (2016). Acute toxicity and environmental risks of five veterinary pharmaceuticals for aquatic macroinvertebrates. Bulletin of Environmental Contamination and Toxicology 96, 139–143.

[59] Biswas, S., Shapiro, C. A., Kranz, W. L., Mader, T. L., Shelton, D. P., Snow, D. D., Bartelt-Hunt, S. L., Tarkalson, D. D., van Donk, S. J., Zhang, T. C., Ensley, S. (2013). Current knowledge on the environmental fate, potential impact, and management of growth-promoting steroids used in the US beef cattle industry. Journal of Soil and Water Conservation 68, 325–336.

[60] Fatta-Kassinos, D., Meric, S., Nikolaou, A. (2011). Pharmaceutical residues in environmental waters and wastewater: current state of knowledge and future research. Analytical and Bioanalytical Chemistry 399, 251–275.

[61] Roberts, P. H., Thomas, K. V. (2006). The occurrence of selected pharmaceuticals in wastewater effluent and surface waters of the lower Tyne catchment. Science of The Total Environment 356, 143–153.

[62] Barra Caracciolo, A., Topp, E., Grenni, P. (2015). Pharmaceuticals in the environment: biodegradation and effects on natural microbial communities. A review. Journal of Pharmaceutical and Biomedical Analysis 106, 25–36.

[63] Kraigher, B., Kosjek, T., Heath, E., Kompare, B., Mandic-Mulec, I. (2008). Influence of pharmaceutical residues on the structure of activated sludge bacterial communities in wastewater treatment bioreactors. Water Research 42, 4578–4588.

[64] Wang, S., Gunsch, C. K. (2011). Effects of selected pharmaceutically active compounds on treatment performance in sequencing batch reactors mimicking wastewater treatment plants operations. Water Research 45, 3398–3406.

[65] Lawrence, J. R., Swerhone, G. D., Wassenaar, L. I., Neu, T. R. (2005). Effects of selected pharmaceuticals on riverine biofilm communities. Canadian Journal of Microbiology 51, 655–669.

[66] Corcoll, N., Acuña, V., Barceló, D., Casellas, M., Guasch, H., Huerta, B., Petrovic, M., Ponsatí, L., Rodríguez-Mozaz, S., Sabater, S. (2014). Pollution-induced community tolerance to non-steroidal anti-inflammatory drugs (NSAIDs) in fluvial biofilm communities affected by WWTP effluents. Chemosphere 112, 185–193.

[67] Veach, A., Bernot, M. J., Mitchell, J. K. (2012). The influence of six pharmaceuticals on freshwater sediment microbial growth incubated at different temperatures and UV exposures. Biodegradation 23, 497–507.

[68] Wilson, B. A., Smith, V. H., deNoyelles, F., Larive, C. K. (2003). Effects of three pharmaceutical and personal care products on natural freshwater algal assemblages. Environmental Science & Technology 37, 1713–1719.

[69] Kümmerer, K. (2009). Antibiotics in the aquatic environment – A review – Part I. Chemosphere 75, 417–434.

[70] Rizzo, L., Manaia, C., Merlin, C., Schwartz, T., Dagot, C., Ploy, M., Michael, I., Fatta-Kassinos, D. (2013). Urban wastewater treatment plants as hotspots for antibiotic resistant bacteria and genes spread into the environment: A review. Science of The Total Environment 447, 345–360.

[71] Kümmerer, K., Henninger, A. (2003). Promoting resistance by the emission of antibiotics from hospitals and households into effluent. Clinical microbiology and infection 9, 1203–1214.

[72] Goñi-Urriza, M., Capdepuy, M., Arpin, C., Raymond, N., Caumette, P., Quentin, C. (2000). Impact of an urban effluent on antibiotic resistance of riverine Enterobacteriaceae and Aeromonas spp. Applied and Environmental Microbiology 66, 125–132.

[73] Brandt, K. K., Amézquita, A., Backhaus, T., Boxall, A., Coors, A., Heberer, T., Lawrence, J. R., Lazorchak, J., Schönfeld, J., Snape, J. R., Zhu, Y.-G., Topp, E. (2015). Ecotoxicological assessment of antibiotics: a call for improved consideration of microorganisms. Environment International 85, 189–205.

[74] European Medicines Agency (2006). Guideline on the environmental risk assessment of medicinal products for human use. EMEA/CHMP/SWP/4447/00.

[75] Backhaus, T., Faust, M. (2012). Predictive environmental risk assessment of chemical mixtures: a conceptual framework. Environmental Science & Technology 46, 2564–2573.

[76] Backhaus, T., Karlsson, M. (2014). Screening level mixture risk assessment of pharmaceuticals in STP effluents. Water Research 49, 157–165.

[77] Wadhia, K. (2013). Microbial Assay for Risk Assessment (MARA). In: Férard, J.-F., Blaise, C. (Hrsg.), Encyclopedia of Aquatic Ecotoxicology. Springer Netherlands, Dordrecht, 699–708.

[78] Kosjek, T., Heath, E. (2008). Applications of mass spectrometry to identifying pharmaceutical transformation products in water treatment. TrAC Trends in Analytical Chemistry 27, 807–820.

[79] Zwiener, C. (2007). Occurrence and analysis of pharmaceuticals and their transformation products in drinking water treatment. Analytical and Bioanalytical Chemistry 387, 1159–1162.

[80] Fenner, K., Kooijman, C., Scheringer, M., Hungerbühler, K. (2002). Including transformation products into the risk assessment for chemicals: the case of nonylphenol ethoxylate usage in switzerland. Environmental Science & Technology 36, 1147–1154.

[81] Schmitt-Jansen, M., Bartels, P., Adler, N., Altenburger, R. (2007). Phytotoxicity assessment of diclofenac and its phototransformation products. Analytical and Bioanalytical Chemistry 387, 1389–1396.

[82] Toolaram, A. P., Kümmerer, K., Schneider, M. (2014). Environmental risk assessment of anti-cancer drugs and their transformation products: a focus on their genotoxicity characterization-state of knowledge and short comings. Mutation Research/Reviews in Mutation Research 760, 18–35.

[83] Zonja, B., Aceña, J., Jelic, A., Petrovic, M., Pérez Solsona, S., Barceló, D. (2014). Transformation Products of Emerging Contaminants: Analytical Challenges and Future Needs. In: Transformation Products of Emerging Contaminants in the Environment. Lambropoulou, D. A., Nollet, L. M. L. (Hrsg.). John Wiley and Sons Ltd, Chichester, 303–324.

[84] Brack, W. (2003). Effect-directed analysis: a promising tool for the identification of organic toxicants in complex mixtures? Analytical and Bioanalytical Chemistry 377, 397–407.

[85] Hug, C., Sievers, M., Ottermanns, R., Hollert, H., Brack, W., Krauss, M. (2015). Linking mutagenic activity to micropollutant concentrations in wastewater samples by partial least square regression and subsequent identification of variables. Chemosphere 138, 176–182.

[86] Rastogi, T., Leder, C., Kümmerer, K. (2014). Qualitative environmental risk assessment of photolytic transformation products of iodinated X-ray contrast agent diatrizoic acid. Science of The Total Environment 482-483, 378–388.

Danksagung

Ein riesiges Dankeschön gilt meiner Familie, die mich immer uneingeschränkt unterstützt hat und mir das Studium der Biologie mit anschließender Promotion ermöglichte. Insbesondere meinen Eltern und Großeltern, meiner Schwester Jessica und meinem Onkel Konrad möchte ich hierfür danken.

Besonderer Dank gilt meiner Partnerin Prisca, die mich stets mit ganzer Kraft unterstützte und auch in schwierigen Zeiten immer zu mir gehalten hat.

Ich danke Prof. Kümmerer für das Ermöglichen dieser Arbeit, das ungebrochene Vertrauen in meine Person und die langjährige Förderung meines Werdegangs.

Ich danke Prof. Floeter und Prof. Hamscher für die freundliche Bereitschaft zur Erstellung der Gutachten.

Ich danke der Teilmaßnahme 1.4 des Innovations-Inkubator Lüneburg für die großzügige finanzielle und ideelle Förderung.

Mein besonderer Dank gilt zudem:

Mandy Schneider, Oliver Olsson, Christoph Leder und Annette Haiß, die mir mit der intensiven fachlichen Betreuung und den vielseitigen Denkanstößen sehr bei der Erstellung dieser Arbeit geholfen haben.

Manuel Herrmann und Marco Reich für die tolle Zusammenarbeit und den vielen großartigen Momenten der Freundschaft.

Anju Toolaram, Birte Hensen, Carlos Lutterbeck, Christoph Trautwein, Claudia Kurtz, Dagmar Schuchardt, Dieter Vollert, Elisa Grabitz, Evgenia Logunova, Ewelina Baginska, Franziska Jentzsch, Isabell Zunker, Janin Westphal, Jens Robertson, Karen Kratschmer, Lamia Mahouachi, Lukasz Gutowski, Marcelo Wilde, Matthias Gaßmann, Morten Suk, Nareman Khaleel, Richard Bolek, Stefanie Hinz, Stefanie Wieck, Tarek Haddad, Tushar Rastogi, Waleed Ahmed und Wolf-Ulrich Palm für die fortwährende Hilfsbereitschaft, das ausgesprochen kollegiale Arbeitsklima und die tolle gemeinsame Zeit.

Den Studierenden Julia Müller, Laura Müller und Stephanie Gottschalk für die tolle Mitarbeit im Labor.

Allen Mitgliedern des Instituts für Nachhaltige Chemie und Umweltchemie für die große allgemeine Hilfsbereitschaft und das durchweg nette Arbeitsklima.

Anhang: Veröffentlichungen zur kumulativen Dissertation

Publikation 1: Menz, J., Schneider, M., Kümmerer, K. (2015). Usage pattern-based exposure screening as a simple tool for the regional priority-setting in environmental risk assessment of veterinary antibiotics: A case study of northwestern Germany. *Chemosphere* 127, 42-48.

Publikation 2: Menz, J., Baginska, E., Arrhenius, A., Haiβ, A., Backhaus, T., Kümmerer, K. (2017). Antimicrobial activity of pharmaceutical cocktails in sewage treatment plant effluent - An experimental and predictive approach to mixture risk assessment. *Environmental Pollution* 231, 1507-1517.

Publikation 3: Herrmann, M., Menz, J., Olsson, O., Kümmerer, K. (2015). Identification of phototransformation products of the antiepileptic drug gabapentin: Biodegradability and initial assessment of toxicity. *Water Research* 85, 11-21.

Publikation 4: Herrmann, M., Menz, J., Gassmann, M., Olsson, O., Kümmerer, K. (2016). Experimental and in silico assessment of fate and effects of the antipsychotic drug quetiapine and its bio- and phototransformation products in aquatic environments. *Environmental Pollution* 218, 66-76.

Publikation 5: Wilde, M. L., Menz, J., Trautwein, C., Leder, C., Kümmerer, K. (2016). Environmental fate and effect assessment of thioridazine and its transformation products formed by photodegradation. *Environmental Pollution* 213, 658-670.

Publikation 6: Toolaram, A., Menz, J., Rastogi, T., Leder, C., Schneider, M., Kümmerer, K. (2017). Hazard screening of photo-transformation products from pharmaceuticals: application to selective β1-blockers Atenolol and Metoprolol. *Science of The Total Environment* 571, 1769-1780.

Publikation 7: Menz, J., Toolaram, A., Leder, C., Olsson, O., Kümmerer, K., Schneider, M. (2017). Transformation products in the water cycle and the unsolved problem of their proactive assessment: a combined in vitro/in silico approach. *Environment International* 98, 171-180.

Nachdruck mit freundlicher Genehmigung des Elsevier Verlags

Tabelle A1: Autoren- und Publikationsstatus der Veröffentlichungen.

Publikation	Autorenstatus / Erklärung zur Autorenschaft	Gewichtung	Publikationsstatus	Konferenzbeiträge
1	**Mit-Autorenschaft mit überwiegendem Anteil** Konzeption des Forschungsansatzes, Entwicklung von Forschungsmethoden, Erhebung und Aufbereitung von Daten, Analyse/Interpretation von Daten, Schreiben des Manuskripts	1	Chemosphere 127, 42-48 IF= 3,698 (2015)*	Menz, J., Müller, J., Munck, M., Gottschalk, S., Kümmerer, K. (2015). Prioritization of veterinary antibiotics for environmental analysis using a simple screening approach. SETAC Europe 25th Annual Meeting, 3.–7. Mai 2015, Barcelona. Menz, J., Schneider, M., Olsson, O., Kümmerer K. (2015). Veterinärantibiotika in der Umwelt - Abschätzung von Eintragsmengen auf der Basis von Verbrauchsdaten. BfR-Symposium Antibiotikaresistenz in der Lebensmittelkette, 2.–3. November 2015, Berlin.
2	**Mit-Autorenschaft mit gleichem Anteil** Konzeption des Forschungsansatzes, Entwicklung von Forschungsmethoden, Erhebung und Aufbereitung von Daten, Analyse/Interpretation von Daten, Schreiben des Manuskripts	1	Environmental Pollution 231, 1507-1517 IF= 4,839 (2015)*	
3	**Mit-Autorenschaft mit wichtigem Anteil** Erhebung und Aufbereitung von Daten, Durchführung der Forschung, Analyse/Interpretation von Daten, Schreiben des Manuskripts	0,5	Water Research 85, 11-21 IF= 5,991 (2015)*	

*Impact Factor (IF), Thomson Reuters Journal Citation Reports 2017

Tabelle A1: Autoren- und Publikationsstatus der Veröffentlichungen (Fortsetzung).

Publikation	Autorenstatus / Erklärung zur Autorenschaft	Gewichtung	Publikationsstatus	Konferenzbeiträge
4	**Mit-Autorenschaft mit wichtigem Anteil** Erhebung und Aufbereitung von Daten, Analyse/Interpretation von Daten, Schreiben des Manuskripts	0,5	Environmental Pollution 218, 66-76 IF= 4,839 (2015)*	
5	**Mit-Autorenschaft mit wichtigem Anteil** Erhebung und Aufbereitung von Daten, Analyse/Interpretation von Daten, Schreiben des Manuskripts	0,5	Environmental Pollution 218, 66-76 IF= 4,839 (2015)*	Menz, J., Trautwein, C., Wilde, M.L., Schneider, M., Kümmerer, K. (2014). Initial microbial ecotoxicity assessment of Thioridazine, Thioridazine 5-Sulfoxide and photolytic mixtures of Thioridazine. SETAC Europe 24th Annual Meeting. 11.–15. Mai 2014, Basel.
6	**Mit-Autorenschaft mit gleichem Anteil** Konzeption des Forschungsansatzes, Entwicklung von Forschungsmethoden, Erhebung und Aufbereitung von Daten, Analyse/Interpretation von Daten, inhaltliche Überarbeitung des Manuskripts	1	Science of The Total Environment 571, 1769-1780. IF= 3,976 (2015)*	Schneider, M., Toolaram, A., Menz, J., Rastogi, T., Kümmerer, K. (2014). Genotoxicity and ecotoxicity screening of photolytic mixtures from the selective β1-receptor blockers Atenolol and Metoprolol. SETAC Europe 24th Annual Meeting. 11.–15. Mai 2014, Basel.
7	**Mit-Autorenschaft mit überwiegendem Anteil** Konzeption des Forschungsansatzes, Entwicklung von Forschungsmethoden, Erhebung und Aufbereitung von Daten, Analyse/Interpretation von Daten, Schreiben des Manuskripts	1	Environment International 98, 171-180 IF= 5,929 (2015)*	Menz, J., Rastogi, T., Leder, C., Schneider, M., Kümmerer, K. (2013). First-time application of a modified luminescent bacteria test for the initial ecotoxicity assessment of beta-blockers after phototransformation. SETAC North America 34th Annual Meeting. 17.–21. November 2013, Nashville, Tennessee.

*Impact Factor (IF), Thomson Reuters Journal Citation Reports 2017

Publikation 1

Usage pattern-based exposure screening as a simple tool for the regional priority-setting in environmental risk assessment of veterinary antibiotics: A case study of northwestern Germany

Menz, J., Schneider, M., Kümmerer, K.

(2015)

Chemosphere 127, 42-48

DOI: 10.1016/j.chemosphere.2014.12.091

Chemosphere 127 (2015) 42–48

Contents lists available at ScienceDirect

Chemosphere

journal homepage: www.elsevier.com/locate/chemosphere

Usage pattern-based exposure screening as a simple tool for the regional priority-setting in environmental risk assessment of veterinary antibiotics: A case study of north-western Germany

J. Menz, M. Schneider, K. Kümmerer *

Institute of Sustainable and Environmental Chemistry, Leuphana University Lüneburg, Scharnhorststraße 1/C13, 21335 Lüneburg, Germany

HIGHLIGHTS

- Usage pattern-based exposure screening of veterinary antibiotics in soil.
- A case study based on approximated scenarios for north-western Germany.
- Predicted manure concentrations provide a strong basis for soil exposure modeling.
- 14 Antibiotics exceeded soil concentrations of 100 μg kg^{-1} in the worst-case scenario.
- A new approach for priority-setting in environmental risk assessment is proposed.

ARTICLE INFO

Article history:
Received 26 September 2014
Received in revised form 17 December 2014
Accepted 28 December 2014
Available online 2 February 2015

Handling Editor: I. Cousins

Keywords:
Veterinary pharmaceuticals
Antimicrobials
Environment
Exposure
Assessment
Risk

ABSTRACT

Veterinary antibiotics (VAs) are widely recognized as important environmental contaminants. Despite the extensive use of antibiotic agents in meat and poultry production and the known resistance problems in human and veterinary medicine, detailed knowledge about usage patterns of VAs in Germany is still scarce. This lack of knowledge severely impacts current research on the environmental risk of VAs, but it is expected that recently established surveillance programs for antimicrobial drug usage will close this knowledge gap. Therefore, a spatially more precise environmental risk assessment and management might become possible in the near future. In this study, a new usage pattern-based exposure screening (UPES) approach for the comprehensive environmental exposure assessment of veterinary antibiotics was preliminarily assessed using approximated scenarios of antimicrobial substance usage in German meat and poultry production. Resulting predicted manure concentrations covered seven orders of magnitude ranging from ng kg^{-1} to g kg^{-1} dry weight (dw). Beyond that 14 antibiotic substances of 10 different antimicrobial classes were predicted to have the potential to occur in soil concentrations higher than 100 μg kg^{-1} dw. These findings raise further questions regarding the environmental exposure and risks of frequently used VAs, especially in regions with higher-than-average livestock density. With this case study we demonstrate that UPES simplifies to account for differing local agricultural factors and therefore facilitates priority-setting on a regional level. In this context a simple prioritization scheme for environmental assessment of VAs, considering both the expected environmental concentration and the frequency of application, is proposed in this paper.

1. Introduction

Antibiotics are used in greater quantities in healthy food producing animals than in the treatment of disease in human patients (World Health Organization, 2012). In Germany, the amount of consumed antibiotics in veterinary medicine is 2–3 times higher than the amount currently used for the treatment of humans (UBA, 2014). The use of antibiotic agents has become an integral part of large-scale livestock farming and contributes significantly to the high efficiency and productivity of this agricultural sector. However, the adverse effects caused by the extensive consumption of antimicrobial agents in animal husbandry have attracted growing attention over the past decades. In fact, there is increasing evidence that intensive antibiotic treatment of livestock facilitates the emergence and spread of antibiotic–resistant bacteria and that intensively treated food animals

* Corresponding author. Tel.: +49 4131 677 2893; fax: +49 4131 677 2894.
E-mail addresses: jakob.menz@leuphana.de (J. Menz), mandy.schneider@leuphana.de (M. Schneider), klaus.kuemmerer@uni.leuphana.de (K. Kümmerer).

http://dx.doi.org/10.1016/j.chemosphere.2014.12.091
0045-6535/

play a fundamental role as reservoirs of resistant human pathogens (Aarestrup, 1999; Teuber, 2001; Smith et al., 2002; Angulo et al., 2004; World Health Organization, 2012). Further, veterinary antibiotics (VAs) are widely recognized as important environmental contaminants (Kemper, 2008; Martinez, 2009) and were frequently detected in the environment throughout the last years (Thiele-Bruhn, 2003; Küster et al., 2013). Many antibiotics used in meat and poultry production undergo incomplete resorption and metabolism leading to a large fraction of the originally applied substances being excreted as active parent compound or as metabolites in urine or feces (Addison, 1984; Sarmah et al., 2006; Kemper, 2008). Therefore, mixtures of antimicrobially active substances enter the terrestrial environment via land application of contaminated manure and might impact environmental microbiota (Kumar et al., 2005; Martinez, 2009).

Before any new veterinary pharmaceutical product can obtain marketing authorization, its efficacy, quality and safety to public health as well as to the environment must to be thoroughly evaluated by the competent authorities (Koschorreck et al., 2002). In this context the European Medicines Agency (EMA) provides a guidance document on the environmental risk assessment for veterinary medicinal products (EMEA/CVMP/055/96). This guidance represents a tiered procedure that includes an environmental exposure assessment as a first stage (phase I). The outcome of phase I, the predicted environmental concentration (PEC), will decide whether a detailed environmental assessment (phase II) is required. The so-called trigger value for phase II assessments is defined as 100 $\mu g\ kg^{-1}$ (soil) and 1 $\mu g\ L^{-1}$ (aquatic environment), respectively. However, the majority of VAs currently used in Germany was approved for market before 1998, when the EMA guidance on Environmental Risk Assessment for Veterinary Medicinal Products (EMEA/CVMP/055/96) came into force (Winckler and Grafe, 2000). This means that most of the commonly used VAs in Germany belong to the category "existing medicinal product" and did not undergo a stringent environmental risk assessment procedure even though the expected environmental concentration in soil might exceed the authoritative trigger value of 100 $\mu g\ kg^{-1}$ for phase II fate and effect assessments. Moreover, environmental risk assessment (ERA) within new market applications usually is conducted under the assumption that the used daily dose (UDD) is identical to the defined animal daily dose (ADD) given by the product's Summary of Product Characteristics (SPC). However, it was recently demonstrated that ADD and UDD can differ significantly (Merle et al., 2014), which means that prospective environmental exposure considerations may not necessarily reflect the real situation. In addition, prospective estimations are usually conducted on a non-standardized case by case basis, using vague assumptions regarding the application frequency and the fraction of animals treated within a population. This means that a comparison in terms of priority-setting between different active compounds based on independent prospective estimations is difficult. Therefore, a comprehensive and homogeneous retrospective assessment of the possible environmental impact of all VAs on the market, applying up-to-date usage data, is highly necessary.

Despite the widespread use of antibiotic agents in food-producing animals and the possible risk to human health and the environment, antibiotic consumption patterns in livestock farming are still poorly characterized (Winckler and Grafe, 2000; Sarmah et al., 2006; Landers et al., 2012). It is expected for most countries in the coming years that knowledge about antimicrobial use will be limited to national total sales data (Bondt et al., 2013). Until recently, veterinarians in Germany were allowed to dispense drugs directly to the farmers without any further reporting to a central database, which severely complicated the monitoring of VA usage (LANUV, 2007; Merle et al., 2012). A first step towards more sophisticated consumption surveillance was realized with the European Surveillance of Veterinary Antimicrobial Consumption (ESVAC) project, which was initiated by the European Medicines Agency (EMA) in 2009 and implemented in Germany by the Federal Office of Consumer Protection and Food Safety (BVL) in 2011. As a result, information about the total sales volume of veterinary antibiotics in Germany was available for the first time, revealing a nationwide consumption of veterinary antimicrobial agents of 1.706 t for the year 2011, 1.619 t for the year 2012 and 1.452 t for the year 2013 (BVL, 2014). Unfortunately, consumption data was not collected and categorized yet by animal species, farming type and weight class, which severely limits the informative value. As for the time being, knowledge about usage patterns of VAs in Germany is limited to sporadic pilot studies with a regional scope that can give only a fragmented picture of the overall situation. This lack of crucial knowledge severely hampers the retrospective evaluation of the potential environmental impact of these compounds. However, it can be expected that knowledge about region and farming type-specific consumption of VAs will improve in future, because the supervisory powers of the state agencies were recently strengthened with the enforcement of the 16th amendment of the Pharmaceutical Products Act (AMG).

In this study, a new usage pattern-based exposure screening (UPES) approach for the comprehensive lower-tier environmental exposure assessment of VAs was developed and exemplarily applied to the region of north-western Germany. Moreover, the applicability of recently established surveillance variables for VA consumption to the existing exposure assessment models was evaluated using approximated usage scenarios. Beyond that, a more integrated scheme for the prioritization of antibiotic substances for higher-tier environmental risk assessment, considering both the expected environmental concentration and the frequency of application, is proposed in this paper.

2. Material and methods

2.1. Dataset description

Antibiotic consumption patterns were approximated by combining datasets from different references. Numbers on administered amounts of active ingredient and the respective dosing were adopted from references related to the feasibility study VetCab, which investigated antibiotic applications to farm animals in north-western Germany from September 2006 to August 2007. A more detailed description of the VetCab study design and outcome can be found elsewhere (Robanus, 2011; Hegger-Gravenhorst, 2012; Merle et al., 2012; Merle et al., 2014). The numbers of applied daily doses were adopted from another surveillance program that was initiated by the Lower Saxony State Office for Consumer Protection and Food Safety (LAVES) in 2010. In this study, the total number of antibiotic applications was investigated for different types of farming, using the same electronic database that was established within the VetCab study (LAVES, 2011).

2.2. Estimation of relative application frequencies

Relative frequencies of antibiotic substance application were approximated for different animal species (poultry, pig, cattle) on the basis of applied substance amounts and average UDDs according to VetCab (see Section 2.1). If no UDD was reported in the above-mentioned reference, the ADD according to publicly available literature (e.g. DANMAP 2012, 2013) was applied instead. The theoretical amount of treated animal biomass (*B_treat*) per antibiotic substance (i) and year was estimated for each investigated animal species (j) according to formula (1).

$$B\_treat_{ij} = m_{ij}/DD_{ij} \quad (1)$$

B_treat_{ij}, treated animal biomass per antibiotic substance i, animal species j and year in kg a^{-1}.
m_{ij}, consumption of the antibiotic substance i by animal species j in mg a^{-1}.
DD_{ij}, UDD or ADD for the main indication and administration route of the antibiotic substance i and animal species j in mg kg^{-1}.

B was used for the calculation of the relative application frequency (F) according to formula (2) and (3).

$$B\_tot_j = \sum_{i=1}^{n} B\_treat_{ij} \quad (2)$$

B_tot_j, total amount of theoretically treated biomass per animal species j in kg a^{-1}.

$$F_{ij} = B\_treat_{ij}/B\_tot_j \quad (3)$$

Fij, relative application frequency of the antibiotic substance i and animal species j.

A complete list of applied *DDs* and resulting relative application frequencies for all active ingredients used for the three investigated species in significant amounts is given in the supplementary material (Table S1).

2.3. Prediction of potential antibiotic substance concentration in manure

The concentration of each consumed antibiotic agent in manure was predicted for manure from different representative livestock categories (broiler, fattening pig and fattening calf). First, the number of applied daily doses per substance, animal and year (*n_DD*) was estimated for each investigated antibiotic agent and livestock category (formula 4).

$$n\_DD_{ij} = n\_treat_j * n\_cyle_j * F_{ij} \quad (4)$$

n_DD_{ij}, theoretically applied number of daily doses per animal and year.
n_treat_j, total number of treatments per animal and production cycle.
n_cyle_j, number of production cycles per year.
F_{ij}, relative application frequency.

Calculation of *n_DD* was conducted for two different scenarios, based on surveillance data of the LAVES report (LAVES, 2011). In the average scenario (A) the average number of reported antibiotic treatments per production cycle was applied as default value. In the worst-case scenario (WC) the highest observed number of antibiotic treatments was used. Applied default values for the calculation of *n_DD* are provided in the supplementary material (Table S2).

The potential concentration of antibiotic substance in manure was calculated on the basis of the total residue approach, using the previously estimated *n_DD*, as well as livestock-specific bodyweights and nitrogen production standards (formula 5).

$$PEC\_manure\ N_{ij} = n\_DD_{ij} * DD_{ij} * \overline{m_j}/N\_excreted_j \quad (5)$$

PEC_manure N_{ij}, predicted amount of substance in manure per kg excreted nitrogen in mg kg^{-1} N.
DD_{ij}, daily dose in mg kg^{-1}.
$\overline{m_j}$, animal bodyweight in kg.
$N\_excreted_j$, nitrogen production per animal and year in kg N.

Before the calculation of initial antibiotic concentrations in soil, the *PEC_manure N* was subjected to a qualitative evaluation by comparing predicted manure concentrations to monitoring data from published literature. This required conversion of the nitrogen-based *PEC_manure N* into a concentration by manure dry weight (*PEC_manure dw*) using average nitrogen and dry-matter contents from literature (formula 6).

$$PEC\_manure\ dw_{ij} = PEC\_manure\ N_{ij} * N\_manure_j/dm\_manure_j \quad (6)$$

PEC_manure dw_{ij}, predicted amount of substance in manure by dry weight in mg t^{-1} dw.
N_manure_j, average nitrogen content in kg N t^{-1} or kg N m^{3-1}.
dm_manure_j, average dry-matter content.

Applied default values for the calculation of *PEC_manure N* and *PEC_manure dw* are provided in the supplementary material (Table S3).

2.4. Prediction of initial antibiotic substance concentration in soil

Initial concentrations in soil (*PEC_soil initial*) were estimated in compliance with phase I of the EMA's revised Guideline on Environmental Impact Assessment for Veterinary Medicinal Products (European Medicines Agency, 2008). Assuming a single manure application event per year, *PEC_soil initial* calculations (formula 7) were conducted for both, the average (A) and the worst-case (WC) scenario, to provide the required margin of safety for a lower-tier ERA.

$$PEC\_soil\ initial_{ij} = PEC\_manure\ N_{ij} * N\_max/(D\_soil * CONV\_area * DEPTH\_field) \quad (7)$$

PEC_soil initial$_{ij}$, predicted substance concentration in soil in mg kg^{-1} dw.
N_max, annual nitrogen immission standard in kg N ha^{-1}.
D_soil, bulk density of soil in kg m^{-3}.
CONV_area, conversion factor for the area of the agricultural field in m^2 ha^{-1}.
DEPTH_field, mixing depth with soil in m.

Contrary to standard manure application, poultry manure is not spread as a slurry onto the land but is usually applied during tillage. Therefore, the *PEC_soil initial* after application of chicken manure was only calculated for arable land (i.e. *DEPTH_field* = 20 cm), but not for grassland (i.e. *DEPTH_field* = 5 cm). Applied default values for the calculation of *PEC_soil initial* are provided in the supplementary material (Table S4).

3. Results and discussions

3.1. Prediction of antibiotic substance concentrations in manure

According to the VetCab data, 45 active substances from 12 antibiotic classes were applied in significant amounts and therefore can potentially occur in the manure of respective animals. Predicted manure concentrations for these active substances covered seven orders of magnitude ranging from ng kg^{-1} dw to g kg^{-1} dw, depending on the substance usage pattern and the applied scenario (Tables S6 and S7). Within the average scenario (A), the highest predicted antibiotic concentration was estimated for Chlortetracycline in cattle manure (0.67 g kg^{-1} dw). Application of the worst-case scenario (WC) resulted in a maximum concentration of 1.8 g kg^{-1} dw for Tetracycline in pig manure. Beyond that, Amoxicillin, Sulfadiazine, Trimethoprim, Tylosin, Colistin, Benzylpenicillin–Procaine and Oxytetracycline were predicted to have the potential to occur in noticeably high manure concentrations (>100 mg kg^{-1} dw).

3.2. Evaluation of predicted manure concentrations

Measured concentrations in manure from German and Austrian livestock were extracted from published literature and the highest reported concentrations were compared to the corresponding predicted manure concentrations to evaluate if the applied scenarios (A, WC) provide plausible results and a sufficient margin of safety to be used in a conservative screening approach. In total, 17 measured peak concentrations from literature covering three different manure species (chicken, pig, cattle) and 11 different antibiotic substances were available for a qualitative evaluation. A summary of measured peak concentrations used for the evaluation of predicted manure concentrations is presented in Table S5. Regarding the average scenario (A), an underestimation of the highest reported measured concentration was observed in 11 of 17 value pairs, but in 13 of 17 cases predicted and measured concentrations were within the same order of magnitude (Fig. 1). The observed outliers resulted all from predictions for chicken manure (Oxytetracycline, Chlortetracycline, Sulfadiazine, Trimethoprim). Applying the worst-case approach (WC), four predicted substance concentrations [Chlortetracycline (chicken), Sulfadiazine (chicken), Trimethoprim (chicken), Tetracycline (cattle)] were lower than the highest measured concentration, but deviated not more than one order of magnitude (Fig. 1). Beyond that, in 6 of 17 cases [Oxytetracycline (chicken), Tetracycline (pig), Chlortetracycline (pig), Sulfamerazine (pig), Sulfadiazine (pig, cattle)] the highest measured concentration was more than one order of magnitude lower than the corresponding predicted value.

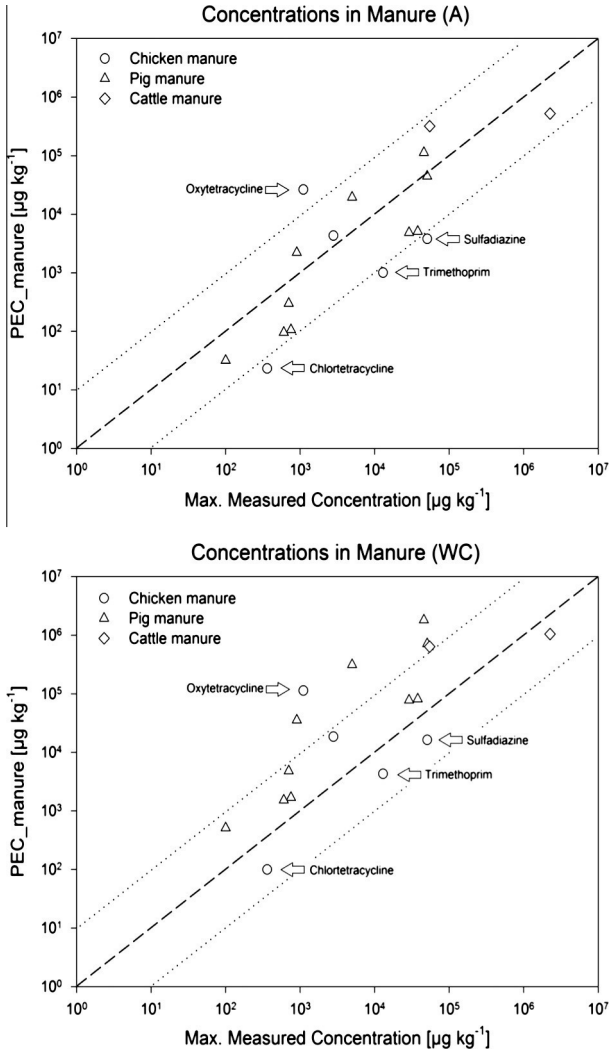

Fig. 1. Comparison between predicted and measured concentrations in manure showing the average scenario (A) and the worst-case scenario (WC). The dashed lines resemble the angle bisectors. Value pairs between dotted lines lie within the same order of magnitude.

It has to be noted that the initial estimations presented in this study do not account for substance alterations by animal metabolism to meet the requirements of a lower-tier screening (total residue approach). This means that comparisons of predicted manure concentrations with monitoring data limited to parent compounds might inevitably indicate an overestimation, especially when taking into account that fractions of excreted residues from 15% to 87% have been reported for the available reference compounds (see Table S5). Further, the measured data does not necessarily include the absolute peak values that might be only reached in specific cases. In contrast, drastic underestimations of measured concentrations should be regarded more critical, because they might lead to an underestimation of the potential environmental risk. Under this aspect, the average scenario (A) provides an insufficient margin of safety to be used as conservative screening model in ERA, as in 3 of 17 cases underestimated values deviated more than one order of magnitude. However, regarding that predicted values were compared to measured peak values a tendency towards underestimation would be the primary expectation for the average scenario. Therefore it can be assumed that this scenario might indeed give a realistic picture of the normal case, as only in one value pair a drastic overestimation was observed. Regarding the worst-case scenario (WC), substantial shortcomings i.e. drastic underestimations under worst-case assumptions were not revealed in this qualitative evaluation approach. In most cases, measured and predicted concentrations were within the same order of magnitude, which is acceptable taking into account the uncertainties of input numbers and monitoring data. Therefore it can be concluded that the predicted manure concentrations provide a strong basis for soil exposure modeling.

3.3. Prediction of initial antibiotic substance concentrations in soil

Predicted initial soil concentrations range from pg kg^{-1} to mg kg^{-1} dw with a worst-case peak value of 4.4 mg kg^{-1} dw for Tetracycline after application of pig manure. Regarding the average scenario, potential antibiotic concentrations up to 1.1 mg kg^{-1} dw (Chlortetracycline) were predicted to occur in soil directly after manure application. Beyond that, Amoxicillin and Sulfadiazine reached theoretical soil concentrations above 1.0 mg kg^{-1} dw under worst-case assumptions. In total, 14 antibiotic substances of 10 different antimicrobial classes were predicted to have the potential to occur in initial soil concentrations higher than 100 µg kg^{-1} dw. The highest predicted antibiotic concentrations in soil are summarized for grassland (pig, cattle) and arable land (chicken) in Figs. 2 and 3. A full overview of predicted soil concentrations is provided in the supplementary material (Tables S6 and S7). Interestingly, in some cases the overall rank order of active substances from highest to lowest concentration changes between scenario A and WC. This can be explained by the high fluctuations within the numbers of applied daily doses (*n_DD*) for pigs. The ranking in the average scenario (A) is more dominated by cattle, as the average *n_DD* is rather low for pigs. This relation is reversed in the worst-case scenario (WC) when the extreme values are applied. Therefore, both scenarios should be considered in terms of priority-setting.

3.4. Significance of the predicted concentrations in soil

As stated before, predicted initial soil concentrations range from pg kg^{-1} dw to mg kg^{-1} dw. Regarding that nearly all reported antibiotic soil concentrations summarized by the LANUV literature

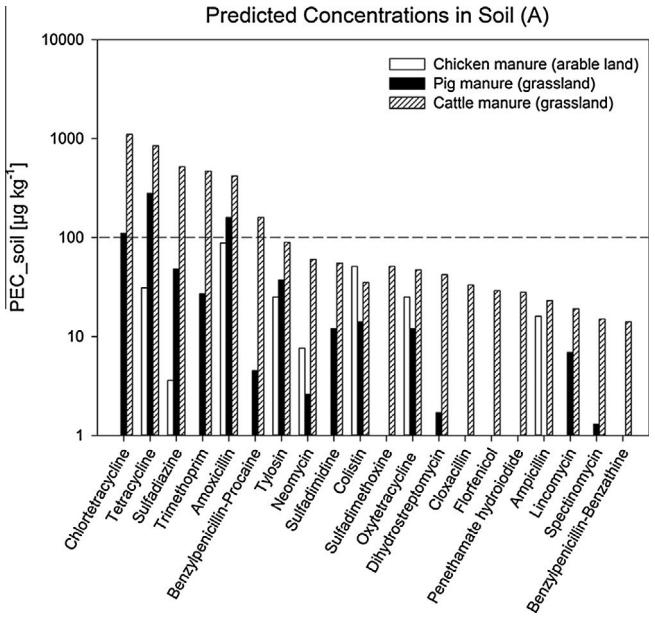

Fig. 2. Predicted initial antibiotic substance concentrations in soil (*PEC_soil*) in the average scenario (A) after application of manure from chicken, pig and cattle onto arable and grassland, respectively. The dashed line shows the EMA trigger value of 100 µg kg^{-1} for phase II assessments. Predicted concentrations in arable land are always four times lower than in grassland due to the assumptions on mixing depth with soil (20 cm instead of 5 cm).

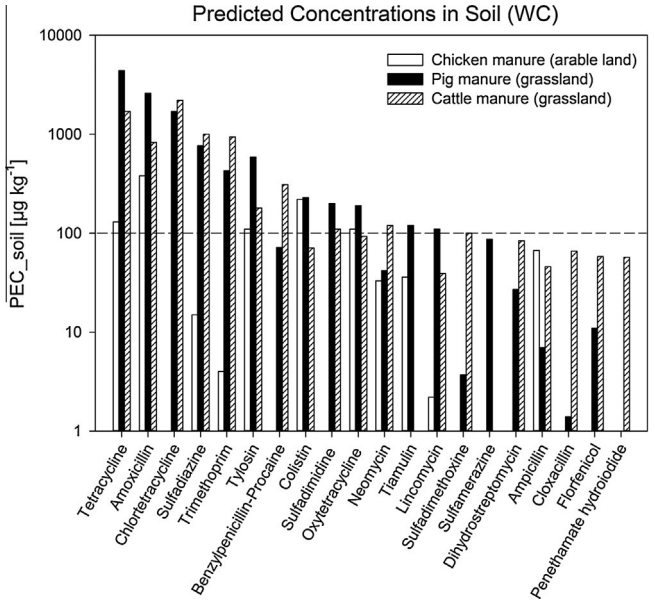

Fig. 3. Predicted initial antibiotic substance concentrations in soil (*PEC_soil*) in the worst-case scenario (WC) after application of manure from chicken, pig and cattle onto arable and grassland, respectively. The dashed line shows the EMA trigger value of 100 µg kg^{-1} for phase II assessments. Predicted concentrations in arable land are always four times lower than in grassland due to the assumptions on mixing depth with soil (20 cm instead of 5 cm).

review peak in the µg to mg kg^{-1} range (LANUV, 2007) the predicted soil concentrations seem realistic. However, comparisons between potential and measured concentrations in soil can be highly misleading because substance degradation in manure and soil, as well as transport processes were not considered in the previously described calculations. Moreover, the formation of non-extractable residues in soil samples might contribute to noticeable deviations between predicted and measured concentrations. Selected environmental fate parameters that might explain possible overestimations of measured soil concentrations are summarized for selected compounds in Table S5 to support the previous considerations. This data clearly shows that various parameters, like the excretion pattern, persistence in manure and soil and sorption to soil organic matter, might influence the recovery of originally applied active substances in soil samples. In addition these parameters are highly variable and only partially available, which is why the consideration of these factors within the initial screening level is not feasible. Nonetheless, the potential input of active substance into soil is basically a function of the amount of manure applied (which is assumed to be constant) and the predicted manure concentration, which was demonstrated to provide a sufficient margin of safety for selected compounds in the worst-case scenario. A previously conducted prediction of Tetracycline concentrations in soil after application of pig manure by Winckler and Grafe ranged from 0.9 to 2.1 mg kg^{-1} dw (Winckler and Grafe, 2000), while the new pattern-based prediction was 0.28–4.4 mg kg^{-1} dw (Tables S6 and S7). This argues for a good congruency of the individual UPES predictions with previously conducted single-substance estimations and demonstrates that recently established variables for the description of the use of veterinary pharmaceuticals in food-producing animals, like the number of applied daily doses per animal year (*n_DD*) and the used daily dose (UDD), are fully compatible with existing standards in environmental exposure assessment. However, this does not change the fact that after the identification of critical hotspots, a further substance-specific refinement of initially predicted environmental concentrations is absolutely necessary, providing that strong data on the fate of the active substance after its administration is available. The EMA's revised Guideline on Environmental Impact Assessment for Veterinary Medicinal Products provides detailed information on possible PEC-refinements that can be directly applied to the initial estimations obtained in this study. Additionally, it has to be considered that the previously described calculations were conducted with the assumption of a uniformly distributed antibiotic consumption, a single manure application event per year and a homogeneous distribution of antibiotic residues in manure and soil. Moreover, the applied consumption patterns do not account for differences in antibiotic consumption between different livestock categories within the same animal species (e.g. beef cattle and dairy cattle), which contributes to the high uncertainty of this first approach. Therefore, a recalculation will be necessary, as soon as more differentiated usage data becomes available.

3.5. Implications for environmental risk assessment of VAs

A higher-than-average livestock density for pigs, cattle and poultry can be found in north-western regions of Germany (Bäurle and Tamásy, 2012) and sales data clearly unmasks this area as a hotspot of VA consumption (Federal Office of Consumer Protection and Food Safety, 2014). Therefore it can be assumed that these regions are particularly affected by the disposal of contaminated livestock manure to agricultural land and that antibiotic usage patterns from this region are suitable to develop a representative worst-case scenario.

The EMA trigger value for phase II assessment of 100 µg kg^{-1} was exceeded for 6 active substances regarding the average scenario (A) and for 14 substances assuming the worst-case (WC). Even with consideration of manure incorporation into soil, the trigger value for phase II assessment was exceeded for 5 (A) and 8 (WC) of the investigated antimicrobials (Figs. 2 and 3). This means that these substances might have to undergo phase II assessments, if today's standards for market authorization would apply for existing medicinal products. But even if this regulation would

Table 1
Suggested two factor priority grouping of veterinary antimicrobials for higher-tier environmental risk assessment. The maximum value of the three investigated species was used for priority-setting.

Priority group	Scenario	Priority-setting criteria	Substances
1	Average (A) arable land	Application frequency (F) > 0.1 or *PEC_soil* > 100 μg kg^{-1}	Amoxicillin Chlortetracycline Colistin Enrofloxacin Sulfadiazine Tetracycline Trimethoprim
2	Average (A) grassland	*PEC_soil* > 100 μg kg^{-1}	Benzylpenicillin
3	Worst-case (WC) arable land	*PEC_soil* > 100 μg kg^{-1}	Oxytetracycline Tylosin
4	Worst-case (WC) grassland	*PEC_soil* > 100 μg kg^{-1}	Lincomycin Neomycin Sulfadimethoxine Sulfadimidine Tiamulin

apply, the trigger value approach would be still debatable as the intrinsic biological activity of a substance is not considered. This problem becomes obvious, when taking a closer look at compounds that did not exceed the phase II action limit, but showed a comparatively high relative application frequency (F). For example, Enrofloxacin was estimated to account for 18.3% of all applied daily doses in poultry, but reaches a rather low *PEC_soil initial* of 17.4 μg kg^{-1} (WC). This can be explained by the high potency of the active substance and also by the comparatively low molecular weight, which leads to a very low *DD* of 1.4 mg kg^{-1} and subsequently to a low *PEC_soil initial*. Therefore not only the potential environmental concentration, but also the application frequency should be considered in substance prioritization. Furthermore, the different levels of conservatism between the applied scenarios allow a categorization of active substances into different priority groups for ERA. A two factor priority grouping scheme of frequently used VAs considering both, the expected environmental concentration and the frequency of application, is suggested in Table 1. In this case, a relative application frequency (F) of 0.1 as additional cut-off value significantly influenced the grouping of two VAs (Colistin and Enrofloxacin) as the EMA trigger value was not exceeded in the average scenario or the worst-case scenario, respectively, even though these compounds were used in a high frequency. This example shows that the relative application frequency as additional cut-off value might represent a valuable supplement of the trigger value approach that should be further evaluated. Moreover, 5 out of 7 active substances of priority group 1 have already been detected in soil samples (Hamscher et al., 2002; Sattelberger et al., 2005; Martínez-Carballo et al., 2007), which confirms the predicted high potential of these compounds to enter the terrestrial environment and demonstrates a good reliability of the applied UPES approach for the identification of environmentally relevant VAs. As a further measure, the high-priority substances identified with UPES should be included in targeted environmental monitoring campaigns on a regular basis to provide an early recognition of possible risks and to allow a close reasoning in case of significant impacts on human health and the environment. Moreover, UPES can be used to account for differing local agricultural factors in research conception, providing that differentiated data from spatially inclusive and comprehensive surveillance programs will be available in the future.

4. Conclusion

In present environmental risk assessment of VAs, exposure predictions are usually conducted only for selected substances and are often based on vague assumptions regarding the dosage, application frequency and fraction of animals treated. The utilization of upcoming differentiated usage patterns for environmental exposure assessment allows an improved lower-tier ERA as it facilitates the prioritization of VAs for higher-tier investigations on a regional level. Moreover, we demonstrated that shortcomings of the conventional priority-setting based on the trigger value approach can be attenuated by considering both, the potential environmental concentration and the frequency of substance application. The predicted high levels of potential soil concentrations gave rise to further questions regarding the environmental occurrence and safety of specific VAs, especially in regions with higher-than-average livestock density. Therefore, a usage pattern-based exposure screening (UPES) can provide valuable information for the conceptualization of further studies on the environmental occurrence, fate and effects of veterinary antibiotics.

Acknowledgements

This work was supported by the Innovations-Inkubator Lüneburg (Teilmaßnahme 1.4, Graduate School) with a scholarship for Jakob Menz. The authors wish to thank Anju Priya Toolaram, Dr. Matthias Gaßmann and Dr. Oliver Olsson for sharing their wide knowledge and for proofreading the manuscript. We also thank the anonymous reviewers for their constructive comments.

Appendix A. Supplementary material

Supplementary data associated with this article can be found, in the online version, at http://dx.doi.org/10.1016/j.chemosphere.2014.12.091.

References

Aarestrup, F.M., 1999. Association between the consumption of antimicrobial agents in animal husbandry and the occurrence of resistant bacteria among food animals. Int. J. Antimicrob. Agents 12 (4), 279–285. http://dx.doi.org/10.1016/S0924-8579(99)90059-6.

Addison, J.B., 1984. Antibiotics in sediments and run-off waters from feedlots. In: Gunther, F., Gunther, J. (Eds.), Residue Reviews, vol. 92. Springer, New York, pp. 1–28.

Angulo, F.J., Nargund, V.N., Chiller, T.C., 2004. Evidence of an association between use of anti-microbial agents in food animals and anti-microbial resistance among bacteria isolated from humans and the human health consequences of such resistance. J. Vet. Med. Ser. B 51 (8–9), 374–379. http://dx.doi.org/10.1111/j.1439-0450.2004.00789.x.

Bäurle, H., Tamásy, C., 2012. Regionale Konzentrationen der Nutztierhaltung in Deutschland (Regional Concentrations of Livestock Farming in Germany).

Institute for Spatial Analysis and Planning in Areas of Intensive Agriculture, Vechta.
Bondt, N., Jensen, V.F., Puister-Jansen, L.F., van Geijlswijk, I.M., 2013. Comparing antimicrobial exposure based on sales data. Preventive Vet. Med. 108 (1), 10–20. http://dx.doi.org/10.1016/j.prevetmed.2012.07.009.
BVL (Federal Office of Consumer Protection and Food Safety), 2014. Dritte Datenerhebung zur Antibiotikaabgabe in der Tiermedizin (third data collection for antibiotic consumption in veterinary medicine), Berlin.
DANMAP, 2013. Use of antimicrobial agents and occurrence of antimicrobial resistance in bacteria from food animals, food and humans in Denmark.
European Medicines Agency, 2008. Revised guideline on environmental impact assessment for veterinary medicinal products, London.
Hamscher, G., Sczesny, S., Höper, H., Nau, H., 2002. Determination of persistent tetracycline residues in soil fertilized with liquid manure by high-performance liquid chromatography with electrospray ionization tandem mass spectrometry. Anal. Chem. 74 (7), 1509–1518. http://dx.doi.org/10.1021/ac015588m.
Hegger-Gravenhorst, C., 2012. Die Erfassung von Verbrauchsmengen für Antibiotika bei Lebensmittel liefernden Tieren vor dem Hintergrund der tierärztlichen Betreuung (monitoring of antibiotic consumption in livestock in relation to veterinary attendance). Inaugural-Dissertation, Hannover.
Kemper, N., 2008. Veterinary antibiotics in the aquatic and terrestrial environment. Ecol. Ind. 8 (1), 1–13. http://dx.doi.org/10.1016/j.ecolind.2007.06.002.
Koschorreck, J., Koch, C., Rönnefahrt, I., 2002. Environmental risk assessment of veterinary medicinal products in the EU—a regulatory perspective. Toxicol. Lett. 131 (1–2), 117–124. http://dx.doi.org/10.1016/S0378-4274(02)00047-4.
Kumar, K., Gupta, C., Satish, Chander, Y., Singh, A.K., 2005. Antibiotic use in agriculture and its impact on the terrestrial environment. In: Sparks, Donald L. (Ed.), Advances in Agronomy, vol. 87. Academic Press.
Küster, A., Lehmann, S., Hein, A., Schönfeld, S., 2013. Antibiotika in der Umwelt – Wirkung mit Nebenwirkung (antibiotics in the environment – effect with side-effects). In: UMID 01/2013: Schwerpunkt Chemikalien, Umwelt und Gesundheit, Berlin.
Landers, T.F., Cohen, B., Wittum, T.E., Larson, E.L., 2012. A review of antibiotic use in food animals: perspective, policy, and potential. Public Health Rep. 127 (1), 4–22.
LANUV (North Rhine-Westphalia. State Agency for Nature, Environment and Consumer Protection), 2007. Eintrag von Arzneimitteln und deren Verhalten und Verbleib in der Umwelt: Literaturstudie (input of pharmaceuticals and the behaviour and fate in the environment: literature review), Recklinghausen.
LAVES (Lower Saxony State Office for Consumer Protection and Food Safety), 2011. Bericht über den Antibiotikaeinsatz in der landwirtschaftlichen Nutztierhaltung in Niedersachsen (report on antibiotic drug consumption in agricultural livestock farming in Lower-Saxony), Hannover.
Martinez, J.L., 2009. Environmental pollution by antibiotics and by antibiotic resistance determinants. Environ. Pollut. 157 (11), 2893–2902. http://dx.doi.org/10.1016/j.envpol.2009.05.051.
Martínez-Carballo, E., González-Barreiro, C., Scharf, S., Gans, O., 2007. Environmental monitoring study of selected veterinary antibiotics in animal manure and soils in Austria. Environ. Pollut. 148 (2), 570–579. http://dx.doi.org/10.1016/j.envpol.2006.11.035.
Merle, R., Hajek, P., Kasbohrer, A., Hegger-Gravenhorst, C., Mollenhauer, Y., Robanus, M., Ungemach, F.-R., Kreienbrock, L., 2012. Monitoring of antibiotic consumption in livestock: a German feasibility study. Preventive Vet. Med. 104 (1–2), 34–43. http://dx.doi.org/10.1016/j.prevetmed.2011.10.013.
Merle, R., Robanus, M., Hegger-Gravenhorst, C., Mollenhauer, Y., Hajek, P., Käsbohrer, A., Honscha, W., Kreienbrock, L., 2014. Feasibility study of veterinary antibiotic consumption in Germany – comparison of ADDs and UDDs by animal production type, antimicrobial class and indication. BMC Vet. Res. 10 (1), 7. http://dx.doi.org/10.1186/1746-6148-10-7.
Robanus, M., 2011. Antibiotika-Verbrauchsmengenerfassung bei landwirtschaftlichen Nutztieren in ausgewählten Betrieben und Tierarztpraxen in Niedersachsen und Nordrhein-Westfalen unter Berücksichtigung pharmakologischer Parameter (pharmacological aspects of monitored consumption of antibiotics of agricultural animals in selected farms and veterinary surgeries in Lower Saxony and Northrhine-Westfalia). Inaugural-Dissertation, Leipzig.
Sarmah, A.K., Meyer, M.T., Boxall, A.B., 2006. A global perspective on the use, sales, exposure pathways, occurrence, fate and effects of veterinary antibiotics (VAs) in the environment. Chemosphere 65 (5), 725–759. http://dx.doi.org/10.1016/j.chemosphere.2006.03.026.
Sattelberger, R., Gans, O., Martínez, E., 2005. Veterinärantibiotika in Wirtschaftsdünger und Boden (veterinary antibiotics in farmyard manure and soil), Wien.
Smith, D.L., Harris, A.D., Johnson, J.A., Silbergeld, E.K., Morris, J.G., 2002. Animal antibiotic use has an early but important impact on the emergence of antibiotic resistance in human commensal bacteria. Proc. Natl. Acad. Sci. 99 (9), 6434–6439. http://dx.doi.org/10.1073/pnas.082188899.
Teuber, M., 2001. Veterinary use and antibiotic resistance. Curr. Opin. Microbiol. 4 (5), 493–499. http://dx.doi.org/10.1016/S1369-5274(00)00241-1.
Thiele-Bruhn, S., 2003. Pharmaceutical antibiotic compounds in soils – a review. J. Plant Nutr. Soil Sci. 166 (2), 145–167. http://dx.doi.org/10.1002/jpln.200390023.
UBA (Federal Environmental Agency), 2014. Antibiotika und Antiparasitika im Grundwasser unter Standorten mit hoher Viehbesatzdichte (Antibiotics and antiparasitics in the ground water at locations with high livestock density), Dessau-Roßlau.
Winckler, C., Grafe, A., 2000. Charakterisierung und Verwertung von Abfällen aus der Massentierhaltung unter Berücksichtigung verschiedener Böden (Characterization and Utilization of Wastes from Intensive Animal Production with Regard to Soil). Federal Environmental Agency, Berlin.
World Health Organization, 2012. The Evolving Threat of Antimicrobial Resistance: Options for Action. World Health Organization, Geneva.

Supplementary material

Table S1: Assumed daily doses (*DD*) and relative application frequencies (*F*) used for the prediction of antibiotic substance concentration in manure.

Antibiotic Substance	Poultry		Pig		Cattle	
	DD **[mg kg^{-1}]**	***F***	***DD*** **[mg kg^{-1}]**	***F***	***DD*** **[mg kg^{-1}]**	***F***
Acetylisovaleryltylosin	-	-	3.7	0.000	-	-
Amoxicillin	21.8	0.258	35.8	0.162	25.5	0.069
Ampicillin	16.0	0.062	15.4	0.001	15.0	0.006
Apramycin	-	-	7.0	0.001	-	-
Benzylpenicillin (-potassium, -sodium)	14.5	0.042	12.0	0.000	9.4	0.002
Benzylpenicillin-Benzathine	-	-	20.0	0.001	20.0	0.003
Benzylpenicillin-Procaine	20.0	0.000	27.8	0.006	18.1	0.037
Cefoperazone	-	-	-	-	0.4	0.003
Cefquinome	-	-	1.7	0.002	1.4	0.023
Ceftiofur	-	-	3.6	0.001	1.7	0.023
Chlortetracycline	232.3	0.000	36.4	0.107	53.2	0.086
Cloxacillin	-	-	92.6	0.000	6.3	0.022
Colistin	19.2	0.169	7.4	0.069	9.4	0.016
Danofloxacin	-	-	2.0	0.002	2.7	0.003
Difloxacin	-	-	-	-	6.8	0.000
Dihydrostreptomycin	-	-	25.0	0.002	12.5	0.014
Doxycycline	-	-	10.0	0.003	14.1	0.000
Enrofloxacin	1.4	0.183	3.9	0.002	3.6	0.016
Erythromycin	-	-	12.6	0.000	10.9	0.001
Florfenicol	-	-	21.4	0.001	22.6	0.005
Gentamicin	-	-	5.6	0.000	4.7	0.005
Kanamycin	-	-	11.8	0.000	7.1	0.000
Lincomycin	16.7	0.002	9.6	0.026	7.3	0.011
Marbofloxacin	-	-	2.4	0.002	2.2	0.008
Neomycin	15.0	0.032	13.0	0.007	7.4	0.034
Oxacillin	-	-	-	-	6.2	-
Oxytetracycline	50.0	0.032	23.8	0.018	32.1	0.006
Penethamate hydroiodide	-	-	9.6	0.000	14.4	0.008
Spectinomycin	33.3	0.002	7.9	0.006	6.0	0.010
Sulfaclozine	70.0	0.002	-	-	-	-
Sulfadiazine	35.0	0.006	25.0	0.068	25.0	0.088
Sulfadimethoxine	-	-	25.0	0.000	30.0	0.007
Sulfadimidine	-	-	65.1	0.007	69.6	0.003
Sulfadoxine	28.5	0.000	13.4	0.001	13.3	0.003
Sulfamerazine	-	-	28.5	0.007	-	-
Sulfamethoxazole	28.0	0.000	-	-	-	-
Sulfamethoxpyridazine	-	-	57.9	0.000	61.7	0.000
Sulfathiazole	-	-	28.5	0.000	28.5	0.001
Tetracycline	20.2	0.098	55.8	0.176	57.3	0.063
Tiamulin	40.5	0.013	9.4	0.027	-	-

Tilmicosin	17.5	0.002	12.7	0.004	33.3	0.001
Trimethoprim	5.6	0.011	5.0	0.191	5.0	0.399
Tulathromycin	4.0	0.000	4.0	0.001	2.8	0.006
Tylosin	18.4	0.086	13.1	0.099	25.6	0.015
Valnemulin	-	-	0.7	0.000	-	-

Table S2: Parameters and default values for the calculation of *n_DD*

Symbol	Input / output parameter	Default value						Unit
		Chicken (Broiler)		Pig (Fattening pig)		Cattle (Fattening calf)		
		A	WC	A	WC	A	WC	
n_treat_j	Total number of treatments per animal and production cycle	6.8[a]	30[a]	4.6[a]	80[a]	39.9[a]	80[a]	$animal^{-1}$
n_cyle_j	Number of production cycles per year	9.1[a]		2.9[a]		1.9[a]		a^{-1}
F_{ij}	Relative application frequency	Table S1						-
n_DD_{ij}	Theoretically applied number of daily doses per animal and year	-						$animal^{-1}\ a^{-1}$

[a] LAVES, 2011

Table S3: Parameters and default values for the calculation of *PEC_manure N* and *PEC_manure dw*

Symbol	Input / output parameter	Default value			Unit
		Chicken (Broiler)	Pig (Fattening pig)	Cattle (Fattening calf)	
$\overline{m_j}$	Animal bodyweight	1.0[b]	65[b]	140[b]	kg
$N\_excretedj$	Nitrogen production per animal and year	0.23[b]	7.5[b]	10.0[b]	kg $animal^{-1}\ a^{-1}$
n_DD_{ij}	Theoretically applied number of daily doses per animal and year		-		$animal^{-1}\ a^{-1}$
DD_{ij}	Daily dose		Table S1		mg kg^{-1}
$PEC\_manure\ N_{ij}$	Predicted amount of substance in manure per kg excreted nitrogen		-		mg kg^{-1} N
N_manure_j	Average nitrogen content	18.1[c]	6.5[c]	2.8[c]	kg N t^{-1} / kg N m^{3-1}
dm_manure_i	Average dry-matter content	30[c]	7[c]	2[c]	%
$PEC\_manure\ dw_{ij}$	Predicted amount of substance in manure by dry weight	-	-	-	mg t^{-1} dw

[b] Montforts, 2006, [c] North-Rhine-Westphalian Chamber of Agriculture, 2012

Table S4: Parameters and default values for the calculation of *PEC_soil initial*

Symbol	Input / output parameter	Default value	Unit
N_max	Annual nitrogen immission standard	170	kg N ha^{-1}
D_soil	Bulk density of soil	1500	kg m^{-3}
CONV_area	Conversion factor for the area of the agricultural field	10000	$m^2\ ha^{-1}$
DEPTH_field	Mixing depth with soil	0.2 (arable land) 0.05 (grassland)	m
$PEC\_manure\ N_{ij}$	Predicted amount of substance in manure per kg excreted nitrogen	-	mg kg^{-1} N
$PEC\_soil\ initial_{ij}$	Predicted substance concentration in soil (by dry weight)	-	mg kg^{-1} dw

Table S5: Highest reported antibiotic substance concentrations in manure used for the evaluation of predicted values and environmental fate parameters that might influence the recovery of respective antibiotics in manure and soil samples.

Group	Antibiotic substance	Highest reported concentrations in manure			Excretion	Degradation/half-life in manure	Half-life in soil	Soil adsorption coefficient (K_{OC}) [L kg^{-1}]
		Chicken [µg kg^{-1} dw]	Pig [µg kg^{-1} dw]	Cattle [µg kg^{-1} dw]				
Tetracyclines	Chlortetracycline	360[j]	50800[e]	n.a.	17-75% (cattle)[g]	0-44% after 30 d[d]	30 d[m]	n.a.
	Doxycycline	n.a.	700[e]	n.a.	n.a.	n.a.	n.a.	n.a.
	Oxytetracycline	1100[j]	29000[j]	n.a.	90%[j]	43.8-79 d[m]	18-21 d[m]	27790-93320[i]
	Tetracycline	n.a.	46000[e]	2265000[a]	72% (pig)[n]	4.5 d[m]; 55-105 d[n]	30 d[m]	40000[m]
Fluorchinolones	Enrofloxacin	2800[j]	750[j]	n.a.	87% (chicken)[b]; 15-50% (pig)[j]	142 d[b]	123-297 d[m]; 359-696 d[b]	16500-770000[h]
Sulfonamides	Sulfadiazine	51000[j]	5000[e]	55000[a]	50%[j]	0% in 16 weeks[e]	n.a.	81[m]; 124[k]
	Sulfadimethoxine	n.a.	600[e]	n.a.	n.a.	30% in 16 weeks[e]	n.a.	1672[m]
	Sulfadimidine	n.a.	38000[e]	n.a.	n.a.	0% in 16 weeks[e]	18.6 d[m]	80-170[f]
	Sulfamerazine	n.a.	900[e]	n.a.	n.a.	0% in 16 weeks[e]	n.a.	n.a.
	Sulfathiazole	n.a.	100[e]	n.a.	n.a.	30% in 16 weeks[e]	n.a.	n.a.
Diamino-pyrimidines	Trimethoprim	13000[j]	n.a.	n.a.	22% (pig)[c]	70% in 16 weeks[e]; 31.5 d[m]	110 d[m]	2835[m]

n.a. = not available; References:

[a]BLAC (National and Regional Committee for the Safety of Chemicals), 2003. Arzneimittel in der Umwelt - Auswertung der Untersuchungsergebnisse (Pharmaceuticals in the environment - Evaluation of the survey results), Hamburg (estimated by reported wet weight assuming a dry-matter content of 2%).

[b]Bayer Corporation, 1996. Environmental Assessment for Enrofloxacin.

[c]European Medicines Agency, Committee for Medicinal Products for Veterinary Use (CVMP), 1997. Trimethoprim: Summary report.

[d]Gavalchin, J., Katz, S.E., 1994. The persistence of fecal-borne antibiotics in soil. Journal of AOAC International, 77(2), 481-485.

[e]Harms, K., Bauer, J., 2011. Detection and Occurrence of Antibiotics and Their Metabolites in Pig Manure in Bavaria (Germany), in: Keen, P.L., Montforts,Mark H. M. M (Eds.), Antimicrobial Resistance in the Environment. John Wiley & Sons, Inc, Hoboken, NJ, USA, pp. 291–307.

[f]Langhammer J.P., Büning-Pfaue H., 1989. Bewertung von Arzneistoff- Rückständen aus der Gülle im Boden (Evaluation of pharmaceutical residues from manure in soil). Lebensmittelchemie und gerichtliche Chemie 43, 108.

[g]Montforts, M.H., Kalf, D.F., van Vlaardingen, P.L., Linders, J.B., 1999. The exposure assessment for veterinary medicinal products. Science of The Total Environment 225 (1-2), 119–133. DOI: 10.1016/S0048-9697(98)00338-6.

[h]Nowara, A., Burhenne, J., Spiteller, M., 1997. Binding of fluoroquinolone carboxylic acid derivatives to clay minerals. Journal of Agricultural and Food Chemistry 45 (4), 1459–1463. DOI: 10.1021/jf960215l.

[i]Rabølle, M., Spliid, N.H., 2000. Sorption and mobility of metronidazole, olaquindox, oxytetracycline and tylosin in soil. Chemosphere 40 (7), 715–722. DOI: 10.1016/S0045-6535(99)00442-7.
[j]Sattelberger, R., Gans, O., Martínez, E., 2005. Veterinärantibiotika in Wirtschaftsdünger und Boden (Veterinary antibiotics in farmyard manure and soil), Wien.
[k]Thiele-Bruhn, S.; Seibicke, T.; Schulten, H-R; Leinweber, P., 2004. Sorption of sulfonamide pharmaceutical antibiotics on whole soils and particle-size fractions. Journal of Environmental Quality 33 (4), 1331–1342.
[l]Thurman, E.M., Lindsey, M.E., 2000. Transport of antibiotics in soil and their potential for ground-water contamination. Poster presented at The SETAC World Congress, Brighton, May 2000.
[m]University of Hertfordshire, 2013. The Veterinary Substance Database (VSDB) developed by the Agriculture & Environment Research Unit (AERU), University of Hertfordshire, 2011-2013.
[n]Winckler, C., Grafe, A., 2000. Charakterisierung und Verwertung von Abfällen aus der Massentierhaltung unter Berücksichtigung verschiedener Böden (Characterization and utilization of wastes from intensive animal production with regard to soil), Federal Environmental Agency, Berlin.

Table S6: Predicted antibiotic substance concentrations (µg kg^{-1} dw) in manure from chicken, pigs and cattle and estimated initial soil concentrations in the average scenario (A).

Group	Antibiotic substance	Chicken		Pig			Cattle		
		PEC_manure	*PEC_soil initial* arable land	*PEC_manure*	*PEC_soil initial* grassland	*PEC_soil initial* arable land	*PEC_manure*	*PEC_soil initial* grassland	*PEC_soil initial* arable land
Amino-glycosides	Apramycin	n.a.	n.a.	67	0.16	0.041	n.a.	n.a.	n.a.
	Dihydrostreptomycin	n.a.	n.a.	700	1.7	0.43	26000	42	10
	Gentamicin	n.a.	n.a.	28	0.068	0.017	3200	5.2	1.3
	Kanamycin	n.a.	n.a.	0.29	0.0007	0.00017	19	0.031	0.0076
	Neomycin	8100	7.6	1100	2.6	0.66	37000	60	15
	Spectinomycin	1100	1	540	1.3	0.33	9200	15	3.7
Beta-Lactames	Amoxicillin	94000	88	67000	160	41	260000	420	100
	Ampicillin	17000	16	180	0.44	0.11	14000	23	5.7
	Benzylpenicillin (-potassium, -sodium)	10000	9.7	16	0.039	0.0097	3200	5.2	1.3
	Benzylpenicillin-Benzathine	n.a.	n.a.	230	0.56	0.14	8300	14	3.4
	Benzylpenicillin-Procaine	0.11	0.00011	1900	4.5	1.1	96000	160	39
	Cloxacillin	n.a.	n.a.	35	0.086	0.021	20000	33	8.2
	Penethamate hydroiodide	n.a.	n.a.	1.9	0.0047	0.0012	18000	28	7.1
Cephalo-sporins	Cefoperazone	n.a.	n.a.	n.a.	n.a.	n.a.	160	0.26	0.064
	Cefquinome	n.a.	n.a.	38	0.092	0.023	4500	7.3	1.8
	Ceftiofur	n.a.	n.a.	40	0.097	0.024	5700	9.2	2.3
Phenicols	Florfenicol	n.a.	n.a.	280	0.68	0.17	18000	29	7.2
Fluor-chinolones	Danofloxacin	n.a.	n.a.	44	0.11	0.027	1200	2	0.49
	Difloxacin	n.a.	n.a.	n.a.	n.a.	n.a.	370	0.59	0.15
	Enrofloxacin	4300	4.1	110	0.26	0.065	8100	13	3.3
	Marbofloxacin	n.a.	n.a.	61	0.15	0.037	2600	4.2	1
Lincos-	Lincomycin	560	0.52	2800	6.9	1.7	12000	19	4.8

amides									
Makrolides	Acetylisovaleryltylosin	n.a.	n.a.	1.9	0.0047	0.0012	n.a.	n.a.	n.a.
	Erythromycin	n.a.	n.a.	6.1	0.015	0.0037	1600	2.6	0.65
	Tilmicosin	560	0.53	520	1.3	0.32	2500	4	1
	Tulathromycin	0.11	0.00011	35	0.085	0.021	2400	3.9	0.97
	Tylosin	26000	25	15000	37	9.2	55000	90	22
Pleuro-mutilines	Tiamulin	8800	8.3	3000	7.2	1.8	n.a.	n.a.	n.a.
	Valnemulin	n.a.	n.a.	1.9	0.0045	0.0011	n.a.	n.a.	n.a.
Poly-peptides	Colistin	54000	51	5900	14	3.6	22000	35	8.8
Sulfon-amides	Sulfaclozine	2800	2.6	n.a.	n.a.	n.a.	n.a.	n.a.	n.a.
	Sulfadiazine	3800	3.6	20000	48	12	320000	520	130
	Sulfadimethoxine	n.a.	n.a.	96	0.23	0.058	32000	51	13
	Sulfadimidine	n.a.	n.a.	5100	12	3.1	34000	55	14
	Sulfadoxine	55	0.051	170	0.41	0.1	6300	10	2.6
	Sulfamerazine	n.a.	n.a.	2200	5.4	1.4	n.a.	n.a.	n.a.
	Sulfamethoxazole	11	0.011	n.a.	n.a.	n.a.	n.a.	n.a.	n.a.
	Sulfamethoxpyridazine	n.a.	n.a.	6.6	0.016	0.004	59	0.095	0.024
	Sulfathiazole	n.a.	n.a.	32	0.078	0.02	2100	3.4	0.85
Tetra-cyclines	Chlortetracycline	23	0.022	45000	110	27	670000	1100	270
	Doxycycline	n.a.	n.a.	300	0.74	0.18	220	0.36	0.089
	Oxytetracycline	26000	25	4900	12	3	29000	47	12
	Tetracycline	33000	31	110000	280	69	530000	850	210
Diamino-pyrimidines	Trimethoprim	1000	0.94	11000	27	6.7	290000	470	120

n.a. = not applied

Table S7: Predicted antibiotic substance concentrations (µg kg^{-1} dw) in manure from chicken, pigs and cattle and estimated initial soil concentrations in the worst-case scenario (WC).

Group	Antibiotic substance	Chicken		Pig			Cattle		
		PEC_manure	***PEC_soil initial* arable land**	***PEC_manure***	***PEC_soil initial* grassland**	***PEC_soil initial* arable land**	***PEC_manure***	***PEC_soil initial* grassland**	***PEC_soil initial* arable land**
Amino-glycosides	Apramycin	n.a.	n.a.	1100	2.6	0.66	n.a.	n.a.	n.a.
	Dihydrostreptomycin	n.a.	n.a.	11000	27	6.8	52000	84	21
	Gentamicin	n.a.	n.a.	450	1.1	0.27	6400	10	2.6
	Kanamycin	n.a.	n.a.	4.6	0.011	0.0028	38	0.061	0.015
	Neomycin	35000	33	17000	42	10	74000	120	30
	Spectinomycin	4800	4.5	8600	21	5.3	18000	30	7.4
Beta-Lactames	Amoxicillin	400000	380	1100000	2600	650	510000	830	210
	Ampicillin	71000	67	2900	7	1.8	28000	46	11
	Benzylpenicillin (-potassium, -sodium)	44000	42	250	0.62	0.15	6500	10	2.6
	Benzylpenicillin-Benzathine	n.a.	n.a.	3700	9	2.2	17000	27	6.8
	Benzylpenicillin-Procaine	0.49	0.00046	30000	72	18	190000	310	78
	Cloxacillin	n.a.	n.a.	560	1.4	0.34	41000	66	16
	Penethamate hydroiodide	n.a.	n.a.	31	0.076	0.019	35000	57	14
Cephalo-sporins	Cefoperazone	n.a.	n.a.	n.a.	n.a.	n.a.	320	0.51	0.13
	Cefquinome	n.a.	n.a.	610	1.5	0.37	9100	15	3.7
	Ceftiofur	n.a.	n.a.	640	1.6	0.39	11000	18	4.6
Phenicols	Florfenicol	n.a.	n.a.	4500	11	2.7	36000	58	14
Fluor-chinolones	Danofloxacin	n.a.	n.a.	710	1.7	0.43	2400	3.9	0.98
	Difloxacin	n.a.	n.a.	n.a.	n.a.	n.a.	730	1.2	0.3
	Enrofloxacin	19000	17	1700	4.2	1	16000	26	6.5
	Marbofloxacin	n.a.	n.a.	980	2.4	0.6	5200	8.4	2.1

Lincos-amides	Lincomycin	2400	2.2	46000	110	28	24000	39	9.6
Makrolides	Acetylisovaleryltylosin	n.a.	n.a.	31	0.076	0.019	n.a.	n.a.	n.a.
	Erythromycin	n.a.	n.a.	98	0.24	0.06	3200	5.2	1.3
	Tilmicosin	2400	2.3	8400	20	5.1	4900	8	2
	Tulathromycin	0.49	0.00046	550	1.4	0.34	4800	7.8	1.9
	Tylosin	110000	110	240000	590	150	110000	180	45
Pleuro-mutilines	Tiamulin	38000	36	47000	120	29	n.a.	n.a.	n.a.
	Valnemulin	n.a.	n.a.	30	0.073	0.018	n.a.	n.a.	n.a.
Poly-peptides	Colistin	230000	220	95000	230	58	44000	71	18
Sulfon-amides	Sulfaclozine	12000	11	n.a.	n.a.	n.a.	n.a.	n.a.	n.a.
	Sulfadiazine	16000	15	310000	770	190	640000	1000	260
	Sulfadimethoxine	n.a.	n.a.	1500	3.7	0.94	63000	100	26
	Sulfadimidine	n.a.	n.a.	82000	200	50	69000	110	28
	Sulfadoxine	230	0.22	2700	6.6	1.6	13000	21	5.1
	Sulfamerazine	n.a.	n.a.	36000	87	22	n.a.	n.a.	n.a.
	Sulfamethoxazole	49	0.046	n.a.	n.a.	n.a.	n.a.	n.a.	n.a.
	Sulfamethoxpyridazine	n.a.	n.a.	100	0.26	0.064	120	0.19	0.047
	Sulfathiazole	n.a.	n.a.	510	1.2	0.31	4200	6.8	1.7
Tetra-cyclines	Chlortetracycline	100	0.094	720000	1700	440	1300000	2200	540
	Doxycycline	n.a.	n.a.	4800	12	2.9	440	0.71	0.18
	Oxytetracycline	110000	110	78000	190	48	58000	93	23
	Tetracycline	140000	130	1800000	4400	1100	1100000	1700	430
Diamino-pyrimidines	Trimethoprim	4300	4	180000	430	110	580000	940	230

n.a. = not applied

Publikation 2

Antimicrobial activity of pharmaceutical cocktails in sewage treatment plant effluent - An experimental and predictive approach to mixture risk assessment

Menz, J., Baginska, E., Arrhenius, A., Haiβ, A., Backhaus, T., Kümmerer, K.

(2017)

Environmental Pollution 231, 1507-1517

DOI: 10.1016/j.envpol.2017.09.009

Environmental Pollution 231 (2017) 1507–1517

Contents lists available at ScienceDirect

Environmental Pollution

journal homepage: www.elsevier.com/locate/envpol

Antimicrobial activity of pharmaceutical cocktails in sewage treatment plant effluent – An experimental and predictive approach to mixture risk assessment☆

Jakob Menz [a], Ewelina Baginska [a], Åsa Arrhenius [b], Annette Haiß [a], Thomas Backhaus [b], Klaus Kümmerer [a, *]

[a] Sustainable Chemistry and Material Resources, Institute of Sustainable and Environmental Chemistry, Leuphana University Lüneburg, Scharnhorststrasse 1, DE-21335 Lüneburg, Germany
[b] Department of Biological and Environmental Sciences, University of Gothenburg, Carl Skottsbergs Gata 22B, Box 461, 40530 Gothenburg, Sweden

ARTICLE INFO

Article history:
Received 22 April 2017
Received in revised form
31 August 2017
Accepted 5 September 2017
Available online 28 September 2017

Keywords:
Antibiotics
Mixture toxicity
Environmental bacteria
Microbial communities

ABSTRACT

Municipal wastewater contains multi-component mixtures of active pharmaceutical ingredients (APIs). This could shape microbial communities in sewage treatment plants (STPs) and the effluent-receiving ecosystems. In this paper we assess the risk of antimicrobial effects in STPs and the aquatic environment for a mixture of 18 APIs that was previously detected in the effluent of a European municipal STP. Effects on microbial consortia (collected from a separate STP) were determined using respirometry, enumeration of culturable microorganisms and community-level physiological profiling. The mixture toxicity against selected bacteria was assessed using assays with *Pseudomonas putida* and *Vibrio fischeri*. Additional data on the toxicity to environmental bacteria were compiled from literature in order to assess the individual and expected joint bacterial toxicity of the pharmaceuticals in the mixture. The reported effluent concentration of the mixture was 15.4 nmol/l and the lowest experimentally obtained effect concentrations (EC_{10}) were 242 nmol/l for microbial consortia in STPs, 225 nmol/l for *P. putida* and 73 nmol/l for *V. fischeri*. The lowest published effect concentrations (EC_{50}) of the individual antibiotics in the mixture range between 15 and 150 nmol/l, whereas 0.9–190 μmol/l was the range of bacterial EC_{50} values found for the non-antibiotic mixture components. Pharmaceutical cocktails could shape microbial communities at concentrations relevant to STPs and the effluent receiving aquatic environment. The risk of antimicrobial mixture effects was completely dominated by the presence of antibiotics, whereas other pharmaceutical classes contributed only negligibly to the mixture toxicity. The joint bacterial toxicity can be accurately predicted from the individual toxicity of the mixture components, provided that standardized data on representative bacterial strains becomes available for all relevant compounds. These findings argue for a more sophisticated bacterial toxicity assessment of environmentally relevant pharmaceuticals, especially for those with a mode of action that is known to specifically affect prokaryotic microorganisms.

1. Introduction

Most active pharmaceutical ingredients (APIs) undergo only incomplete resorption and metabolism within the human body and therefore enter the raw sewage as active compounds or as metabolites (Jelić et al., 2012). Furthermore, parent APIs can enter raw sewage via the inappropriate disposal of out-of-date or unwanted drugs (Kümmerer, 2008). These pharmaceutical residues form multi-component mixtures in municipal wastewater that are only insufficiently removed during the passage through the sewage treatment plant (STP) (Fatta-Kassinos et al., 2011; Heberer, 2002; Roberts and Thomas, 2006). The ecotoxicological risk of pharmaceutical mixtures typically exceeds the risk of each individual compound (Backhaus, 2016). Consequently, there is an urgent need for ecotoxicity assessment of pharmaceutical mixtures in environmentally realistic settings, i.e. scenarios where several interacting

☆ This paper has been recommended for acceptance by Charles Wong.

* Corresponding author.
E-mail address: klaus.kuemmerer@leuphana.de (K. Kümmerer).

https://doi.org/10.1016/j.envpol.2017.09.009
0269-7491/

species are exposed to a multitude of pharmaceuticals from different classes (Backhaus, 2014; Vasquez et al., 2014).

The occurrence of APIs in the environment impacts microbial communities in different ways (Barra Caracciolo et al., 2015). Microbial communities can acquire tolerance in polluted environments as a result of an adaptation or acclimatization of populations or from shifts in species composition due to altered competitive interactions under toxic exposure (Tlili et al., 2015). The ability of complex microbial communities to adapt to the presence of multiple toxic compounds is important for the process stability in biological wastewater treatment systems (Kong et al., 1993). It was found that the chemical, rather than the bacterial composition of the incoming wastewater represents the main factor in shaping the microbial community structure in activated sludge (Shchegolkova et al., 2016). Therefore, it is not surprising that mixtures of APIs from different classes were shown to potentially influence activated sludge communities (Kraigher et al., 2008; Wang and Gunsch, 2011). In this context, antibiotic agents are of particular interest, since they possess a high intrinsic potential to affect the microbial degradation of organic matter in STPs (Kümmerer, 2009). Moreover, their presence in STPs at sub-inhibitory concentrations may promote the selection and spread of antibiotic resistance (Rizzo et al., 2013). There are many indications that APIs, either in mixtures or even as single compounds, may shape not only microbial communities in STPs, but also sensitive natural microbial communities in the aquatic environment (Corcoll et al., 2014; Ebert et al., 2011; Lawrence et al., 2005; Veach et al., 2012; Wilson et al., 2003). Such effects may have far-reaching consequences, since alterations of the natural microbial composition could impact ecosystem functioning (Reed and Martiny, 2007). Moreover, antibiotics can exert a selective pressure at concentrations up to several hundred-fold below the minimal inhibitory concentration of susceptible bacteria (Gullberg et al., 2011) and reported antibiotic concentrations in STP effluent often exceeded predicted no effect concentrations for resistance selection (Bengtsson-Palme and Larsson, 2016; Kümmerer and Henninger, 2003). As a consequence, the combined discharge of antibiotics and antibiotic-resistant bacteria from STPs may contribute to the maintenance and spread of antibiotic resistance in the aquatic environment (Goñi-Urriza et al., 2000).

The current guideline of the European Medicines Agency (EMA) for the environmental risk assessment of medicinal products for human use (EMEA/CHMP/SWP/4447/00 corr 2) does not require the mandatory evaluation of antimicrobial effects for all pharmaceuticals prior to marketing authorization (EMA, 2006). The first step (phase I) of the tiered assessment procedure estimates the exposure of the environment to the drug substance. If phase I results in a predicted environmental concentration (PEC) for the aquatic compartment equal to or above 0.01 μg/l, a screening-level assessment of aquatic fate and effects should be conducted in Tier A of phase 2. The Tier A assessment of antimicrobial effects, i.e. the inhibition of activated sludge respiration and cyanobacteria growth, is only mandatory for pharmaceuticals used for antimicrobial purposes. If a risk for effects on microorganisms cannot be excluded in Tier A, additional testing on specific bacteria species (e.g. *Pseudomonas putida*) is required as part of Tier B of phase II.

The importance of making more use of ecotoxicological endpoints targeting microorganisms and microbial communities in environmental risk assessment of antibiotics was recently pointed out (Brandt et al., 2015). Besides, the EMA guideline does not address the effects of mixtures that are formed unintentionally in sewage and the aquatic environment. The risk assessment of pharmaceutical cocktails represents a challenging task since environmental mixtures are highly variable in terms of composition and concentration (Vasquez et al., 2014). Moreover, the high demands on data availability still impede the accurate modeling of cocktail effects (Backhaus, 2016). However, a tiered approach for the predictive screening-level risk assessment of chemical mixtures on the basis of the Concentration Addition (CA) concept was introduced in 2012 (Backhaus and Faust, 2012) and the first tier of this approach was applied to multi-component pharmaceutical mixtures that reportedly occurred in European STP effluents (Backhaus and Karlsson, 2014). This resulted in the indication of substantial risks that were mainly attributed to the specific toxicity of antibiotic agents against cyanobacteria. Hence, pharmaceutical mixtures in the effluent of municipal STPs may pose a particular risk to prokaryotic microorganisms.

This study seeks to further characterize the risk of antimicrobial effects that was previously indicated for a pharmaceutical mixture that was found in the effluent of a STP in Europe (Andreozzi et al., 2003; Backhaus and Karlsson, 2014). For this purpose, a synthetic multi-component mixture of 18 APIs was designed according to the effluent monitoring data that was originally reported by Andreozzi et al. (2003). This mixture was tested for its toxicity to microbial communities in STPs and to selected bacterial species using a multiple endpoint approach. In addition, available data on the toxicity to environmental bacteria were compiled from peer-reviewed literature in order to determine the individual and the estimated joint bacterial toxicity of the individual mixture components.

2. Material and methods

2.1. Preparation of the pharmaceutical mixture

A master solution containing 18 different APIs was prepared on the basis of measured effluent concentrations (MECs) that were previously reported for a European STP (M1-I: Latina, Italy) (Andreozzi et al., 2003). Stock solutions of the 18 individual pharmaceuticals were prepared in methanol and stored at −18 °C until further use. Aliquots of the stock solutions were combined, evaporated under a gentle stream of air until dryness and redissolved in 500 ml ultrapure water to produce a 40,000 fold concentrate of the MEC. The reported MEC and the nominal concentration in the master solution of each component are presented in Table 1. The total measured concentration of the mixture, i.e. the sum of the individual MECs, was 15.4 nmol/l.

2.2. Testing of effects on microbial communities from STPs

The specific characteristics of the investigated exposure scenario necessitated some adaptations of the standard information requirements, i.e. the respiration inhibition test according to OECD TG 209, which can be justified as follows.

i) The conventional respiration inhibition test (OECD 209) fails to assess the effects of antibiotics because of the short test duration (Kümmerer et al., 2004). Therefore, a prolonged test was conducted in analogy to OECD guideline 301 F, which is a continuous respirometric method that was originally developed for the assessment of ready biodegradability (OECD, 1992). The toxicity control of OECD TG 301 F can be considered reliable for observing inhibitory effects of the testing material (European Commission, 2003; ECHA, 2016).

ii) Concentrations of the investigated pharmaceuticals in the influent and within the STP were not available. Therefore, the toxicity of the mixture found in the effluent was determined by using STP effluent as inoculum instead of activated sludge. The bioavailable concentration in the aeration tank, i.e. the dissolved concentration to which the microorganisms are exposed, can be expected to be approximately equal to the effluent concentration

Table 1
Substance names (salt form) of chemicals used for the preparation of the master solution, nominal concentrations in the master solution and measured effluent concentrations (MEC) of the active substances according to Andreozzi et al. (2003).

Substance	CAS	Supplier	Master solution (μmol/l)	MEC[a] (nmol/l)
Acebutolol (hydrochloride)	34381-68-5	Sigma-Aldrich Sweden	4.3	0.12
Carbamazepine	298-46-4	Sigma-Aldrich Sweden	50.8	1.3
Ciprofloxacin	85721-33-1	Fluka	8.5	0.21
Clofibric acid	882-09-7	Sigma-Aldrich Sweden	126.7	3.2
Diclofenac (sodium salt)	15307-79-6	Sigma-Aldrich Sweden	59.1	1.6
Enoxacin	74011-58-8	Sigma-Aldrich Sweden	3.7	0.094
Fenofibrate	49562-28-9	Sigma-Aldrich Sweden	17.7	0.44
Gemfibrozil	25812-30-0	Sigma-Aldrich Sweden	129.4	3.2
Ibuprofen	15687-27-1	Sigma-Aldrich Sweden	34.9	0.87
Lomefloxacin (hydrochloride)	98079-52-8	Sigma-Aldrich Sweden	33.0	0.91
Metoprolol (tartrate)	56392-17-7	Sigma-Aldrich Sweden	0.58	0.037
Naproxen	22204-53-1	Fluka	50.4	1.3
Norfloxacin	70458-96-7	Sigma-Aldrich Sweden	8.8	0.22
Ofloxacin	82419-36-1	Sigma-Aldrich Sweden	64.2	1.6
Oxprenolol (hydrochloride)	6452-73-9	Moravek Biochemicals	1.3	0.038
Propranolol (hydrochloride)	3506-09-0	Fluka	1.4	0.039
Sulfamethoxazole	723-46-6	Sigma-Aldrich Sweden	1.6	0.040
Trimethoprim	738-70-5	Fluka	5.5	0.14

[a] Converted to nmol/l from originally published data in μg/l.

(ECHA, 2016). Moreover, the bacterial community structure of activated sludge can be expected to be similar to the community structure of the final effluent (e.g. Tang et al., 2016).

The number of culturable microorganisms and community-level physiological profiles were monitored in addition to the respirometric activity in order to obtain a more comprehensive picture of the effects on the microbial community.

2.2.1. Preparation of exposure cultures

The test medium was prepared in accordance with OECD guideline 301 F (OECD, 1992). On the day of testing, a grab sample from the effluent of a municipal STP (Lüneburg, Germany, 73,000 inhabitant equivalents) was collected and filtered through a folded paper filter. The exposure cultures were inoculated with the effluent filtrate and supplemented with six different dilutions of the master solution. The final inoculum concentration was 80 ml/l and the exposure concentration of the master solution was 0.1 fold MEC (1.54 nmol/l) to 4000 fold MEC (61.6 μmol/l).

2.2.2. Manometric respirometry

The exposure cultures (control: n = 3, treatments: n = 2) were supplemented with 38.5 mg/l sodium acetate as readily biodegradable substrate, which corresponds to a theoretical oxygen demand (ThOD) of 30 mg/l. Each exposure culture was accompanied by two blank vessels, which contained STP effluent and the test article but no sodium acetate. The test vessels were kept in dark at 20 ± 1 °C under gentle stirring and the biochemical oxygen demand (BOD) resulting from the aerobic biodegradation of sodium acetate was monitored using the OxiTop® system (WTW, Weilheim, Germany).

2.2.3. Enumeration of culturable microorganisms

The exposure cultures (n = 3) were aliquoted into 24 well culture plates and incubated at 20 °C in the dark on a horizontal shaker for 24 and 48 h. After incubation, 10-fold serial dilutions of the exposure cultures were prepared in mineral medium and 0.1 ml of each dilution was plated on yeast extract agar culture medium (ISO, 1999). Colony forming units (CFUs) were determined after incubation for 72 h at 20 °C.

2.2.4. Community-level physiological profiling

The exposure cultures (n = 3) were aliquoted into 24 well culture plates and incubated on a horizontal shaker at 20 °C in the dark for 24 and 48 h. After the exposure period, the test suspensions were diluted 3.5-fold with mineral media and one set of the triplicate wells of a Biolog EcoPlate™ (Biolog, Inc., Hayward, CA) was inoculated with one exposure triplicate. The inoculated EcoPlates™ were incubated at 20 °C for 72 h before an absorbance reading at 590 nm was conducted. The obtained metabolic profiles were analyzed with regard to overall metabolic rate, diversity and similarity as detailed elsewhere (Garland, 1997). The overall metabolic rate was evaluated by calculation of the average well color development (AWCD) over the 31 substrates of the plate. The substrate diversity was evaluated using the Shannon diversity index (H′) as a measure of metabolic richness and evenness as previously described in connection with community-level physiological profiling by Staddon et al. (1997):

$$H' = \sum p_i \ln p_i \quad (1)$$

where p_i is the proportional color development of the *ith* well over total color development of all positive wells. An absorbance threshold of 0.25 was used for the determination of H′ in order to eliminate weak false positive wells (Garland, 1997).

The patterns of substrate utilization were evaluated after correction of measured absorbance values by the AWCD of the respective plate. The relative contribution of different types of substrates to the total well color development was analyzed with respect to substrate categories according to Weber and Legge (2009) (Supporting information, Table S1). In addition, a principal component analysis (PCA) followed by a *t*-test for the screening of variables was conducted to evaluate the similarity of substrate utilization patterns, i.e. the relative rate of well color development among substrates, and to identify the variables (substrates) that were mainly responsible for the differences between the treatments.

2.3. Testing of toxicity to Vibrio fischeri and Pseudomonas putida

2.3.1. Sample preparation

The master solution was sterilized by filtration (PES, 0.22 μm) and stored in aliquots at −150 °C until further usage. On the day of testing, two fold serial dilutions were prepared in ultrapure water to achieve a final test concentrations between 0.25 fold MEC

(3.85 nmol/l) and 20,000 fold MEC (308 μmol/l). In case of the modified luminescent bacteria test, all samples were supplemented with 20 mg/ml sodium chloride.

2.3.2. Modified luminescent bacteria test

This bioassay was especially designed for the assessment of short-term (30 min) and long-term (24 h) inhibition of bacterial luminescence (Menz et al., 2013). In addition, the growth inhibition was evaluated at the transition to the stationary phase after 14 h incubation. An overnight culture of *Vibrio fischeri* NRRL-B-11177 (Hach-Lange GmbH, Düsseldorf) was prepared in SSWC media (5 g/l peptone from casein, 0.5 g/l yeast extract, 3 ml/l glycerol, 30 g/l NaCl, 5.3 g/l NaH_2PO_4, 2.1 g/l K_2HPO_4, 0.2 g/l $MgSO_4$*$7H_2O$, 0.5 g/l $(NH_4)_2HPO_4$) and incubated at 20 °C for 22 ± 2 h. The overnight culture was diluted with fresh SSWC media to an initial density of 20 formazine turbidity units (FTU) and aliquots of 100 μl were transferred into a 96-well microplate. After 30 min preincubation at 15 °C, an initial measurement of luminescence emission and optical density (578 nm) was conducted. Subsequently, the test cultures (n = 3) were supplemented with 100 μL of the respective sample and a continuous measurement of luminescence and optical density was carried out for 24 h at 15 °C.

2.3.3. Modified P. putida cell multiplication inhibition test

The growth inhibition of *P. putida* mt-2 KT2440 (DSM 6125, DSMZ, Braunschweig) was assessed in a modified version of the method according to ISO 10712:1995 (ISO, 1995). Fifty ml of preculture media (1000 mg/l $NaNO_3$, 240 mg/l K_2HPO_4, 120 mg/l KH_2PO_4, 100 mg/l yeast extract, 4000 mg/l $C_6H_{12}O_6$*H_2O, 400 mg/l $MgSO_4$*$7H_2O$, 1 mg/l Fe (III) citrate) were inoculated from a frozen stock culture and incubated for 24 h at 20 °C. This overnight culture was diluted with test media (1000 mg/l $NaNO_3$, 240 mg/l K_2HPO_4, 120 mg/l KH_2PO_4, 4000 mg/l $C_6H_{12}O_6$*H_2O, 400 mg/l $MgSO_4$*$7H_2O$, 1 mg/l Iron(III) citrate) to an initial density of 10 FTU and aliquots of 100 μl were transferred into a 96-well microplate. The test cultures (n = 3) were supplemented with 100 μL of the respective sample and the optical density (600 nm) was determined directly after sample addition and at the transition to the stationary phase after 20 h exposure. In between, the exposure plate was incubated on a horizontal shaker at 20 °C and 150 rpm.

2.4. Chemical analysis

The sterile filtrate of the master solution and the exposure cultures for the testing of effects on mixed inocula were further analyzed in order to provide an approximate confirmation of the nominal exposure concentrations and to confirm that the mixture was not significantly degraded over the course of the experiment. The approximate recovery of the whole pharmaceutical mixture was determined as sum parameter by means of the Non-Purgeable Organic Carbon (NPOC) using a Shimadzu TOC-VCPN analyzer. The addition of hydrochloric acid (2 M) was 1.5% and the sparge time was set to 3 min. The instrument was calibrated with standard solutions of potassium hydrogen phthalate corresponding to 0, 10, 25, 50 ppm NPOC. The recovery of selected substances was determined by LC-MS analysis. The seven antibiotic agents in the mixture were chosen for mass spectrometric analysis, since they were expected to be major drivers of antimicrobial activity. Moreover, the highly lipophilic substances fenofibrate [Log K_{OW} = 5.19 (KOWWIN v1.67 estimate)] and gemfibrozil [Log K_{OW} = 4.77 (KOWWIN v1.67 estimate)] were monitored because their nominal concentrations may have exceeded the reported water solubility. LC-MS analysis was conducted using a Shimadzu Prominence HPLC system coupled to a Shimadzu LCMS-2020 single quadrupole mass spectrometer equipped with an electrospray ion (ESI) source. A Phenomenex kinetex C18 100A column (100 × 2.1 mm, 2.6μ) and mobile phases consisting of 0.1% formic acid (eluent A) and 100% methanol (eluent B) were used for the chromatographic separation. The following gradient program was used: 0.01–1 min 10% B, 1–3 min 98% B, 15–16.5 min 10% B, 16.5–22 min 10% B. The flow rate, column oven temperature and injection volume were set to 0.2 ml min^{-1}, 40 °C and 2 μL, respectively. The mass-spectrometric detection was performed in the selected ion monitoring (SIM) mode with the following m/z and retention times being used for the monitoring of positive ions: ciprofloxacin (332.1; 14.9 min), enoxacin (321.1; 11.7 min), fenofibrate (360.1; 11.3 min), lomefloxacin (352.1; 14.7 min), norfloxacin (320.1; 13.2 min), ofloxacin (362.1; 12.1 min), sulfamethoxazole (254.0; 9.3 min) and trimethoprim (291.1; 9.4 min). Gemfibrozil (249.1; 11.0 min) was monitored in the negative ionization mode. The DL/Qarray voltage was individually optimized for each target analyte through an automated process. The quantification of target substances was done by external standard calibration with a minimum of five calibration points. Standard solutions for the external calibration were prepared in acetonitrile.

2.5. Statistical analysis

The analysis of variance and the modeling of monophasic concentration-response relationships were done with the software package SigmaPlot 11 (Systat Software). The statistical significance of differences between treatments was tested by two-tailed ANOVA, followed by Dunnett's post test to correct for multiple comparisons. Monophasic concentration-response relationships were described by non-linear regression analysis using a four-parameter Hill model. Multiphasic concentration-response relationships were analyzed using the Dr-Fit software (Di Veroli et al., 2015), which automatically generates and ranks dose-response models with varying degrees of multiphasic features using a generalized Hill model. The respective equations of the used concentration-response models are presented together with the obtained parameter estimates in the Supporting information (Tables S4 and S5). PCA followed by a *t*-test for the screening of variables was performed using the Excel add-in Multibase 2015 package (Numerical Dynamics, 2015).

2.6. Literature review

Data on the toxicity of the tested pharmaceuticals to environmental bacteria were extracted from the peer-reviewed literature with the help of electronic databases [WikiPharma (MistraPharma, 2009), ECOTOX (US EPA, 2000)] and substance-specific queries in Scopus (www.scopus.com) using the search string “substance name AND toxicity AND bacteria”. Effect concentrations were obtained as half maximal effective concentration (EC_{50}) or in case of the microbial assay for risk assessment (MARA) as microbial toxic concentration (MTC). In some cases, literature data was only available for the salt forms of the APIs and not for the free acid or free base. Therefore, mass concentrations from the literature were converted into the molar concentration to allow a direct comparison between different forms of a certain API and measured environmental concentrations, respectively. In cases where more than one effect concentration was available for the same pharmaceutical, the lowest obtained value was chosen for the risk characterization. All considered values were traced back to the referenced original publication and are listed in the Supporting information (Table S6).

2.7. Risk characterization

2.7.1. Antimicrobial effects in STPs

The predicted no effect concentration for microorganisms in

STPs ($PNEC_{MICROORGANISM}$) was obtained by dividing the EC_{10} for the STP effluent community by an assessment factor (AF) of 10, which is the default AF recommended by of the EMA guideline (EMA, 2006). In case of the specific testing on bacteria, i.e. *P. putida* growth inhibition, the $PNEC_{MICROORGANISM}$ was derived from the EC_{10} without using an AF as recommended elsewhere (European Commission, 2003; ECHA, 2008). Data on *V. fischeri* was not considered for STP risk assessment, since this species has no direct relevance for STP functioning (ECHA, 2008). Risk quotients (RQ) for antimicrobial effects in STPs were obtained by dividing the MEC by the $PNEC_{MICROORGANISM}$ of the mixture:

$$RQ = \frac{MEC}{PNEC_{MICROORGANISM}} \quad (2)$$

The obtained RQs were interpreted using a commonly applied classification scheme: RQ < 0.1, low risk; RQ = 0.1–1, medium risk; RQ > 1, high risk (e.g. Hernando et al., 2006; Souza et al., 2009; Zhou et al., 2016).

2.7.2. Bacterial toxicity in the aquatic environment

The EMA guideline does not provide a risk assessment framework for bacterial toxicity in the aquatic environment. We assessed the risks for the aquatic environment using toxic units (TUs) as a measure for the effluent toxicity. The TUs of the mixture as a whole were derived from the whole-mixture testing with *P. putida* and *V. fischeri* for a specific effect size of *x* % according to Equation (3).

$$TU_{x,Mix} = \frac{MEC_{Mix}}{EC_{x,\ Mix}} \quad (3)$$

where MEC_{Mix} is the measured effluent concentration of the mixture and $EC_{x,Mix}$ is the concentration of the mixture which provokes x % effect. In addition, the joint toxicity of the mixture components was estimated from literature data on multiple species and endpoints by the sum of toxic units (STUs) for an effect size of 50% according to Equation (4).

$$STU_{50} = \sum_{i=1}^{n} \frac{MEC_i}{EC_{50,i}} \quad (4)$$

where MEC_i is the measured effluent concentration and $EC_{50,i}$ is the half-maximal effective concentration of mixture component i.

3. Results and discussion

3.1. Measured exposure concentrations

The determination of NPOC indicated a total recovery of organic carbon in the sterile filtered master solution and the initial exposure cultures of 83% and 85%, respectively. The average recovery of the seven antibiotic substances was 113% in the filtered master solution and 101% in the initial exposure culture. The measured concentration of enoxacin in the master solution (6.3 μmol/l) was considerably higher than the nominal concentration (3.7 μmol/l), whereas the measured concentration of enoxacin in the initial exposure culture (0.41 μmol/l) was close to the nominal concentration (0.37 μmol/l). The measured concentration of the lipophilic substance gemfibrozil was close to the nominal concentration in all cases. In contrast, fenofibrate was not detectable in any of the analyzed samples, which may be explained by the high lipophilicity and the possibly resulting adsorption to container surfaces. The presented exposure concentrations only represent approximate values due to the limitations of the applied analytical methods. On grounds of efficiency and economy, single MS was applied instead of MS/MS or high resolution MS and the used calibration methods did not correct for potential matrix effects. Nevertheless, eight out of nine analyzed compounds showed a sufficient recovery in the exposure cultures over the whole course of the experiment (Supporting information, Table S2), indicating robust measurements and no significant losses of the test material. Since only minor deviations occurred between the nominal and the measured exposure concentrations, the usage of nominal concentrations in the following toxicity analyses seems justified.

3.2. Effects on effluent microbial communities

The initial oxygen uptake of the mixed inoculum was increasingly reduced at concentrations starting from 100 fold MEC, but this effect disappeared after a plateau was reached in all exposure cultures (Fig. 1A). This plateau can be explained by a growth limitation that occurred after a specific BOD was reached. The achievement of a similar plateau level in all test cultures shows that parts of the exposed microbial community must have retained metabolic activity even under a high toxic pressure, thus being able to catch up with the non-exposed control after a prolonged adaptation phase. Moreover, the initial lag phase was shortened at 1 and 10 fold MEC (Fig. 1A), which led to a transiently increased BOD in these treatments (Fig. 1B). The shorter lag phase may have resulted either from a direct stimulatory effect of the pharmaceutical mixture or from altered competitive interactions within the microbial community. The additional organic carbon stemming from the pharmaceutical mixture can be excluded as a possible cause for the increased BOD, since the additional ThOD at 1 fold MEC and 10 fold MEC was only 0.008 and 0.08 mg/l, respectively.

The numbers of culturable microorganisms in the raw effluent and the initial exposure culture were $7.1*10^3$ (SD = $1.3*10^3$) CFU/ml and $1.0*10^3$ (SD = $7.2*10^1$) CFU/ml, respectively. Even though no additional substrate was added to the exposure cultures, there was a 3 log stages increase of the CFU count in the control within the initial 24 h. However, CFU were only marginally increased between 24 and 48 h (Fig. 2A), implying that, similar to the BOD measurement, a growth limitation was achieved with prolonged exposure. In comparison to the control sample, the log CFU values were significantly reduced at 1000 fold MEC after 24 h and at 4000 fold MEC after 48 h exposure (Fig. 2A).

The overall metabolic activity, measured as AWCD, was affected at lower concentrations than CFU, since there was already a statistically significant reduction of AWCD at 100 fold MEC and 1 fold MEC after 24 and 48 h exposure, respectively (Fig. 2B). However, in contrast to 1 fold MEC, a statistically significant difference to the control was not indicated for 10 fold MEC due to a slightly higher standard deviation. The decline of ACDW after 24 h at 1000 fold MEC was most probably a side-effect of the reduced culture density (CFU), since these parameters are known to be correlated (Garland and Mills, 1991). However, after 48 h exposure to 1000 fold MEC, AWCD was still significantly reduced, but CFU was not. This shows that the reduced metabolic activity after 48 h was probably not resulting from a reduced inoculum density, but rather from a generally reduced respiration and/or an altered microbial community structure. The Shannon diversity index (H′) significantly declined only after an exposure to 1000 fold MEC after 24 h and to 4000 fold MEC after 48 h exposure (Fig. 2C). This shows that the observed reduction of metabolic activity (AWCD) at lower concentrations was not accompanied by a decline of metabolic diversity.

3.2.1. Effects on metabolic patterns

The relative contribution of different substrate categories to the total well colour development was not significantly altered in the

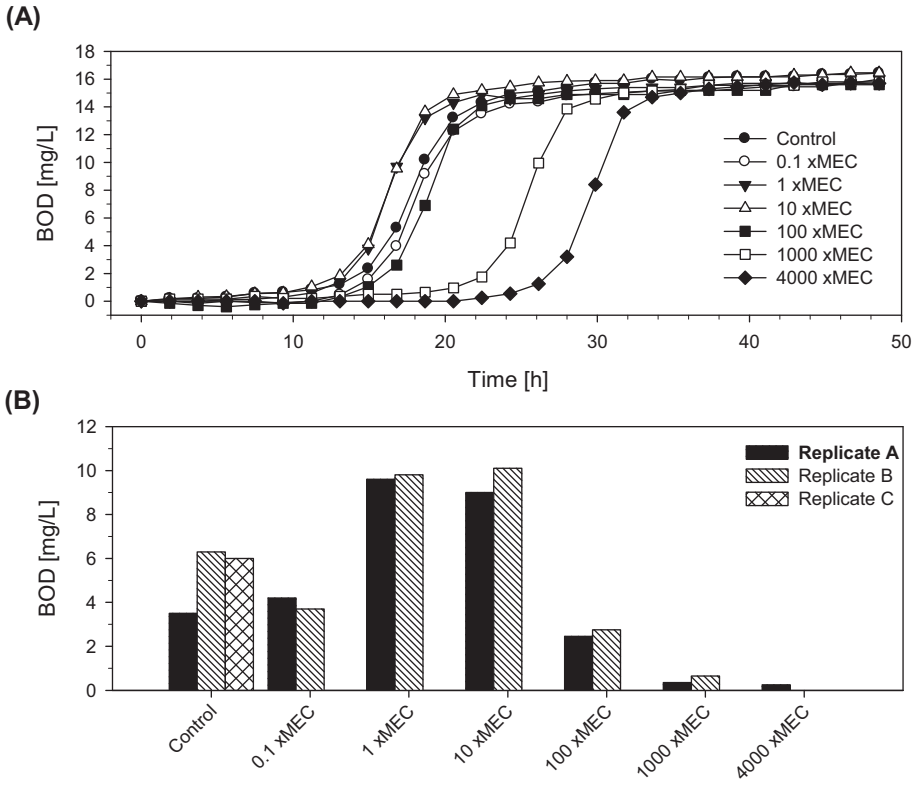

Fig. 1. A: Development of the biochemical oxygen demand (BOD) in the exposure cultures supplemented with 38.5 mg/l sodium acetate and different concentrations of the pharmaceutical mixture (mean values, control: n = 3, treatments: n = 2). B: BOD in the exposure cultures at the endpoint measurement with t = 17 h. The measured effluent concentration (MEC) of the mixture was 15.4 nmol/l.

range of 0.1–10 fold MEC, whereas the relative proportions became increasingly different starting from 100 fold MEC (Supporting information, Fig. S1). The shift at 100 fold MEC became even more evident after 48 h. This was attributed to a significantly increased ($p < 0.05$) proportion of carbohydrates and to a significantly reduced ($p < 0.05$) proportion of amines/amides and carboxylic/acetic acids.

The outcome of the principal component analysis (PCA) showed that the reduction of AWCD at 10 fold MEC and above was also accompanied by an alteration of the metabolic patterns within the microbial community. After 24 h exposure, 34.2% and 13.6% of the total variance were explained in the first two principal components (Fig. 3A). The metabolic profile of the 100 fold MEC treatment was grouped differently from the main cluster, whereas the patterns of 0.1 fold MEC, 1 fold MEC and 10 fold MEC were still clustered similar to the control. After 48 h, 38.8% and 11% of the total variance were explained in the first two principal components. The treatments with 10 fold MEC and 100 fold MEC were grouped differently from the control (Fig. 3B) and the shift between 10 fold MEC and 100 fold MEC became more pronounced with increasing exposure time. A variable screening was conducted for the treatment with 10 fold MEC to extract variables that contributed most to the observed difference to the control. The obtained differential scores are based on the mean ratio and the *t*-test p value (Numerical Dynamics, 2015). The substrates D,L-α-glycerol phosphate (score = 6.118), glycyl-L-glutamic acid (score = 3.338) and L-threonine (score = 2.999) contributed most as significantly increased variables ($p < 0.05$). The substrates phenylethylamine (score = 2.358), D-cellobiose (score = 1.818) and D-galacturonic acid (score = 1.360) were contributing most as decreased variables, but the differences to the control were not significant ($p > 0.05$).

3.2.2. Concentration-response relationships for quantitative risk assessment

The community-level endpoints BOD after 17 h and AWCD after 48 h showed the highest sensitivity and were therefore considered in the risk characterization. The concentration-response curve for BOD was well described by a biphasic model with an initial stimulatory effect in the range of 1–10 fold MEC (Fig. 4A), whereas the observations for AWCD could be fitted with a monophasic concentration-response model (Fig. 4B). The different curve shapes can be explained by the different assay principles, since BOD is based on a single substrate whereas AWCD represents the average over 31 substrates. The derived inhibitory EC_{10} values for risk characterization were 61 fold MEC (939 nmol/l) for BOD and 15.7 fold MEC (242 nmol/l) for AWCD. Stimulatory effects were not considered for risk characterization, but it should be recognized that the stimulatory EC_{10} for BOD of 0.67 fold MEC (10.3 nmol/l) was even lower than the MEC.

3.3. Toxicity to specific bacteria

3.3.1. Mixture toxicity to P. putida and V. fischeri

The testing of the whole mixture resulted in EC_{10} values for growth inhibition in *P. putida* and *V. fischeri* of 14.6 fold MEC (225 nmol/l) and 5.4 fold MEC (83 nmol/l), respectively (Fig. 5A). In case of *V. fischeri*, the effective concentration range for the inhibition of long-term luminescence was similar to inhibition of growth, but the effective range for short-term luminescence inhibition was several orders of magnitude higher (Fig. 5B). The short-term luminescence is mainly regarded as an endpoint for unspecific baseline toxicity (Escher et al., 2008; Lee et al., 2013; Neale et al., 2017) or direct impacts on the bacterial energy metabolism

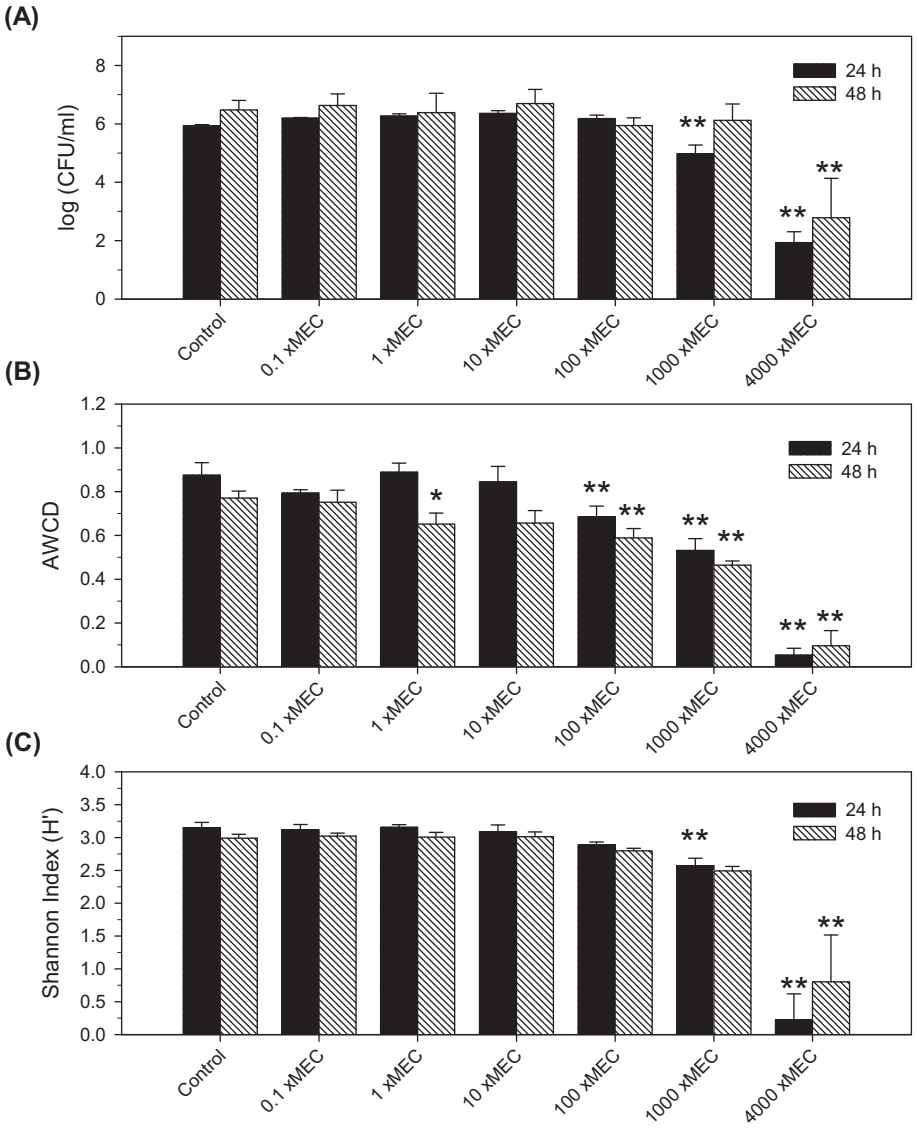

Fig. 2. A: Colony forming units (CFU), B: average well colour development (AWCD) and C: substrate diversity (H′) of the test cultures after 24 h and 48 h exposure to different concentrations of the pharmaceutical mixture (mean ± SD, n = 3, *p < 0.05, **p < 0.01). The measured effluent concentration (MEC) of the mixture was 15.4 nmol/l.

(Backhaus et al., 1997; Altenburger et al., 2000). In contrast, endpoints that are related to bacterial cell multiplication, such as long-term luminescence and growth, are much more sensitive to substances that specifically interfere with biosynthetic pathways (Backhaus et al., 1997; Majewsky et al., 2014; Menz et al., 2013; Neale et al., 2017). Therefore, it is assumed that the observed antibacterial effect of the pharmaceutical mixture is mainly caused by the antibiotic agents in the mixture. This was fully supported by the relative contributions to the sum of toxic units that was estimated from literature data (Table 4).

3.3.2. Literature review of single-substance toxicity

The literature review on antibacterial activity yielded 89 effect concentrations for 12 different species and 16 mixture components (Supporting information, Table S6). In case of the β-blockers acebutolol and oxprenolol no data on antibacterial activity could be obtained. The lowest published effect concentrations (EC_{50}) of the individual antibiotics in the mixture range between 15 and 150 nmol/l, whereas 0.9–190 μmol/l was the range of bacterial EC_{50} values found for the non-antibiotic mixture components. It should be noted that about half of the available effect data was based either on short-term (5–30 min) or long-term (16–72 h) inhibition of bacterial luminescence, whereby the latter is usually more sensitive but maybe ecologically less significant than the inhibition of growth (Gellert, 2000). Moreover, there was only short-term data on luminescence inhibition available in case of ibuprofen. As previously outlined in Section 3.3.1, the delayed onset of effects is a well-established feature of substances that specifically interfere with biosynthetic pathways of prokaryotic cells (e.g. antibiotics). This explains the strong differences between the reported short-term and long-term/growth inhibition data of some antibiotic agents. Moreover, the literature review provided evidence for considerable interspecies variations, which highlights the necessity of multispecies testing with regard to antibacterial effects. This may be especially important to the risk assessment of narrow spectrum antibiotics that are only active against specific groups of bacterial types.

3.4. Risk characterization

3.4.1. Antimicrobial effects in STPs

A medium risk was identified for mixed microbial communities in STPs considering BOD and AWCD as the most sensitive

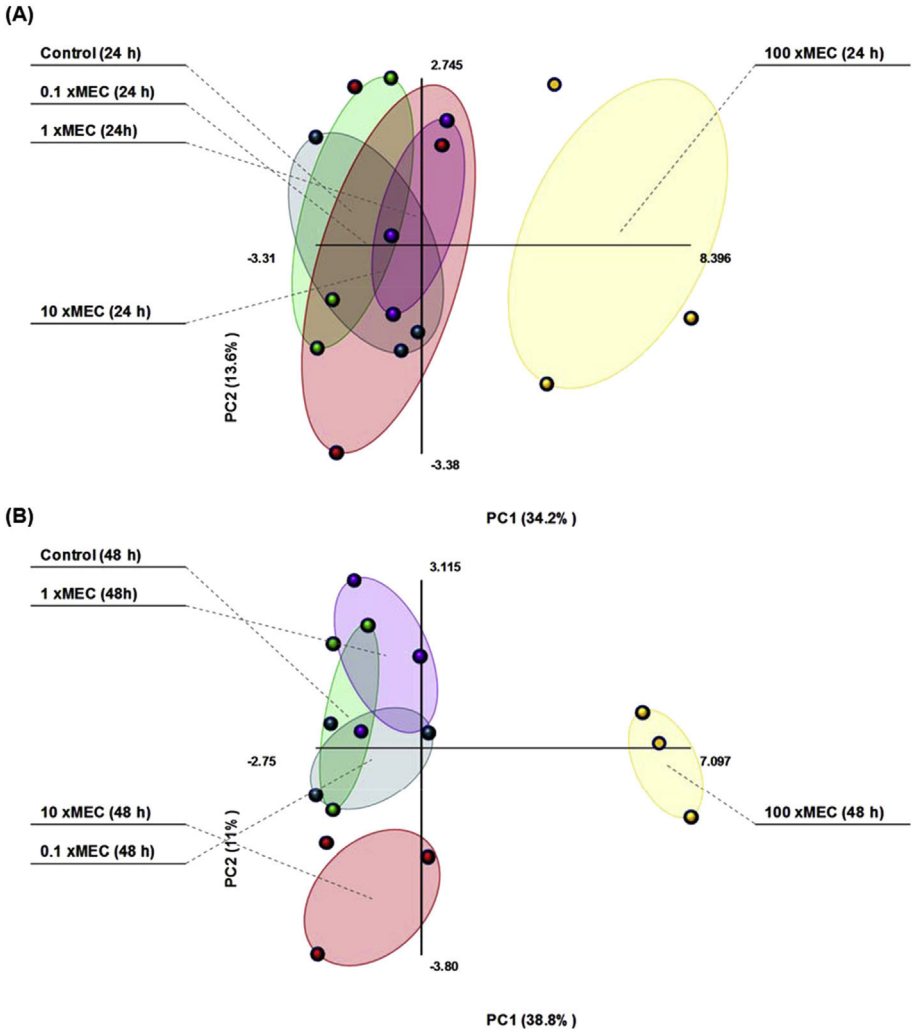

Fig. 3. Ordination produced from PCA of metabolic patterns in the exposure cultures after 24 h (A) and 48 h exposure (B) to the pharmaceutical mixture at 0.1 fold MEC (blue), 1 fold MEC (purple), 10 fold MEC (red) and 100 fold MEC (yellow) in comparison to the control (green). The measured effluent concentration (MEC) of the mixture was 15.4 nmol/l. The component loadings are presented in the Supporting information (Table S3). (For interpretation of the references to colour in this figure legend, the reader is referred to the web version of this article.)

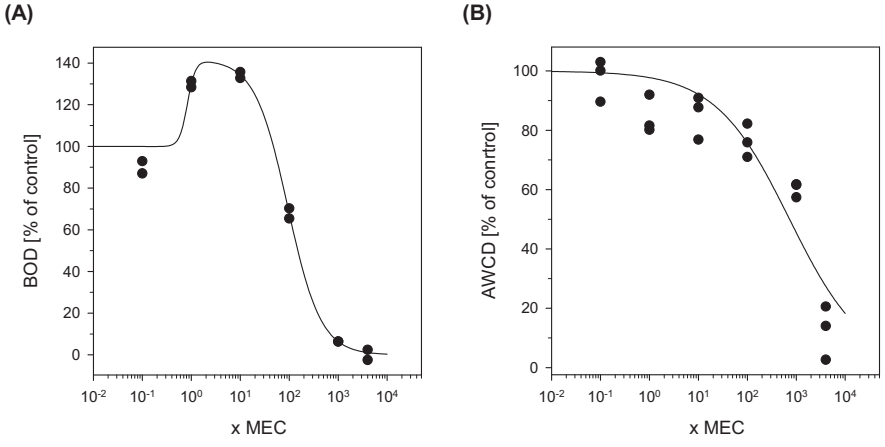

Fig. 4. Concentration-response curves of the pharmaceutical mixture for the community-level endpoints A: biochemical oxygen demand (BOD) and B: average well color development (AWCD).The measured effluent concentration (MEC) of the mixture was 15.4 nmol/l.

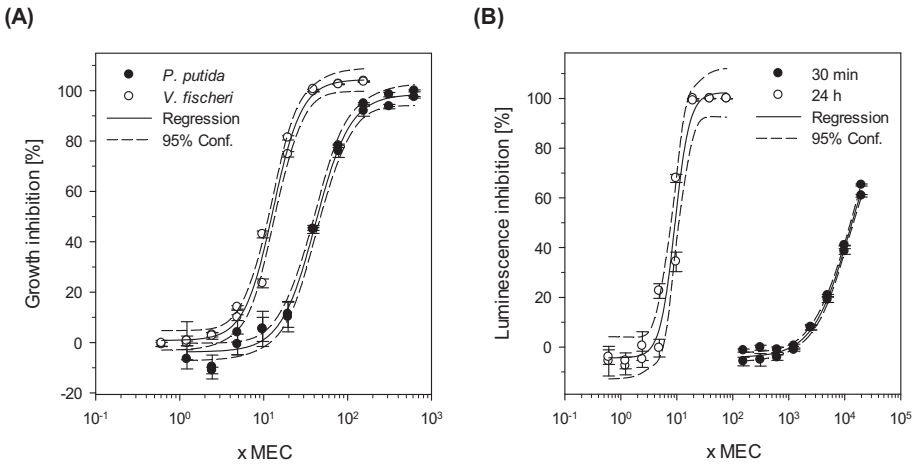

Fig. 5. Concentration-response curves of the pharmaceutical mixture for the toxicity to specific bacteria A: inhibition of bacterial growth (mean ± SD, n = 3) and B: inhibition of bioluminescence in *V. fischeri* (mean ± SD, n = 3). The measured effluent concentration (MEC) of the mixture was 15.4 nmol/l.

endpoints. However, the initially identified risk on a multispecies level was not confirmed by the testing of a specific bacterial species (Table 2). It should be noted that different assessment factors were used for the derivation of multispecies and single-species PNEC values. Moreover, *P. putida* is known to be very tolerant to chemical stress in comparison to other bacterial species (Dworkin et al., 2006; Isken et al., 1999) and indications for this comparatively high tolerance were also found in the present study (Fig. 5A). Hence, it must be questioned in general whether the current EMA guideline approach is sufficiently protective for microbial communities in STPs, especially since the conventional respiration inhibition test (OECD 209) reportedly failed to assess the effects of antibiotics (Kümmerer et al., 2004). In contrast, the adapted multispecies approach of the present study must be regarded as comparatively sensitive, since it was able to detect a response even in the environmental concentration range. The observed alterations of substrate utilization rates and patterns suggest that pharmaceutical cocktails could principally shape microbial communities in the activated sludge and the final effluent. However, the relevance of such effects with regard to STP functioning and resistance selection is not yet established.

3.4.2. Bacterial toxicity in the aquatic environment

The experimental testing of the whole mixture resulted in TU_{50} values between 0.024 and 0.11 for the different species and endpoints in relation to the MEC (Table 3). This means that the mixture concentration in the effluent is approximately 10 times lower than the concentration that could cause an effect of 50%. If a conservative factor of 10 is assumed for the extrapolation from the EC_{50} down to an acceptable no-effect concentration, the remaining margin of exposure for the aquatic environment would solely depend on the actual dilution factor of the recipient stream. According to published literature, actual dilution factors can vary at least from 1.4 to 50 (Backhaus and Karlsson, 2014). However, this margin does still not account for the remaining uncertainties (e.g. laboratory to field extrapolation and interspecies variations), which means that a risk for environmental bacteria cannot be ruled out. This conclusion would be in good agreement with previous studies that identified a significant risk for specific antibiotics in the aquatic environment (Ebert et al., 2011; Halling-Sørensen et al., 2000; Robinson et al., 2005).

Table 2
Calculation of risk quotients (RQ) for antimicrobial effects in STPs. The 10% effect concentration (EC_{10}), the measured effluent concentration (MEC) and the predicted no effect concentration (PNEC) is given as mixture concentration in nmol/l.

Community/Species	Endpoint	EC_{10}	AF	PNEC	MEC	RQ	Risk
STP Effluent	BOD	939	10	93.9	15.4	0.16	medium
	AWCD	242	10	24.2	15.4	0.64	medium
P. putida	growth	225	1	225	15.4	0.07	low

Table 3
Estimation of toxic units (TU) for antibacterial activity at the measured effluent concentration (MEC). The effective concentrations (EC_{10}, EC_{50}) and the MEC of the pharmaceutical mixture are presented as mixture concentration in nmol/l.

Species	Endpoint	EC_{10}	EC_{50}	MEC	TU_{10}	TU_{50}
P. putida	growth	225	640	15.4	0.068	0.024
V. fischeri	growth	84	199	15.4	0.183	0.077
	luminescence (24 h)	73	142	15.4	0.211	0.108

The estimated joint activity of the mixture was clearly dominated by the components with known antibiotic activity, which contributed with 98% to the STU_{50} (Table 4). The fluoroquinolone antibiotics ofloxacin, lomefloxacin and ciprofloxacin were identified as the most important contributors with individual TU_{50} values of 0.064, 0.014 and 0.014, respectively, corresponding to 64%, 14% and 14% of the total STU_{50}.

The experimentally determined TU_{50} values of the mixture for *V. fischeri* were in very good agreement with the calculated STU_{50} (Tables 3 and 4), which demonstrates that an approximate estimation of the bacterial toxicity in complex mixtures by using the Concentration Addition model is feasible. Similar findings were previously reported for less heterogeneous pharmaceutical mixtures containing only quinolones (Backhaus et al., 2000) and for mixtures of antibiotics and non-antibiotic pharmaceuticals (Neale et al., 2017). However, it should be noted that in case of *P. putida*, the literature-based TU_{50} of ofloxacin is considerably higher than the experimentally determined TU_{50} of the whole mixture (Tables 3 and 4). This inconsistency is most probably attributed to modifications of the experimental setup that are detailed elsewhere (Kümmerer et al., 1996, 2000). This example shows the importance of a high degree of standardization for an accurate component-based prediction of mixture toxicity.

3.5. Implications for risk assessment

The presented risk assessment does not account for any non-

Table 4
Toxic units (TU_{50}) of individual mixture components and their sum of toxic units (STU_{50}) for antibacterial activity at the measured effluent concentration based on the lowest reported EC_{50} value of each mixture component. An exhaustive summary of underlying effect concentrations with references is provided in the supporting information (Table S4).

Substance	Species	Endpoint	EC_{50}[b] (nmol/l)	(S)TU_{50}
Ofloxacin[a]	*Pseudomonas putida*	growth	2.5E+01	6.4E-02
Lomefloxacin[a]	*Vibrio fischeri*	luminescence (24 h)	6.4E+01	1.4E-02
Ciprofloxacin[a]	*Microcystis aeruginosa*	growth	1.5E+01	1.4E-02
Norfloxacin[a]	*Vibrio fischeri*	luminescence (24 h)	6.9E+01	3.2E-03
Trimethoprim[a]	*Bacillus pumilus*	growth	9.6E+01	1.5E-03
Naproxen	*Vibrio fischeri*	luminescence (16 h)	9.3E+02	1.4E-03
Enoxacin[a]	*Vibrio fischeri*	luminescence (24 h)	1.5E+02	6.1E-04
Sulfamethoxazole[a]	*Synechococcus leopoliensis*	growth	1.1E+02	3.8E-04
Diclofenac	*Vibrio fischeri*	luminescence (16 h)	6.2E+03	2.6E-04
Gemfibrozil	*Vibrio fischeri*	luminescence (16 h)	1.5E+04	2.1E-04
Fenofibrate	*Vibrio fischeri*	luminescence (30 min)	4.8E+03	9.2E-05
Propranolol	*Synechococcus leopoliensis*	growth	2.3E+03	1.7E-05
Clofibric acid	*Synechococcus leopoliensis*	growth	1.9E+05	1.7E-05
Ibuprofen	*Vibrio fischeri*	luminescence (15 min)	5.9E+04	1.5E-05
Carbamazepine	*Synechococcus leopoliensis*	growth	1.4E+05	9.1E-06
Metoprolol	*Vibrio fischeri*	luminescence (15 min)	5.4E+04	6.8E-07
Acebutolol	–	–	n.a.	n.d.
Oxprenolol	–	–	n.a.	n.d.
Mixture	–	–	1.5E+02	1.0E-01

[a] Antibiotic substance.
[b] Converted to nmol/l if the original data was published in mg/l or μg/l.

surveyed APIs, metabolites or transformation products. Consequently, this study is inevitably biased towards underestimating the actual risk of pharmaceutical mixtures. Nevertheless, a possible risk was identified for microorganisms in STPs and the aquatic environment using a combination of experimental and predictive methods. These findings underline the importance of considering the joint effects on microbial communities in the environmental assessment of pharmaceuticals.

A major obstacle in mixture risk assessment of pharmaceuticals is the high variability of environmental mixtures, which clearly argues for a component-based modeling approach and against the testing of whole mixtures. Our findings suggested that a reliable estimation of the joint bacterial toxicity in complex pharmaceutical mixtures is principally feasible. However, the lower the degree of standardization in the underlying data set, the more uncertain are resulting mixture-level estimations. Hence, it is of utmost importance to collect more harmonized data with a standardized testing protocol for all potentially relevant compounds. This assessment should include a well-defined base set of representative bacterial strains in order to account for differences in species sensitivity and to include a variety of functional traits. Once available, this data could be used for the retrospective determination of species- and site-specific STU values in order to predict the relative impact of each contaminant on a variety of bacterial species and their associated ecosystem functions.

4. Conclusions

Pharmaceutical cocktails shape microbial communities at concentrations relevant to STPs and the effluent receiving aquatic environment. However, the risk of antimicrobial mixture effects was completely dominated by the presence of antibiotics, whereas other pharmaceutical classes contributed only negligibly to the mixture toxicity. The joint bacterial toxicity can be estimated with sufficient accuracy from the individual toxicity of the mixture components, provided that existing data gaps will be closed. An important step into this direction would be the collection of more standardized data on a systematically selected base set of representative environmental bacteria. In the overall view, the outcome of this study argues for a more sophisticated bacterial toxicity assessment of environmentally relevant pharmaceuticals, especially for those with a mode of action that is known to specifically affect prokaryotic microorganisms.

Acknowledgments

The authors would like to thank Janin Westphal and Stefanie Wieck (both Leuphana University) for the great support in the chemical analysis. This work was supported by the European Union (European Commission, FP7 projects PHARMAS and SOLUTIONS, grants no. 265346 and 603437), the University of Gothenburg (Centre for Antibiotic Resistance Research, CARe (care.gu.se)), and by a scholarship (J. Menz) within the Innovations-Inkubator Lüneburg (Teilmaßnahme 1.4, Graduate School).

Appendix A. Supplementary data

Supplementary data related to this article can be found at https://doi.org/10.1016/j.envpol.2017.09.009.

References

Altenburger, R., Backhaus, T., Boedeker, W., Faust, M., Scholze, M., Grimme, L.H., 2000. Predictability of the toxicity of multiple chemical mixtures to Vibrio fischeri: mixtures composed of similarly acting chemicals. Environ. Toxicol. Chem. 19, 2341–2347.
Andreozzi, R., Raffaele, M., Nicklas, P., 2003. Pharmaceuticals in STP effluents and their solar photodegradation in aquatic environment. Chemosphere 50, 1319–1330.
Backhaus, T., Scholze, M., Grimme, L.H., 2000. The single substance and mixture toxicity of quinolones to the bioluminescent bacterium Vibrio fischeri. Aquat. Toxicol. 49, 49–61.
Backhaus, T., 2014. Medicines, shaken and stirred: a critical review on the ecotoxicology of pharmaceutical mixtures. Philos. Trans. R. Soc. Lond., B, Biol. Sci. 369, 20130585.
Backhaus, T., 2016. Environmental risk assessment of pharmaceutical mixtures: demands, gaps, and possible bridges. AAPS J. 18, 804–813.
Backhaus, T., Faust, M., 2012. Predictive environmental risk assessment of chemical mixtures: a conceptual framework. Environ. Sci. Technol. 46, 2564–2573.
Backhaus, T., Froehner, K., Altenburger, R., Grimme, L.H., 1997. Toxicity testing with Vibrio fischeri: a comparison between the long term (24 h) and the short term (30 min) bioassay. Chemosphere 35, 2925–2938.
Backhaus, T., Karlsson, M., 2014. Screening level mixture risk assessment of pharmaceuticals in STP effluents. Water. Res. 49, 157–165.
Barra Caracciolo, A., Topp, E., Grenni, P., 2015. Pharmaceuticals in the environment: biodegradation and effects on natural microbial communities. A review.

J. Pharm. Biomed. 106, 25–36.
Bengtsson-Palme, J., Larsson, D.J., 2016. Concentrations of antibiotics predicted to select for resistant bacteria: proposed limits for environmental regulation. Environ. Int. 86, 140–149.
Brandt, K.K., Amézquita, A., Backhaus, T., Boxall, A., Coors, A., Heberer, T., Lawrence, J.R., Lazorchak, J., Schönfeld, J., Snape, J.R., Zhu, Y.-G., Topp, E., 2015. Ecotoxicological assessment of antibiotics: a call for improved consideration of microorganisms. Environ. Int. 85, 189–205.
Corcoll, N., Acuña, V., Barceló, D., Casellas, M., Guasch, H., Huerta, B., Petrovic, M., Ponsatí, L., Rodríguez-Mozaz, S., Sabater, S., 2014. Pollution-induced community tolerance to non-steroidal anti-inflammatory drugs (NSAIDs) in fluvial biofilm communities affected by WWTP effluents. Chemosphere 112, 185–193.
Di Veroli, G.Y., Fornari, C., Goldlust, I., Mills, G., Koh, S.B., Bramhall, J.L., Richards, F.M., Jodrell, D.I., 2015. An automated fitting procedure and software for dose-response curves with multiphasic features. Sci. Rep. 5, 14701.
Dworkin, M., Falkow, S., Rosenberg, E., Schleifer, K.-H., Stackebrandt, E. (Eds.), 2006. The Prokaryotes. Springer, New York.
Ebert, I., Bachmann, J., Kühnen, U., Küster, A., Kussatz, C., Maletzki, D., Schlüter, C., 2011. Toxicity of the fluoroquinolone antibiotics enrofloxacin and ciprofloxacin to photoautotrophic aquatic organisms. Environ. Toxicol. Chem. 30, 2786–2792.
Escher, B.I., Bramaz, N., Mueller, J.F., Quayle, P., Rutishauser, S., Vermeirssen, E.L.M., 2008. Toxic equivalent concentrations (TEQs) for baseline toxicity and specific modes of action as a tool to improve interpretation of ecotoxicity testing of environmental samples. J. Environ. Monit. 10, 612–621.
ECHA (European Chemicals Agency), 2008. Guidance on Information Requirements and Chemical Safety Assessment. Chapter R.10: Characterisation of dose [concentration]-response for environment.
ECHA (European Chemicals Agency), 2016. Guidance on Information Requirements and Chemical Safety Assessment. Chapter R. 16: Environmental Exposure Estimation.
EMA (European Medicines Agency), 2006. Guideline on the Environmental Risk Assessment of Medicinal Products for Human Use. Doc. Ref. EMEA/CHMP/SWP/4447/00 corr 2.
European Commission, 2003. Technical Guidance Document on Risk Assessment in Support of Commission Directive 93/67/EEC on Risk Assessment for New Notified Substances Part II. Commission Regulation (EC) No 1488/94 on risk assessment for existing substances and of directive 98/8/EC of the European Parliament and of the Council concerning the placing of biocidal products on the market: Part II Environmental risk assessment. Office for Official Publications of the European Communities, Luxembourg.
Fatta-Kassinos, D., Meric, S., Nikolaou, A., 2011. Pharmaceutical residues in environmental waters and wastewater: current state of knowledge and future research. Anal. Bioanal. Chem. 399, 251–275.
Garland, J.L., 1997. Analysis and interpretation of community-level physiological profiles in microbial ecology. FEMS Microbiol. Ecol. 24, 289–300.
Garland, J.L., Mills, A.L., 1991. Classification and characterization of heterotrophic microbial communities on the basis of patterns of community-level sole-carbon-source utilization. Appl. Environ. Microbiol. 57, 2351–2359.
Gellert, G., 2000. Sensitivity and significance of luminescent bacteria in chronic toxicity testing based on growth and bioluminescence. Ecotoxicol. Environ. Saf. 45, 87–91.
Goñi-Urriza, M., Capdepuy, M., Arpin, C., Raymond, N., Caumette, P., Quentin, C., 2000. Impact of an urban effluent on antibiotic resistance of riverine Enterobacteriaceae and Aeromonas spp. Appl. Environ. Microb. 66, 125–132.
Gullberg, E., Cao, S., Berg, O.G., Ilbäck, C., Sandegren, L., Hughes, D., Andersson, D.I., 2011. Selection of resistant bacteria at very low antibiotic concentrations. PLoS Pathog. 7, e1002158.
Halling-Sørensen, B., Lützhøft, H.C., Andersen, H.R., Ingerslev, F., 2000. Environmental risk assessment of antibiotics: comparison of mecillinam, trimethoprim and ciprofloxacin. J. Antimicrob. Chemother. 46 (Suppl. 1), 53–58.
Heberer, T., 2002. Occurrence, fate, and removal of pharmaceutical residues in the aquatic environment: a review of recent research data. Toxicol. Lett. 131, 5–17.
Hernando, M.D., Mezcua, M., Fernandez-Alba, A.R., Barcelo, D., 2006. Environmental risk assessment of pharmaceutical residues in wastewater effluents, surface waters and sediments. Talanta 69, 334–342.
Isken, S., Derks, A., Wolffs, P.F., de Bont, J.A., 1999. Effect of organic solvents on the yield of solvent-tolerant Pseudomonas putida S12. Appl. Environ. Microbiol. 65, 2631–2635.
ISO, 1999. Water Quality - Enumeration of Culturable Micro-organisms - Colony Count by Inoculation in a Nutrient Agar Culture Medium (ISO 6222:1999). German version EN ISO 6222:1999.
ISO, 1995. Water Quality - Pseudomonas Putida Growth Inhibition Test (Pseudomonas Cell Multiplication Inhibition Test) (ISO 10712:1995). German version EN ISO 10712:1995.
Jelić, A., Gros, M., Petrović, M., Ginebreda, A., Barceló, D., 2012. Occurrence and elimination of pharmaceuticals during conventional wastewater treatment. In: Guasch, H., Ginebreda, A., Geiszinger, A. (Eds.), Emerging and Priority Pollutants in Rivers, vol. 19. The Handbook of Environmental Chemistry. Springer, Berlin, Heidelberg.
Kong, Z., Vanrolleghem, P., Verstraete, W., 1993. An activated sludge-based biosensor for rapid IC50 estimation and on-line toxicity monitoring. Biosens. Bioelectron. 8, 49–58.
Kraigher, B., Kosjek, T., Heath, E., Kompare, B., Mandic-Mulec, I., 2008. Influence of pharmaceutical residues on the structure of activated sludge bacterial communities in wastewater treatment bioreactors. Water Res. 42, 4578–4588.
Kümmerer, K., 2008. Pharmaceuticals in the environment – a brief summary. In: Kümmerer, K. (Ed.), Pharmaceuticals in the Environment: Sources, Fate, Effects and Risks. Springer, Berlin, Heidelberg, pp. 3–21.
Kümmerer, K., 2009. Antibiotics in the aquatic environment – a review – Part I. Chemosphere 75, 417–434.
Kümmerer, K., Al-Ahmad, A., Mersch-Sundermann, V., 2000. Biodegradability of some antibiotics, elimination of the genotoxicity and affection of wastewater bacteria in a simple test. Chemosphere 40, 701–710.
Kümmerer, K., Al-Ahmad, A., Steger-Hartmann, T., 1996. Epirubicin hydrochloride in the aquatic environment - biodegradation and bacterial toxicity [in German] Umweltmed. Forsch. Prax. 1, 133–137.
Kümmerer, K., Alexy, R., Huttig, J., Scholl, A., 2004. Standardized tests fail to assess the effects of antibiotics on environmental bacteria. Water Res. 38, 2111–2116.
Kümmerer, K., Henninger, A., 2003. Promoting resistance by the emission of antibiotics from hospitals and households into effluent. Clin. Microbiol. Infect. 9, 1203–1214.
Lawrence, J.R., Swerhone, G.D., Wassenaar, L.I., Neu, T.R., 2005. Effects of selected pharmaceuticals on riverine biofilm communities. Can. J. Microbiol. 51, 655–669.
Lee, S.-Y., Kang, H.-J., Kwon, J.-H., 2013. Toxicity cutoff of aromatic hydrocarbons for luminescence inhibition of Vibrio fischeri. Ecotoxicol. Environ. Saf. 94, 116–122.
Majewsky, M., Wagner, D., Delay, M., Bräse, S., Yargeau, V., Horn, H., 2014. Antibacterial activity of sulfamethoxazole transformation products (TPs): general relevance for sulfonamide TPs modified at the para position. Chem. Res. Toxicol. 27, 1821–1828.
Menz, J., Schneider, M., Kümmerer, K., 2013. Toxicity testing with luminescent bacteria – characterization of an automated method for the combined assessment of acute and chronic effects. Chemosphere 93, 990–996.
MistraPharma, 2009. WikiPharma Database on Publicly Available Ecotoxicity Data for Active Pharmaceutical Ingredients. Accessed 5 November 2016. http://www.wikipharma.org.
Neale, P.A., Leusch, F.D.L., Escher, B.I., 2017. Applying mixture toxicity modelling to predict bacterial bioluminescence inhibition by non-specifically acting pharmaceuticals and specifically acting antibiotics. Chemosphere 173, 387–394.
Numerical Dynamics, 2015. Multibase 2015 Excel Add-in. Accessed 5 November 2016. http://www.numericaldynamics.com.
OECD (Organisation for Economic Co-operation and Development), 1992. Test No. 301: Ready Biodegradability.
Reed, H.E., Martiny, J.B.H., 2007. Testing the functional significance of microbial composition in natural communities. FEMS Microbiol. Ecol. 62, 161–170.
Rizzo, L., Manaia, C., Merlin, C., Schwartz, T., Dagot, C., Ploy, M., Michael, I., Fatta-Kassinos, D., 2013. Urban wastewater treatment plants as hotspots for antibiotic resistant bacteria and genes spread into the environment: a review. Sci. Total Environ. 447, 345–360.
Roberts, P.H., Thomas, K.V., 2006. The occurrence of selected pharmaceuticals in wastewater effluent and surface waters of the lower Tyne catchment. Sci. Total Environ. 356, 143–153.
Robinson, A.A., Belden, J.B., Lydy, M.J., 2005. Toxicity of fluoroquinolone antibiotics to aquatic organisms. Environ. Toxicol. Chem. 24, 423–430.
Shchegolkova, N.M., Krasnov, G.S., Belova, A.A., Dmitriev, A.A., Kharitonov, S.L., Klimina, K.M., Melnikova, N.V., Kudryavtseva, A.V., 2016. Microbial community structure of activated sludge in treatment plants with different wastewater compositions. Front. Microbiol. 7, 112.
Souza, S.M.L. de, Vasconcelos, E.C.d., Dziedzic, M., Oliveira, C.M.R. de, 2009. Environmental risk assessment of antibiotics: an intensive care unit analysis. Chemosphere 77, 962–967.
Staddon, Duchesne, Trevors, 1997. Microbial diversity and community structure of postdisturbance forest soils as determined by sole-carbon-source utilization patterns. Microb. Ecol. 34 (2), 125–130.
Tang, J., Bu, Y., Zhang, X.-X., Huang, K., He, X., Ye, L., Shan, Z., Ren, H., 2016. Metagenomic analysis of bacterial community composition and antibiotic resistance genes in a wastewater treatment plant and its receiving surface water. Ecotoxicol. Environ. Saf. 132, 260–269.
Tlili, A., Berard, A., Blanck, H., Bouchez, A., Cássio, F., Eriksson, K.M., Morin, S., Montuelle, B., Navarro, E., Pascoal, C., Pesce, S., Schmitt-Jansen, M., Behra, R., 2015. Pollution-induced community tolerance (PICT): towards an ecologically relevant risk assessment of chemicals in aquatic systems. Freshw. Biol. 61, 2141–2151.
US EPA (US Environmental Protection Agency), 2000. ECOTOX Database. Accessed 5 November 2016. https://cfpub.epa.gov/ecotox.
Vasquez, M., Lambrianides, A., Schneider, M., Kümmerer, K., Fatta-Kassinos, D., 2014. Environmental side effects of pharmaceutical cocktails: what we know and what we should know. J. Hazard. Mater 279, 169–189.
Veach, A., Bernot, M.J., Mitchell, J.K., 2012. The influence of six pharmaceuticals on freshwater sediment microbial growth incubated at different temperatures and UV exposures. Biodegradation 23, 497–507.
Wang, S., Gunsch, C.K., 2011. Effects of selected pharmaceutically active compounds on treatment performance in sequencing batch reactors mimicking wastewater treatment plants operations. Water Res. 45, 3398–3406.
Weber, K.P., Legge, R.L., 2009. One-dimensional metric for tracking bacterial community divergence using sole carbon source utilization patterns. J. Microbiol. Methods 79, 55–61.
Wilson, B.A., Smith, V.H., deNoyelles, F., Larive, C.K., 2003. Effects of three pharmaceutical and personal care products on natural freshwater algal assemblages. Environ. Sci. Technol. 37, 1713–1719.
Zhou, H., Ying, T., Wang, X., Liu, J., 2016. Occurrence and preliminarily environmental risk assessment of selected pharmaceuticals in the urban rivers, China. Sci. Rep. 6, 34928.

Supporting Information

for

Antimicrobial activity of pharmaceutical cocktails in sewage treatment plant effluent – An experimental and predictive approach to mixture risk assessment

Jakob Menz[1], Ewelina Baginska[1], Åsa Arrhenius[2], Annette Haiβ[1], Thomas Backhaus[2], Klaus Kümmerer[1*]

[1]Sustainable Chemistry and Material Resources, Institute of Sustainable and Environmental Chemistry, Leuphana University Lüneburg, Scharnhorststrasse 1, DE-21335 Lüneburg, Germany

[2]Department of Biological and Environmental Sciences, University of Gothenburg, Carl Skottsbergs Gata 22B, Box 461, 40530 Gothenburg, Sweden

[*] Corresponding author: klaus.kuemmerer@leuphana.de; tel.: +49 4131 677 2893; fax: +49 4131 677 2848.

Table S1. Biolog EcoPlate™ carbon source guild groupings according to Weber and Legge (2009).

Well no.	*ID*	*C-source*	
Well1	C0	Water (blank)	
Well2	C1	Pyruvic acid methyl ester	Carbohydrates
Well3	C2	Tween 40	Polymers
Well4	C3	Tween 80	Polymers
Well5	C4	α-cyclodextrin	Polymers
Well6	C5	Glycogen	Polymers
Well7	C6	D-cellobiose	Carbohydrates
Well8	C7	α-D-lactose	Carbohydrates
Well9	C8	β-methyl-D-glucoside	Carbohydrates
Well10	C9	D-xylose	Carbohydrates
Well11	C10	i-erythritol	Carbohydrates
Well12	C11	D-mannitol	Carbohydrates
Well13	C12	N-acetyl-D-glucosamine	Carbohydrates
Well14	C13	D-glucosaminic acid	Carboxylic & acetic acids
Well15	C14	Glucose-1-phosphate	Carbohydrates
Well16	C15	D,L-α-glycerol phosphate	Carbohydrates
Well17	C16	D-galactonic acid-γ-lactone	Carboxylic & acetic acids
Well18	C17	D-galacturonic acid	Carboxylic & acetic acids
Well19	C18	2-Hydroxy benzoic acid	Carboxylic & acetic acids
Well20	C19	4-Hydroxy benzoic acid	Carboxylic & acetic acids
Well21	C20	γ-hydroxybutyric acid	Carboxylic & acetic acids
Well22	C21	Itaconic acid	Carboxylic & acetic acids
Well23	C22	α-ketobutyric acid	Carboxylic & acetic acids
Well24	C23	D-malic acid	Carboxylic & acetic acids
Well25	C24	L-arginine	Amino acids
Well26	C25	L-asparagine	Amino acids
Well27	C26	L-phenylalanine	Amino acids
Well28	C27	L-serine	Amino acids
Well29	C28	L-threonine	Amino acids
Well30	C29	Glycyl-L-glutamic acid	Amino acids
Well31	C30	Phenylethylamine	Amines/amides
Well32	C31	Putrescine	Amines/amides

Table S2. Measured concentrations and recovery in percent of the nominal concentration (C_{nom}) of APIs in the sterile filtered master solution at 40,000 fold MEC and the exposure cultures at fold 4,000 MEC.

Substance	**Master solution**		**Exposure Culture (0 h)**		**Exposure Culture (24 h)**		**Exposure Culture (48 h)**	
	mg/l	***% C_{nom}***	***mg/l***	***% C_{nom}***	***mg/l***	***% C_{nom}***	***mg/l***	***% C_{nom}***
Organic carbon (NPOC)	86.0	83	8.8	84.8	-	-	-	-
Ciprofloxacin	3.22	114	0.26	93	0.28	101	0.28	101
Enoxacin	2.03	169	0.13	112	0.14	119	0.14	116
Fenofibrate	n.d.	n.d.	n.d.	n.d.	n.d.	n.d.	n.d.	n.d.
Gemfibrozil	29.12	90	3.17	98	3.27	101	3.34	103
Lomefloxacin hydrochloride	15.89	124	1.27	99	1.37	107	1.38	108
Norfloxacin	2.80	100	0.26	94	0.26	93	0.25	89
Ofloxacin	23.22	100	2.60	112	2.69	116	2.67	115
Sulfamethoxazole	0.38	94	0.03	85	0.04	95	0.04	99
Trimethoprim	1.46	91	0.18	113	0.18	112	0.19	117

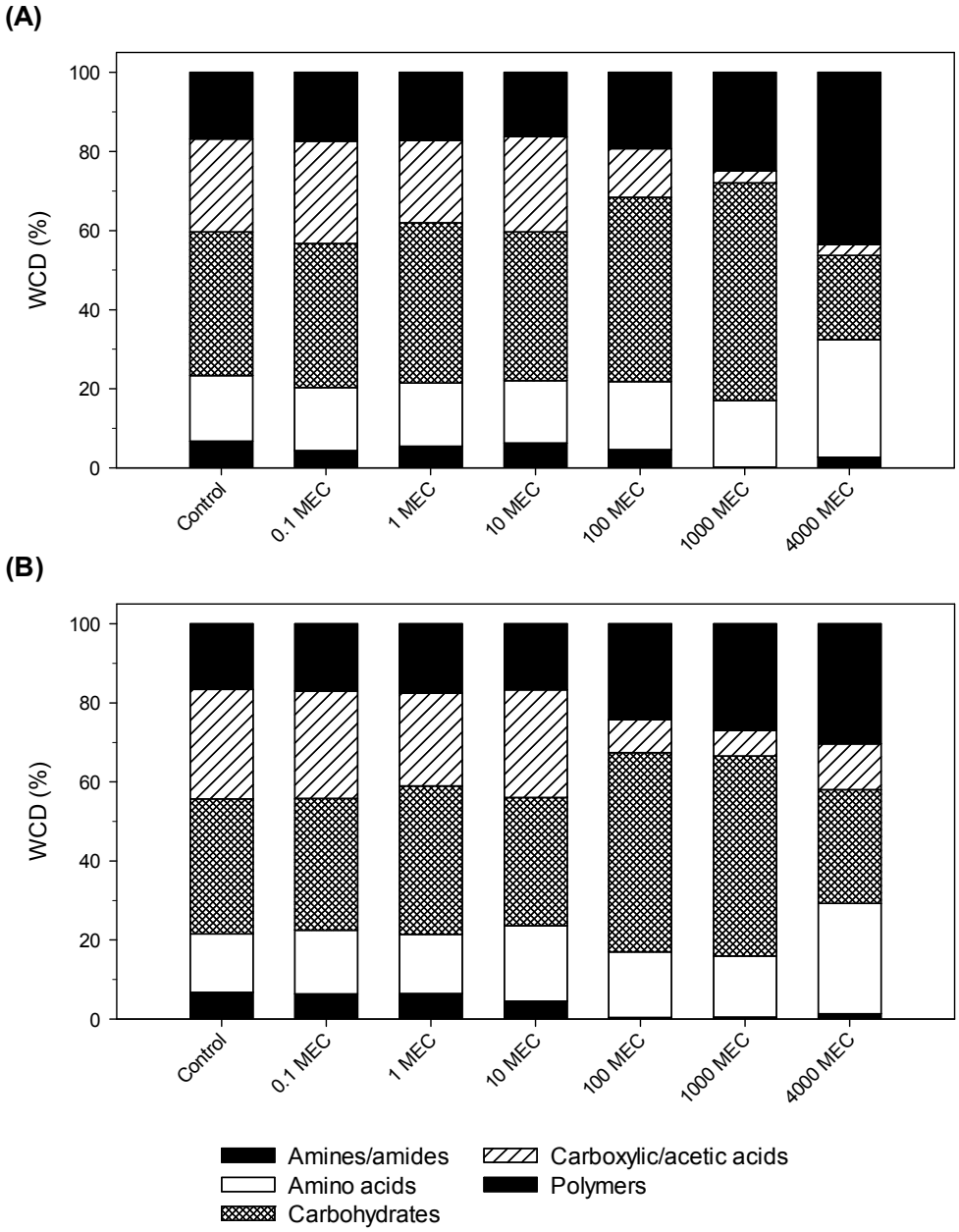

Figure S1. Metabolic profiles of the exposure cultures after 24 h (A) and 48 h (B) contact to different concentrations of the pharmaceutical mixture. The contribution of each substrate group is depicted as percentage of the total well colour development (WCD). The measured effluent concentration (MEC) of the mixture was 15.4 nmol/l.

Table S3. Correlations between the principal components and the original variables (component loadings).

Variables	***24 h Exposure***			***48 h Exposure***		
	Comp 1	***Comp 2***	***Comp 3***	***Comp 1***	***Comp 2***	***Comp 3***
2-Hydroxy Benzoic Acid	-0.18	-0.20	-0.18	-0.17	-0.25	0.05
4-Hydroxy Benzoic Acid	-0.15	0.31	-0.06	-0.21	-0.20	0.05
D,L-α-Glycerol Phosphate	0.25	-0.05	-0.14	0.23	-0.08	0.14
D-Cellobiose	0.28	0.00	0.07	0.22	0.12	0.02
D-Galactonic Acid γ-Lactone	-0.21	-0.18	0.24	-0.24	-0.01	-0.06
D-Galacturonic Acid	-0.21	-0.08	-0.02	-0.19	0.23	0.08
D-Glucosaminic Acid	-0.26	0.08	-0.08	-0.20	0.18	-0.07
D-Malic Acid	-0.14	-0.10	0.41	-0.17	-0.18	0.03
D-Mannitol	0.23	-0.10	-0.01	0.18	-0.07	-0.24
D-Xylose	-0.15	0.24	-0.06	-0.13	0.07	-0.03
Glucose-1-Phosphate	0.10	0.02	-0.35	0.13	-0.10	-0.03
Glycogen	0.09	-0.03	-0.31	0.20	0.14	0.01
Glycyl-L-Glutamic Acid	0.16	-0.26	0.00	0.16	-0.20	0.31
i-Erythritol	-0.13	-0.03	-0.41	-0.02	0.29	0.18
Itaconic Acid	-0.18	0.25	-0.09	-0.03	0.19	0.29
L-Arginine	0.11	0.25	-0.02	0.03	-0.37	-0.34
L-Asparagine	0.05	0.43	0.07	-0.05	-0.42	-0.11
L-Phenylalanine	-0.18	-0.09	-0.09	-0.20	0.11	-0.21
L-Serine	0.15	-0.02	-0.20	0.14	-0.20	0.24
L-Threonine	0.15	-0.21	-0.14	0.04	-0.20	0.38
N-Acetyl-D-Glucosamine	0.20	0.15	0.01	0.21	0.05	0.02
Phenylethyl-amine	-0.24	-0.05	-0.13	-0.24	0.09	-0.08
Putrescine	0.00	0.16	0.12	-0.22	0.08	-0.04
Pyruvic Acid Methyl Ester	0.18	0.20	0.11	0.22	0.02	-0.20
Tween 40	0.28	0.04	0.08	0.23	-0.12	-0.18
Tween 80	0.23	-0.07	0.19	0.25	-0.03	-0.03
α-Cyclodextrin	-0.13	-0.23	-0.03	0.11	0.04	0.09
α-D-Lactose	0.22	0.18	-0.10	0.24	0.21	-0.03
α-Ketobutyric Acid	-0.09	0.10	-0.20	-0.13	-0.23	0.39
β-Methyl-D-Glucoside	0.18	-0.19	-0.26	0.23	0.08	-0.07
γ-Hydroxybutyric Acid	-0.02	0.28	-0.16	0.08	0.14	0.24

Table S4. Parameter estimates of the monophasic Hill model [E(C)=min+(max-min)/(1+(C/EC_{50})^(-H))].

Endpoint	***Parameters***			
	min	***max***	***EC_{50} (xMEC)***	***H***
AWCD (48 h)	0	100	728.9	-0.57
P. Putida (growth)	-3.71	98.58	41.53	2.1
V. fischeri (growth)	0.84	104.42	12.92	2.54
V. fischeri (lum. 30 min)	-4.2	100	12,678	1.3
V. fischeri (lum. 24 h)	-4.32	102.39	9.22	3.29

Table S5. Parameter estimates of the generalized Hill model [E(C)=((1+($E_{max\ 1}$-1)/(1+($EC_{50\ 1}$/C)^H_1)*(1+($E_{max\ 2}$-1)/(1+($EC_{50\ 2}$/C)^H_2))*100].

Endpoint	***Parameters***					
	$EC_{50\ 1}$ (xMEC)	***H_1***	***$E_{max\ 1}$***	***$EC_{50\ 2}$ (xMEC)***	***H_2***	***$E_{max\ 2}$***
BOD (17 h)	0.835	5.32	1.42	93.62	1.29	5.52E-12

Table S6: Toxicity to environmental bacteria of individual mixture components.

Substance	***CAS no***	***MW [g/mol]***	***Species***	***Endpoint***	***EC_{50} [mg/l]***	***Reference***
Carbamazepine	298-46-4	236.27	*Synechococcus leopoliensis*	growth	33.6	Ferrari 2004
Carbamazepine	298-46-4	236.27	*Vibrio fischeri*	luminescence (30 min)	49.4	Neale 2017
Carbamazepine	298-46-4	236.27	*Vibrio fischeri*	luminescence (16 h)	50.5	Neale 2017
Carbamazepine	298-46-4	236.27	*Vibrio fischeri*	luminescence (30 min)	>81	Ferrari 2004
Ciprofloxacin	85721-33-1	331.34	*Microcystis aeruginosa*	growth	0.005	Halling-Sørensen 2000
Ciprofloxacin	85721-33-1	331.34	*Anabaena flos-aquae*	yield	0.010	Ebert 2011
Ciprofloxacin	85721-33-1	331.34	*Anabaena flos-aquae*	growth	0.036	Ebert 2011
Ciprofloxacin HCl	86393-32-0	367.80	*Citrobacter freudii*	growth	0.012	Nalecz-Jawecki 2010
Ciprofloxacin HCl	86393-32-0	367.80	*Microcystis aeruginosa*	growth	0.017	Robinson 2005
Ciprofloxacin HCl	86393-32-0	367.80	*Pseudomonas putida*	growth	0.080	Kümmerer 2000
Ciprofloxacin HCl	86393-32-0	367.80	*Vibrio fischeri*	luminescence (15 min)	235	Ortiz de Garcia 2016
Clofibric acid	882-09-7	214.65	*Synechococcus leopoliensis*	growth	40.2	Ferrari 2004
Clofibric acid	882-09-7	214.65	*Anabaena sp. 4337*	luminescence (24 h)	48.1	Rosal 2010
Clofibric acid	882-09-7	214.65	*Vibrio fischeri*	luminescence (5 min)	87.5	Ortiz de Garcia 2016
Clofibric acid	882-09-7	214.65	*Vibrio fischeri*	luminescence (30 min)	91.8	Ferrari 2004
Clofibric acid	882-09-7	214.65	*Vibrio fischeri*	luminescence (30 min)	100	Henschel 1997

Substance	***CAS no***	***MW [g/mol]***	***Species***	***Endpoint***	***EC_{50} [mg/l]***	***Reference***
Clofibric acid	882-09-7	214.65	*Vibrio fischeri*	luminescence (30 min)	241	Rosal 2010
Diclofenac	15307-86-5	296.15	*Vibrio fischeri*	luminescence (16 h)	1.8	Neale 2017
Diclofenac	15307-86-5	296.15	*Vibrio fischeri*	luminescence (30 min)	3.8	Neale 2017
Diclofenac	15307-86-5	296.15	*Vibrio fischeri*	luminescence (15 min)	14.0	Czech 2014
Diclofenac	15307-86-5	296.15	*Vibrio fischeri*	luminescence (30 min)	16.3	Dökmeci 2014
Diclofenac sodium	15307-79-6	318.13	*Vibrio fischeri*	luminescence (30 min)	11.5	Ferrari 2004
Diclofenac sodium	15307-79-6	318.13	*Vibrio fischeri*	luminescence (15 min)	13.7	Farré 2001
Diclofenac sodium	15307-79-6	318.13	*Synechococcus leopoliensis*	growth	14.5	Ferrari 2004
Diclofenac sodium	15307-79-6	318.13	*Vibrio fischeri*	luminescence (15 min)	17.4	Gheorghe 2016
Diclofenac sodium	15307-79-6	318.13	*Vibrio fischeri*	luminescence (5 min)	21.3	Ortiz de Garcia 2016
Enoxacin	74011-58-8	320.32	*Vibrio fischeri*	luminescence (24 h)	0.049	Backhaus 2000
Fenofibrate	49562-28-9	360.83	*Vibrio fischeri*	luminescence (30 min)	1.7	Rosal 2010
Fenofibrate	49562-28-9	360.83	*Anabaena sp. 4337*	luminescence (24 h)	10.8	Rosal 2010
Gemfibrozil	25812-30-0	250.33	*Vibrio fischeri*	luminescence (16 h)	3.9	Neale 2017
Gemfibrozil	25812-30-0	250.33	*Anabaena sp. 4337*	luminescence (24 h)	4.4	Rosal 2010
Gemfibrozil	25812-30-0	250.33	*Vibrio fischeri*	luminescence (30 min)	17.3	Neale 2017
Gemfibrozil	25812-30-0	250.33	*Vibrio fischeri*	luminescence (15 min)	18.8	Farré 2001
Gemfibrozil	25812-30-0	250.33	*Vibrio fischeri*	luminescence (30 min)	29.1	Rosal 2010
Ibuprofen	15687-27-1	206.28	*Vibrio fischeri*	luminescence (15 min)	12.1	Farré 2001
Ibuprofen	15687-27-1	206.28	*Vibrio fischeri*	luminescence (15 min)	39.9	Gheorghe 2016
Ibuprofen	15687-27-1	206.28	*Vibrio fischeri*	luminescence (30 min)	39.9	Dökmeci 2014
Ibuprofen sodium	31121-93-4	228.26	*Vibrio fischeri*	luminescence (15 min)	50.8	Ortiz de Garcia 2016
Lomefloxacin	98079-51-7	351.35	*Vibrio fischeri*	luminescence (24 h)	0.022	Backhaus 2000
Lomefloxacin	98079-51-7	351.35	*Microcystis aeruginosa*	growth	0.19	Robinson 2005
Lomefloxacin HCl	98079-52-8	387.81	*Citrobacter freudii*	growth	0.075[a]	Nalecz-Jawecki 2010
Metoprolol	51384-51-1	267.36	*Vibrio fischeri*	luminescence (15 min)	14.5	Czech 2014
Metoprolol tartrate	56392-17-7	684.81	*Vibrio fischeri*	luminescence (15 min)	65.0	Rubirola 2014
Metoprolol tartrate	56392-17-7	684.81	*Vibrio fischeri*	growth	259	Toolaram 2016
Metoprolol tartrate	56392-17-7	684.81	*Vibrio fischeri*	luminescence (24 h)	527	Toolaram 2016

Substance	*CAS no*	*MW [g/mol]*	*Species*	*Endpoint*	*EC_{50} [mg/l]*	*Reference*
Metoprolol tartrate	56392-17-7	684.81	*Vibrio fischeri*	luminescence (30 min)	>100	Maszkowska 2014
Metoprolol tartrate	56392-17-7	684.81	*Vibrio fischeri*	luminescence (30 min)	>2000	Toolaram 2016
Naproxen	22204-53-1	230.26	*Vibrio fischeri*	luminescence (16 h)	0.21	Neale 2017
Naproxen	22204-53-1	230.26	*Vibrio fischeri*	luminescence (30 min)	0.78	Neale 2017
Naproxen	22204-53-1	230.26	*Anabaena flos-aquae*	growth	12.3	Straub 2007
Naproxen	22204-53-1	230.26	*Vibrio fischeri*	luminescence (15 min)	20.0	Gheorghe 2016
Naproxen	22204-53-1	230.26	*Vibrio fischeri*	luminescence (15 min)	21.2	Farré 2001
Naproxen	22204-53-1	230.26	*Vibrio fischeri*	luminescence (30 min)	47.1	Dökmeci 2014
Norfloxacin	70458-96-7	319.33	*Vibrio fischeri*	luminescence (24 h)	0.022	Backhaus 2000
Norfloxacin	70458-96-7	319.33	*Microcystis wesenbergii*	growth	0.038	Ando 2007
Norfloxacin	70458-96-7	319.33	*Citrobacter freudii*	growth	0.047[a]	Nalecz-Jawecki 2010
Norfloxacin	70458-96-7	319.33	*Anabaena cylindrica*	growth	0.053	Ando 2007
Norfloxacin	70458-96-7	319.33	*Microcystis aeruginosa*	growth	0.062	Ando 2007
Norfloxacin	70458-96-7	319.33	*Anabaena variabilis*	growth	0.19	Ando 2007
Norfloxacin	70458-96-7	319.33	*Anabaena flos-aquae*	growth	0.29	Ando 2007
Norfloxacin	70458-96-7	319.33	*Synechococcus leopoliensis*	growth	0.63	Ando 2007
Norfloxacin	70458-96-7	319.33	*Synechococcus sp. PCC 7002*	growth	0.63	Ando 2007
Norfloxacin	70458-96-7	319.33	*Nostoc sp. PCC 7120*	growth	1.7	Ando 2007
Norfloxacin	70458-96-7	319.33	*Anabaena sp. CPB4337*	luminescence (72 h)	5.6	González-Pleiter 2013
Norfloxacin	70458-96-7	319.33	*Vibrio fischeri*	luminescence (15 min)	23.6	Ortiz de Garcia 2016
Ofloxacin	82419-36-1	361.37	*Vibrio fischeri*	luminescence (24 h)	0.014	Backhaus 2000
Ofloxacin	82419-36-1	361.37	*Synechococcus leopoliensis*	growth	0.016	Ferrari 2004
Ofloxacin	82419-36-1	361.37	*Microcystis aeruginosa*	growth	0.021	Robinson 2005
Ofloxacin	82419-36-1	361.37	*Citrobacter freudii*	growth	0.036[a]	Nalecz-Jawecki 2010
Ofloxacin	82419-36-1	361.37	*Vibrio fischeri*	luminescence (30 min)	>90	Ferrari 2004
Ofloxacin HCl	118120-51-7	397.83	*Pseudomonas putida*	growth	0.010	Kümmerer 2000
Propranolol HCl	318-98-9	295.80	*Synechococcus leopoliensis*	growth	0.67	Ferrari 2004
Propranolol HCl	318-98-9	295.80	*Vibrio fischeri*	luminescence (24 h)	57.7	Menz 2017
Propranolol HCl	318-98-9	295.80	*Vibrio fischeri*	luminescence (30 min)	61.0	Ferrari 2004

Substance	*CAS no*	*MW [g/mol]*	*Species*	*Endpoint*	*EC_{50} [mg/l]*	*Reference*
Propranolol HCl	318-98-9	295.80	*Vibrio fischeri*	grwoth	178	Menz 2017
Propranolol HCl	318-98-9	295.80	*Vibrio fischeri*	luminescence (30 min)	227	Menz 2017
Propranolol HCl	318-98-9	295.80	*Vibrio fischeri*	luminescence (30 min)	>100	Maszkowska 2014
Sulfamethoxazole	723-46-6	253.28	*Synechococcus leopoliensis*	growth	0.027	Ferrari 2004
Sulfamethoxazole	723-46-6	253.28	*Bacillus pumilus*	growth	0.052	van der Grinten 2010
Sulfamethoxazole	723-46-6	253.28	*Microcystis aeruginosa*	photosynthetic yield	0.55	van der Grinten 2010
Sulfamethoxazole	723-46-6	253.28	*Vibrio fischeri*	luminescence (16 h)	0.88	Neale 2017
Sulfamethoxazole	723-46-6	253.28	*Vibrio fischeri*	luminescence (24 h)	1.8	Majewsky 2014
Sulfamethoxazole	723-46-6	253.28	*Vibrio fischeri*	luminescence (24 h)	2.8	Wang 2016
Sulfamethoxazole	723-46-6	253.28	*Vibrio fischeri*	luminescence (30 min)	14.6	Neale 2017
Sulfamethoxazole	723-46-6	253.28	*Vibrio fischeri*	luminescence (15 min)	49.5	Ortiz de Garcia 2016
Sulfamethoxazole	723-46-6	253.28	*Vibrio fischeri*	luminescence (30 min)	140	Majewsky 2014
Sulfamethoxazole	723-46-6	253.28	*Vibrio fischeri*	growth	152	Majewsky 2014
Sulfamethoxazole	723-46-6	253.28	*Vibrio fischeri*	luminescence (30 min)	>84	Ferrari 2004
Trimethoprim	738-70-5	290.32	*Bacillus pumilus*	growth	0.028	van der Grinten 2010
Trimethoprim	738-70-5	290.32	*Microcystis aeruginosa*	photosynthetic yield	6.9	van der Grinten 2010
Trimethoprim	738-70-5	290.32	*Anabaena variabilis*	growth	11.0	Ando 2007
Trimethoprim	738-70-5	290.32	*Nostoc sp. PCC 7120*	growth	53.0	Ando 2007
Trimethoprim	738-70-5	290.32	*Microcystis aeruginosa*	growth	112	Halling-Sørensen 2000
Trimethoprim	738-70-5	290.32	*Microcystis aeruginosa*	growth	150	Ando 2007
Trimethoprim	738-70-5	290.32	*Anabaena flos-aquae*	growth	253	Kolar 2014
Trimethoprim	738-70-5	290.32	*Anabaena cylindrica*	growth	>200	Ando 2007
Trimethoprim	738-70-5	290.32	*Anabaena flos-aquae*	growth	>200	Ando 2007
Trimethoprim	738-70-5	290.32	*Microcystis wesenbergii*	growth	>200	Ando 2007
Trimethoprim	738-70-5	290.32	*Synechococcus leopoliensis*	growth	>200	Ando 2007
Trimethoprim	738-70-5	290.32	*Synechococcus sp. PCC 7002*	growth	>200	Ando 2007

[a]microbial toxic concentration (MTC).

References

Ando, T., Nagase, H., Eguchi, K., Hirooka, T., Nakamura, T., Miyamoto, K., Hirata, K., 2007. A novel method using cyanobacteria for ecotoxicity test of veterinary antimicrobial agents. Environ. Toxicol. Chem. 26, 601–606.

Backhaus, Scholze, Grimme, 2000. The single substance and mixture toxicity of quinolones to the bioluminescent bacterium Vibrio fischeri. Aquat. Toxicol. 49, 49–61.

Czech, B., Josko, I., Oleszczuk, P., 2014. Ecotoxicological evaluation of selected pharmaceuticals to Vibrio fischeri and Daphnia magna before and after photooxidation process. Ecotoxicol. Environ. Saf. 104, 247–253.

Dökmeci, A.H., Dökmeci, I., Ibar, H., 2014. The determination of single and mixture toxicity at high concentrations of some acidic pharmaceuticals via Aliivibrio fischeri. Environ. Process. 1, 95–103.

Ebert, I., Bachmann, J., Kühnen, U., Küster, A., Kussatz, C., Maletzki, D., Schlüter, C., 2011. Toxicity of the fluoroquinolone antibiotics enrofloxacin and ciprofloxacin to photoautotrophic aquatic organisms. Environ. Toxicol. Chem. 30, 2786–2792.

Farré, M., Ferrer, I., Ginebreda, A., Figueras, M., Olivella, L., Tirapu, L., Vilanova, M., Barceló, D., 2001. Determination of drugs in surface water and wastewater samples by liquid chromatography–mass spectrometry: Methods and preliminary results including toxicity studies with Vibrio fischeri. J. Chromatogr. A 938, 187–197.

Ferrari, B., Mons, R., Vollat, B., Fraysse, B., Paxéus, N., Lo Giudice, R., Pollio, A., Garric, J., 2004. Environmental risk assessment of six human pharmaceuticals: are the current environmental risk assessment procedures sufficient for the protection of the aquatic environment? Environ. Toxicol. Chem. 23, 1344–1354.

Gheorghe, S., Petre, J., Lucaciu, I., Stoica, C., Nita-Lazar, M., 2016. Risk screening of pharmaceutical compounds in Romanian aquatic environment. Environ. Monit. Assess. 188, 379.

González-Pleiter, M., Gonzalo, S., Rodea-Palomares, I., Leganés, F., Rosal, R., Boltes, K., Marco, E., Fernández-Piñas, F., 2013. Toxicity of five antibiotics and their mixtures towards photosynthetic aquatic organisms: Implications for environmental risk assessment. Water Res. 47, 2050–2064.

Halling-Sørensen, B., Lützhøft, H.C., Andersen, H.R., Ingerslev, F., 2000. Environmental risk assessment of antibiotics: comparison of mecillinam, trimethoprim and ciprofloxacin. J. Antimicrob. Chemother. 46 (suppl 1), 53-58.

Henschel, K.P., Wenzel, A., Diedrich, M., Fliedner, A., 1997. Environmental hazard assessment of pharmaceuticals. Regul. Toxicol. Pharmacol. 25, 220–225.

Kolar, B., Arnus, L., Jeretin, B., Gutmaher, A., Drobne, D., Durjava, M.K., 2014. The toxic effect of oxytetracycline and trimethoprim in the aquatic environment. Chemosphere 115, 75–80.

Kümmerer, K., Al-Ahmad, A., Mersch-Sundermann, V., 2000. Biodegradability of some antibiotics, elimination of the genotoxicity and affection of wastewater bacteria in a simple test. Chemosphere 40, 701–710.

Majewsky, M., Wagner, D., Delay, M., Bräse, S., Yargeau, V., Horn, H., 2014. Antibacterial activity of sulfamethoxazole transformation products (TPs): General relevance for sulfonamide TPs modified at the para position. Chem. Res. Toxicol. 27, 1821–1828.

Maszkowska, J., Stolte, S., Kumirska, J., Lukaszewicz, P., Mioduszewska, K., Puckowski, A., Caban, M., Wagil, M., Stepnowski, P., Bialk-Bielinska, A., 2014. Beta-blockers in the environment: part II. Ecotoxicity study. Sci. Total Environ. 493, 1122–1126.

Menz, J., Toolaram, A.P., Rastogi, T., Leder, C., Olsson, O., Kummerer, K., Schneider, M., 2017. Transformation products in the water cycle and the unsolved problem of their proactive assessment: A combined in vitro/in silico approach. Environ. Int. 98, 171–180.

Nalecz-Jawecki, G., Wadhia, K., Adomas, B., Piotrowicz-Cieslak, A.I., Sawicki, J., 2010. Application of microbial assay for risk assessment biotest in evaluation of toxicity of human and veterinary antibiotics. Environ. Toxicol. 25, 487–494.
Neale, P.A., Leusch, F.D.L., Escher, B.I., 2017. Applying mixture toxicity modelling to predict bacterial bioluminescence inhibition by non-specifically acting pharmaceuticals and specifically acting antibiotics. Chemosphere 173, 387–394.
Ortiz de Garcia, S., Garcia-Encina, P.A., Irusta-Mata, R., 2016. Dose-response behavior of the bacterium Vibrio fischeri exposed to pharmaceuticals and personal care products. Ecotoxicology 25, 141–162.
Robinson, A.A., Belden, J.B., Lydy, M.J., 2005. Toxicity of fluoroquinolone antibiotics to aquatic organisms. Environ. Toxicol. Chem. 24, 423–430.
Rosal, R., Rodea-Palomares, I., Boltes, K., Fernández-Piñas, F., Leganés, F., Gonzalo, S., Petre, A., 2010. Ecotoxicity assessment of lipid regulators in water and biologically treated wastewater using three aquatic organisms. Environ. Sci. Pollut. Res. 17, 135–144.
Rubirola, A., Llorca, M., Rodriguez-Mozaz, S., Casas, N., Rodriguez-Roda, I., Barcelo, D., Buttiglieri, G., 2014. Characterization of metoprolol biodegradation and its transformation products generated in activated sludge batch experiments and in full scale WWTPs. Water Res. 63, 21–32.
Straub, J.O., Stewart, K.M., 2007. Deterministic and probabilistic acute-based environmental risk assessment for naproxen for western Europe. Environ. Toxicol. Chem. 26, 795–806.
Toolaram, A.P., Menz, J., Rastogi, T., Leder, C., Kummerer, K., Schneider, M., 2016. Hazard screening of photo-transformation products from pharmaceuticals: Application to selective beta1-blockers atenolol and metoprolol. Sci. Total Environ. (article in press).
van der Grinten, E., Pikkemaat, M.G., van den Brandhof, E.-J., Stroomberg, G.J., Kraak, M.H., 2010. Comparing the sensitivity of algal, cyanobacterial and bacterial bioassays to different groups of antibiotics. Chemosphere 80, 1–6.
Wang, T., Wang, D., Lin, Z., An, Q., Yin, C., Huang, Q., 2016. Prediction of mixture toxicity from the hormesis of a single chemical: A case study of combinations of antibiotics and quorum-sensing inhibitors with gram-negative bacteria. Chemosphere 150, 159–167.
Weber, K.P., Legge, R.L., 2009. One-dimensional metric for tracking bacterial community divergence using sole carbon source utilization patterns. J. Microbiol. Methods 79, 55–61.

Publikation 3

Identification of phototransformation products of the antiepileptic drug gabapentin: Biodegradability and initial assessment of toxicity

Herrmann, M., Menz, J., Olsson, O., Kümmerer, K.

(2015)

Water Research 85, 11-21

DOI:10.1016/j.watres.2015.08.004

Water Research 85 (2015) 11–21

Contents lists available at ScienceDirect

Water Research

journal homepage: www.elsevier.com/locate/watres

Identification of phototransformation products of the antiepileptic drug gabapentin: Biodegradability and initial assessment of toxicity

Manuel Herrmann [a, b], Jakob Menz [a], Oliver Olsson [a], Klaus Kümmerer [a, *]

[a] Sustainable Chemistry and Material Resources, Institute of Sustainable and Environmental Chemistry, Leuphana University of Lüneburg, C13, Scharnhorstrasse 1, DE-21335 Lüneburg, Germany
[b] Hospital Pharmacy, Ortenau Klinikum Offenburg-Gengenbach, Ebertplatz 12, DE-77654 Offenburg, Germany

ARTICLE INFO

Article history:
Received 13 February 2015
Received in revised form
20 July 2015
Accepted 1 August 2015
Available online 4 August 2015

Keywords:
Closed Bottle Test (CBT)
High-resolution mass spectrometry
Luminescent bacteria test
Umu-test
UV photolysis

ABSTRACT

The anticonvulsant drug Gabapentin (GAB) is used for the treatment of various diseases (e.g. epilepsy, bipolar disorder, neuropathic pain) and is being consumed in high amounts. As GAB is not metabolized and shows a weak elimination in sewage treatment plants (STPs), it has been detected in surface water and even in raw potable water. Moreover, the confirmed teratogenic effects of GAB indicate the need for further investigations regarding options for the elimination of GAB in the water cycle. Little is known about the behavior of GAB during treatment with UV light, which is normally used for the disinfection of potable water and discussed for advanced wastewater treatment. In this study, GAB was exposed to polychromatic UV irradiation at different initial concentrations in aqueous solution. Afterwards the structures of the resulting phototransformation products (PTPs) were identified and elucidated by means of high-resolution mass spectrometry. GAB and photolytic mixtures were submitted to the Closed Bottle Test (CBT; OECD 301 D) to assess biodegradability. Furthermore, the toxicity of GAB and its photolytic mixtures was initially addressed on screening level using a modified luminescent bacteria test (LBT) and the umu-test (ISO/FDIS 13829). Environmentally realistic concentrations of GAB were disclosed by predicting STP influent concentrations (24.3 and 23.2 μg L^{-1}). GAB with initial concentration of 100 mg L^{-1} was eliminated by 80% after 128 min of direct UV irradiation, but just 9% of non-purgeable organic carbon (NPOC) was removed indicating the formation of dead-end transformation products (TPs). Structures of different PTPs were elucidated and several identical PTPs could also be identified at lower initial treatment concentrations (20 mg L^{-1}, 5 mg L^{-1}, 1 mg L^{-1} and 0.1 mg L^{-1}). GAB was classified as not readily biodegradable. Moreover, photo treatment did not result in better biodegradable PTPs. With increasing UV treatment duration, photolytic mixtures of GAB showed an increased inhibition of both, the bacterial luminescence emission as well as the growth in the modified LBT. In the umu-test no significant induction of the umuC gene as an indicator of genotoxicity was observed. Our results show that UV irradiation of GAB containing water would lead to the formation of recalcitrant PTPs. Considering that GAB was found in raw drinking water, the formation of toxic PTPs during drinking water treatment with UV light might be possible. Therefore, further studies should be conducted regarding the fate and effects on human health and the environment of GAB and the PTPs identified within this study.

1. Introduction

The occurrence and assessment of pharmaceuticals in the environment plays an important role in environmental research, since the variety and the consumption of pharmaceuticals is still rising (OECD, 2011). Many different compounds from several classes, like analgesics, antihypertensive agents or antibiotics have been detected in different environmental compartments (Capdeville and Budzinski, 2011; Nödler et al., 2010). The environmental risk emanating from pharmaceuticals has been frequently assessed by several studies (Escher et al., 2011; Sanderson et al., 2004; Verlicchi et al., 2012). For some pharmaceuticals the potential environmental risk is obvious. Antibiotics can affect the

* Corresponding author. Nachhaltige Chemie und Stoffliche Ressourcen, Institut für Nachhaltige Chemie und Umweltchemie, Fakultät für Nachhaltigkeit, Leuphana Universität Lüneburg, Scharnhorststraße 1/C13, D-21335 Lüneburg, Germany.
E-mail addresses: manuel.herrmann@leuphana.de (M. Herrmann), jakob.menz@leuphana.de (J. Menz), oliver.olsson@leuphana.de (O. Olsson), klaus.kuemmerer@leuphana.de (K. Kümmerer).

http://dx.doi.org/10.1016/j.watres.2015.08.004
0043-1354/

population dynamics of microbial communities, hormones can cause changes in the endocrine system of water organisms and cytostatics are apparently highly toxic to actively dividing eukaryotic cells. In contrast, the effect being caused by pharmaceuticals such as psychotropic drugs in the environment is not easily assessable. Still, they should receive more attention, because they have been found in different environmental aqueous compartments (Writer et al., 2013), as well as in drinking water (Huerta-Fontela et al., 2011).

For medical use the antiepileptic drug gabapentin (GAB) arouse high concern in previous years. Besides its regulatory medical indications like epilepsy and neuropathic pain, GAB is off-label used for several other indications, such as bipolar disorder (Carta et al., 2003), migraine prophylaxis (Mathew et al., 2001) or restless legs syndrome (Happe et al., 2003). In 2009, according to Lai et al. (2011) 6.7 t of GAB were consumed in Australia. In the same year the consumption in Germany (data for public health insurance, around 85% of the population) was 58.9 t (Schwabe and Paffrath, 2010) with a steady linear annual increase to 73.3 t in 2012 (Schwabe and Paffrath, 2013). GAB represents about 1% of the whole pharmaceutical consumption in Germany (Ebert et al., 2014) and is excreted entirely unchanged (PFIZER PHARMA GmbH (Parke-Davis), 2014). Therefore, GAB is expected to have a high concentration at influents of sewage treatment plants (STPs).

Some pharmaceuticals are not entirely eliminated in STPs, thus being able to reach surface waters (Kasprzyk-Hordern et al., 2009a) or even drinking water (Huerta-Fontela et al., 2011; Zühlke et al., 2004). In the case of GAB, sewage concentrations up to 25 μg L^{-1} and 37 μg L^{-1} were detected in influents of STPs (Kasprzyk-Hordern et al., 2009b), whereas Yu et al. (2006) quantified 1 μg L^{-1}. Ottmar et al. (2010) modeled GAB concentrations at influents of five STPs ranging from 1 μg L^{-1} to 28 μg L^{-1} by means of drug prescription data, which shows that modeled concentrations are very close to measured concentrations. However, there is inconsistent data on the elimination of GAB in STPs. Yu et al. (2006) observed full elimination of GAB in an STP, whereas other studies reported high concentrations of GAB in STP effluents up to 1.7 and 6.5 μg L^{-1}, respectively (De la Cruz et al., 2012; Reungoat et al., 2010). Kasprzyk-Hordern et al. (2009a) in turn compared two STPs with different secondary treatment technologies and concluded that filter bed STPs are not able to eliminate GAB sufficiently, but STPs working with activated sludge are to some degree. The weak elimination of GAB in STPs leads to frequent detection of GAB in surface waters up to 1.9 μg L^{-1} receiving effluent from STPs (Kasprzyk-Hordern et al., 2008; Writer et al., 2013). Morasch et al. (2010) even detected GAB in raw drinking water (0.4 μg L^{-1}) sampled at a drinking water plant receiving river water downstream of an STP. The uptake of GAB via drinking water could be dreadful, because some studies showed teratogenic effects for GAB (Afshar et al., 2007; Prakash et al., 2008).

GAB has a high mobility potential (log p −1.25 (Zhu et al., 2002)) and has been found in every possible aqueous environmental compartment. Therefore, more detailed information about the environmental behavior of GAB should be available.

In connection with the constant release of pharmaceuticals to the environment, advanced treatment processes, like treatment with UV light, are discussed as a feasible method to eliminate pharmaceutical residues from wastewater (De la Cruz et al., 2012). Several possibilities to eliminate GAB after secondary wastewater treatment in STPs have already been studied. Neamţu et al. (2014) identified GAB as one of the most persistent compounds towards UV_{254}/H_2O_2/Fe(II) treatment in ultrapure, lake and wastewater. In comparison GAB was sufficiently eliminated from wastewater by UV/H_2O_2 treatment as reported by De la Cruz et al. (2012), whereas simple UV treatment leads to the elimination of only 10% (De la Cruz et al., 2012). As UV irradiation is commonly used for drinking water disinfection (Canonica et al., 2008; Hijnen et al., 2006), micro-pollutants like GAB are constantly exposed to UV light and should therefore also be investigated in this respect.

However, the above-mentioned studies only monitored GAB with regard to its primary elimination. An entire mineralization of the parent compound was not compulsive, which means that unknown transformation products (TPs) could be formed. Moreover, TPs formed from GAB during drinking water disinfection with UV light have not been taken into account. The only possibility for identification of TPs is to access intermittent databases (Gómez et al., 2010). Moreover, structural elucidation of TPs leads to the possibility of assessing the potential toxicity and persistence in the environment (Haddad and Kümmerer, 2014; Trautwein and Kümmerer, 2012). Recent studies showed that TPs could have a negative effect on environmental organisms or be more persistent than the parent compound itself (Illés et al., 2014; Trautwein et al., 2014). To the best of our knowledge there have been no literature information on TPs formed from GAB.

In this study the consumption of GAB for a medium-sized city located in the west of Germany with around 40,000 inhabitants was assessed to approximate GAB's potential sewage concentration for the simulation of UV treatment. In a first step, photodegradation experiments with an initial GAB concentration of 100 mg L^{-1} were performed to generate photolytic mixtures that allowed the identification and characterization of phototransformation products (PTPs). Photolytic mixtures were analyzed using high-resolution mass spectrometry, further investigated in the Closed Bottle Test (CBT), a modified luminescent bacteria test (LBT) (Menz et al., 2013) and the umu-test to assess changes in biodegradability, antibacterial activity and genotoxicity, respectively. Finally, samples with consecutively lower, i.e. environmentally realistic initial concentrations of GAB were also treated with UV light to check the transferability of the test results to environmental conditions.

2. Data sets, material and methods

2.1. Mass balanced prediction of gabapentin (GAB) in municipal wastewater

For the prediction of GAB influent concentration in an STP, the medium-sized city Dülmen with 46,300 citizens, located in the west of Germany, was chosen. Data of the amount of applied GAB in the allocated hospitals (general hospital (200 beds) and psychiatry (108 beds)) for the year 2012 was collected from the hospital pharmacy. The consumption of pharmaceuticals by the general population was calculated based on drug sales data provided by the local wholesaler for pharmaceuticals and cross checked with data of the annually published report for prescribed drugs in Germany Arzneiverordnungs-Report (AVP) 2013 (based on 2012 data). The predicted influent concentration (PIC), indicating the 'worst-case scenario', with GAB being excreted entirely unchanged, was calculated according to Eq. (1):

$$PIC(GAB) = \frac{\left(A_{hospitals} + A_{domestic}\right) \times f_{nm}}{366 \times P \times V_E} \quad (1)$$

where: $A_{hospitals}$ is the consumption in hospitals, $A_{domestic}$ is the consumption in households (from the wholesaler and AVP, respectively), f_{nm} is the non-metabolized fraction of GAB (100% (Pfizer Pharma GmbH (Parke-Davis), 2014)), P is the number of inhabitants and V_E is the water consumption per capita and day (121 L (Federal Statistical Office DESTATIS, 2015)).

2.2. Chemicals and reagents

GAB (certified purity 99.9%, traceable to USP standard) was purchased from Sigma–Aldrich Chemie GmbH (Steinheim, Germany). Ammonium acetate (HiPerSolv CHROMANORM® for HPLC) and methanol (HiPerSolv CHROMANORM® for HPLC, LC-MS grade) were purchased from VWR International GmbH (Darmstadt, Germany). 2-Propanol (purity ≥99.5%, Ph.Eur.) was purchased from Carl Roth GmbH & Co. KG (Karlsruhe, Germany). Aqueous mobile phase, standard solutions and solutions for photodegradation experiments were prepared with ultrapure water (Q1:16.6 mΩ and Q2: 18.2 mΩ).

2.3. Simulated UV treatment (direct UV photolysis)

The test solutions of GAB with initial concentrations of 100 mg L^{-1}, 20 mg L^{-1}, 5 mg L^{-1}, 1 mg L^{-1} and 0.1 mg L^{-1} were freshly prepared with ultrapure water in order to determine non-purgeable organic carbon (NPOC) and further elucidate PTPs. To obtain information about the photochemical role of reactive oxygen species (ROS) during the photolysis process, an aqueous solution of GAB (100 mg L^{-1}) with 1% 2-Propanol (v/v) was also prepared to undergo photolysis. Additionally, the concentration of dissolved oxygen was measured throughout the experiment by an optical oxygen sensor FDO® 925 (WTW GmbH, Weilheim, Germany). The photolysis experiments were carried out in a 1000 mL batch immersion tube photo reactor using 800 mL of sample volume. Magnetic stirring ensured continuous mixing of the solution. Constant temperature (20 ± 1 °C) was achieved by using a cooling system (WKL230, LAUDA, Berlin, Germany).

The polychromatic irradiation source used in the experiments was a medium-pressure mercury lamp (TQ 150, UV Consulting Peschl, Mainz, Germany). The lamp was surrounded by a cooling jacket separated from the test solution by an ilmasil quartz glass to guarantee unlimited irradiation. The applied UV fluence for experiments is shown in Fig. 1F. Additionally, the measured emission spectrum of polychromatic light after a total operating time of 500 h and the measured absorbance spectrum of GAB is shown in Fig. S1, SM (supplementary material). GAB has a high absorption in the lower wavelength range, and therefore, it is not expected to be mainly eliminated by direct photolysis.

The photolysis experiment was conducted for 128 min. Samples for each test concentration were collected before (0 min), after 2, 4, 8, 16, 32, 64 and 128 min of treatment for LC-MS^n analysis (primary elimination and structural elucidation), as well as for NPOC determination (mineralization). Analogous sampling in the case of 100 mg L^{-1} initial concentration was conducted and subsequently submitted to the LBT and the umu-test. For the CBT, samples (initial concentration 100 mg L^{-1}) were collected at the beginning (0 min), after 32, 64 and 128 min.

2.4. Biodegradation testing according to OECD 301 D (Closed Bottle Test (CBT))

The CBT was performed with little modifications according to the Organisation for Economic Co-operation and Development (OECD) test guidelines (OECD, 1992) using a low content of nutrients (mineral medium) and bacteria to simulate ready biodegradability in the aquatic environment. The concentration of GAB was 2.3 mg L^{-1} corresponding to a theoretical oxygen demand (ThOD) of 5 mg L^{-1}. The final concentration of the photolytic mixtures after 32, 64 and 128 min, respectively, was adjusted according to the remaining NPOC concentration to reach a comparable ThOD.

During the whole test the biochemical oxygen demand (BOD) was monitored by measuring the dissolved oxygen concentration (Friedrich et al., 2013). According to the test guidelines, degradation of 60%, expressed as a percentage of oxygen consumed in the test bottle, classifies a chemical as readily biodegradable. Additional information regarding the test procedure and validation criteria can be found in Text S1, SM.

Samples from the beginning and the end of the test (after 28 days) were taken for LC-MS^n analysis.

2.5. Analytical conditions

2.5.1. Non-purgeable organic carbon (NPOC) analysis

To monitor the degree of mineralization a Total Organic Carbon Analyzer (TOC 5000, Shimadzu GmbH, Duisburg, Germany) was used. Linear calibration for the measured range was performed with dried potassium phthalate.

2.5.2. Primary elimination of gabapentin (GAB) and structural elucidation of phototransformation products (PTPs)

LC-MS^n analysis was performed on an Agilent 1100 series HPLC system (Agilent Technologies, Waldbronn, Germany) coupled with a Bruker Esquire 6000^{plus} mass spectrometer with an ESI source (Bruker Daltonics, Bremen, Germany) (LC-ITMS), and a Dionex Ultimate 3000 UHPLC system (Dionex, Idstein, Germany) coupled with an LTQ Orbitrap-XL high-resolution mass spectrometer with H-ESI source (Thermo Scientific, Bremen, Germany) (LC-HRMS). Detailed information about chromatographic and mass spectrometric conditions can be found in Text S2, SM.

All photolysis samples with different initial concentrations (100 mg L^{-1}, 20 mg L^{-1}, 5 mg L^{-1}, 1 mg L^{-1} and 0.1 mg L^{-1}) were measured for primary elimination by LC-ITMS injecting 5 μL of the sample volume.

To obtain information about the occurrence of formed PTPs during photolysis experiment, samples with initial concentration of 100 mg L^{-1} GAB were analyzed by LC-ITMS. The peak area A of each newly occurring m/z value with corresponding retention time (t_R) was related to GAB's peak area A_0 at time point 0 min, as the absolute peak area is no indicator for the concentration of unknown PTPs. No correlation between peak area and concentration can be established for unknown compounds because the ionization rate in the MS is different for every compound. The injection volume was 5 μL.

Structural elucidation was performed for every PTP considering a threshold exceeding 2% among the ratio between PTP peak area (A) and GAB's peak area at time point 0 min (A_0) during the photolysis process. A threshold of 2% meets OECD guidelines for the testing of chemicals (OECD, 2010). The guideline recommends the inclusion of PTP >10% on an amount basis for environmental fate assessment, since PTPs in lower occurring amounts do not seem to have a potential effect on the environment. To get further information about the structure of the formed PTPs during the photolysis experiment, PTPs were screened and structural elucidated by ITMS. Structures were ensured with further HRMS fragmentation up to MS^4. Moreover, t_Rs and accurate *m/z* values of GAB and its PTPs were compared within different initial concentrations to study concentration effects on the formation of PTPs.

Samples from CBT were assessed by LC-ITMS using the recovered peak areas of GAB and its PTPs S/S_0 (S is the peak area of the PTP at day 28 and S_0 is the peak area of the PTP at day 0). Due to lower concentrations of the investigated compounds in CBT compared to the photolysis test, the injection volume was 50 μL.

2.6. Toxicity screening of photolytic mixtures

GAB and the mixtures obtained after photolysis were screened for toxicity using a set of two bioassays. The modified LBT according

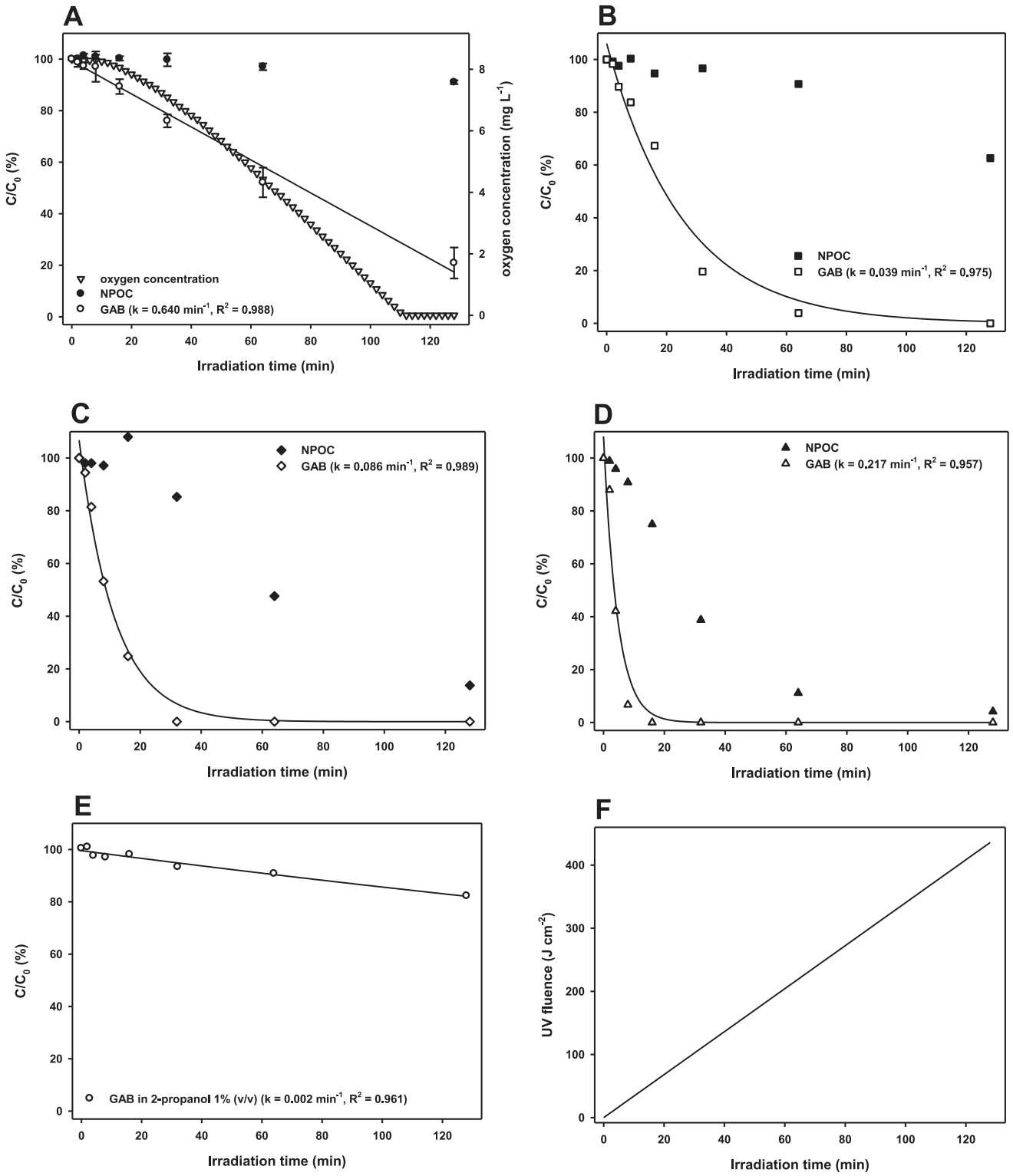

Fig. 1. [A–D] Gabapentin (GAB) and non-purgeable organic carbon (NPOC) elimination during photolysis with different initial concentrations of GAB in ultrapure water (A: 100 mg L^{-1} (n = 4), B: 20 mg L^{-1}, C: 5 mg L^{-1}, D: 1 mg L^{-1}) showing recovery by means of the ratio of the concentration at the specific time point C and the concentration at 0 min C_0, the rate constant k, and the correlation R^2 to the kinetic model. [E] GAB elimination during photolysis with initial concentration of 100 mg L^{-1} in aqueous solution of 1% 2-propanol (v/v). [F] Applied UV fluence as a function of irradiation time.

to Menz et al. (2013), using the luminescent bacteria strain Vibrio *fischeri* NRRL-B-11177 (Hach-Lange GmbH), was employed for the combined assessment of short-term luminescence inhibition after 30 min (LI_{30min}), long-term luminescence inhibition after 24 h (LI_{24h}) and growth inhibition after 14 h (GI_{14h}). Moreover, the photolytic mixtures of GAB were subject to a genotoxicity screening using the umu-test with *Salmonella typhimurium* TA1535 psk 1002 (German Collection of Microorganisms and Cell Cultures GmbH)

according to ISO/FDIS 13829 (ISO/FDIS, 1999). Initial photodegradation concentration (C_0) of GAB for toxicity screening purposes was 100 mg L^{-1}. More detailed information about testing procedures can be found in Text S3, SM.

3. Results and discussion

3.1. Predicted influent concentration (PIC) of gabapentin (GAB)

In 2012, 48.7 kg (1.052 g capita^{-1}) (estimated data from AVR) and 46.3 kg (1.000 g capita^{-1}) (data from the cognizant wholesaler) of GAB was consumed in households of the city Dülmen (46,300 citizens), respectively. 1.1 kg (3.571 g bed^{-1}) of GAB was consumed in hospitals. Consumption data based on a per capita consumption were slightly different from the Suisse city Lausanne with surrounding communities (221,000 citizens). In Lausanne, in households the consumption was lower with 107.0 ± 53.5 kg year^{-1} (0.484 ± 0.242 g capita^{-1} year^{-1}), and in hospitals also comparably lower with 8.6 ± 4.3 kg year^{-1} (2.429 ± 1.215 g bed^{-1} year^{-1}) (Chèvre et al., 2013).

PIC of GAB obtained from Eq. (1) with the data of AVP 2013 was 24.3 μg L^{-1}. With data from the pharmacies' wholesaler and the domestic hospital pharmacy a value of 23.2 μg L^{-1} was calculated. These calculations were confirmed by information found in literature (Kasprzyk-Hordern et al., 2009b; Ottmar et al., 2010). Considering that GAB is not eliminated in STPs (Morasch et al., 2010), the concentration in the effluent might not change, resulting in high STP effluent concentrations in comparison to other pharmaceutical compounds (Petrie et al., 2015).

3.2. UV photolysis: primary elimination and mineralization

The fate of GAB at UV treatment was evaluated by monitoring the primary elimination and mineralization. For the initial concentration of 100 mg L^{-1} the process was performed four times to cope with experimental uncertainties and potential fluctuation in lamp emission.

Using the initial concentration of 100 mg L^{-1}, 50% of GAB was eliminated after approximately 1 h (Fig. 1A). At the end of the test, the concentration was around 20% of the initial concentration. Due to the high initial concentration, the elimination of GAB followed a zero order kinetics, with a half-life $t_{1/2}$ of 78 min. The NPOC concentration remained unchanged over almost the whole photolysis time. Mineralization started after around 1 h of photolysis and NPOC elimination was only 9% after 128 min. The low degree of mineralization and the primary elimination of 80% indicate the formation of PTPs.

The elimination kinetics for the initial concentrations of 20 mg L^{-1}, 5 mg L^{-1}, 1 mg L^{-1} used in photolysis experiments following a first order model are shown in Fig. 1B–D, respectively. The quantum yields for initial concentrations fitting a first order model were calculated according to Zepp (1978) by means of the respective rate constants, measured lamp irradiance, and the molar extinction coefficient of GAB. Accordingly, the estimated quantum yield was increasing with decreasing initial concentration (20 mg L^{-1}: 0.015, 5 mg L^{-1}: 0.032, 1 mg L^{-1}: 0.082). At an initial concentration of 0.1 mg L^{-1}, GAB concentration was below limit of detection (LOD) after 4 min of photolysis (data not shown) and kinetic fitting was not conducted. Due to insufficient detection limits of the TOC analyzer, NPOC measurement was not carried out for this concentration. The elimination kinetics for GAB and the corresponding NPOC were slower with increasing initial concentration of GAB. Likewise, rate constants were decreasing, because more intermediates and PTPs were formed from UV light with high initial start concentration. These intermediates are in concurrence to GAB and may absorb UV light partially, before the UV light can pass through the whole solution (Chelme-Ayala et al., 2010; Ding et al., 2013).

As shown in Fig. 1E, the elimination of GAB in aqueous solution with 1% 2-propanol (v/v) was slower compared to the elimination of GAB in ultrapure water (Fig. 1A) fitting a first order kinetic model. It can be assumed that 2-propanol is acting as a radical scavenger, quenching the reaction of ROS, generated from dissolved oxygen, with GAB. As shown in Fig. 1A, the dissolved oxygen concentration was constantly decreasing during the treatment process in ultrapure water. Du et al. (2014) have found that ROS are generated from dissolved oxygen through UV irradiation. In their study the decay of gallic acid was mainly induced by ROS oxidation. Likewise, the elimination of gallic acid through direct photolysis was less important. Therefore, it is expected that GAB's degradation will be predominately caused by ROS. As an explanation, GAB could be transitioned to its excited state by means of UV irradiation energy. Further reaction with dissolved oxygen could lead to the formation of superoxide anions and hydroperoxyl radicals (Du et al., 2014), which induce the elimination of GAB and the formation of PTPs. Additionally, in every taken sample the hydrogen peroxide concentration was measured semi-quantitatively with MQuant Peroxide test strips (Merck Chemicals GmbH, Schwalbach, Germany). At the beginning of the test, no hydrogen peroxide could be determined. After 32 and 64 min, 0–0.5 mg L^{-1} hydrogen peroxide was detected. Whereas, the highest observed concentration range (0.5–2.0 mg L^{-1}) was found after 128 min (test end). The formation of hydrogen peroxide can be explained by the recombination of superoxide anions with hydroperoxyl radicals (Bielski et al., 1985). Before the biodegradation and toxicity tests were performed, the hydrogen peroxide concentration had been measured again. As a result, the concentration was even lower than 0.5 mg L^{-1} in the sample after 128 min probably due to further reaction of hydrogen peroxide with GAB and PTPs.

3.3. Occurrence and structural elucidation of PTPs

Table 1 shows GAB and the PTPs formed during the course of the photolysis at different initial concentrations. 27 PTPs as newly occurring peaks were identified showing eight different *m/z* values with different t_Rs indicating the formation of isomers. The time course of newly formed PTPs and a tentative photodegradation pathway for initial concentration of 100 mg L^{-1} is shown in Figs. 2 and 3, respectively. Potential chemical mechanisms for the formation of PTPs are described in the following. The fragmentation pattern as well as the fragmentation pathway listed according to m/z values for the PTPs can be found in Text S4, SM.

In this study, most of the PTPs were found to be more polar than GAB. Accordingly to their fragmentation pattern, they were mostly formed by hydroxylation during photolysis (Mahmoud et al., 2013).

PTP 204 and PTP3 160 were renamed to PTP 204a and PTP 204b, as well as to PTP3 160a and PTP160b, respectively. In LC-ITMS PTP 204 and PTP3 160, occurred as one peak. However, in LC-HRMS the PTPs were separated, allowing to propose the formation of constitutional isomers. As LC parameters for both instruments were the same, the better separation resulted from the UHPLC working in LC-HRMS, achieving better peak separation compared to LC-ITMS.

M/z values 128, 154, 168 and 188 were identified as primarily formed PTPs. The course of the curves for these PTPs – except for 168 m/z – showed a steep slope during the beginning of the photolysis experiment (Fig. 2A, C and G). PTPs were immediately formed after starting the experiment, constantly increasing up to 64 min and then decreasing, in favor for the formation of follow-up PTPs or mineralization. PTP 154 was probably formed after the loss of water resulting in the formation of a cyclic lactam ring

Table 1
Gabapentin (GAB) and its phototransformation products (PTPs) in chronologic order according to LC-ITMS retention time (t_R), showing the highest observed A/A_0 during photolysis and corresponding LC-HRMS t_R with detected accurate mass in LC-HRMS (A is the peak area of the PTP and A_0 is the peak area of GAB at time point 0 min). PTPs were named with m/z value and numbered according to their t_R. The occurrence of PTPs was compared in different concentrations (showing • for occurrence and ◦ for absence during photolysis process).

PTP/GAB	LC-ITMS t_R (min)	Highest observed A/A_0 (%)	LC-HRMS t_R (min)	Detected mass (m/z)	Occurrence of PTPs during photolysis				
					100 mg L^{-1}	20 mg L^{-1}	5 mg L^{-1}	1 mg L^{-1}	0.1 mg L^{-1}
PTP 204a	1.8	10.2	1.70	204.1224	•	•	•	◦	◦
PTP 204b	1.8	10.2	1.91	204.1224	•	•	•	•	◦
PTP1 188	2.1	1.8	1.95	188.1274	•	•	•	•	◦
PTP 168	2.1	4.9	1.79	168.1014	•	•	•	◦	◦
PTP1 186	2.2	3.1	2.08	186.1121	•	•	•	•	•
PTP1 160	2.2	0.2	2.00	160.0966	•	•	◦	◦	◦
PTP2 188	2.4	1.4	2.25	188.1274	•	•	•	•	◦
PTP3 188	2.6	5.8	2.42	188.1275	•	•	•	•	◦
PTP2 160	3.0	0.3	2.88	160.1326	•	•	◦	◦	◦
PTP1 144	3.1	0.2	2.16	144.1378	•	•	◦	◦	◦
PTP4 188	3.2	1.4	3.05	188.1275	•	•	•	•	◦
PTP2 186	3.3	0.4	3.18	186.1115	•	•	•	•	•
PTP5 188	3.4	1.3	3.35	188.1274	•	•	•	•	◦
PTP3 186	4.0	0.8	4.28	186.1118	•	•	◦	◦	◦
PTP3 160a	4.0	2.5	3.81	160.1327	•	•	◦	◦	◦
PTP3 160b	4.0	2.5	3.98	160.1326	•	•	◦	◦	◦
PTP4 186	4.3	0.6	4.62	186.1115	•	•	◦	◦	◦
PTP2 144	4.9	0.4	3.60	144.1380	•	•	◦	◦	◦
PTP3 144	5.4	0.8	3.90	144.1380	•	•	•	◦	◦
PTP5 186	6.1	3.7	6.63	186.1119	•	•	•	◦	◦
PTP4 160	6.2	0.1	6.12	160.1322	•	•	◦	◦	◦
PTP5 160	6.8	0.6	6.75	160.1325	•	•	◦	◦	◦
GAB	7.9	100	7.34	172.1327	•	•	•	•	•
PTP4 144	10.4	0.1	7.64	144.1385	•	•	•	◦	◦
PTP5 144	11.0	0.3	8.02	144.1384	•	•	•	◦	◦
PTP6 144	11.4	0.4	8.48	144.1016	•	•	•	◦	◦
PTP 128	14.2	5.9	10.81	128.1430	•	•	•	◦	◦
PTP 154	16.1	2.3	13.31	154.1220	•	•	•	◦	◦

(Fig. 3). The proposed lactam structure induced myoclonic and generalized clonic seizures in kindled rats (Potschka et al., 2000). In contrast, the expected effect of an antiepileptic drug, like GAB, is preventing from seizures. The lactam is GAB's main degradation product. Its formation becomes more probable after long-time storage or temperatures higher than room temperature and was reported in several other studies (Ciavarella et al., 2007; Hsu and Lin, 2009; Lin et al., 2010). As the photolysis was carried out at controlled temperature of 20 ± 1 °C, it could also be formed during photolysis.

PTP 128 could be formed by decarboxylation of GAB, which results in a typical loss of 44 Da accounting for the carbonic acid moiety (Fig. 3). Several other studies also reported the loss of a carbonic acid moiety during photolysis processes (Rastogi et al., 2014; Sheu et al., 2003; Wang and Lin, 2012).

160 m/z were probably formed as secondary PTPs. PTP3 160a and PTP3 160b were formed after two hydroxylation steps from PTP 128. Position 4 on the cyclohexane is preferred for hydroxylation, because the other positions are sterically hindered. Fragmentation pattern (Text S4, SM) revealed a second hydroxylation in position 1 on the methenamine chain for PTP3 160b and on the methyl group for PTP3 160a.

PTPs formed with 188 m/z are primarily formed by single hydroxylation (Fig. 2G). As a result of the fast further transformation of mono hydroxylated GAB, only PTP3 188 exceeded the threshold of 2% A/A_0. The most probable position for the hydroxylation was position 4 on the cyclohexane ring, because the other positions are sterically hindered. A further hydroxylation step is proposed to explain the formation of PTP 204a and PTP 204b (Fig. 3) as a follow-up PTP of PTP3 188.

It can be assumed that PTP1 186 and PTP5 186 could stem from an intermediary, not analytically detected, structure with 170 m/z. During UV treatment, 170 m/z would be formed from PTP3 188 after dehydroxylation in combination with formation of a double bond in the cyclohexane ring (loss of water). Further hydroxylation, as in the case of PTP 204a and PTP 204b, would lead to PTP1 186 and PTP5 186, respectively (Fig. 3).

PTP 168 is proposed to be formed directly from the parent compound GAB and presented an increasing slope during the course of the photolysis (Fig. 2E). The proposed structure comprehends to the formation of a cyano group by dehydrogenation of the aminoethyl side chain (Fig. 3). The PTP 168 has been described as one of GAB's impurities by the United States Pharmacopeia (USP, 2013).

The occurrence of each PTP identified at the initial concentration of 100 mg L^{-1} was checked at consecutively lower concentrations (Table 1) as well, in order to evaluate if the PTPs formed at lower concentrations are identical to the ones identified at higher initial concentration of photolysis. This would allow an estimation of the significance of PTPs and their properties to environmentally relevant concentration levels.

As can be seen, each PTP identified at the initial concentration of 100 mg L^{-1} also occurred during photolysis of 20 mg L^{-1} GAB. In the same way, at initial concentration of 5 mg L^{-1} still more than the half of the PTPs were also identified. On the other hand, at initial concentration of 0.1 mg L^{-1} only 2 PTPs could be identified. As a result, for environmentally realistic concentrations not every PTPs, detected at higher concentrations, could be identified. Possible reasons for this could be (i) a different photodegradation pathway, (ii) non-sufficient detections limits, (iii) faster elimination kinetics of PTPs or (iv) the occurrence of PTPs within determined sampling points. Nevertheless, it cannot be excluded that PTPs formed at higher concentrations are formed at lower concentrations as well, which is why further targeted analysis must be conducted to clarify the relevance of suspected PTPs under environmentally realistic conditions.

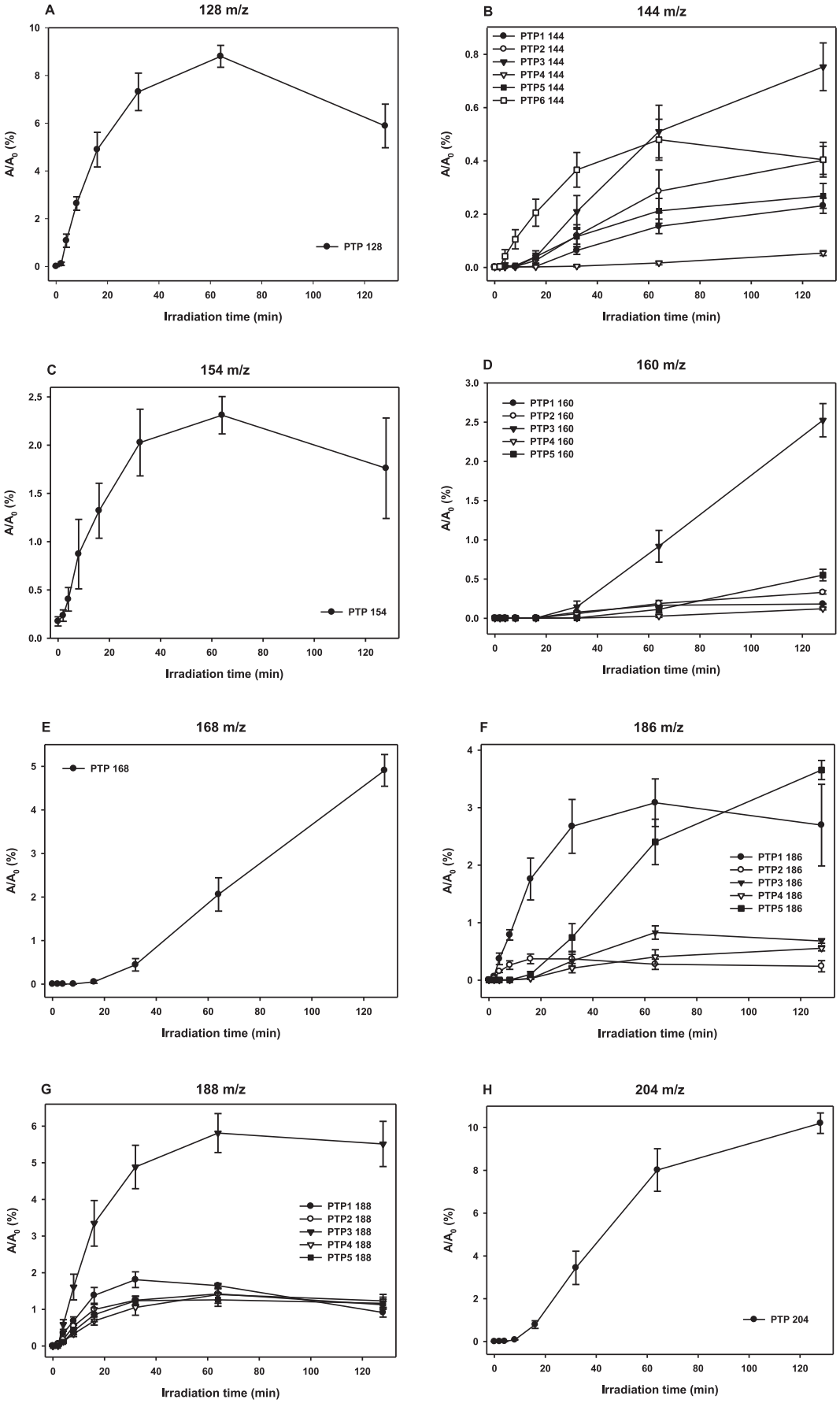

Fig. 2. Relative peak area A/A_0 (%) of phototransformation products (PTPs) during photolysis assigned to their m/z ratio (A is the peak area of the PTP at a specific time point, A_0 is the peak area of GAB at 0 min) (n = 4).

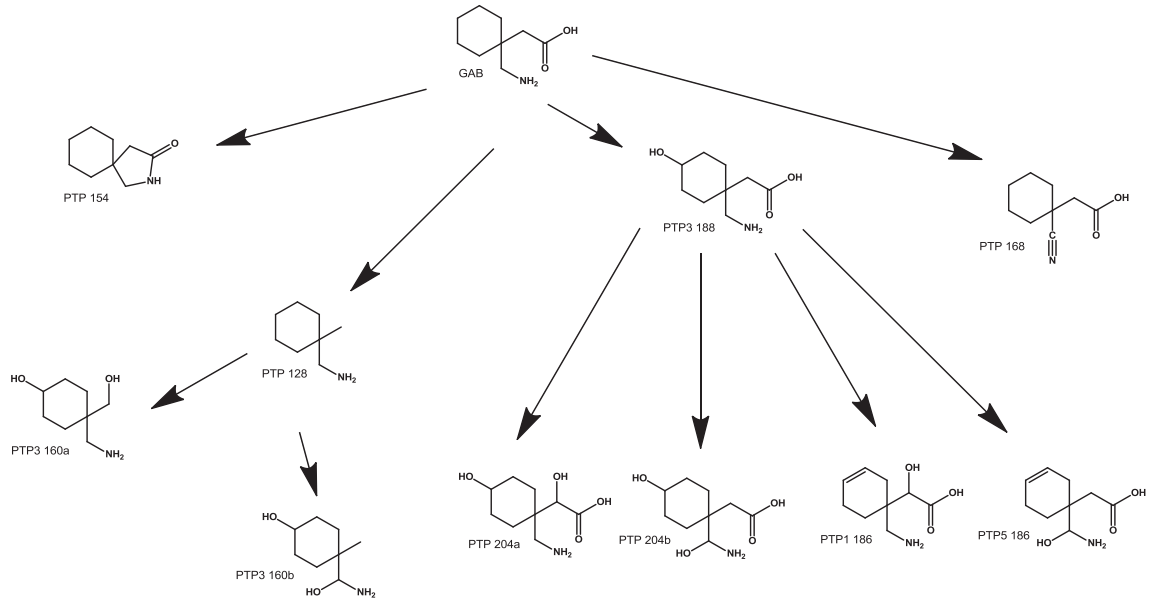

Fig. 3. Tentative phototransformation pathway of structural elucidated phototransformation products (PTPs) during UV photolysis of gabapentin (GAB) with initial concentration of 100 mg L^{-1}.

3.4. Biodegradation testing

All validity criteria of the OECD guideline for CBT were fulfilled.

GAB showed low degradation regarding ThOD achieving 7.9 ± 3.6% after 28 days. Accordingly, GAB has to be classified as a not readily biodegradable compound (OECD, 1992). The recovery of GAB regarding the peak area ratio S/S_0 was 99.6 ± 0.13% (n = 4) indicating that no biodegradation TP from GAB was formed. These findings agree with the studies of De la Cruz et al. (2012) and Reungoat et al. (2010), which even showed that GAB was not eliminated in sewage sludge, which contains a much higher density and diversity of bacteria. In conclusion Kasprzyk-Hordern et al. (2008) and Writer et al. (2013) detected GAB in river water. Because of GAB's persistence and increasing consumption, in the future, higher concentrations of GAB in the environment have to be expected.

As the CBT is used to study ready biodegradability for single chemicals with known elementary composition (OECD, 1992), the interpretation on biodegradability for the photolytic mixtures was assessed by means of measured BOD. The BOD time course of ready biodegradable sodium acetate (quality control, control substance), GAB and photolytic mixtures can be seen in Fig. 4A. GAB and photolytic mixtures at time points 32, 64 and 128 min showed no biodegradation, as BOD over the whole test period was very low. In contrast, the BOD for readily biodegradable sodium acetate increased significantly over 28 days. Samples from CBT were also evaluated by means of LC-ITMS. The TIC didn't show any newly occurring peak. Due to comparably low concentrations of the investigated compounds in CBT, only the elimination of GAB and structural elucidated PTPs were taken into account. The peak recovery after 28 days (S/S_0) of GAB and most PTPs was around 100% in every prepared CBT sample (Fig. 4B), thereby excluding any microbial biotransformation. Only PTP 154 showed a slight elimination in the CBT.

3.5. Toxicity screening of photolytic mixtures

In the modified LBT, untreated GAB did not exert a significant effect at the lowest tested dilution level of 1:2 (C_0 = 100 mg L^{-1}). In contrast, photolytic mixtures obtained after photolysis times of 64 and 128 min caused a significant inhibition (>20%) at the same dilution level (long-term luminescence inhibition (LI_{24h}) and growth inhibition (GI_{14h}), respectively, Fig. 5). Analysis of variance (ANOVA) confirmed a significant difference between untreated GAB (0 min) and the photolytic mixtures after 64 and 128 min for all investigated endpoints ($P < 0.001$).

The strongest inhibitory effects occurred after 128 min of irradiation, indicating an increasing short-term bacterial cytotoxicity (LI_{30min}) and an even more pronounced long-term antibacterial activity (LI_{24h} and GI_{14h}) for the samples collected during UV-photolysis of GAB. This time-dependency argues for a moderate impact on the biological fitness of the bacterial cells that is mainly expressed by a lowered cell multiplication rate. However, it must be assumed that this impact is not limited to specific biosynthetic pathways in prokaryotes because the short-term luminescence inhibition, as an indicator for immediate disturbances of the cell's integrity and physiology, was also significantly affected. Moreover, GAB was already partly mineralized (10% of NPOC-elimination) but not fully primarily eliminated (approx. 13% recovery) after 128 min which contributes to the finding that PTPs of GAB might possess a considerably higher intrinsic toxic potential than the original parent compound. According to the kinetics of PTP formation (Fig. 2), the following structural elucidated PTPs are suspected candidates for the observed effects: PTP 168, PTP5 186, PTP 204a and PTP 204b. Still, as only whole reaction mixtures were tested, synergistic effects (cocktail-effects) between individual PTPs and the parent compound cannot be excluded. Further, reaction by-products such as ROS might also contribute to the observed mixture toxicity. Therefore, suspected candidates should be tested individually in future experiments to confirm their expected toxic potential.

In the umu-test, a significant induction of the umuC gene was neither observed for GAB, nor for the photolytic samples at the lowest applied dilution level of 1:1.5 (C_0 = 100 mg L^{-1}). As the growth factor (G) was above 0.5 for all investigated samples, false negative results due to cytotoxicity can be excluded.

It has to be noted that the applied screening tests in this study cannot replace a sound evaluation of environmental toxicity and

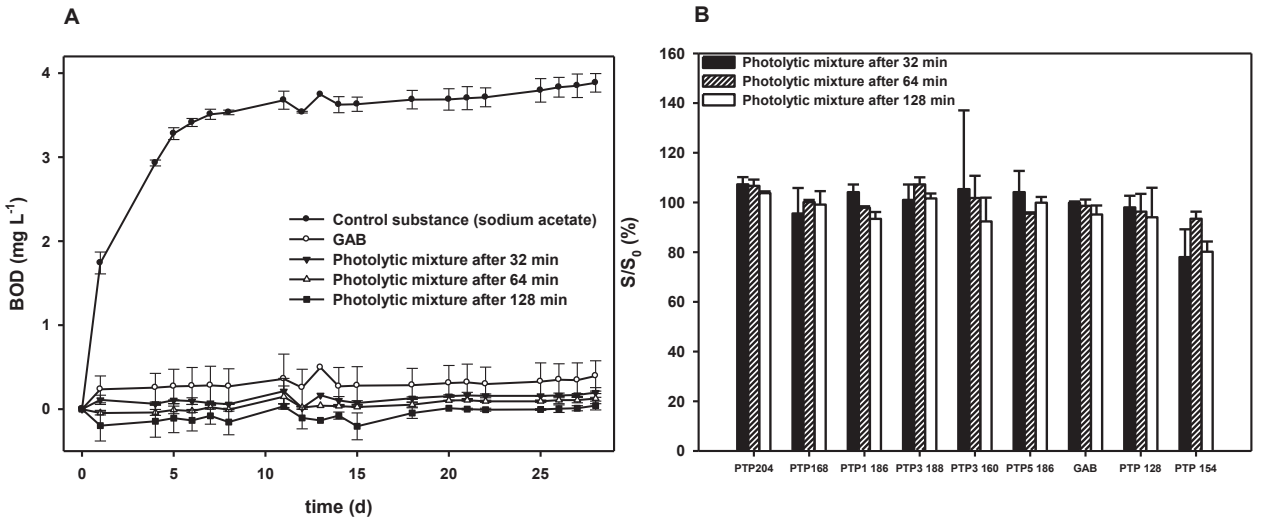

Fig. 4. [A] Time course of biochemical oxygen demand (BOD) over 28 days in the Closed Bottle Test (CBT) showing control substance, gabapentin (GAB) and its photolytic mixtures after 32, 64 and 128 min of UV treatment, respectively (n = 2). [B] Recovery of GAB and its phototransformation products (PTPs) (A/A_0 >2%) showing relative peak area S/S_0 after 28 days related to day 0 of Closed Bottle Test (CBT) in different photolytic mixtures (n = 2).

possible effects on human health. But they provided clear evidence that PTPs of GAB can have altered (eco)toxicological properties that might be worth receiving further attention. As for the parent compound GAB teratogenicity is already confirmed, the teratogenicity and other possible "side-effects" of environmentally relevant PTPs should also be considered in this context using a read-across approach. However, appropriate testing of all relevant PTPs for teratogenicity and other important toxicological endpoints would require extensive in vitro and in vivo experiments to generate data of ecological relevance. Moreover, the isolation or synthesis of PTPs in appropriate amounts for performance of such assays is difficult, cost-intensive and often not possible. The chemical structures of PTPs were sufficiently elucidated within this study to provide access to powerful in silico tools on the basis of (quantitative) structure-activity relationships ((Q)SARs). Such (Q)SAR-predictions could provide further evidence that might help to develop intelligent strategies for (eco)toxicity testing.

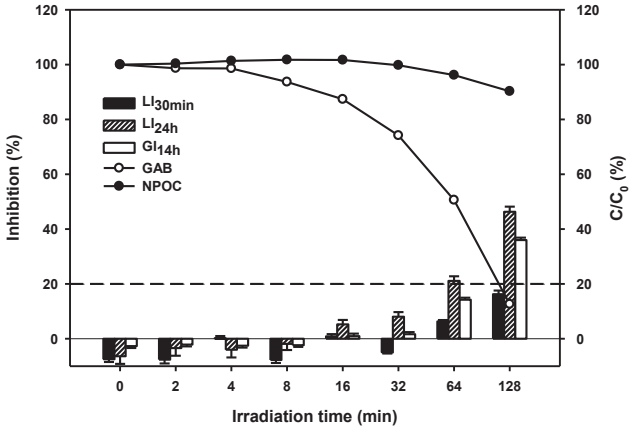

Fig. 5. Toxification of gabapentin (GAB) during UV-photolysis by means of short-term luminescence inhibition (LI_{30min}), long-term luminescence inhibition (LI_{24h}) and growth inhibition (GI_{14h}) in the modified LBT (bars). Initial photolysis concentration (C_0) of GAB was 100 mg L^{-1}. Luminescent bacteria were exposed to photolytic samples in a final dilution of 1:2. Primary elimination and mineralization of GAB during photolysis is shown as percentage of the initial treatment concentration (C/C_0) according to measured peak areas and NPOC concentrations, respectively.

4. Conclusions

GAB was neither entirely eliminated nor fully mineralized by UV photolysis at high elevated concentrations in ultrapure water. Even close to realistic environmental concentrations, a technically long irradiation time was necessary to mineralize GAB. Additionally, newly formed PTPs are not eliminated after biodegradation testing, and therefore could be persistent in the environment. It was demonstrated that some PTPs of GAB might possess altered toxicological properties e.g. toxicity against environmental bacteria. Therefore, further investigations should be conducted regarding the environmental occurrence and the adverse effects of newly formed PTPs of GAB. As for the parent compound GAB teratogenicity is already confirmed, the teratogenicity of PTPs should also be considered in this context.

Moreover, due to the limited sensitivity of (bio)analytical methods, the characterization and elucidation of PTPs should be conducted with initial concentrations that are higher than the environmentally realistic concentrations as to take more formed PTPs into account. However, we recommend to conduct photolysis at different concentration levels to confirm that certain types of PTPs are independent from the initial concentration. Finally, the environmental relevance of PTPs that are suspected to be persistent and/or toxic should be clarified using targeted analysis.

Acknowledgments

The authors would like to thank the Federal Ministry of Research and Education for their financial support (grant no. 02WRS1280A - J), the Ministry for Climate Protection, environment, agriculture and environment and consumer protection North Rhine-Westphalia for their financial support which was co-founded by the EU INTERREG IVb program (Project DSADS), the Innovations-Inkubator Lüneburg (Teilmaβnahme 1.4, Graduate School) for providing a scholarship for Jakob Menz, the local pharmacists for providing consumption data for GAB, Dr. Annette Haiβ and Evgenia Logunova for planning the aerobic biodegradation tests, Janin Westphal for analytical support, Stefanie Hinz for the help with toxicity testing, Dr. Marcelo L. Wilde and Karen Kratschmer for proofreading the manuscript, and Markus Herrel and Rainer Fiehn (Ortenau Klinikum Offenburg-Gengenbach) for their general support and

patience. We also thank the anonymous reviewers for their constructive comments.

Appendix A. Supplementary data

Supplementary data related to this article can be found at http://dx.doi.org/10.1016/j.watres.2015.08.004.

References

Afshar, M., Golalipoor, M.J., Azadeh, T., 2007. Teratogenic effects of gabapentin on neural tube and skeletal development in mice. Reprod. Toxicol. 24 (1), 66–67.

Bielski, B.H.J., Cabelli, D.E., Arudi, R.L., Ross, A.B., 1985. Reactivity of HO2/O−2 radicals in aqueous solution. J. Phys. Chem. Ref. Data 14 (4), 1041.

Canonica, S., Meunier, L., Gunten, U. von, 2008. Phototransformation of selected pharmaceuticals during UV treatment of drinking water. Water Res. 42 (1–2), 121–128.

Capdeville, M., Budzinski, H., 2011. Trace-level analysis of organic contaminants in drinking waters and groundwaters. TrAC-Trend Anal. Chem. 30 (4), 586–606.

Carta, M.G., Hardoy, M.C., Hardoy, M.J., Grunze, H., Carpiniello, B., 2003. The clinical use of gabapentin in bipolar spectrum disorders. J. Affect Disord. 75 (1), 83–91.

Chelme-Ayala, P., El-Din, M.G., Smith, D.W., 2010. Degradation of bromoxynil and trifluralin in natural water by direct photolysis and UV plus H(2)O(2) advanced oxidation process. Water Res. 44 (7), 2221–2228.

Chèvre, N., Coutu, S., Margot, J., Wynn, H.K., Bader, H.-P., Scheidegger, R., Rossi, L., 2013. Substance flow analysis as a tool for mitigating the impact of pharmaceuticals on the aquatic system. Water Res. 47 (9), 2995–3005.

Ciavarella, A.B., Gupta, A., Sayeed, V.A., Khan, M.A., Faustino, P.J., 2007. Development and application of a validated HPLC method for the determination of gabapentin and its major degradation impurity in drug products. J. Pharm. Biomed. 43 (5), 1647–1653.

De la Cruz, N., Giménez, J., Esplugas, S., Grandjean, D., de Alencastro, L.F., Pulgarín, C., 2012. Degradation of 32 emergent contaminants by UV and neutral photo-fenton in domestic wastewater effluent previously treated by activated sludge. Water Res. 46 (6), 1947–1957.

Ding, S.-L., Wang, X.-K., Jiang, W.-Q., Meng, X., Zhao, R.-S., Wang, C., Wang, X., 2013. Photodegradation of the antimicrobial triclocarban in aqueous systems under ultraviolet radiation. Environ. Sci. Pollut. Res. Int. 20 (5), 3195–3201.

Du, Y., Chen, H., Zhang, Y., Chang, Y., 2014. Photodegradation of gallic acid under UV irradiation: insights regarding the pH effect on direct photolysis and the ROS oxidation-sensitized process of DOM. Chemosphere 99, 254–260.

Ebert, I., Amato, R., Hein, A., Konradi, Sabine, 2014. Pharmaceuticals in the Environment: Avoiding, Reducing, Monitoring. Federal Environmental Agency (in German).

Escher, B.I., Baumgartner, R., Koller, M., Treyer, K., Lienert, J., McArdell, C.S., 2011. Environmental toxicology and risk assessment of pharmaceuticals from hospital wastewater. Water Res. 45 (1), 75–92.

Federal Statistical Office DESTATIS, 2015. Water Management. Water supply from 1991 to 2010 (accessed 02.02.2015). https://www.destatis.de/DE/ZahlenFakten/GesamtwirtschaftUmwelt/Umwelt/UmweltstatistischeErhebungen/Wasserwirtschaft/Tabellen/Wasserabgabe1991_2010.html (in German).

Friedrich, J., Längin, A., Kümmerer, K., 2013. Comparison of an electrochemical and luminescence-based oxygen measuring system for use in the biodegradability testing according to closed bottle test (OECD 301D). Clean-Soil Air Water 41 (3), 251–257.

Gómez, M., Gómez-Ramos, M., Malato, O., Mezcua, M., Férnandez-Alba, A., 2010. Rapid automated screening, identification and quantification of organic microcontaminants and their main transformation products in wastewater and river waters using liquid chromatography–quadrupole-time-of-flight mass spectrometry with an accurate-mass database. J. Chromatogr. A 1217 (45), 7038–7054.

Haddad, T., Kümmerer, K., 2014. Characterization of photo-transformation products of the antibiotic drug ciprofloxacin with liquid chromatography-tandem mass spectrometry in combination with accurate mass determination using an LTQ-Orbitrap. Chemosphere 115, 40–46.

Happe, S., Sauter, C., Klösch, G., Saletu, B., Zeitlhofer, J., 2003. Gabapentin versus ropinirole in the treatment of idiopathic restless legs syndrome. Neuropsychobiology 48 (2), 82–86.

Hijnen, W.A.M., Beerendonk, E.F., Medema, G.J., 2006. Inactivation credit of UV radiation for viruses, bacteria and protozoan (oo)cysts in water: a review. Water Res. 40 (1), 3–22.

Hsu, C.-H., Lin, S.-Y., 2009. Rapid examination of the kinetic process of intramolecular lactamization of gabapentin using DSC–FTIR. Thermochim. Acta 486 (1–2), 5–10.

Huerta-Fontela, M., Galceran, M.T., Ventura, F., 2011. Occurrence and removal of pharmaceuticals and hormones through drinking water treatment. Water Res. 45 (3), 1432–1442.

Illés, E., Szabó, E., Takács, E., Wojnárovits, L., Dombi, A., Gajda-Schrantz, K., 2014. Ketoprofen removal by O_3 and O_3/UV processes: kinetics, transformation products and ecotoxicity. Sci. Total Environ. 472, 178–184.

ISO/FDIS 13829:1999(E), 1999. Water Quality-Determination of the Genotoxicity of Water and Waste Water Using the Umu-test.

Kasprzyk-Hordern, B., Dinsdale, R.M., Guwy, A.J., 2008. The occurrence of pharmaceuticals, personal care products, endocrine disruptors and illicit drugs in surface water in South Wales, UK. Water Res. 42 (13), 3498–3518.

Kasprzyk-Hordern, B., Dinsdale, R.M., Guwy, A.J., 2009a. Illicit drugs and pharmaceuticals in the environment–forensic applications of environmental data, Part 2: pharmaceuticals as chemical markers of faecal water contamination. Environ. Pollut. 157 (6), 1778–1786.

Kasprzyk-Hordern, B., Dinsdale, R.M., Guwy, A.J., 2009b. The removal of pharmaceuticals, personal care products, endocrine disruptors and illicit drugs during wastewater treatment and its impact on the quality of receiving waters. Water Res. 43 (2), 363–380.

Lai, F.Y., Ort, C., Gartner, C., Carter, S., Prichard, J., Kirkbride, P., Bruno, R., Hall, W., Eaglesham, G., Mueller, J.F., 2011. Refining the estimation of illicit drug consumptions from wastewater analysis: co-analysis of prescription pharmaceuticals and uncertainty assessment. Water Res. 45 (15), 4437–4448.

Lin, S.-Y., Hsu, C.-H., Ke, W.-T., 2010. Solid-state transformation of different gabapentin polymorphs upon milling and co-milling. Int. J. Pharm. 396 (1–2), 83–90.

Mahmoud, W.M.M., Trautwein, C., Leder, C., Kümmerer, K., 2013. Aquatic photochemistry, abiotic and aerobic biodegradability of thalidomide: identification of stable transformation products by LC–UV–MSn. Sci. Total Environ. 463–464, 140–150.

Mathew, N.T., Rapoport, A., Saper, J., Magnus, L., Klapper, J., Ramadan, N., Stacey, B., Tepper, S., 2001. Efficacy of gabapentin in migraine prophylaxis. Headache 41 (2), 119–128.

Menz, J., Schneider, M., Kümmerer, K., 2013. Toxicity testing with luminescent bacteria – characterization of an automated method for the combined assessment of acute and chronic effects. Chemosphere 93 (6), 990–996.

Morasch, B., Bonvin, F., Reiser, H., Grandjean, D., de Alencastro, Luiz Felippe, Perazzolo, C., Chèvre, N., Kohn, T., 2010. Occurrence and fate of micropollutants in the Vidy Bay of Lake Geneva, Switzerland. Part II: micropollutant removal between wastewater and raw drinking water. Environ. Toxicol. Chem. 29 (8), 1658–1668.

Neamțu, M., Grandjean, D., Sienkiewicz, A., Le Faucheur, S., Slaveykova, V., Colmenares, Julia Janeth Velez, Pulgarín, C., de Alencastro, Luiz Felippe, 2014. Degradation of eight relevant micropollutants in different water matrices by neutral photo-fenton process under UV254 and simulated solar light irradiation – a comparative study. Appl. Catal. B Environ. 158–159, 30–37.

Nödler, K., Licha, T., Bester, K., Sauter, M., 2010. Development of a multi-residue analytical method, based on liquid chromatography–tandem mass spectrometry, for the simultaneous determination of 46 micro-contaminants in aqueous samples. J. Chromatogr. A 1217 (42), 6511–6521.

OECD, 1992. Guidelines for the Testing of Chemicals: Ready Biodegradability.

OECD, 2010. Guidelines for the Testing of Chemicals: Phototransformation of Chemicals in Water – Direct Photolysis.

OECD, 2011. Health at a Glance 2011. OECD Publishing.

Ottmar, K.J., Colosi, L.M., Smith, J.A., 2010. Development and application of a model to estimate wastewater treatment plant prescription pharmaceutical influent loadings and concentrations. Bull. Environ. Contam. Toxicol. 84 (5), 507–512.

Petrie, B., Barden, R., Kasprzyk-Hordern, B., 2015. A review on emerging contaminants in wastewaters and the environment: current knowledge, understudied areas and recommendations for future monitoring. Water Res. 72, 3–27.

Pfizer Pharma GmbH (Parke-Davis), 2014. NEURONTIN® FDA Approved Labeling.

Potschka, H., Feuerstein, T.J., Löscher, W., 2000. Gabapentin-lactam, a close analogue of the anticonvulsant gabapentin, exerts convulsant activity in amygdala kindled rats. N-S Arch. Pharmacol. 361 (2), 200–205.

Prakash, Prabhu, L.V., Rai, R., Pai, M.M., Yadav, S.K., Madhyastha, S., Goel, R.K., Singh, G., Nasar, M.A., 2008. Teratogenic effects of the anticonvulsant gabapentin in mice. Singap. Med. J. 49 (1), 47–53.

Rastogi, T., Leder, C., Kümmerer, K., 2014. Qualitative environmental risk assessment of photolytic transformation products of iodinated X-ray contrast agent diatrizoic acid. Sci. Total Environ. 482–483, 378–388.

Reungoat, J., Macova, M., Escher, B.I., Carswell, S., Mueller, J.F., Keller, J., 2010. Removal of micropollutants and 5-6 ozonation and activated carbon filtration. Water Res. 44 (2), 625–637.

Sanderson, H., Johnson, D.J., Reitsma, T., Brain, R.A., Wilson, C.J., Solomon, K.R., 2004. Ranking and prioritization of environmental risks of pharmaceuticals in surface waters. Regul. Toxicol. Pharmacol. 39 (2), 158–183.

Schwabe, U., Paffrath, D., 2010. Drug Prescription Report 2010: Current Data, Expenses, Trends and Comments. Springer-Verlag Berlin Heidelberg, Berlin, Heidelberg (in German).

Schwabe, U., Paffrath, D., 2013. Drug Prescription Report 2013: Current Data, Expenses, Trends and Comments. Springer Verlag, Berlin (in German).

Sheu, M.-T., Ho, H.-O., Wang, P.-Y., Liou, Y.-B., Wu, A.-B., 2003. Photolysis of NSAIDs. I. photodegradation products of carprofen determined by LC-ESI-MS. J. Chromatogr. Sci. 41 (4), 200–204.

Trautwein, C., Berset, J.-D., Wolschke, H., Kümmerer, K., 2014. Occurrence of the antidiabetic drug metformin and its ultimate transformation product guanylurea in several compartments of the aquatic cycle. Environ. Int. 70, 203–212.

Trautwein, C., Kümmerer, K., 2012. Ready biodegradability of trifluoromethylated phenothiazine drugs, structural elucidation of their aquatic transformation products, and identification of environmental risks studied by LC-MS(n) and QSAR. Environ. Sci. Pollut. Res. Int. 19 (8), 3162–3177.

USP 37-NF 32 The United States Pharmacopeia and National Formulary, 2013. Main Edition Plus Supplements 1 and 2.

Verlicchi, P., Al Aukidy, M., Galletti, A., Petrovic, M., Barceló, D., 2012. Hospital effluent: Investigation of the concentrations and distribution of pharmaceuticals and environmental risk assessment. Sci. Total Environ. 430, 109–118.
Wang, X.-H., Lin, A.Y.-C., 2012. Phototransformation of cephalosporin antibiotics in an aqueous environment results in higher toxicity. Environ. Sci. Technol. 46 (22), 12417–12426.
Writer, J.H., Ferrer, I., Barber, L.B., Thurman, E.M., 2013. Widespread occurrence of neuro-active pharmaceuticals and metabolites in 24 Minnesota rivers and wastewaters. Sci. Total Environ. 461–462, 519–527.
Yu, J.T., Bouwer, E.J., Coelhan, M., 2006. Occurrence and biodegradability studies of selected pharmaceuticals and personal care products in sewage effluent. Agr. Water Manage. 86 (1–2), 72–80.
Zepp, R.G., 1978. Quantum yields for reaction of pollutants in dilute aqueous solution. Environ. Sci. Technol. 12 (3), 327–329.
Zhu, C., Jiang, L., Chen, T.-M., Hwang, K.-K., 2002. A comparative study of artificial membrane permeability assay for high throughput profiling of drug absorption potential. Eur. J. Med. Chem. 37 (5), 399–407.
Zühlke, S., Dünnbier, U., Heberer, T., 2004. Detection and identification of phenazone-type drugs and their microbial metabolites in ground and drinking water applying solid-phase extraction and gas chromatography with mass spectrometric detection. J. Chromatogr. A 1050 (2), 201–209.

Publikation 4

Experimental and in silico assessment of fate and effects of the antipsychotic drug quetiapine and its bio- and phototransformation products in aquatic environments

Herrmann, M., Menz, J., Gassmann, M., Olsson, O., Kümmerer, K.

(2016)

Environmental Pollution 218, 66-76

DOI: 10.1016/j.envpol.2016.08.040

Environmental Pollution 218 (2016) 66–76

Contents lists available at ScienceDirect

Environmental Pollution

journal homepage: www.elsevier.com/locate/envpol

Experimental and *in silico* assessment of fate and effects of the antipsychotic drug quetiapine and its bio- and phototransformation products in aquatic environments☆

Manuel Herrmann [a, b], Jakob Menz [a], Matthias Gassmann [c], Oliver Olsson [a], Klaus Kümmerer [a, *]

[a] Sustainable Chemistry and Material Resources, Institute of Sustainable and Environmental Chemistry, Leuphana University of Lüneburg, C13, Scharnhorststrasse 1, DE-21335 Lüneburg, Germany
[b] Hospital Pharmacy, Ortenau Klinikum Offenburg-Gengenbach, Ebertplatz 12, DE-77654 Offenburg, Germany
[c] Water Quality Management – Modelling and Simulation, Institute of Water, Waste and Environment, Kurt-Wolters-Strasse 3, DE-34125 Kassel, Germany

ARTICLE INFO

Article history:
Received 21 April 2016
Received in revised form
12 August 2016
Accepted 13 August 2016
Available online 20 August 2016

Keywords:
Closed Bottle Test (CBT)
High-resolution mass spectrometry
Luminescent bacteria test
Manometric Respirometry Test (MRT)
Quetiapine carboxylic acid
Umu-test

ABSTRACT

The antipsychotic drug quetiapine (QUT) has been frequently detected in sewage treatment plants. However, information on the fate of QUT in aquatic environments and its behavior during UV treatment is limited. In this study, QUT is shown not to be readily biodegradable in the Closed Bottle Test and the Manometric Respirometry Test according to OECD guidelines. The main biotransformation product (BTP) formed in the tests, a carboxylic acid derivative, was identified by means of high-resolution mass spectrometry. This BTP is presumably a human metabolite and showed higher detection rates than QUT in a river sampling campaign conducted in northern Germany. UV elimination kinetics of QUT at different initial concentrations (226.5, 45.3, 11.3, and 2.3 μmol L^{-1}) were faster at lower initial concentrations. All seven phototransformation products (PTPs) could be still identified at initial concentration of 11.3 μmol L^{-1}. The photolytic mixture generated after 128 min of photolysis of QUT was not better biodegradable than QUT. Initial UV treatment of QUT led to the formation of several additional BTPs. Four of them were identified. The bacterial cytotoxicity and genotoxicity before and after phototransformation of QUT in a modified luminescent bacteria test (LBT) and the umu-test (ISO/FDIS 13829) showed cytotoxic effects in the LBT for QUT. Furthermore, PTPs had similar cytotoxic effects on luminescent bacteria. The umu-test did not reveal any genotoxic activity for QUT or PTPs. In conclusion, the release of QUT into sewage treatment plants and aquatic environments could result in the formation of a main BTP. Additional UV treatment of QUT would lead to the formation of additional BTPs. Moreover, treatment did not result in lower toxicity to tested organisms. In conclusion, UV treatment of QUT should be considered critically as a potential treatment for QUT in aquatic systems.

1. Introduction

The occurrence of active pharmaceutical ingredients (APIs) in the environment is a well-known issue in environmental research (Al Aukidy et al., 2012; Kümmerer, 2009; Petrie et al., 2015). APIs of various classes, including neurological drugs, have been found in different environmental compartments (Mackuľak et al., 2015; Nödler et al., 2010; Subedi et al., 2013). As the worldwide consumption of especially second-generation antipsychotics increased in recent years (Lertxundi et al., 2012; Verdoux et al., 2010), it can be assumed that higher amounts of these kinds of drugs are being discharged into the environment. In particular, quetiapine (QUT) has been used in high amounts for the treatment of psychiatric diseases in England and Canada (Ilyas and Moncrieff, 2012; Pringsheim and Gardner, 2014). Likewise, QUT had the highest prescription volume of all antipsychotic drugs in German

☆ This paper has been recommended for acceptance by Chen Da.

* Corresponding author. Nachhaltige Chemie und Stoffliche Ressourcen, Institut für Nachhaltige Chemie und Umweltchemie, Fakultät für Nachhaltigkeit, Leuphana Universität Lüneburg, Scharnhorststraße 1/C13, D-21335 Lüneburg, Germany.
E-mail addresses: manuel.herrmann@leuphana.de (M. Herrmann), jakob.menz@leuphana.de (J. Menz), gassmann@uni-kassel.de (M. Gassmann), oliver.olsson@leuphana.de (O. Olsson), klaus.kuemmerer@leuphana.de (K. Kümmerer).

http://dx.doi.org/10.1016/j.envpol.2016.08.040
0269-7491/

households with a calculated consumption of 24.9 t in 2014 (Schwabe and Paffrath, 2015).

QUT is almost entirely metabolized in human bodies (AstraZeneca Pharmaceuticals, 2013). However, recent studies have shown that QUT can be found in influents of sewage treatment plants (STPs) at average concentrations of 90 ng L^{-1} (Gurke et al., 2015) and up to 43.6 ng L^{-1} (Subedi and Kannan, 2015). The excreted fraction of unchanged QUT can be primarily eliminated up to 87% by STPs (Subedi and Kannan, 2015). However, other studies observed QUT in even higher concentrations in effluents of different STPs (up to 100 ± 100 ng L^{-1} and 1168 ± 66 ng L^{-1}) (Oliveira et al., 2015; Yuan et al., 2013; respectively).

Comprehensive information on the environmental fate and effects of QUT in general and biodegradation in aquatic systems in particular is not available. There are a few indications for the non-ready biodegradability of QUT (Food and Drug Administration, 2007). Data on possible biotransformation products (BTPs) resulting from incomplete mineralization of the parent compound in STPs or aquatic environments is, however, missing. As the known metabolite QUT carboxylic acid is not active in humans (Food and Drug Administration, 2007), no studies have been conducted regarding the occurrence and fate of this compound in the environment. Mahmoud et al. (2013) already showed that human metabolites and environmental BTPs can be identical. Therefore, it is very likely that the carboxylic acid product of QUT is also formed by bacteria in aquatic systems in oxidation processes. Moreover, some studies have already shown that BTPs can be produced in high amounts by bacteria in surface water (Mahmoud and Kümmerer, 2012; Trautwein and Kümmerer, 2011).

Since QUT can be seen as an API consumed in high amounts at psychiatric hospitals and nursing homes (Herrmann et al., 2015a), the elimination of QUT and its metabolites at the emission source could reduce influent concentrations at STPs. UV irradiation has been discussed as a potential decentralized treatment option (Kovalova et al., 2013). Furthermore, UV radiation is often applied for the finishing of potable water. Different studies have assessed the performance of UV treatment regarding the elimination of APIs from water (Kim et al., 2009; Pereira et al., 2007). However, these decentralized treatment systems have to completely degrade, i.e mineralize substances into non-toxic compounds such as carbon dioxide and water, as incomplete degradation could result in environmental and health problems originating either from the parent compound or its phototransformation products (PTPs). UV treatment of QUT was assessed in the study by Skibiński (2012), who identified five PTPs formed from QUT in methanol by means UV-C irradiation. Data on the fate and effects of these PTPs is, however, still missing. Consequently, an analysis of the degradation efficiency of QUT, the identification of PTPs, and their assessment are required if one is to assess whether UV treatment systems could be used to eliminate QUT from wastewater or potable water finishing (Herrmann et al., 2015b; Mahmoud et al., 2014). Recent studies have shown that PTPs or BTPs could have a negative effect on environmental organisms and be more persistent than the parent compound itself (Gutowski et al., 2015; Illés et al., 2014).

In light of the findings discussed above, the main objectives of this study were (i) to provide new insights concerning the fate of QUT in aquatic environments, (ii) to determine the effect of UV radiation on the behavior of QUT in aqueous solution to evaluate the degradation and mineralization efficiency and suitability of UV treatment, and (iii) to obtain additional information on the formation of BTPs and PTPs. To fulfill these objectives, the biodegradability and biotransformation of QUT in the Closed Bottle Test (CBT) and the MRT according to Organisation for Economic Co-operation and Development (OECD) 301 D and F, respectively, were studied. In addition, selective water sampling was conducted at six rivers of a rural county in northern Germany for analytical determination of QUT and the BTP that was observed in laboratory testing. Moreover, QUT, at different initial concentrations in aqueous solution, was treated with UV light to investigate elimination kinetics, degree of mineralization and to elucidate the structure of its PTPs. The primary elimination of QUT and structure elucidation was performed by LC-UV-MS^n. Photolytic mixtures of QUT and the generated PTPs were also analyzed in terms of biodegradability, i.e. mineralization and the possible formation of BTPs. The bacterial cytotoxicity and genotoxicity of QUT and the photolytic mixtures were also assessed in a modified luminescent bacteria test (LBT) and the umu-test according to ISO/FDIS 13829, respectively.

2. Materials and methods

2.1. Chemicals and reagents

All tests were conducted with QUT hemifumarate (certified purity 98%) purchased from LGC Standards GmbH (Wesel, Germany). Sodium fumarate dibasic (purity ≥ 99%) was purchased from Sigma-Aldrich Chemie GmbH (Steinheim, Germany). Ammonium acetate (HiPerSolv CHROMANORM® for HPLC) and methanol (HiPerSolv CHROMANORM® for HPLC, LC-MS grade) were purchased from VWR International GmbH (Darmstadt, Germany). Aqueous mobile phase, standard solutions, and solutions for photolysis treatments were prepared with ultrapure water.

2.2. Simulated UV treatment

The test solutions were freshly prepared with ultrapure water, and 100, 20, 5, and 1 mg L^{-1} of QUT hemifumarate to reach corresponding initial concentrations of 226.5, 45.3, 11.3, and 2.3 μmol L^{-1} of QUT, respectively. Photolysis experiments were carried out in a 1 L batch immersion tube photo reactor using 0.8 L of sample volume. A medium-pressure mercury lamp (TQ 150, UV Consulting Peschl, Mainz, Germany) surrounded by ilmasil quartz glass was used as a polychromatic radiation source. Information on the relative emission spectrum of the lamp can be found in the SM (supplementary material), Text S1. The actual absolute photon flux of the lamp was determined by chemical actinometry. Using this information and the molar extinction coefficient of QUT, the quantum yield of QUT was calculated (SM, Text S2). Magnetic stirring ensured continuous mixing of the solution. Constant temperature (20 ± 1 °C) was guaranteed by using a cooling system (WKL230, LAUDA, Berlin, Germany).

The photolysis experiments were carried out for 128 min. Samples were collected before treatment, and after 2, 4, 8, 16, 32, 64, and 128 min of treatment for an LC-UV-MS^n analysis (primary elimination and structure elucidation) (see Section 2.4) and dissolved organic carbon (DOC) determination for degree of total mineralization (see Section 2.4). For toxicity screening, samples at initial UV treatment concentration of 226.5 μmol L^{-1} of QUT were collected at the identical time points (see Section 2.6). In addition, photolytic samples after 128 min of treatment at initial concentration of 226.5 μmol L^{-1} were collected for biodegradation testing (see Section 2.3). Kinetic curve fitting was performed with SigmaPlot 11 (Systat Software, San Jose, USA).

2.3. Biodegradation testing

QUT hemifumarate and the photolytic mixture after 128 min of UV irradiation at initial concentration of 226.5 μmol L^{-1} underwent two biodegradation tests with different contents in terms of test substance, minerals, and inoculum according to OECD guidelines

301 D (CBT) and 301 F (MRT), respectively. All biodegradation tests were performed in duplicates (n = 2). The applied inoculum was collected from the effluent of the municipal STP in Lüneburg, Germany (144,000 population equivalents). In both tests, a chemical is classified as readily biodegradable if the measured biochemical oxygen demand (BOD) reaches at least 60% of the theoretical oxygen demand (ThOD) (OECD, 1992). As the standard substance of QUT was only available as a fumaric acid salt, partial degradation could be attributed to readily biodegradable fumaric acid. To confirm this assumption, the CBT was also conducted with fumaric acid to measure its extent of biodegradability compared to QUT hemifumarate.

Samples taken at the beginning and the end of both tests underwent LC-MS^n analysis (see Section 2.4). In the case of the MRT, a DOC analysis (see Section 2.4) was also performed.

2.3.1. Closed Bottle Test (CBT)

The CBT was performed according to OECD test guidelines (OECD, 1992) using a low content of minerals and inoculum. Likewise, ready biodegradability in aquatic environments was simulated. 1 L of mineral medium was inoculated with two drops of STP effluent. The test was conducted in the dark for 28 days at a temperature of 20 ± 1 °C. The initial concentration of QUT hemifumarate was 2.6 mg L^{-1} (5.9 μmol L^{-1}) corresponding to a ThOD of 5 mg L^{-1}. The final concentration of the photolytic mixture after 128 min was adjusted according to the remaining DOC concentration to reach a similar ThOD. The test concentration of fumaric acid in the CBT was 8.3 mg L^{-1} (71.5 μmol L^{-1}) corresponding to a ThOD of 5 mg L^{-1}. Detailed information is prodived in the SM, Text S3.

2.3.2. Manometric Respirometry Test (MRT)

The MRT was also performed according to OECD guidelines (OECD, 1992). This test has a higher inoculum density than the CBT. 1 L of mineral medium was inoculated with 80 mL of STP effluent. The test was also conducted in the dark for 28 days at a temperature of 20 ± 1 °C. The test concentration of QUT hemifumarate was 15.3 mg L^{-1} (34.7 μmol L^{-1}) corresponding to a ThOD of 30 mg L^{-1}. The final concentration of the photolytic mixture after 128 min was adjusted according to the remaining DOC concentration to reach a similar ThOD. Fumaric acid was not measured in the MRT because it was assumed that it is very likely to be readily biodegradable in the CBT. Detailed information is prodived in the SM, Text S4.

2.4. Analytical conditions

The degree of mineralization for photolysis experiments and the MRT was analyzed by a Total Organic Carbon Analyzer (TOC 5000, Shimadzu GmbH, Duisburg, Germany). Primary elimination by UV absorption at 254 nm in all photolytic samples were tested on a Shimadzu Prominence HPLC (Shimadzu GmbH, Duisburg, Germany) (SM, Text S5).

An LC-MS^n analysis was performed a) for screening on an Agilent 1100 series HPLC system (Agilent Technologies, Waldbronn, Germany) coupled to a Bruker Esquire 6000^{plus} low resolution mass spectrometer with an ESI source (Bruker Daltonics, Bremen, Germany) (LC-ITMS) and b) a Dionex Ultimate 3000 UHPLC system (Dionex, Idstein, Germany) coupled with a LTQ Orbitrap-XL high-resolution mass spectrometer with a H-ESI source (Thermo Scientific, Bremen, Germany) (LC-HRMS) for confirmation of the chemical structure of the transformation products. The chromatographic method described above was also for LC-MS^n analysis (see SM, Text S5).

At initial concentration of 226.5 μmol L^{-1} the peak area A of PTPs were related to the peak area of QUT A_0 at time point 0 min. Every PTP exceeding 1% of A/A_0 was structurally elucidated. Detailed information on the mass spectrometric method regarding peak area ratios can be found in SM, Text S6. Structures were analyzed using the ITMS in Auto-MS Mode and, to improve the reliability of results, the HRMS up to MS^3 (see SM, Text S7). Moreover, the occurrence of PTPs at different initial concentrations was compared to confirm that the formation of PTPs is not depending on initial concentration.

Samples from both biodegradation tests were analyzed with the help of LC-ITMS using recovered peak areas of QUT and its PTPs S/S_0 (S is the peak area of the PTP at day 28, and S_0 is the peak area of the PTP at day 0). Structural elucidation was conducted for each BTP at each new peak in the total ion chromatogram of the MRT. Structures were established with the help of ITMS in Auto-MS Mode and verified with the help of HRMS up to MS^3 (see SM, Text S7). In addition, the biotransformation pathway of QUT and PTPs was predicted using Meta software (version 1.8.1, Multicase Inc. Beachwood, USA) and Eawag Biocatalysis/Biodegradation Database (Eawag, 2016) to improve the reliability of the structural elucidation of BTP. Further information on Meta software can be found in the SM, Text S8.

2.5. Sampling site and surface water analysis

QUT and its main biotransformation product BTP 398 were monitored in six tributaries of the Ilmenau River, a tributary to the Elbe River, in the district of Lüneburg, Lower Saxony, Germany. A map is available in the SM, Fig. S4, Text S9. Grab sampling, similar to González Alonso et al. (2010) and López-Serna et al. (2012), was conducted every month at seven locations between October 2014 and February 2015 resulting in a total number of 35 samples, which were then analyzed in triplicates using LC-HRMS. Further information on sample preparation and instrumental analysis can be found in the SM, Text S9. As no analytical standard for BTP 398 was available and the chemical structure was similar, QUT was used as a surrogate for analysis. Likewise, it was assumed that mass spectrometric ionization and the behavior during solid phase extraction of BTP 398 were similar to QUT. The limit of detection (LOQ) and limit of quantification (LOQ) for QUT were 1.3 ng and 3.8 ng L^{-1}, respectively.

2.6. In vitro bioassays

The cytotoxic effect on bacteria was assessed in a modified LBT with *Vibrio fischeri* NRRL-B-11177 (Hach-Lange GmbH, Düsseldorf, Germany) following Menz et al. (2013). This test allows for the combined assessment of short-term (30 min) and long-term (24 h) inhibition of bacterial luminescence emission. In addition, the impact on bacterial cell proliferation was evaluated during the transition from exponential growth to the stationary phase after 14 h of incubation. The exposure cultures were prepared in triplicates (n = 3) and the final sample concentration in the test media was 50% (v/v). A detailed description of the experimental procedure is presented in the SM, Text S10. Concentration-response relationships in the modified LBT were established by fitting the experimental data to a four parametric Hill-function (Eq. (1)),

$$y = min + (max - min) \Big/ \left(1 + (x/EC_{50})^{-Hillslope}\right) \quad (1)$$

y is the inhibition in %, min is the bottom of the curve, max is the top of the curve, Hillslope is the slope of the curve at its midpoint, and EC_{50} is the half-maximal effective concentration. Curve fitting was performed with the statistical software SigmaPlot 11 (Systat Software, San Jose, USA).

The genotoxic effect on bacteria was assessed using the umu-

test with *Salmonella typhimurium* TA1535 psk 1002 (German Collection of Microorganisms and Cell Cultures GmbH, Braunschweig, Germany) according to ISO/FDIS 13829. The umu-test is based on the colorimetric measurement of the *umuC* gene induction, which is upregulated in the applied tester strain as response to genotoxic lesions in the DNA (ISO/FDIS, 1999). Therefore, the *umuC* induction ratio (*IR*) provides useful information on the genotoxic potential of the tested sample. The exposure cultures were prepared in triplicates (n = 3) and the final sample concentration in the test media was 66.7% (v/v). A detailed description of the experimental procedure is presented in the SM, Text S10.

3. Results and discussion

3.1. Biodegradation of the parent compound quetiapine (QUT) hemifumarate in the Closed Bottle Test (CBT) and the Manometric Respirometry Test (MRT)

3.1.1. Assessment of ready biodegradability

All validity criteria in the CBT were fulfilled. As degradation rates reached 16.6 ± 1.5%, QUT hemifumarate has to be, according to OECD guidelines (OECD, 1992), classified as not readily biodegradable. Moreover, a partial degradation of QUT hemifumarate of up to 6% can be attributed to fumaric acid (ThOD of fumarate: 0.3 mg L^{-1}), because it was readily biodegradable in the CBT (degradation of 86.1 ± 1.0%). Elimination of QUT was assessed for recovered peak area S/S_0. After 28 days, 80 ± 4% of the peak area was recovered. Therefore, it can be assumed that BTPs were formed.

In the MRT, all validity criteria were fulfilled. QUT hemifumarate was degraded to an extent of −1.9 ± 3.2%. Therefore, QUT hemifumarate has to be classified as not readily biodegradable according to OECD test guidelines (OECD, 1992) in the MRT as well. Likewise, the measured DOC was eliminated by 5.5 ± 1.7%. In contrast, QUT was recovered by only 11 ± 11% according to peak area ratio S/S_0. As no mineralization was observed and QUT was almost entirely eliminated, the formation of BTPs is even more likely in the MRT than in the CBT. In the study by Trautwein and Kümmerer (2012), it was also shown that numerous BTPs were formed in biodegradation tests, especially at tests which are using higher inoculum density and diversity such as MRT compared to CBT.

3.1.2. Biotransformation of quetiapine (QUT)

Only one product with an m/z value of 398 was formed (see SM, MRT chromatogram in Fig. S5A, Text S11). Structure elucidation was conducted from samples of the MRT, as BTP 398 was formed in both biodegradation tests (Table 1). The most likely structure proposed for BTP 398 based on analytical results is that of a carboxylic acid derivative. It was formed as a result of the oxidation of the alcohol group and the formation of a group characterized by a carboxylic function with an aldehyde as an intermediate product. Oxidation via addition of oxygen on the sidechain of QUT was confirmed by MS spectra. However, the exact position could not be proven (SM, Text S12). Meta software also predicted that carboxylic acid derivative is a possible BTP (SM, Text S8, Fig. S2). Suggested mechanisms are oxidation by alcohol dehydrogenase and aldehyde dehydrogenase to form aldehyde and carboxylic acid, respectively. Therefore, oxidation of QUT resulting in the carboxylic acid derivative was considered to be the most likely explanation. Eawag Biodegradation Database did not predict suitable biodegradation patterns. It suggested as a first biotransformation step, cleavage on the nitrogen of the tricyclic ring system. Further transformation did not lead to the observed m/z values and fragmentation patterns in MS spectra.

The same structure is formed in high amounts by oxidation in the human metabolism recovering 14.7% of QUT as carboxylic acid metabolite in plasma (DeVane and Nemeroff, 2001). According to Food and Drug Administration (2007), 29% of a given dose was excreted as the carboxylic acid metabolite. As the carboxylic acid derivative of QUT is formed in the human metabolism and by bacteria, several biotic processes promote the formation of the compound. Therefore, high detection rates in surface water were assumed to be very likely. To strengthen this hypothesis, a small monitoring campaign for QUT and BTP 398 was conducted.

Table 2 presents the results of the sampling campaign. QUT was not detected in any sample. At two sampling points of the same river (MP3 and MP4), BTP 398 was detected in almost every sample. The data shows that the concentrations in the river increased downstream, indicating additional BTP sources after the first sampling point (MP3). Continuous positive detection of BTP 398 at MP3 and MP4 might be due to STP effluents. Furthermore, the highest detection rates were at sampling points with a high density of small STPs in the catchments, indicating a possible influence of small STPs on the sampled concentrations. However, despite the presence of an STP and the highest density of small STPs in the catchment of MP5, no BTP was detected in these samples. As a result, BTP 398 showed high detection rates compared to QUT. This is very likely because BTP 398 is formed in relatively large quantity during human metabolism, biological wastewater treatment and by bacteria in surface water.

3.2. UV treatment of quetiapine (QUT)

3.2.1. Primary elimination and mineralization

Fig. 1A shows QUT elimination by irradiation with UV light at different initial concentrations in ultrapure water. At an initial concentration of 226.5 μmol L^{-1}, elimination of QUT followed zero-order kinetics with a rate constant k of 0.478 min^{-1} ($R^2 = 0.996$). The calculated half-life $t_{1/2}$ was 101 min. Likewise, QUT was not fully eliminated after 128 min of irradiation. The residual QUT recovery rate was 39%. As DOC was only eliminated for 1% (data not shown), it can be assumed that the loss of QUT is due to the formation of one or several PTPs during the treatment. The color of the test solution constantly changed from clear colorless to clear yellowish. Therefore, QUT was probably transformed to PTPs absorbing light in a comparably higher wavelength range. At an initial concentration of 45.3 and 11.3 μmol L^{-1}, QUT elimination followed first-order kinetics (Fig. 1A), a result that is identical with that by Skibiński (2012), who performed tests at an initial concentration of 26 μmol L^{-1}. After 64 min, QUT was entirely eliminated at an initial concentration of 45.3 μmol L^{-1}. In contrast, DOC was only eliminated for 5% at the end of the test (data not shown). The rate constant k was determined to be 0.0155 min^{-1} ($R^2 = 0.976$) with a half-life of 45 min.

At an initial concentration of 11.3 μmol L^{-1}, QUT was under the LOQ after 32 min of treatment. At the end of the test, approximately 70% of DOC was eliminated. The rate constant k was 0.0692 min^{-1} ($R^2 = 0.973$) with a half-life of 10 min. At an initial concentration of 2.3 μmol L^{-1}, QUT was eliminated after 16 min. Kinetic fitting and DOC measurement was not possible.

It was only possible to calculate the quantum yield for initial concentrations of 45.3 and 11.3 μmol L^{-1} following first-order kinetics. The quantum yield was determined to be 0.0001 and 0.0006, respectively. It is possible that QUT was also eliminated due to indirect photolysis and that this process may have affected the findings concerning the quantum yield. Indirect photolysis may have also contributed to faster primary elimination kinetics (Nick and Schöler, 1995). Likewise, different quantum yields were probably obtained due to different initial photolysis concentrations with a different role of indirect photolytic elimination of QUT. Moreover, the reaction of PTPs might lead to different elimination kinetics as

Table 1
LC-MS parameters and structures of biotransformation products (BTPs) formed after biotransformation of quetiapine (QUT) and phototransformation products (PTPs). Positive determination of BTP (●) or non-detectable BTP (○) are indicated with spots.

PTPs/QUT	t_R LC-ITMS (min)	BTP identified at the test end of		Presumably formed from	t_R LC-HRMS (min)	Detected mass HRMS (m/z)	Theoretical mass (m/z)	Mass error (Δmmu)	Proposed structure
		CBT	MRT						
BTP 356	16.23	●	●	n/a	13.43	356.1027	356.1063	−3.619	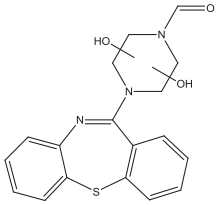
BTP 398	17.41	●	●	QUT	14.78	398.1536	398.1533	0.271	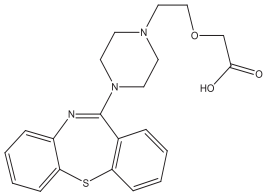
BTP 400	16.41	●	●	n/a	13.83	400.1313	400.1326	−1.203	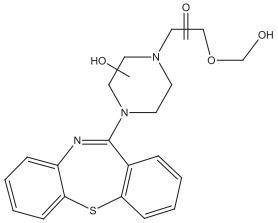
BTP 414	15.68	●	●	PTP2 400	12.96	414.1451	414.1482	−3.063	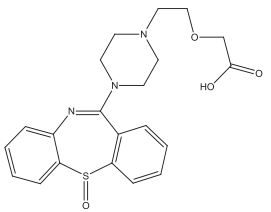

Table 2
Sampling network and corresponding number of STPs (n_{STP}) and density of small STPs (d_{SSTP}) in the corresponding catchments. f_{QTP} and f_{BTP} are the fraction of samples above LOD for QUT and BTP 398, respectively.

Sampling point (MP)	River	n_{STP}	d_{SSTP} km^{-2}	f_{QUT}(%)	f_{BTP}(%)
MP1	Hasenburger Bach	0	0.29	0	20
MP2	Barmbeck-Melbecker Bach	0	0.76	0	0
MP3	Neetze	1	1.21	0	80
MP4	Neetze (mouth)	2	0.95	0	100
MP5	Bruchwetter	1	1.35	0	0
MP6	Marschwetter	0	0.32	0	0
MP7	Roddau	0	0.42	0	40

well (Ding et al., 2013). The number and the concentration of PTPs during UV treatment is usually different at different initial concentrations (Herrmann et al., 2015b).

Ultrapure water was used to study UV elimination kinetics of QUT. Changing the experimental design by using matrices like wastewater, surface water, or potable water containing different amounts of organic matter and minerals could have affected the results found here. Liu et al. (2016) and Neamţu et al. (2014) observed slower UV elimination kinetics in natural waters compared to pure water for their studied organic molecules due to scavenging effects. However, as the amount and the diversity of organic matter and minerals differs greatly in aqueous matrices, suggestions for the specific behavior of QUT cannot be provided.

3.2.2. Peak area profile and structural elucidation of phototransformation products (PTPs)

During UV treatment, several PTPs were formed (see SM, chromatogram Fig. S6, Text S13). Fig. 1B shows the time courses of seven PTPs and QUT at an initial concentration of 226.5 μmol L^{-1}. All of them show A/A_0 ratios lower than 7%, assuming that PTPs were formed in, compared to QUT, low concentrations. Six of them were even lower than 3%. Nevertheless, peak area ratios cannot depict real concentrations, because the ionization and the respective abundance of compounds depend on the chemical structure and can, therefore, only be approximated.

Table 3 shows QUT and all seven PTPs, which are referred to their different m/z values. The fragmentation pattern for each PTP can be found in the SM, Text S14. The proposed photochemical mechanisms and the extent of abundance A/A_0 during UV treatment are described in the following paragraphs.

PTP 251 is likely formed as a secondary PTP. Accordingly, Fig. 1B shows a low slope for PTP 251 at the beginning of the UV treatment. It is possible that PTP 251 is formed due to the cleavage of the moiety on the tertiary amino groups of a PTP with a hydroxylation on the piperazine ring and the subsequent elimination of water.

PTP 296 is probably directly formed from QUT. The ethoxyethanol group is eliminated from the piperazine ring after cleaving at the tertiary amino group which is an often observed pattern. The peak area profile showed a steep slope at the beginning of photolysis with decreasing slope over the entire time course.

PTP 358 also showed a steep slope at the beginning of photolysis (Fig. 1B) with the highest peak ratio A/A_0 after 64 min of treatment. Therefore, it is very likely that PTP 358 is formed as a primary PTP of QUT. It is likely that two carbons are eliminated from the piperazine ring, resulting in the formation of two secondary amines. MS^2 spectrum showed the characteristic 2-(2-(ethylamino)ethoxy) ethanol fragment, a finding supporting the assumption that carbon was eliminated (SM, Text S14).

PTPs can also be formed as a result of multiple hydroxylations on the ring system, the ethoxyethanol sidechain, and the piperazine ring of QUT. PTP1 400 may be formed due to the hydroxylation of the piperazine ring. The fragmentation pattern indicated monohydroxylation on the carbon next to the tertiary amine, which is connected to the dibenzothiazepine ring system. It is likely that PTP3 400 is also formed as a result of hydroxylation of the piperazine ring. In this case, the carbon, which is connected to the tertiary amine and the ethoxyethanol side chain, was hydroxylated.

It can be assumed that PTP2 400 is formed as a result of oxidation of QUT. The preferred atom to be oxidized is the sulfur included in the dibenzothiazepine ring. Skibiński (2012) also identified the sulfoxide formed during photolysis of QUT. QUT sulfoxide is also formed in the human metabolism (Fisher et al., 2012). As PTP2 400 absorbs light in a higher wavelength range than QUT, this PTP could be responsible for the color change of the photolysis test solution from clear colorless to clear yellowish (see Section 3.2.1). PTP2 400 has an additional absorption peak at

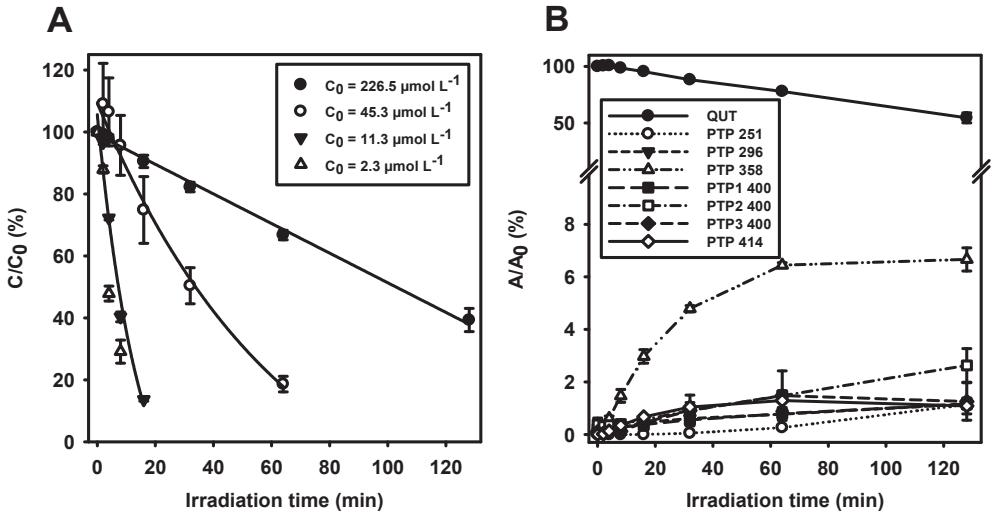

Fig. 1. [A] Kinetic plots of quetiapine (QUT) at different initial concentrations (C_0) (n = 2). C is the concentration at specific time points. QUT at C_0 of 226.5 μmol L^{-1} fits a zero order model. QUT at C_0 of 45.3 and 11.3 μmol L^{-1} fits a first order model. Kinetic fitting at C_0 of 2.3 μmol L^{-1} was not possible. [B] Peak area profile of QUT and phototransformation products (PTPs) at initial QUT concentration of 226.5 μmol L^{-1} (n = 2). A_0 is the peak area of QUT at the beginning of UV photolysis. A is the peak area of QUT and PTPs at specific time points.

Table 3
LC-MS parameters and structures of phototransformation products (PTPs) and quetiapine (QUT). Positive determination of PTP (●) and the time point of highest abundance in parentheses, or non-detectable PTP (○) at different initial concentrations are indicated with spots.

PTPs/QUT	t_R LC-ITMS (min)	Highest abundance for peak (A/A_0) at time point (min) for different initial concentrations				t_R LC-HRMS (min)	Detected mass HRMS (m/z)	Theoretical mass (m/z)	Mass error (Δmmu)	Proposed structure
		226.5 μmol L^{-1}	45.3 μmol L^{-1}	11.3 μmol L^{-1}	2.3 μmol L^{-1}					
PTP 251	18.16	● (128 min)	● (64 min)	● (16 min)	○	15.90	251.0637	251.0637	−0.026	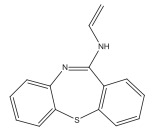
PTP 296	17.63	● (128 min)	● (64 min)	● (8 min)	● (4 min)	15.11	296.1219	296.1216	0.355	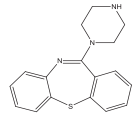
PTP 358	16.84	● (64 min)	● (32 min)	● (16 min)	● (4 min)	14.33	358.1584	358.1584	0.076	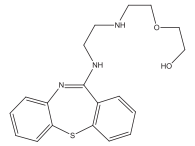
PTP1 400	16.79	● (128 min)	● (32 min)	● (8 min)	○	14.25	400.1672	400.1689	−1.699	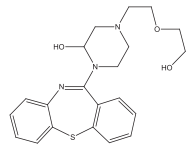
PTP2 400	17.09	● (128 min)	● (32 min)	● (8 min)	○	14.65	400.1691	400.1689	0.131	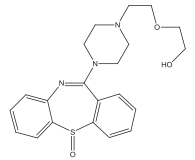
PTP3 400	17.71	● (64 min)	● (32 min)	● (8 min)	○	14.88	400.1688	400.1689	−0.149	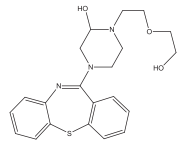
PTP 414	17.79	● (64 min)	● (16 min)	● (8 min)	● (4 min)	15.43	414.1477	414.1482	−0.533	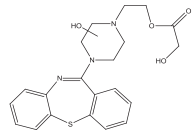
QUT	18.48	● (0 min)	● (0 min)	● (0 min)	● (0 min)	16.21	384.1749	384.1740	0.876	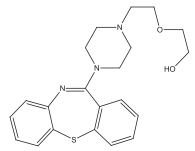

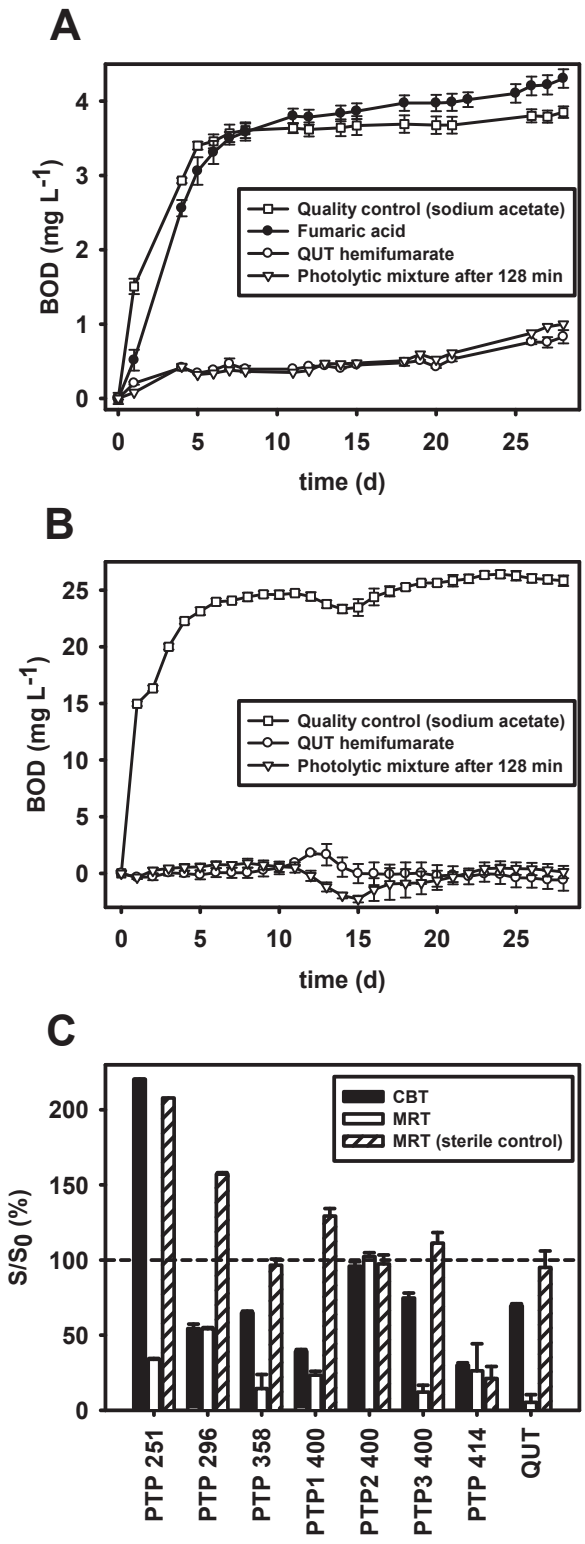

Fig. 2. Biochemical oxygen demand (BOD) as an indicator for biodegradation of sodium acetate, fumaric acid, quetiapine (QUT) hemifumarate and the photolytic mixture created after 128 min of photolysis of 226.5 μmol L^{-1} of QUT in the [A] Closed Bottle Test (CBT) and the [B] Manometric Respirometry Test (MRT) (n = 2). [C] Peak area recovery S/S_0 of QUT and selected phototransformation products (PTPs) after 28 days in the CBT and the MRT.

around 350 nm (SM, Text S15). Therefore, it could be further transformed by sunlight in the environment. For other PTPs, no significant change of absorption spectra could be observed compared to QUT. The fragmentation pattern indicated the characteristic elimination of sulfur monoxide (SM, Text S14) due to the formation of a phenantridine ring system. PTP2 400 constantly increased during photolysis.

PTP 414 is most likely quickly formed as a primary PTP of QUT by means of hydroxylation on a position of the piperazine ring that cannot be determined. In addition, the fragmentation pattern suggested oxidation of the carbon next to the ether group. Fig. 1B shows a steep slope for PTP 414 at the beginning of the UV treatment with the highest ratio of A/A_0 after 64 min.

All of the seven structurally elucidated PTPs at an initial concentration of 226.5 μmol L^{-1} could also be identified at initial concentrations of 45.3 and 11.3 μmol L^{-1} (Table 3). However, at an initial concentration of 2.3 μmol L^{-1}, only three PTPs were detected. Likewise, it was shown that the formation PTPs is not greatly influenced by the initial photolysis concentration. The possible reasons why they cannot be detected at the lowest initial concentration include a different photodegradation pathway, non-sufficient detection limits, or the faster elimination kinetics of PTPs (Herrmann et al., 2015b). The PTPs identified in this study were formed in ultrapure water by a medium-pressure mercury lamp. The use of UV light is discussed for the elimination of organic pollutants from wastewater (Köhler et al., 2012) and normally used during finishing of potable water (Hijnen et al., 2006). Therefore, it seems reasonable that different systems with a different irradiation time applied, different aqueous matrices containing QUT and different type of lamps could lead to the formation of other PTPs. However, studies indicated that PTPs can be identical when using different aqueous matrices (Cermola et al., 2005; Liu et al., 2009) or different type of lamps (Haddad and Kümmerer, 2014). Likewise, the types of PTPs found in this study are assumed to be the same like in UV treatment facilities.

3.3. Biodegradation of phototransformation products (PTPs) in the Closed Bottle Test (CBT) and the Manometric Respirometry Test (MRT)

3.3.1. Assessment of biodegradability

As can been seen in Fig. 2A, readily biodegradable sodium acetate (quality control) and fumaric acid show a high BOD up to 4 mg L^{-1} in the CBT. In contrast, QUT hemifumarate and the photolytic mixture, after 128 min of photolysis at a concentration of 226.5 μmol L^{-1} QUT, show a low BOD (>1 mg L^{-1}). As a result, photo-treatment did not significantly increase the biodegradability. However, phototransformation occurred. The recovered peak areas S/S_0 of PTPs and QUT in the photolytic mixture (sample after 128 min) can be seen in Fig. 2C. The relative peak area of one PTP increased, whereas that of five PTPs decreased during the CBT. The peak area of PTP 251 more than doubled after 28 days in the CBT. This increase might be correlated with the decrease of PTP 358 after the 2-(2-aminoethoxy)ethanol side chain was separated from the rest of the molecule by biological transformation of the molecule. The peak area of QUT sulfoxide (PTP2 400) remained stable. The peak areas of PTP 296, PTP1 400, PTP3 400, PTP 414, and QUT decreased, and it can be assumed that different BTPs could have been formed from these PTPs.

The BOD of photolytic mixture after 128 min of UV light exposure did not show a significant increase compared to that of QUT hemifumarate (Fig. 2B), and in this sense, the results of the MRT were similar to those of the CBT. In the MRT, readily biodegradable sodium acetate showed a BOD of up to almost 26 mg L^{-1}. As a result, QUT and PTPs were turned into BTPs, and this transformation was suggested by the peak areas of QUT and the PTPs (Fig. 2C). QUT was almost entirely transformed by biotic transformation processes.

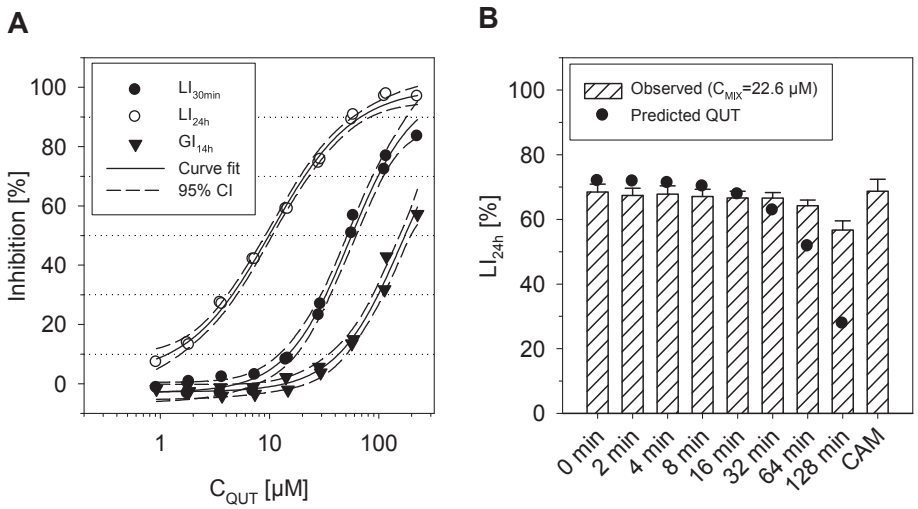

Fig. 3. [A] Concentration-dependent bacterial cytotoxicity of quetiapine (QUT) by means of luminescence inhibition after 30 min (LI_{30min}), luminescence inhibition after 24 h (LI_{24h}) and growth inhibition after 14 h (GI_{14h}). [B] Observed luminescence inhibition after 24 h (LI_{24h}) of the tenfold diluted photolytic mixture of 226.5 µmol L^{-1} QUT (C_{MIX} = 22.6 µmol L^{-1}) and the predicted individual effect of measured QUT in the mixture. 0.15 µmol L^{-1} chloramphenicol (CAM) was used as positive control.

PTP 251 and PTP 296 showed a significant decrease in the inoculated test vessel, but increased in the sterile control vessel. Therefore, abiotic transformation processes seem to be the reason for the formation of these PTPs, whereas biotic transformation could be a relevant pathway for their removal. PTP 358 was also transformed by bacteria. As the sterile control vessel showed no change, transformation could only be attributed to bacterial activity. QUT sulfoxide (PTP2 400) did not show a significant change regarding peak area. PTP1 400 and PTP3 400 only decreased in the inoculated vessel, and PTP 414 decreased in the inoculated vessel and the sterile control. Therefore, abiotic transformation of PTP 414 is very likely.

3.3.2. *Biotransformation in the photolytic mixture*

Each BTP identified in the MRT was also formed in the CBT (see Table 1). Because the MRT yielded higher concentrations, structure elucidation was done from samples of this test. Four BTPs were identified based on new peaks (see SM, chromatogram in Text S12). BTP 398 could also be identified in the sample of the photolytic mixture. It is likely that it was formed from residual QUT; all other BTPs identified here were formed from PTPs (for fragmentation patterns, see SM, Text S12). The proposed structure of BTP 356 could not be traced back to any PTP, but it is possible that it is the result of double hydroxylation on the piperazine ring and degradation of the QUT side chain. BTP 400 was also formed by a PTP. The position of the oxidized carbon on the side chain could not be determined with the help of MS spectra. It is likely that the second hydroxyl group was added to the piperazine ring, but the exact position could not be determined. BTP 414 was probably formed from QUT sulfoxide (PTP2 400). Meta software also predicted BTP 414 as a possible BTP of PTP2 400 (SM, Text S8, Fig. S3). An identical mechanism was also proposed for the formation of BTP 398. The exact position of the carboxylic group could not be determined. It is, however, very likely that BTP 414 is formed after oxidation of the alcohol group. The oxidation of the sulfur was shown by the characteristic elimination of sulfur monoxide.

3.4. *In vitro effects of quetiapine (QUT) and photolytic mixtures*

The bacterial cytotoxicity before and after the phototransformation of 226.5 µmol L^{-1} QUT was monitored using a modified LBT. QUT was cytotoxic to *V. fischeri* with EC_{50} values of 10.3, 54.3, and 167.3 µmol L^{-1}, depending on the endpoint and the time of exposure (Fig. 3A). The most sensitive endpoint was the luminescence inhibition after 24 h (LI_{24h}), followed by the luminescence inhibition after 30 min (LI_{30min}), and the inhibition of growth after 14 h (GI_{14h}), which was also the case for the photolytic mixtures. Therefore, only LI_{24h} of the tenfold-diluted photolytic mixture (C_{MIX} = 22.6 µmol L^{-1}) will be presented as an example here (Fig. 3B). The observed luminescence inhibition of the dark control sample (0 min) was explained by the measured concentration of QUT and the independently determined concentration-response curve, which indicated that QUT itself still had an effect in the photodegradation samples. However, phototransformation of QUT resulted only in a minor decrease of bacterial luminescence inhibition, which did not follow the predicted decrease of the individual effect of QUT. This means that the elimination of QUT during UV irradiation is not necessarily accompanied by a reduction of bacterial cytotoxicity. Moreover, one can expect that most of the PTPs in the photolytic mixture are, in terms of potency, similar to QUT.

The umu-test with and without metabolic activation did not provide any evidence for genotoxic activity of 226.5 µmol L^{-1} QUT before and after the phototransformation at the lowest investigated dilution level (C_{MIX} = 151 µmol L^{-1}).

4. Conclusions

In this paper, many new insights concerning the fate and behavior of QUT in aquatic environments were obtained. The results indicate that it is probable that while QUT and its PTPs are not readily biodegradable in aquatic environments, there is some evidence that QUT is transformed in surface water. The main BTP is very likely to be the carboxylic acid derivative, which is also formed by the human metabolism. Because it was observed more often in water samples of the rivers receiving inflows from STPs, one could argue that the BTP is likely to have a greater impact on the environment than QUT. That in turn underlines the necessity to include not just the parent compound into an environmental risk assessment but also possibly formed transformation products.

For the first time, data on the UV elimination kinetics of QUT at different initial concentrations was provided. Moreover, it was

shown that the elimination of QUT from the water cycle by means of UV treatment could result in the formation of multiple hitherto unknown PTPs. Moreover, it was shown that the formation of these main PTPs is not affected by the initial photolysis concentration over two orders of magnitude. Therefore, it was possible to use a comparably high initial concentration of QUT under experimental conditions to identify and determine the characteristic fate and effects of PTPs.

It can be concluded that it is not sufficient to monitor only processes of primary elimination of the parent compound because PTPs may have a similar or even more pronounced toxic effect than the parent compound. Furthermore, primarily formed PTPs can undergo further biological transformation resulting in again different molecules of different fate and effects. In the case of QUT, further research is needed to identify and characterize the PTPs that contributed to the bacteriotoxic effect of the reaction mixture.

Moreover, PTPs were not more biodegradable than QUT. Multiple formation of PTPs even led to a wide range of BTPs, which makes the characterization of resulting transformation products even more difficult. As suggested by these preliminary findings, it seems that UV treatment should not be considered as a possible treatment option for the elimination of QUT from the water cycle.

In general, more information on transformation products of APIs is needed. More specifically, environmental risk assessment studies on metabolites and transformation products have to be conducted because these also have the potential to have an adverse effect on the environment. Furthermore, measures at the source such as proper use as well as better biodegradable molecules should be given more attention to reduce the introduction of pharmaceuticals to the environment at the very beginning.

Acknowledgments

The authors would like to thank the Federal Ministry of Education and Research for financial support (grant no. 02WRS1280A - J), the Innovations-Inkubator Lüneburg (Teilmaßnahme 1.4, Graduate School) for providing a scholarship for Jakob Menz, Dr. Annette Haiß and Evgenia Logunova for planning the biodegradation tests, Dr. Christoph Leder for computing the absorption spectra, Stefanie Hinz and Julian Michael for assistance in the experimental work, Micha Edlich for proofreading the manuscript, and Multicase Inc. for providing Meta software. Manuel Herrmann wants to thank Markus Herrel and Rainer Fiehn (Ortenau Klinikum Offenburg-Gengenbach) for their general support and patience.

Appendix A. Supplementary data

Supplementary data related to this article can be found at http://dx.doi.org/10.1016/j.envpol.2016.08.040.

References

Al Aukidy, M., Verlicchi, P., Jelic, A., Petrovic, M., Barcelò, D., 2012. Monitoring release of pharmaceutical compounds: occurrence and environmental risk assessment of two WWTP effluents and their receiving bodies in the Po Valley, Italy. Sci. Total Environ. 438, 15–25.

AstraZeneca Pharmaceuticals, 2013. Seroquel FDA Approved Label.

Cermola, M., DellaGreca, M., Iesce, M.R., Previtera, L., Rubino, M., Temussi, F., Brigante, F., 2005. Phototransformation of fibrate drugs in aqueous media. Environ. Chem. Lett. 3, 43–47.

DeVane, C.L., Nemeroff, C.B., 2001. Clinical pharmacokinetics of quetiapine: an atypical antipsychotic. Clin. Pharmacokinet. 40, 509–522.

Ding, S., Wang, X., Jiang, W., Meng, X., Zhao, R., Wang, C., Wang, X., 2013. Photodegradation of the antimicrobial triclocarban in aqueous systems under ultraviolet radiation. Environ. Sci. Pollut. Res. Int. 20, 3195–3201.

Eawag, 2016. Biocatalysis/Biodegradation Database. http://eawag-bbd.ethz.ch/predict/ (accessed 06.04.16.).

Food and Drug Administration (FDA) - Center for Drug Evaluation and Research, 2007. Environmental Assessment and Finding of no Significant Impact for Seroquel®. http://www.accessdata.fda.gov/drugsatfda_docs/nda/2007/022172s000_EA.pdf (accessed 28.02.16.).

Fisher, D.S., Handley, S.A., Taylor, D., Flanagan, R.J., 2012. Measurement of quetiapine and four quetiapine metabolites in human plasma by LC-MS/MS. Biomed. Chromatogr. BMC 26, 1125–1132.

González Alonso, S., Catalá, M., Maroto, R.R., Gil, J.L.R., Miguel ÁG de, Valcárcel Y., 2010. Pollution by psychoactive pharmaceuticals in the Rivers of Madrid metropolitan area (Spain). Environ. Int. 36, 195–201.

Gurke, R., Rößler, M., Marx, C., Diamond, S., Schubert, S., Oertel, R., Fauler, J., 2015. Occurrence and removal of frequently prescribed pharmaceuticals and corresponding metabolites in wastewater of a sewage treatment plant. Sci. Total Environ. 532, 762–770.

Gutowski, L., Baginska, E., Olsson, O., Leder, C., Kümmerer, K., 2015. Assessing the environmental fate of S-metolachlor, its commercial product Mercantor Gold® and their photoproducts using a water-sediment test and in silico methods. Chemosphere 138, 847–855.

Haddad, T., Kümmerer, K., 2014. Characterization of photo-transformation products of the antibiotic drug Ciprofloxacin with liquid chromatography-tandem mass spectrometry in combination with accurate mass determination using an LTQ-Orbitrap. Chemosphere 115, 40–46.

Hijnen, W.A.M., Beerendonk, E.F., Medema, G.J., 2006. Inactivation credit of UV radiation for viruses, bacteria and protozoan (oo)cysts in water: a review. Water Res. 40, 3–22.

Herrmann, M., Olsson, O., Fiehn, R., Herrel, M., Kümmerer, K., 2015a. The significance of different health institutions and their respective contributions of active pharmaceutical ingredients to wastewater. Environ. Int. 85, 61–76.

Herrmann, M., Menz, J., Olsson, O., Kümmerer, K., 2015b. Identification of phototransformation products of the antiepileptic drug gabapentin: biodegradability and initial assessment of toxicity. Water Res. 85, 11–21.

Illés, E., Szabó, E., Takács, E., Wojnárovits, L., Dombi, A., Gajda-Schrantz, K., 2014. Ketoprofen removal by O_3 and O_3/UV processes: kinetics, transformation products and ecotoxicity. Sci. Total Environ. 472, 178–184.

Ilyas, S., Moncrieff, J., 2012. Trends in prescriptions and costs of drugs for mental disorders in England, 1998-2010. Br. J. Psychiatry J. Ment. Sci. 200, 393–398.

ISO/FDIS. 13829, 1999. (E): Water Quality - Determination of the Genotoxicity of Water and Waste Water Using the Umu-test, 1999.

Kim, I., Yamashita, N., Tanaka, H., 2009. Performance of UV and UV/H2O2 processes for the removal of pharmaceuticals detected in secondary effluent of a sewage treatment plant in Japan. J. Hazard. Mater. 166, 1134–1140.

Köhler, C., Venditti, S., Igos, E., Klepiszewski, K., Benetto, E., Cornelissen, A., 2012. Elimination of pharmaceutical residues in biologically pre-treated hospital wastewater using advanced UV irradiation technology: a comparative assessment. J. Hazard. Mater. 239–240, 70–77.

Kovalova, L., Siegrist, H., von Gunten, U., Eugster, J., Hagenbuch, M., Wittmer, A., Moser, R., McArdell, C.S., 2013. Elimination of micropollutants during post-treatment of hospital wastewater with powdered activated carbon, ozone, and UV. Environ. Sci. Technol. 47, 7899–7908.

Kümmerer, K., 2009. The presence of pharmaceuticals in the environment due to human use-present knowledge and future challenges. J. Environ. Manag. 90, 2354–2366.

Lertxundi, U., Echaburu, S.D., Palacios, R.H., 2012. The use of antipsychotics in a medium-long stay psychiatric hospital from 1998 to 2010. Int. J. Psychiatry Clin. Pract. 16, 143–147.

Liu, Q., Williams, T.D., Cumming, R.I., Holm, G., Hetheridge, M.J., Murray-Smith, R., 2009. Comparative aquatic toxicity of propranolol and its photodegraded mixtures: algae and rotifer screening. Environ. Toxicol. Chem. 28, 2622–2631.

Liu, W., Ying, G., Zhao, J., Liu, Y., Hu, L., Yao, L., et al., 2016. Photodegradation of the azole fungicide climbazole by ultraviolet irradiation under different conditions: kinetics, mechanism and toxicity evaluation. J. Hazard. Mater. [Epub ahead of print].

López-Serna, R., Petrović, M., Barceló, D., 2012. Occurrence and distribution of multi-class pharmaceuticals and their active metabolites and transformation products in the Ebro river basin (NE Spain). Sci. Total Environ. 440, 280–289.

Mackuľak, T., Mosný, M., Škubák, J., Grabic, R., Birošová, L., 2015. Fate of psychoactive compounds in wastewater treatment plant and the possibility of their degradation using aquatic plants. Environ. Toxicol. Pharmacol. 39, 969–973.

Mahmoud, W.M., Kümmerer, K., 2012. Captopril and its dimer captopril disulfide: photodegradation, aerobic biodegradation and identification of transformation products by HPLC–UV and LC–ion trap-MSn. Chemosphere 88, 1170–1177.

Mahmoud, W.M., Trautwein, C., Leder, C., Kümmerer, K., 2013. Aquatic photochemistry, abiotic and aerobic biodegradability of thalidomide: identification of stable transformation products by LC–UV–MSn. Sci. Total Environ. 463–464, 140–150.

Mahmoud, W.M., Toolaram, A.P., Menz, J., Leder, C., Schneider, M., Kümmerer, K., 2014. Identification of phototransformation products of thalidomide and mixture toxicity assessment: an experimental and quantitative structural activity relationships (QSAR) approach. Water Res. 49, 11–22.

Menz, J., Schneider, M., Kümmerer, K., 2013. Toxicity testing with luminescent bacteria – characterization of an automated method for the combined assessment of acute and chronic effects. Chemosphere 93, 990–996.

Neamţu, M., Grandjean, D., Sienkiewicz, A., Le Faucheur, S., Slaveykova, V., Velez Colmenares, J.J., Pulgarín, C., de Alencastro, L.F., 2014. Degradation of eight relevant micropollutants in different water matrices by neutral photo-Fenton process under UV254 and simulated solar light irradiation – a comparative study. Appl. Catal. B Environ. 158–159, 30–37.

Nick, K., Schöler, H.F., 1995. Photochemical degradation of herbicides in water by UV-radiation generated by low-pressure arcs (Part I, herbicides). vom Wasser 271–286.
Nödler, K., Licha, T., Bester, K., Sauter, M., 2010. Development of a multi-residue analytical method, based on liquid chromatography–tandem mass spectrometry, for the simultaneous determination of 46 micro-contaminants in aqueous samples. J. Chromatogr. A 1217, 6511–6521.
OECD, 1992. Guidelines for the Testing of Chemicals: Ready Biodegradability.
Oliveira, T.S., Murphy, M., Mendola, N., Wong, V., Carlson, D., Waring, L., 2015. Characterization of Pharmaceuticals and Personal Care products in hospital effluent and waste water influent/effluent by direct-injection LC-MS-MS. Sci. Total Environ. 518–519, 459–478.
Pereira, V.J., Weinberg, H.S., Linden, K.G., Singer, P.C., 2007. UV degradation kinetics and modeling of pharmaceutical compounds in laboratory grade and surface water via direct and indirect photolysis at 254 nm. Environ. Sci. Technol. 41, 1682–1688.
Petrie, B., Barden, R., Kasprzyk-Hordern, B., 2015. A review on emerging contaminants in wastewaters and the environment: current knowledge, understudied areas and recommendations for future monitoring. Water Res. 72, 3–27.
Pringsheim, T., Gardner, D.M., 2014. Dispensed prescriptions for quetiapine and other second-generation antipsychotics in Canada from 2005 to 2012: a descriptive study. CMAJ Open 2, E225.
Schwabe, U., Paffrath, D., 2015. Arzneiverordnungs-Report 2015: Aktuelle Zahlen, Kosten, Trends Und Kommentare. Springer Verlag.
Skibiński, R., 2012. A study of photodegradation of quetiapine by the use of LC-MS/MS method. Central Eur. J. Chem. 10, 232–240.
Subedi, B., Kannan, K., 2015. Occurrence and fate of select psychoactive pharmaceuticals and antihypertensives in two wastewater treatment plants in New York State, USA. Sci. Total Environ. 514, 273–280.
Subedi, B., Lee, S., Moon, H., Kannan, K., 2013. Psychoactive pharmaceuticals in sludge and their emission from wastewater treatment facilities in Korea. Environ. Sci. Technol. 47, 13321–13329.
Trautwein, C., Kümmerer, K., 2011. Incomplete aerobic degradation of the antidiabetic drug Metformin and identification of the bacterial dead-end transformation product Guanylurea. Chemosphere 85, 765–773.
Trautwein, C., Kümmerer, K., 2012. Degradation of the tricyclic antipsychotic drug chlorpromazine under environmental conditions, identification of its main aquatic biotic and abiotic transformation products by LC-MSn and their effects on environmental bacteria. J. Chromatogr. B 889–890, 24–38.
Verdoux, H., Tournier, M., Bégaud, B., 2010. Antipsychotic prescribing trends: a review of pharmaco-epidemiological studies. Acta Psychiatr. Scand. 121, 4–10.
Yuan, S., Jiang, X., Xia, X., Zhang, H., Zheng, S., 2013. Detection, occurrence and fate of 22 psychiatric pharmaceuticals in psychiatric hospital and municipal wastewater treatment plants in Beijing, China. Chemosphere 90, 2520–2525.

Publikation 5

Environmental fate and effect assessment of thioridazine and its transformation products formed by photodegradation

Wilde, M. L., Menz, J., Trautwein, C., Leder, C., Kümmerer, K.

(2016)

Environmental Pollution 213, 658-670

DOI: 10.1016/j.envpol.2016.03.018

Environmental Pollution 213 (2016) 658–670

Contents lists available at ScienceDirect

Environmental Pollution

journal homepage: www.elsevier.com/locate/envpol

Environmental fate and effect assessment of thioridazine and its transformation products formed by photodegradation☆

Marcelo L. Wilde [a], Jakob Menz [a], Christoph Trautwein [b], Christoph Leder [a], Klaus Kümmerer [a, *]

[a] Sustainable Chemistry and Material Resources, Institute of Sustainable Environmental Chemistry, Leuphana University Lüneburg, C13, DE-21335 Lüneburg, Germany

[b] Karlsruhe Institute of Technology, Institute of Microstructure Technology, Hermann-von-Helmholtz-Platz 1, D-76344 Eggenstein-Leopoldshafen, Germany

ARTICLE INFO

Article history:
Received 8 December 2015
Received in revised form
19 February 2016
Accepted 4 March 2016

Keywords:
Photodegradation
Thioridazine
Transformation products
Risk assessment
Toxicity
QSAR

ABSTRACT

An experimental and *in silico* quantitative structure-activity relationship (QSAR) approach was applied to assess the environmental fate and effects of the antipsychotic drug Thioridazine (THI). The sunlight-driven attenuation of THI was simulated using a Xenon arc lamp. The photodegradation reached the complete primary elimination, whereas 97% of primary elimination and 11% of mineralization was achieved after 256 min of irradiation for the initial concentrations of 500 μg L^{-1} and 50 mg L^{-1}, respectively. A non-target approach for the identification and monitoring of transformation products (TPs) was adopted. The structure of the TPs was further elucidated using liquid chromatography–high resolution mass spectrometry (LC–HRMS). The proposed photodegradation pathway included sulfoxidation, hydroxylation, dehydroxylation, and S- and N-dealkylation, taking into account direct and indirect photolysis through a self-sensitizing process in the higher concentration studied. The biodegradability of THI and photolytic samples of THI was tested according to OECD 301D and 301F, showing that THI and the mixture of TPs were not readily biodegradable. Furthermore, THI was shown to be highly toxic to environmental bacteria using a modified luminescent bacteria test with *Vibrio fischeri*. This bacteriotoxic activity of THI was significantly reduced by phototransformation and individual concentration-response analysis confirmed a lowered bacterial toxicity for the sulfoxidation products Thioridazine-2-sulfoxide and Thioridazine-5-sulfoxide. Additionally, the applied QSAR models predicted statistical and rule-based positive alerts of mutagenic activities for carbazole derivative TPs (TP 355 and TP 339) formed through sulfoxide elimination, which would require further confirmatory *in vitro* validation tests.

1. Introduction

Pharmaceuticals are important micropollutants that have been subject of concern in the last decades (Kümmerer, 2001, 2009). They have been quantified up to μg L^{-1} in different environmental compartments such as hospital wastewaters and sewage treatment plants (STP), surface water, groundwater, drinking water (Lapworth et al., 2012; Rodil et al., 2012; Verlicchi et al., 2012) and even at sea water (Trautwein et al., 2014).

In the environment, pharmaceuticals are subject to biotic and abiotic reactions such as biodegradation, hydrolysis and photolysis that can result in the formation of transformation products (TPs) as a consequence of incomplete degradation (Fatta-Kassinos et al., 2011). The most common abiotic transformation process that pharmaceuticals are subjected to in surface waters is photolysis through sunlight (Lin et al., 2013; West and Rowland, 2012).

Very little is known about the fate and effects of TPs until now. They can be recalcitrant, persistent, and often they might show novel properties and activities, e.g. being even more toxic than the parent compounds (Fatta-Kassinos et al., 2011). Small changes in the structure of the parent compounds might lead to similar and

☆ This paper has been recommended for acceptance by B. Nowack.

* Corresponding author. Nachhaltige Chemie und Stoffliche Ressourcen, Institut für Nachhaltige Chemie und Umweltchemie, Fakultät für Nachhaltigkeit, Leuphana Universität Lüneburg, Scharnhorststraße 1/C13, D-21335 Lüneburg, Germany.

E-mail addresses: marcelolw@gmail.com, wilde@leuphana.de (M.L. Wilde), jakob.menz@uni.leuphana.de (J. Menz), christoph.trautwein@kit.edu (C. Trautwein), cleder@leuphana.de (C. Leder), klaus.kuemmerer@uni.leuphana.de (K. Kümmerer).

http://dx.doi.org/10.1016/j.envpol.2016.03.018
0269-7491/

non-target interactions on aquatic organisms, which are affected by the discharge of both parent compounds and TPs (Cwiertny et al., 2014). Therefore, knowledge on occurrence, fate and effects of TPs formed through photodegradation is of great importance to understand the potential risk for human health and the environment (Escher and Fenner, 2011). However, these TPs are often not accessible for experimental testing. This is why *in silico* models, such as quantitative structure-activity relationships (QSAR), have been used to support the environmental assessment of TPs (Mahmoud et al., 2014; Rastogi et al., 2014a, 2014b, 2015).

Psychiatric drugs, including phenothiazine pharmaceuticals, are worldwide prescribed drugs, being extensively used over the past years (Trautwein and Kümmerer, 2012b; Nałecz-Jawecki et al., 2008), and little attention has been given to their environmental fate in comparison to other pharmaceuticals micropollutants. One of the most commonly used phenothiazine pharmaceutical is Thioridazine (THI) achieving a total prescription amount of 153 kg in the year 2013 in Germany (Schwabe and Paffrath, 2014). In total, approximately 30% of orally administered THI is excreted in the urine and 50% of the original dose is excreted in the faeces (Eiduson and Geller, 1963). However, before excretion THI is extensively metabolized in the liver and of a daily dose of THI only 2.5%–7% is excreted as Thioridazine and conjugates, being 0.5% excreted as the parent compound, whereas 0.5% is excreted as Mesoridazine (THI-2-SO) and approximately 1% is excreted as Thioridazine-5-sulfoxide (THI-5-SO) via urine within 24 h (Baselt and Cravey, 1995). Thanacoody (2011) have pointed out that 4% of the original dose appears unchanged in urine. Recent studies have suggested THI as an affordable antimicrobial agent for the treatment of intracellular infections caused by multiresistant strains of *Mycobacterium tuberculosis* (pathogen of tuberculosis) and *Plasmodium falciparum* (pathogen of *Malaria tropica*) (Kristiansen et al., 2015; Thanacoody, 2007, 2011; Weismana et al., 2006). Further THI is a promising 'lead' compound used as antibiotic from the 'non-antibiotic' class and as a 'helper' compound combined with classical antibiotics for the treatment of multidrug-resistant Gram-negative infections (Martins et al., 2008; Worthington and Melander, 2013), and was even discussed as a promising drug for anti-cancer therapy (Nagel et al., 2012). Therefore, consumption and consequently release to the environment of THI and related compounds is expected to increase, especially in resource-poor countries plagued by endemic infectious diseases. At the same time, these countries are often lacking effluent treatment and are exposed to high sunlight intensity, which is why photodegradation in surface water is an important factor in the environmental risk assessment of THI.

Photodegradation of THI by VIS and UVA light has been investigated in the past mainly with regard to phototoxicity *in vitro* assay towards various biological substrates (Elisei et al., 2007; Miolo et al., 2006), and to the bioindicators *Spirostomum ambiguum* (Spirotox) and anostracan crustacean *Thamnocephalus platyurus* (Nałecz-Jawecki et al., 2008). The photochemical instability of phenothiazine pharmaceuticals can lead to phototoxic and photoallergic reactions in the human body (Nałecz-Jawecki et al., 2008). Besides, Nałecz-Jawecki et al. (2008) demonstrated that the protozoan *Spirostomum ambiguum* was very sensitive not only to the parent drugs but also to photodegraded solutions of THI and chlorpromazine. It is also known that psychiatric drugs such as carbamazepine can modulate behavior of aquatic organisms at concentrations in the range of 200–2000 ng L^{-1} and alter freshwater community structure and ecosystem dynamics (Jarvis et al., 2014a, 2014b). Together with the intrinsic antimicrobial activity, this suggests THI and TPs of THI as compounds of relevant environmental concern. However, there is only little information available on the environmental fate and effects of THI and its transformation products formed via photodegradation.

The aim of this study was to assess the environmental fate and effects of THI and its TPs formed after simulated sunlight irradiation. For that, the TPs were elucidated by means of ultra-high performance liquid chromatography–high resolution mass spectrometry (UHPLC–HRMS) using an Orbitrap mass spectrometer. The ready biodegradability of photodegraded samples was tested according to the OECD guidelines 301D and 301F. The impact of phototransformation on bacterial cytotoxicity was investigated using a modified luminescent bacteria test towards *Vibrio fischeri.* Besides, *in silico* QSAR tools were implemented for the initial assessment of mutagenicity of THI and its proposed TPs.

2. Material and methods

2.1. Chemicals

Thioridazine hydrochloride (≥99%, CAS No. 130-61-0), 3,5-Dichlorophenol (97%, CAS No. 591-35-5) and Chloramphenicol (98%, CAS No. 56-75-7) were purchased from Sigma-Aldrich (Deisenhofen, Germany). Thioridazine-2-Sulfoxide (CAS No. 32672-69-8) and Thioridazine-5-Sulfoxide (98%, CAS No.7776-05-8) were acquired from Santa Cruz Biotechnology (Dallas, Texas, USA). Organic solvents were of LC-MS grade and provided by VWR (Darmstadt, Germany). Aqueous solutions were prepared in ultrapure water (Q1:16.6 MΩ·cm and Q2:18.2 MΩ·cm, Ultra Clear UV TM, Barsbüttel, Germany). All other chemicals were of recognized analytical grade and used as received.

2.2. Photodegradation through simulated sunlight irradiation

The photodegradation experiments were carried out in a 1000 mL cylindrical immersion-type batch reactor with ilmasil quartz immersion tube using 800 mL of synthetic solutions of THI diluted in ultrapure water. The sunlight irradiation was simulated by means of an UV/VIS xenon lamp (TXE 150 W, UV Consulting Peschl, Mainz, Germany). The irradiance of the Xe lamp in the range 200–850 nm was measured with Black Comet UV–VIS spectroradiometer model C (StellarNet Inc., Florida, USA) showing the follow irradiance: 200–280 nm: 1.01 W m^{-2}; 280–315 nm: 3.29 W m^{-2}; 315–380 nm: 12.91 W m^{-2} and 380–850 nm: 243.16 W m^{-2}. The spectrum of the lamp and the molar extinction coefficient of THI are depicted in Text S1 (Supplementary material).

Initial concentrations of 500 μg L^{-1} and 50 mg L^{-1} of thioridazine hydrochloride (THI·HCl) were chosen in order to allow reliable experimental evaluations of toxicity, ready biodegradability and in order to produce TPs in a sufficient amount to allow their initial characterization and further assessment in a 'worst case' scenario. The experiments were carried out at pH 6.5 and no adjustments in pH of the solution were carried out during and after the experiments. A dark control in the same conditions as for photolysis was carried out by using an initial concentration of 500 μg L^{-1} of THI·HCl. The temperature was held at 20 (±2) °C with a circulating cooler (WKL230, LAUDA, Berlin, Germany).

2.3. Kinetic modeling of photodegradation

In addition to monitoring the primary elimination of the parent compound, the degree of mineralization is an important parameter and can help to establish an initial benchmark, being indirectly related to the presence of TPs and, consequently, to determine further biodegradation and toxicity studies. Thus, the non-purgeable organic carbon (NPOC) was monitored. According to Legrini et al. (1993), in general NPOC reductions follow an apparent zero order kinetic through direct photolysis. The experimental data of the NPOC removal were fitted in relation to a zero-order kinetic

rate according to Equation (1).

$$\frac{d[NPOC]}{dt} = -k_{NPOC_{obs}} \quad (1)$$

Where [NPOC] is the concentration of dissolved organic carbon and $k_{NPOC_{obs}}$ is the observed rate constant.

The primary elimination of THI can be fitted with first, second, or mixed kinetic orders such as two steps of first-order (Equation (2)) (Legrini et al., 1993). Three different kinetic models were evaluated to fit the normalized experimental data of THI photodegradation (Langdon et al., 2011; Martins et al., 2010; Carstens et al., 2013).

$$\frac{d[THI]}{dt} = -k_{1_{obs}}[THI] - k_{2_{obs}}[THI] \quad (2)$$

Where [THI] is the concentration of Thioridazine and k_{obs}, $k_{1_{obs}}$ and $k_{2_{obs}}$ are the observed kinetic constants.

The kinetic of the experimental data were fitted with the software SigmaPlot 12 (Systat Software, USA) by means of nonlinear model fit regressions. The statistical analysis of the fitting was performed by means of ANOVA.

2.4. Instrumental analysis

2.4.1. Organic carbon and UV–VIS analysis

The mineralization was monitored as NPOC using a total organic carbon analyzer (TOC-Vcpn, Shimadzu GmbH, Duisburg, Germany) with ASI-V auto-sampler. The evolution of the absorbance during the photodegradation was measured by UV–VIS Lambda 24 spectrophotometer (Perkin-Elmer, Germany).

2.4.2. HPLC and LC-MS^n analysis

The primary elimination of THI was analyzed by using a Shimadzu Prominence (Shimadzu, Duisburg, Germany) high pressure liquid chromatography with diode array (DAD) and fluorescence (FLD) detection (HPLC-DAD-FLD) according to the modified method of Trautwein and Kümmerer (2012a).

A non-target approach for the identification and monitoring of TPs was performed by means of LC-ESI-IT-MS^n in positive ion mode, using an Agilent Technologies 1100 series HPLC (Agilent Technologies, Böblingen, Germany) in tandem with an Esquire 6000^{plus} Ion Trap Mass Spectrometer (Bruker Daltonics GmbH, Bremen, Germany).

In order to achieve more accurate elucidation of the previously identified TPs, a Dionex Ultimate 3000 UHPLC system (Dionex, Idstein, Germany) coupled with an LTQ Orbitrap-XL high-resolution mass spectrometer with H-ESI ion source (Thermo Scientific, Bremen, Germany) was used. The UHPLC-HRMS was operated in positive ion mode from 50 to 500 m/z and the fragmentation of the most intense ions was carried out by multiple reaction monitoring (MRM) up to MS^3 by means of collision-induced dissociation (CID) using 25 V.

The chromatographic separation was carried out on a reverse phase column C18 ec (RP18 CC 125-2 mm Nucleodur 100-3) and guard column (RP18 CC 8-2 mm Nucleodur 100-3) (Macherey-Nagel, Düren, Germany). Further information about the HPLC-DAD-FLD, LC–ESI-IT-MS^n and UHPLC-HRMS methodology can be found in Text S2 (Supplementary material).

2.5. Aerobic biodegradation testing

Closed Bottle Test (CBT) is a simple test to evaluate the ready biodegradability of an organic compound in the environment. Substances that pass this test are classified as readily biodegradable and it is assumed to be biodegradable in STP's (Nyholm, 1991).

The CBT was performed according to OECD 301 D guidelines with aerated water, low nutrient load, low bacteria density (10^2–10^5 colony formation unity mL^{-1}) and incubation in the dark at 20 ± 1 °C for a period of 28 days (OECD, 1992). The mineral medium used was solution (A) 8.50 g L^{-1} KH_2PO_4, 21.75 mg L^{-1} K_2HPO_4, 33.40 g L^{-1} $Na_2HPO_4 \cdot 2H_2O$, 0.50 mg L^{-1} NH_4Cl; solution (B) 36.40 mg L^{-1} $CaCl_2 \cdot 2H_2O$; solution (C) 22.50 mg L^{-1} $MgSO_4 \cdot 7H_2O$ and solution (D) 0.25 mg L^{-1} $FeCl_3 \cdot 6H_2O$. From each solution above, 1 mL/L was used, whereas 2 drops/L of the inoculum was added to the test solution (OECD, 1992). The concentration of the tested substance was adjusted to reach a theoretical oxygen demand (ThOD) of 5 mg L^{-1} in the test vessels. The oxygen demand (OD) was monitored using non-invasive optical oxygen sensors in combination with a Fibox 3 oxygen meter (Presens, Regensburg, Germany) (Friedrich et al., 2013).

The Manometric Respirometry Test (MRT) according to OECD 301F guidelines was carried out similarly to CBT with the same mineral medium and incubation in the dark for 28 days at 20 ± 1 °C under constant stirring (OECD, 1992). In contrast to CBT, a high inoculum density (5–10 × 10^6 CFU mL^{-1}) was applied and the dilution water was not aerated before the test. The test substance was added in a comparatively high concentration, equivalent to 30 mg L^{-1} of ThOD. The respirometric system OxiTop® OC-110 (WTW, Weilheim, Germany) was used for the determination of biochemical oxygen demand (BOD) as described in details elsewhere (Mahmoud et al., 2014; Trautwein and Kümmerer, 2011).

In order to further evaluate possible individual transformations of the parent compound and TPs in the biodegradation tests, samples were collected and further analyzed by means of LC-ESI-IT-MS. The inoculum used in CBT and MRT was sampled from a final effluent of the STP Lüneburg (Abwasser, Grün & Lüneburger Service GmbH (AGL), Lüneburg, Germany), which serves a regional population equivalent to 144,000 inhabitants. Further information and the scheme of distribution of samples in CBT and MRT can be found at in Text S3 (Supplementary material).

2.6. Short- and long-term bacterial toxicity by modified luminescent bacteria test

Photolytic mixtures from the photodegradation experiments and standard solutions of identified mixture components were analyzed in a modified luminescent bacteria test (LBT) according to Menz et al. (2013), which allows the combined assessment of short-term (30 min) and long-term (24 h) inhibition of bacterial luminescence emission. Additionally, the impact on bacterial cell proliferation was evaluated after 14 h incubation. A detailed description of the underlying method can be found in Text S4 (Supplementary material). Prior to testing, all samples were supplemented with NaCl to a final salinity of 2% (w/v). Concentration-response relationships were described by fitting the experimental data to a four parametric Hill-function (Equation (3)).

$$y = min + \frac{(max - \min)}{1 + (x/EC_{50})^{-Hillslope}} \quad (3)$$

Where y is the inhibition in %, min is the bottom of the curve, max is the top of the curve, *Hillslope* is the slope of the curve at its midpoint and EC_{50} is the half-maximal effective concentration.

Curve fitting was performed with the statistical software SigmaPlot 12 (Systat Software, USA). The obtained concentration-response curves of individual mixture components were used to evaluate the expected contribution to the observed effect in the photolytic samples. This was done using the concentration addition

(CA) model (Berenbaum, 1985) and the independent action (IA) model (Bliss, 1939) for mixture effect prediction.

2.7. Biodegradability and mutagenicity predictions using quantitative structure-activity relationships (QSARs)

The chemical structures of THI and suggested TPs (neutral form) were converted into SMILES strings by means of the software package ChemBioDraw Ultra (v.12) and were subjected to *in silico* predictions for biodegradability and mutagenic/genotoxic activity by the different QSAR models. The models BioWin v.4.10 (EPI suite™ U.S. EPA), CATABOL BOD 28 days MITI I v.02.03 and CATALOGIC BOD 28 days MITI v.06.07 (Oasis Catalogic v5.11.6 TB, Laboratory of Mathematical Chemistry, 2012) were applied for the preliminary evaluation of ready biodegradability. A combination of statistical and rule-based systems as recommended by the ICH M7 guideline (International Conference on Harmonization (ICH), 2014) was used to predict mutagenic activities of THI and TPs. This included the models GT1_A7B, GT1_AT_ECOLI, GT_EXPERT, PHARM_ECOLI, and PHARM_SALM (Chakravarti et al., 2012; Saiakhov et al., 2013, 2014) of the CASE Ultra software (v. 1.5.2.0 MultiCASE Inc.). In addition, bacterial mutagenicity (*Salmonella typhimurium*) with training sets from 2012 SAR Genetox Database provided by Leadscope® (v. 3.2.3-1) was applied as well (Roberts et al., 2000).

It is worth to remember that some models still carry a level of uncertainty due the limitations on training and validation set of the models. Applicability domains and other criteria of the applied QSAR models can be found in Text S5 (Supplementary material).

3. Results and discussion

3.1. Photodegradation

The photodegradation of THI under simulated sunlight irradiation reached the complete primary elimination after 128 min of photolysis when the initial concentration of THI·HCl was 500 μg L^{-1}, whereas for the initial concentration of 50 mg L^{-1} of THI·HCl the photolysis led to 97.3% of primary elimination and 11.0% of mineralization after 256 min. As depicted in Fig. 1(A), the NPOC removal for the initial concentration of 50 mg L^{-1} of THI·HCl was well fitted with the zero-order kinetic model with a $k_{DOC_{obs}}$ 9.025×10^{-6} mol L^{-1} s^{-1} and a r^2 of 0.878 ($p < 0.05$). The best fitting model to the observed primary elimination of THI in the concentrations studied was the two steps first-order exponential decay (or biexponential) as it can be seen in Fig. 1(A) and Fig. 1(C). A comparison among the different models applied can be seen in Text S6 (Supplementary material). The computed kinetic constants for the photodegradation of THI were $k_{1_{obs}}$ 0.166 min^{-1} and $k_{2_{obs}}$ 0.014 min^{-1} with r^2 0.999 ($p < 0.05$) for the initial concentration of 50 mg L^{-1} of THI·HCl, whereas the kinetic constants observed for the initial concentration of 500 μg L^{-1} of THI·HCl were $k_{1_{obs}}$ 0.805 min^{-1} and $k_{2_{obs}}$ 0.027 min^{-1} with r^2 0.989 ($p < 0.05$). The half-life time ($t_{½}$) of THI during the photodegradation process was 5.84 min and 8.08 min for the initial concentrations of 50 mg L^{-1} and 500 μg L^{-1} of THI·HCl, respectively.

A similar biexponential kinetic behavior was also reported in the literature (Edhlund et al., 2006; Sturini et al., 2010). Sturini et al. (2010) have investigated the degradation of marbofloxacin and enrofloxacin in lower concentrations (5 and 50 μg L^{-1}) in natural waters and using a solar simulator. The degradation of enrofloxacin was reported to follow two steps of first-order in tap water and river water at pH 7.9 and 8.0. Likewise, Edhlund et al. (2006) have identified a biexponential kinetic model in the investigation of the photodegradation of furazolidone in lake water by using a medium-pressure mercury lamp and the initial concentration of 10 μmol L^{-1} of furazolidone. The dark control experiment showed that approximately 10% of the starting concentration of THI undergo hydrolysis. The resulting hydrolytic product was identified as the intermediary TP 387 II (THI-2-SO). The hydrolysis of THI can be attributed to presence of dissolved oxygen and the autocatalytic characteristics of phenothiazine derivatives (Manju et al., 2012).

The kinetic slope methodology was adopted for the estimation of the THI's apparent quantum yield (Zepp and Cline, 1977; Zepp, 1978). Thus, the apparent quantum yield for the protonated species of THI (Φ_{THI}) at pH 6.5 were estimated to be 1.26×10^{-4} ($\pm 2.81 \times 10^{-5}$) mol $Einstein^{-1}$ ($n = 3$) and 5.54×10^{-4} mol $Einstein^{-1}$ ($n = 1$) for the initial concentrations of 50 mg L^{-1} and 500 μg L^{-1} of THI·HCl, respectively (Text S7, Supplementary material). The photolysis of THI was accompanied by an increase of absorbance in the UVA region (320–400 nm) (Fig. 1(B)), which can be explained by the formation of TPs which higher absorbance in the respective wavelength range. Further, a red color was observed in the photodegraded solutions with a λ_{max} in the VIS at 510 nm due to the formation of one or more TPs with a chromophore group. The increase in absorbance in some wavelengths can interfere in the propagation of the irradiation in the whole reactor. Such behavior was also found in the photodegradation of N-methyl phenothiazine as an indicative of self-sensitized photooxidation (Manju et al., 2012). Thus, the suggested two steps of the first-order exponential decay can be attributed to a fast initial degradation of the parent compound, followed by a reduced degradation rate due to the concurrence with newly formed TPs. It can be observed that the first step of first-order kinetic decay of THI occur up to 32 min of photodegradation Fig. 1(A). Comparing the profile of THI and the two main occurring TPs, TP 387 I (THI-5-SO) and TP 387 II (THI-2-SO) in Fig. 3, also known as the main human metabolites of THI (Wójcikowski et al., 2006; Daniel et al., 2000; Borges et al., 2008), it can be seen that they achieve a maximum at 16 min of photodegradation. After this point, it can be inferred that a competition among these three compounds takes place, as the degradation of THI starts to follow the slow kinetic decay. Likewise, after 16 min of photodegradation TP 387 I and TP 387 II are being further transformed. Fig. 1(B) depicts an increasing in absorbance in the range 325–400 nm with the increasing of reaction time, which is due to the formation of intermediaries with structural moieties absorbing in this range. Consequently, it might be assumed that some sort of concurrence takes place among the intermediaries formed and THI, which might explain the slow kinetic of THI's degradation after 32 min. At the concentration of 500 μg L^{-1} of THI·HCl (Fig. 1(C)), the first-order step occur up to 8 min of photodegradation, whereas the second first-order decay occur after 16 min. As above, such behavior can also be related to the concurrence among the parent compound and the TPs 387 I and 387 II as it can be observed in Supplementary material (Text S9).

Such behavior clearly indicate that THI undergo further transformation through abiotic natural attenuation process such as photolysis and the environmental fate of TPs formed should be further investigated.

3.2. Identification of TPs and proposal of degradation pathway

The structural elucidation of TPs was based on their high resolution mass spectra and fragmentation pattern, which are summarized in Text S8 (Supplementary material). Chromatographic peaks with same nominal m/z ($[M+H]^+$) and similar fragmentation patterns, but different retention times (Rt) have indicated the formation of isomers.

A degradation pathway was proposed in Fig. 2. The two mainly occurring peaks were proposed as the pharmacologically active human metabolites of THI, THI-5-SO and THI-2-SO (Wójcikowski

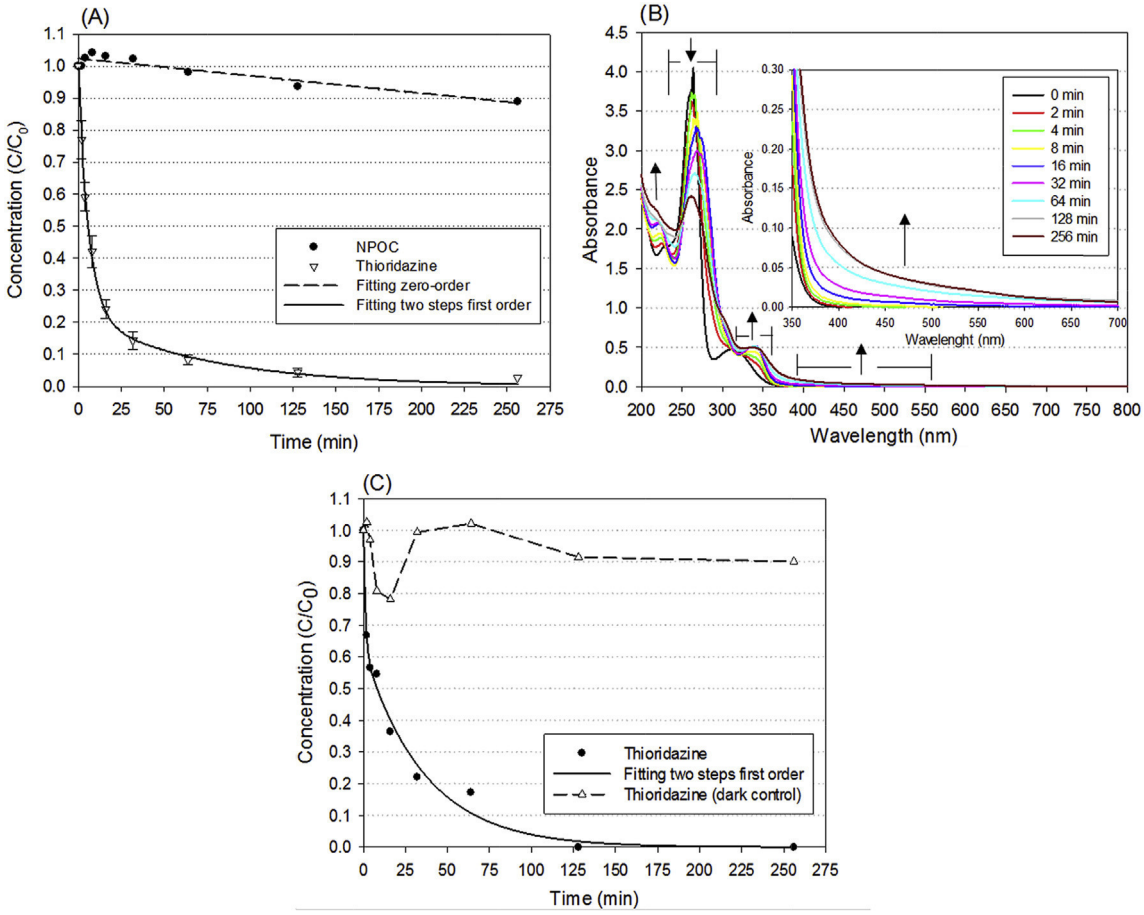

Fig. 1. (A) Non-purgeable organic carbon (NPOC) removal and primary elimination of thioridazine during photodegradation under simulated sunlight irradiation. Initial conditions: [THI·HCl] 50 mg L^{-1}, pH 6.5, temp.: 20 ± 2 °C (n = 3). (B) Evolution of the UV–VIS spectra of all sampling points during THI photodegradation through simulated sunlight irradiation. Initial conditions: [THI·HCl] 50 mg L^{-1}, pH 6.5, temp.: 20 ± 2 °C. (C) Primary elimination of thioridazine during photodegradation under simulated sunlight irradiation and dark control. Initial conditions: [THI·HCl] 500 μg L^{-1}, pH 6.5, temp.: 20 ± 2 °C (n = 1).

et al., 2006; Daniel et al., 2000; Borges et al., 2008), which were identified in both studied concentrations. A sulfoxidation step on phenothiazine derivatives was reported in previous photodegradation studies (Trautwein and Kümmerer, 2012b). The other two TPs with *m/z* $[M+H]^+$ 387 Da were proposed as intermediaries from hydroxylation on the piperidine moiety, according to the product ion of *m/z* 142.1229 ($C_8H_{16}ON$) indicated by the fragmentation pattern of the UHPLC-HRMS.

Eight different TPs with *m/z* $[M+H]^+$ of 403 Da (TPs 403) were found in the initial concentration of 50 mg L^{-1} of THI·HCl, whereas one TP with *m/z* $[M+H]^+$ of 403 Da was found in the initial concentration of 500 μg L^{-1} of THI·HCl. Therefore, according to the Rt and fragmentation pattern, it was proposed that TP 403 V was present in both concentrations. Due to the further transformation of THI-5-SO and THI-2-SO, TPs 403 were proposed to be formed through hydroxylation or sulfoxidation in different positions of the phenothiazine ring and/or on the piperidine ring. Another hydroxylation/sulfoxidation step resulted in two tertiary TPs (TPs 419) and according to the fragmentation pattern, a new hydroxylation/sulfoxidation and even a new sulfoxide oxidation step over TPs 403 can be assumed. Nałecz-Jawecki et al. (2008) have investigated the photodegradation of THI and have found $[M+H]^+$ ions with the *m/z* 387 Da, 403 Da and 419 Da, but no elucidation was proposed. On the other hand, dehydrogenation or dehydroxylation steps took place resulting in TP 369, TP 385 and TP 401. Based on their fragmentation pattern (Text S8, Supplementary material) it is proposed to occur on the piperidine moiety. TP 357 is proposed to be formed through S-dealkylation, which can be explained by the formation and elimination of a sulfone intermediary on the R2 substituent (methanethiol) of THI. The TP 339 and TP 355 are carbazole ring derivatives and were formed through sulfoxide elimination. Manju et al. (2012) have proposed sulfoxide elimination during the exposition of N-methyl phenothiazine for long irradiation times during photolysis. The TP 245 (2-methylthiophenothiazine) is proposed to be formed through N-dealkylation step from THI and elimination of the substituent group R1 on the position N-10. Thus, the use of relative high initial concentration allowed studying a wide range of TPs. Besides, a higher accuracy was achieved in the elucidation of the fragmentation pattern of the TPs.

Fig. 3 presents the profile of the chromatographic peak area ratio (A/A_0), where A is the relative peak area of the TP and A_0 is the relative peak area of THI before photodegradation. THI-5-SO and THI-2-SO achieved up to 33% and 23% of the initial area of the parent compound, respectively. It is worth to note that the peak areas of TPs cannot be related to their absolute concentration, since standards and ionization rates of the TPs in the ESI and H-ESI ion sources of the mass spectrometers were not available. Nevertheless, the relationship among peak area, formation and further transformation of TPs can be observed. The TP 403 VI shows an increase in peak area up to 16 min of photodegradation being then further transformed. The TP 403 VI can further react forming, for instance, TP 357 and TP 355, through S-dealkylation and sulfoxide

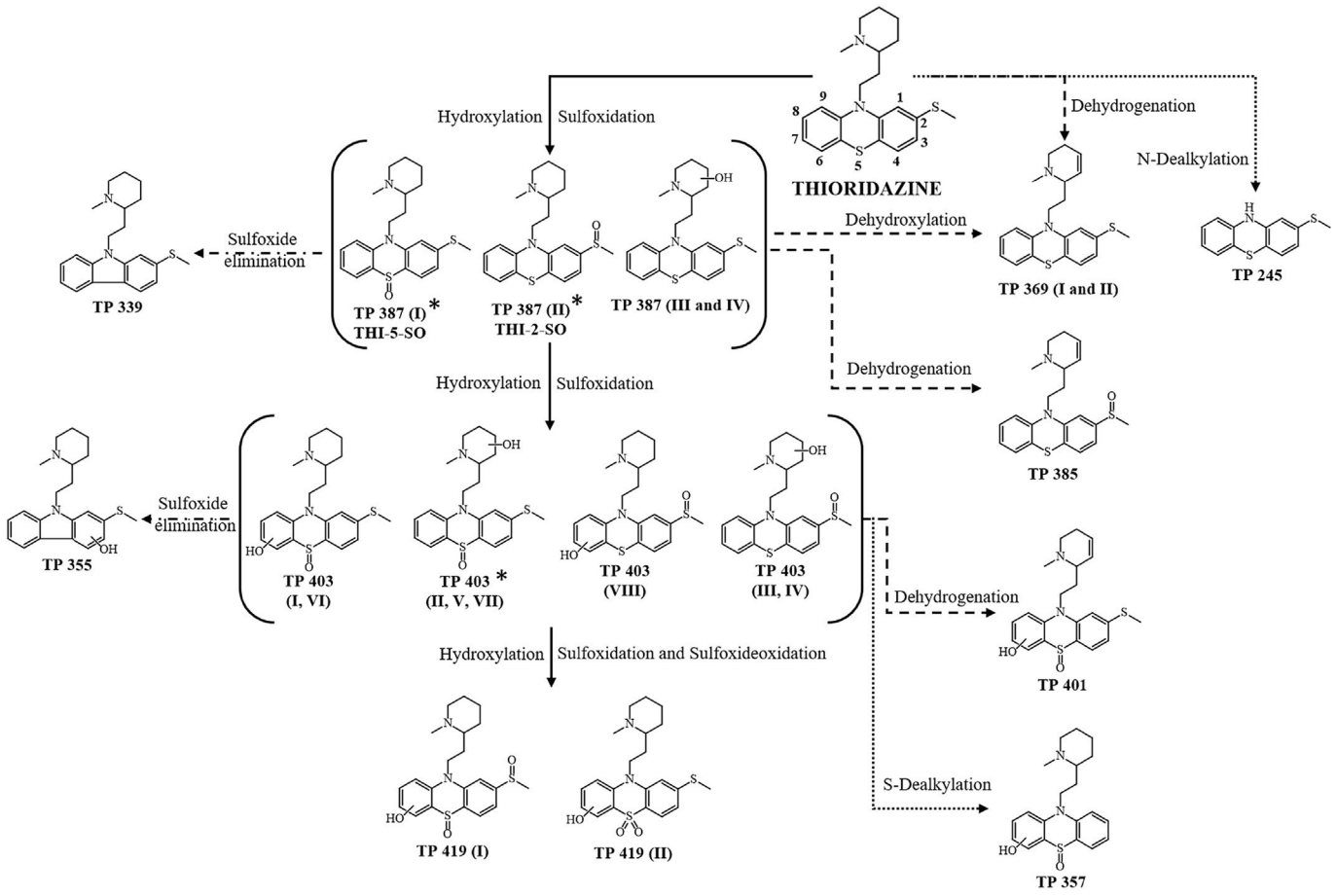

Fig. 2. Proposed photodegradation pathway of THI under simulated sunlight irradiation. Initial conditions of photolysis: 800 mL, $[THI{\cdot}HCl]_0$ 50 mg L^{-1}, pH 6.5 and temperature 20 ± 2 °C. TPs marked with * were found by using the following initial conditions: 800 mL, $[THI{\cdot}HCl]_0$ 500 μg L^{-1}, pH 6.5 and temperature 20 ± 1 °C.

elimination, respectively, once both TPs arise after 16 min of treatment. The same can be assumed for TP 419 I. The TP 403 VII is formed after 32 min of photolysis and can be related directly to the decrease in peak area of TP 387 I. Both, TPs 369 I and TP 369 II rise up after 8 min, which is related to the parent compound. TP 385 arises after 16 min whereas TP 387 II meanwhile presents a decrease in the peak area. The peak area profile of the TPs found for the photolysis of 500 μg L^{-1} of THI·HCl can be seen in Text S9 (Supplementary material).

A plausible explanation for the generation of many different TPs can rely on the direct and indirect photolysis based on the self-sensitization of THI. It is worth to note that self-sensitization is concentration dependent and is likely to occur during photodegradation processes in higher concentrations of the target compound. Manju et al. (2012) have investigated the self-sensitization on the monochromatic photolysis of N-methyl phenothiazine and have proposed a reaction with reactive oxygen species (ROS) leading to the formation of sulfoxidation products. Therefore, the degradation mechanism observed might be through direct and indirect photolysis caused by ROS such as $^1O_2$, $HO_2^{\bullet}$ and H_2O_2 (Latch et al., 2003). Li et al. (2011) have determined the self-sensitization of enrofloxacin through electron spin resonance determining ROS such as $HO^{\bullet}$ and $^1O_2$ in high initial concentrations of the parent compound. However, self-sensitization is unlikely to happen in lower and environmental occurring concentrations (Wammer et al., 2013). In the environment, the formation of ROS such as that is formed through self-sensitization processes can also occur in natural waters via indirect photolysis due to the presence of naturally occurring sensitizers such as humic acids, fulvic acids, nitrate, carbonate (Jacobs et al., 2012; Lin et al., 2013).

Regarding direct photolysis, it can be assumed that THI is excited to a singlet excite state by the absorption of irradiation, where it can further react forming TPs. Formation of a triplet state might also be speculated, as it was reported in the photodegradation of THI in water (Elisei et al., 2007). Elisei et al. (2007) have reported the evidence of intersystem crossing of THI and the formation of S oxygen in polar organic solvents. When a compound is excited to a triplet state, it might further react forming TPs, or may return to the normal state because of the quenching action of the dissolved oxygen (Ryan et al., 2010). On the other hand, Manju et al. (2012) have proposed the generation of ROS through self-sensitization for a phenothiazine derivative through the formation of superoxide anion-like intermediary such as $[THI^{\bullet+}\cdots O_2^{\bullet-}]$, which in acidic medium can further generate H_2O_2.

3.3. Aerobic biodegradability of phototransformation products

According to the “rules of thumb” for the structure/biodegradability relationships, the attachment of groups with an electron donating character (e.g. carboxylic acids, phenols, amines, and hydroxyl) might increase the biodegradability (Howard, 2000). Moreover, substrate concentration, structure and physical-chemical properties have an impact on the rate and pathway of biodegradation. Besides, the presence of aromatic substituents with electron withdrawing character, as it is the case for THI and most of the identified TPs, tends to increase the persistence (Howard, 2000.).

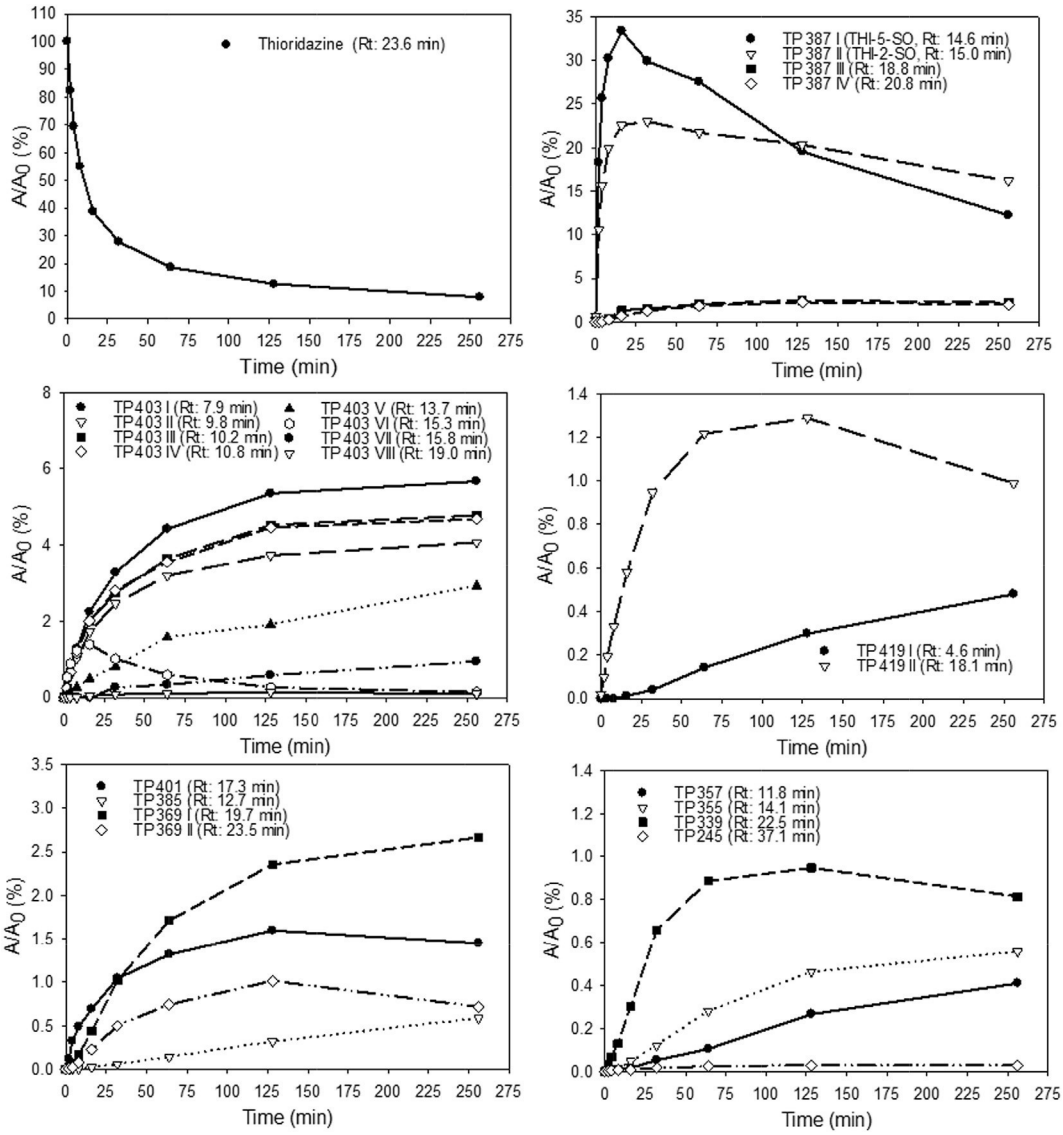

Fig. 3. Profile of the normalized peak area with A/A_0 (%) of Thioridazine (THI) and Transformation Products (TPs) during the photodegradation by means of simulated sunlight irradiation. Data obtained by using the extracted ion chromatogram acquired through LC-ESI-IT-MS^n in full scan mode (50–800 *m/z*). (A) Initial conditions of photolysis: 800 mL, $[THI{\cdot}HCl]_0$ 50 mg L^{-1}, pH 6.5 and temperature 20 ± 2 °C. A is the peak area of the respective TP and A_0 is the initial peak area of THI at time 0 min.

The QSAR predictions provided by EPI Suite™ (US EPA), CATABOL BOD 28 days MITI I v.02.03 and CATALOGIC BOD 28 days MITI v.06.07 (Oasis Catalogic v5.11.6 TB, Laboratory of Mathematical Chemistry, 2012) models indicated that THI and most of the proposed TPs are not readily biodegradable in the aquatic environment (Text S11, Supplementary material). However, Rastogi et al. (2014b, 2015) pointed out that the attachment of an electron-donating group, such as a hydroxyl on the benzene ring of metoprolol and atenolol increased the aerobic biodegradability of the TPs from a photodegradation process. Längin et al. (2009) have tested amoxicillin and piperacillin in CBT and have pointed out that the presence of a phenol moiety in amoxicillin make the biodegradation possible, whereas in the case piperacillin the presence of a benzene moiety plays a role not favoring the biodegradation. Therefore, photolytic samples of THI were subjected experimental biodegradation testing in order to corroborate the QSAR predictions.

In the OECD 301 test series a compound is considered readily biodegradable, when the biochemical oxygen demand (BOD) achieves at least 60% of the theoretical oxygen demand (ThOD). Thus, achieving only 7.15% (±1.83%) and −24.83% (±11.08%) of the ThOD in CBT (OECD 301D) and MRT (OECD 301F), respectively, THI could not be classified as readily biodegradable (Text S10, Supplementary material). Further, the samples collected after 128 min of photolysis, which consisted mainly of TPs, did not show a significant increase of BOD in comparison to the dark control sample (see Fig. S5(B) and S6(B), SI). However, as many TPs might be present in the photolytic mixture only in low concentrations, their individual degradation might not significantly influence the total BOD on whole mixture level. Therefore, the individual fate of each identified TP was monitored by LC-ESI-IT-MS.

As depicted in Fig. 4 (A and C), the peak area of THI before photolysis did not change in CBT within 28 days of testing, whereas in the MRT a reduction of 11.38% (±2.14%) was observed. Possible explanations for this variation between the tests are the higher concentrations of inoculum and test substance that are applied in the MRT. A similar behavior was also observed in other studies on the biodegradability of phenothiazine pharmaceuticals (Trautwein and Kümmerer, 2012a, 2012b).

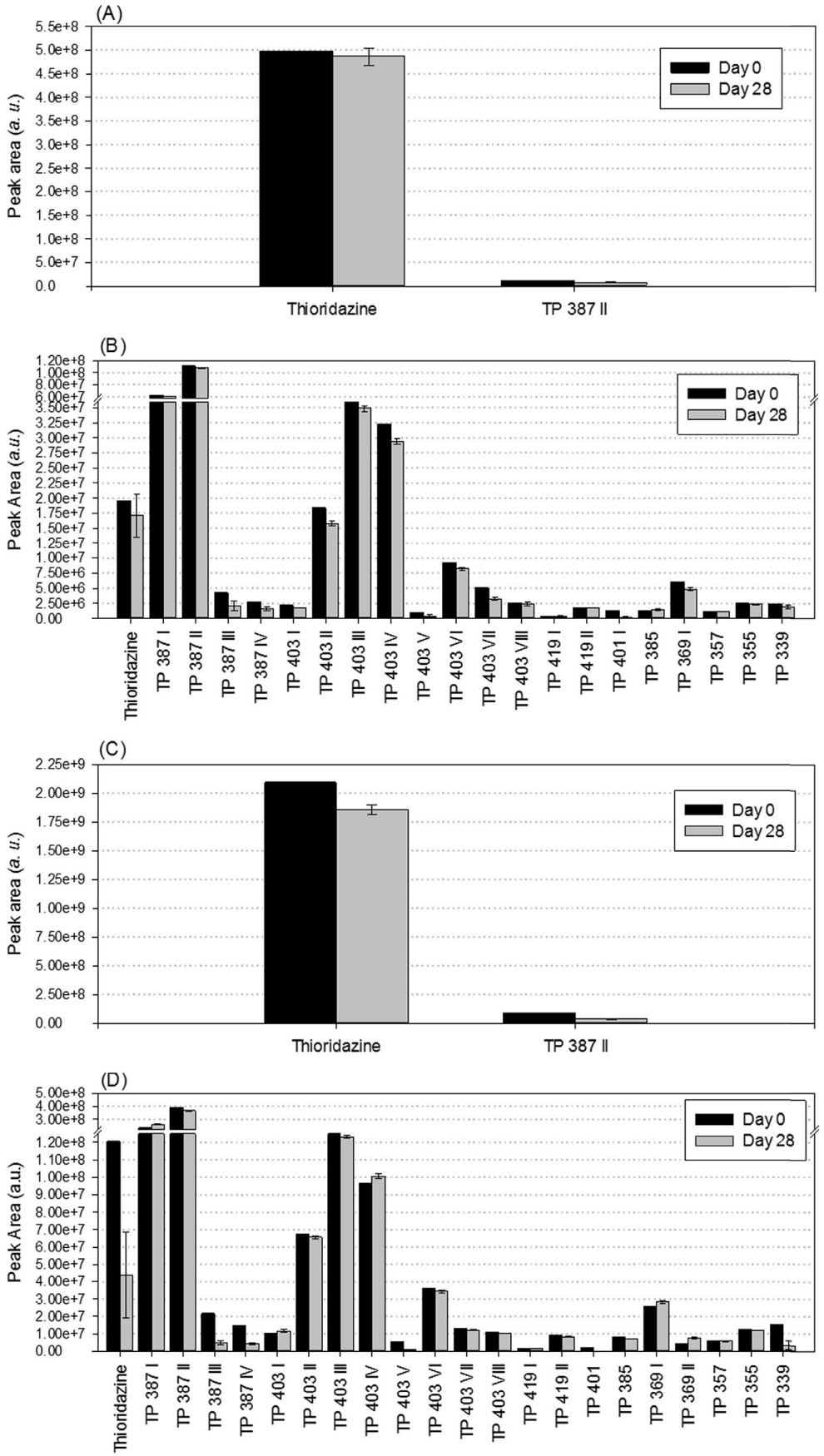

Fig. 4. Peak areas of Thioridazine (THI) and Transformation Products (TPs) before and after 28 days of aerobic biodegradation. (A) Closed Bottle Test of Thioridazine 0 min irradiation, (B) Closed Bottle Test of Thioridazine and Transformation Products after 128 min of irradiation, (C) Manometric Respirometry Test of Thioridazine 0 min irradiation and (D) Manometric Respirometry Test of Thioridazine and Transformation Products after 128 min of irradiation (n = 2).

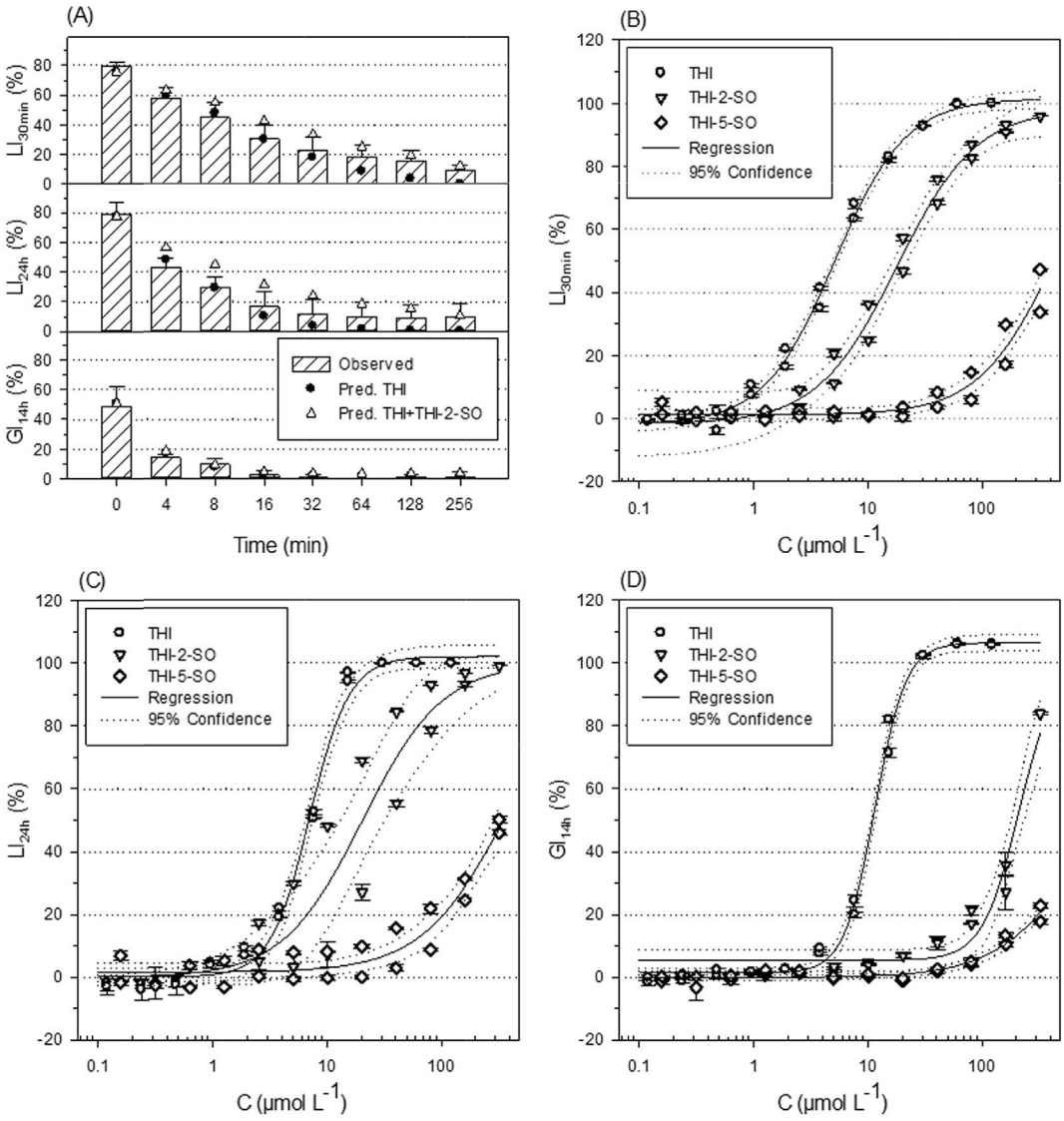

Fig. 5. (A) Observed and predicted bacteriotoxic effects in *V. fischeri* of 50 mg L^{-1} (123 µM) Thioridazine hydrochloride during simulated sunlight irradiation by means of short-term luminescence inhibition after 30 min (LI_{30min}), long-term luminescence inhibition after 24 h (LI_{24h}) and growth inhibition after 14 h (GI_{14h}) [theoretical assay concentration: 12.3 µM]. (B–D) Concentration-response relationships of the mixture components Thioridazine (THI), Thioridazine-2-Sulfoxide (THI-2-SO) and Thioridazine 5-Sulfoxide (THI 5-SO).

Due to the photo-instability of THI (Nałecz-Jawecki et al., 2008) and autocatalytic characteristics of phenothiazine derivatives (Manju et al., 2012), TP 387 II (THI-2-SO) was already present in the sample of THI before photolysis. Fig. 4 (B and D) depicts changes in the peak area of THI and TPs comparing day 0 and day 28 of the biodegradation test with the sample collected after 128 min of photodegradation. In case of CBT, most TPs showed only small changes in peak area after 28 days of test. Such changes might be related to the autocatalytic characteristics of phenothiazine derivatives (Manju et al., 2012), since abiotic transformations cannot be excluded in the CBT without separated studies. In case of MRT, the peak area of THI was decreasing and the peak area of TP 387 I (THI-5-SO) increased during 28 days of MRT. Since the same behavior was found in the abiotic control (sterile control), it can be inferred that THI was transformed abiotically by sulfoxidation due to the presence of dissolved oxygen (Manju et al., 2012). A reduction in terms of peak area was observed for TP 387 II (THI-2-SO), TP 387 III, TP 387 IV, TP 403 V, TP 401 and TP 339 after 28 days of MRT. However, these TPs can also have undergone abiotic transformation such as hydrolysis or due an autocatalytic process due the presence of dissolved oxygen, since the same behavior was observed in the sterile control.

Regarding the "rules of thumb", THI is composed of stable tricycle ring with an electron withdrawing group on the side chain C-2 ($-SCH_3$) and a hydrophilic side chain in the position N-10, which give to phenothiazine a hydrophilic and hydrophobic (surfactant-*like*) behavior (Mahajan and Mahajan, 2013). Such characteristic makes them not accessible for biotransformation. On the other hand, abiotic transformations might occur due to the known autocatalytic characteristic of phenothiazine derivatives with dissolved oxygen (Manju et al., 2012), and transformations were observed on the abiotic control of MRT test (Text S10, Supplementary material).

Concerning the TPs formed, although hydroxylation on the Phenothiazine tricyclic moiety increases the electron donating effect on their structure, the electron withdrawing effect of the side chain $-SCH_3$ might deactivate such effect in the biodegradation. The single oxidation of the side chain increases the electron

Table 1
Effective concentrations (EC_x) of THI, THI-2-SO and THI-5-SO in the modified LBT.

Endpoint	EC_{10} [μmol L^{-1}]			EC_{50} [μmol L^{-1}]		
	THI	THI-2-SO	THI-5-SO	THI	THI-2-SO	THI-5-SO
Luminescence (30 min)	1.1	3.1	80.8	5.1	18.1	>320
Luminescence (24 h)	2.9	3.5	56.5	7.1	20.5	>320
Growth (14 h)	5.9	94.1	150.3	11.6	211.2	>320

withdrawing effect, because it is formed $-S(O)CH_3$, which has a withdrawing effect higher than $-SCH_3$. The higher the withdrawing effect of the side chain the higher is the antipsychotic effect of phenothiazine pharmaceuticals (Jaszczyszyn et al., 2012). When the side chain $-SCH_3$ is oxidized, the electron withdrawing effect increase and consequently increase the antipsychotic action. On the other hand, more than one substitution on the tricycle ring decreases the antipsychotic effect of phenothiazine.

3.4. Bacterial cytotoxicity of photolytic samples and selected TPs of THI

The toxicity against bacteria of THI before and after phototransformation was monitored using a modified luminescent bacteria test. THI was cytotoxic to *V. fischeri* in the range of μmol L^{-1} with EC_{50} values between 5.1 and 11.6 μmol L^{-1} depending on the evaluated endpoint and the time of exposure (Table 1). The most sensitive endpoint was the luminescence emission after 30 min, followed by the luminescence emission after 24 h and the inhibition of growth after 14 h. The observed effect of the dark control sample (0 min) was well explained by the measured concentration of THI and the independently determined concentrations-response curve (Fig. 5), which indicates a good recovery of the individual effect of THI in the photodegradation samples. Irradiation of THI with simulated sunlight resulted in a significant decrease of bacterial cytotoxicity in terms of luminescence and growth inhibition, which followed a similar trend like the predicted individual effect of residual THI in the photolytic mixture (Fig. 5). This means that a lowered antibacterial activity in comparison to the parent compound can be expected for the majority of TPs within the investigated samples, as long as they occur as a mixture. The expected contribution to the observed mixture effect of the TPs THI-2-SO and THI-5-SO was further tested using commercially available reference standards. The obtained EC_{50}-values (Table 1) indicated that THI-2-SO was 3–18 times less potent than THI, depending on the endpoint (luminescence or growth inhibition) and the time of exposure (30 min or 24 h). THI-5-SO was even less active than THI-2-SO, which is why the EC_{50} could not be determined within the tested concentration range. The EC_{10} of THI-2-SO was below the investigated mixture concentration of 12.3 μM, whereas EC_{10} of THI-5-SO was more than 4 times higher. This shows that THI-2-SO might have contributed to the observed residual bacterial toxicity in the photolytic mixtures, whereas THI-5-SO may not have a sufficient potency to cause an effect within the tested concentration range. In order to gain further information on possible interactions, the combined effect of THI and THI-2-SO in the photolytic mixture was predicted using the concentration addition (CA) and the independent action (IA) models (Text S12, Supplementary material). However, only CA will be exemplarily shown and discussed here, because both models provided very similar results. The observed mixture effect of irradiated samples was in some cases slightly lower than the expected combined effect of THI and THI-2-SO, showing that THI and THI-2-SO may have a reduced bacteriotoxic activity when they are part of a synthetic photolytic mixture. Such an antagonism could be explained by a high abundance of structurally similar, but less potent TPs that bind competitively to the same molecular target as THI and THI-2-SO.

3.4.1. QSAR predictions of genotoxic and mutagenic activities

The predicted values and applied QSAR models for genotoxic and mutagenic activities are summarized in Table 2 and in Text S13 (Supplementary material). It is worth to remember that the endpoints do not address any dose-dependence on the results. Besides, considering that many isomers were formed, and the impossibility to confirm the exact attachment position of hydroxyl group for some TPs based on the UHPLC-HRMSn spectrum only, we are considering all possible attachments positions on the structures submitted to the *in silico* QSAR predictions.

Negative alerts for THI were pointed out by the QSAR models, which is in line with the literature (Matter et al., 1983). Matter et al. (1983) have investigated the mutagenicity of THI in the Ames test towards *Salmonella typhimurium* (TA98, TA100, TA1535, TA1537, TA1538) and no mutagenic/genotoxic effects were evidenced. However, THI is known to cause chromosomal aberrations in psychiatric patients (Gocke, 1996; Brambilla et al., 2009).

As showed in Table 2 most of the TPs presented "negative", "inconclusive (IN)" and "out of domain (OD)" estimations. The negative alert indicates that the calculated probability is lower than the model's current classification threshold of 50% and is not within the so-called "gray zone", which is 40%–60% of probability of being positive. Therefore, negative alerts indicated that such structures are predicted to not present mutagenic activities. The "inconclusive (IN)" estimation means that such proposed structures have the calculated probability of being positive falling inside the "gray zone", whereas the "out of domain (OD)" estimation points out that the chemical contains features not covered by the training set of the respective model. Such uncertainty in the predictions might be due to the limitations of the training set of the applied models.

On the other hand, QSAR predictions provided by CASE Ultra and Leadscope® have pointed out positive alerts for mutagenicity in TP 355 and TP 339 for both statistical and rule-based models, which is a strong evidence of the risk associated to this TPs. The predicted structural moieties responsible for the positive alerts for TP 339 and TP 355 are shown in Table S12 and Table S13 (Text S14, supplementary material). In common, both TPs present a carbazole heterocyclic aromatic ring, which is known to be a mutagenic moiety (Weyand et al., 1993; Jha and Bharti, 2002). Consequently, sulfoxide elimination and formation of carbazole derivative compounds during photodegradation of THI can lead to TPs, which could represent a risk for human health and the environment. A confirmatory *in vitro* tests for the evaluation of predicted mutagenicity of TP 355 and TP 339 should be further considered.

4. Conclusions

Thioridazine undergoes photodegradation under simulated sunlight irradiation forming a mixture of TPs as a result of direct and self-sensitized photolysis. The most abundant TPs were identified as THI-5-SO and THI-2-SO, suggesting their environmental relevance not only as human metabolites but also as TPs formed

Table 2
In silico QSAR predictions for mutagenicity of THI and proposed TPs formed during photodegradation according to QSAR models provided by CASE Ultra and Leadscope™.

Compounds[a]	QSAR predictions					
	Case ultra[b]					Leadscope[c]
	A	B	C	D	E	F
Thioridazine	IN	–	–	–	–	–
THI-5-SO	IN	OD	–	OD	–	–
THI-2-SO	IN	–	–	–	–	–
403 (I, VI) a	IN	OD	–	OD	–	OD
403 (I, VI) b	IN	OD	–	OD	–	–
403 (I, VI) c	IN	OD	–	OD	–	–
403 (I, VI) d	IN	OD	–	OD	–	–
403 (I, VI) e	OD	OD	–	OD	–	–
403 (I, VI) f	OD	OD	–	OD	–	–
403 (I, VI) g	IN	OD	–	OD	–	–
403 (VIII) a	IN	–	–	–	–	–
403 (VIII) b	IN	–	–	–	–	–
403 (VIII) c	IN	–	–	–	–	–
403 (VIII) d	IN	–	–	–	–	–
403 (VIII) e	–	–	–	–	–	–
403 (VIII) f	OD	OD	–	–	–	–
403 (VIII) g	IN	OD	–	–	–	–
419 (I) a	OD	OD	–	OD	–	–
419 (I) b	OD	OD	–	OD	–	–
419 (I) c	OD	OD	–	OD	–	OD
419 (I) d	OD	OD	–	OD	–	–
419 (I) e	OD	OD	–	OD	–	–
419 (I) f	OD	OD	–	OD	–	–
419 (I) g	OD	OD	–	OD	–	–
419 (II) a	IN	OD	–	–	–	OD
419 (II) b	IN	OD	–	–	–	OD
419 (II) c	IN	OD	–	–	–	OD
419 (II) d	IN	OD	–	–	–	–
419 (II) e	–	OD	–	–	–	–
419 (II) f	–	OD	–	–	–	OD
419 (II) g	IN	OD	–	–	–	OD
401 a	IN	OD	–	OD	–	–
401 b	IN	OD	–	OD	–	–
401 c	IN	OD	–	OD	–	–
401 d	IN	OD	–	OD	–	–
401 e	OD	OD	–	OD	–	–
401 f	OD	OD	–	OD	–	–
401 g	IN	OD	–	OD	–	–
355 a	+	+	+	+	+	+
355 b	+	+	+	+	+	+
355 c	+	+	+	+	+	+
355 d	+	+	+	+	+	OD
355 e	+	+	+	+	+	OD
355 f	+	+	+	+	+	+
355 g	+	+	+	+	+	+
339	+	+	+	+	+	+

OD (Out of Domain): tested chemical is not covered by the applicability domain of the model.
IN (Inconclusive): the calculated probability of being positive falls inside the "gray zone" (40%–60% of probability).
(+) positive alert (>60%).
(–) negative alert (<40%).
[a] The SMILE codes of the TPs can be seen in Text S13 (Supplementary material).
[b] Case Ultra models according to ICH guideline M7: (A) GT1 A7B Salmonella mutagenicity TA 97,98,100, 1535–1538; (B) GT1 AT *Escherichia coli* A-T mutation *E. coli* and TA102; (C) GT Expert (Expert rules for genotoxicity); (D) Pharm *E coli E. coli* mutagenicity (all strains); (E) Pharm Salm (Salmonella mutagenicity (TA97,98,100,1535–1538)).
[c] Leadscope model: (F) Bacterial mutagenesis towards *Salmonella typhimurium*.

through a natural attenuation processes. THI and the photolytic mixture containing THI and TPs were not readily biodegradable according to CBT and MRT. Only few TPs showed a reduction in their corresponding peak area during the biodegradation tests, providing evidence that most TPs would be recalcitrant to biodegradation in environmental waters. The *in silico* QSAR predictions for ready biodegradability were in line with the experimental results.

The toxicity of THI against *V. fischeri* decreased with the further phototransformation. Moreover, the most abundant TPs, THI-5-SO and THI-2-SO, were proven to be less toxic to *V. fischeri* than THI.

In silico QSAR models provided statistical and rule-based positive alerts for mutagenic/genotoxic activity in case of TP 355 and TP 339, strongly indicating that sulfoxide elimination and formation of a carbazole moiety can lead to compounds that demand further attention. Nevertheless, many proposed structures of TPs showed "inconclusive" and "out of the applicability domain" estimations due to the limitations on the training set of the applied models indicating that such results still should be interpreted carefully.

In terms of bacterial toxicity there was also some evidence for antagonism between the components of the highly concentrated photolytic mixture. This shows that whole mixture testing of photodegradation samples with an elevated initial concentration can also lead to an underestimation of the potential hazard of individual mixture components. Besides, *in silico* QSAR tools should be further developed to cover the gaps on the initial risk assessment regarding TPs, which are not available for experimental testing. Finally, after the successful identification and characterization of potentially hazardous TPs, their relevance in terms of exposure must be further assessed to allow a well-founded evaluation of possible risks.

Acknowledgments

The authors would like to thank the Brazilian program "*Science without borders*" from CNPq/CAPES/CsF (Grant Nr. 2367712012-4) and the Innovations-Inkubator Lüneburg (Teilmaβnahme 1.4, Graduate School) for the scholarships granted to Dr. M.L. Wilde and J. Menz, respectively. The authors would like to thank A. Haiss and E. Logunova for planning the aerobic biodegradation tests and J. Westphal for analytical support. Multicase Inc. and Leadscope Inc. are kindly acknowledged for providing the CASE Ultra and Leadscope QSAR software, respectively.

Appendix A. Supplementary data

Supplementary data related to this article can be found at http://dx.doi.org/10.1016/j.envpol.2016.03.018.

Conflicts of interest

The authors declared to have no conflict of interest.

References

Baselt, R.C., Cravey, R.H., 1995. Disposition of Toxic Drugs and Chemicals in Man, fourth ed. Chemical Toxicology Institute, Foster City, CA, USA.
Berenbaum, M.C., 1985. The expected effect of a combination of agents: the general solution. J. Theor. Biol. 114, 413–431. http://dx.doi.org/10.1016/S0022-5193(85)80176-4.
Bliss, C.I., 1939. The toxicity of poisons applied jointly. Ann. Appl. Biol. 26, 585–615. http://dx.doi.org/10.1111/j.1744-7348.1939.tb06990.x.
Borges, K.B., Borges, W.D.S., Pupo, M.T., Bonato, P.S., 2008. Stereoselective analysis of thioridazine-2-sulfoxide and thioridazine-5-sulfoxide: an investigation of rac-thioridazine biotransformation by some endophytic fungi. J. Pharm. Biomed. Anal. 46, 945–952. http://dx.doi.org/10.1016/j.jpba.2007.05.018.
Brambilla, G., Mattioli, F., Martelli, A., 2009. Genotoxic and carcinogenic effects of antipsychotics and antidepressants. Toxicology 261, 77–88. http://dx.doi.org/10.1016/j.tox.2009.04.056.
Carstens, K.L., Gross, A.D., Moorman, T.B., Coats, J.R., 2013. Sorption and photodegradation processes govern distribution and fate of sulfamethazine in freshwater-sediment microcosms. Environ. Sci. Technol. 47, 10877–10883. http://dx.doi.org/10.1021/es402100g.
Chakravarti, S.K., Saiakhov, R.D., Klopman, G., 2012. Optimizing predictive

performance of CASE Ultra expert system models using the applicability domains of individual toxicity alerts. J. Chem. Inf. Model 52, 2609–2618. http://dx.doi.org/10.1021/ci300111r.
Cwiertny, D.M., Snyder, S.A., Schlenk, D., Kolodziej, E.P., 2014. Environmental designer drugs: when transformation may not eliminate risk. Environ. Sci. Technol. 48, 11737–11745.
Daniel, W.A., Syrek, M., Haduch, A., Wójcikowski, J., 2000. Pharmacokinetics and metabolism of thioridazine during co-administration of tricyclic antidepressants. Br. J. Pharmacol. 131, 287–295. http://dx.doi.org/10.1038/sj.bjp.0703540.
Edhlund, B.L., Arnold, W.a, McNeill, K., 2006. Aquatic photochemistry of nitrofuran antibiotics. Environ. Sci. Pollut. Res. 40, 5422–5427. http://dx.doi.org/10.1021/es0606778.
Eiduson, S., Geller, E., 1963. The excretion and metabolism of ^{35}S-labeled thioridazine in urine, blood, bile, and feces. Biochem. Pharmacol 12, 1429–1435.
Elisei, F., Latterini, L., Gaetano Aloisi, G., Mazzucato, U., Viola, G., Miolo, G., Vedaldi, D., Dall'Acqua, F., 2007. Excited-state properties and in vitro phototoxicity studies of three phenothiazine derivatives. Photochem. Photobiol. 75, 11–21. http://dx.doi.org/10.1562/0031-8655(2002)0750011ESPAIV2.0.CO2.
Escher, B.I., Fenner, K., 2011. Recent advances in environmental risk assessment of transformation products. Environ. Sci. Technol. 45, 3835–3847. http://dx.doi.org/10.1021/es1030799.
Fatta-Kassinos, D., Vasquez, M.I., Kümmerer, K., 2011. Transformation products of pharmaceuticals in surface waters and wastewater formed during photolysis and advanced oxidation processes – degradation, elucidation of byproducts and assessment of their biological potency. Chemosphere 85, 693–709. http://dx.doi.org/10.1016/j.chemosphere.2011.06.082.
Friedrich, J., Längin, A., Kümmerer, K., 2013. Comparison of an electrochemical and luminescence-based oxygen measuring system for use in the biodegradability testing according to closed bottle test (OECD 301D). Clean 41, 251–257. http://dx.doi.org/10.1002/clen.201100558.
Gocke, E., 1996. Review of the genotoxic properties of chlorpromazine and related phenothiazines. Mutat. Res. 366, 9–21.
Howard, P.H., 2000. Biodegradation. In: Mackay, D., Boethling, R.S. (Eds.), Handbook of Property Estimation Methods for Environmental Chemicals. Environmental and Health Sciences. Lewis Publishers, Boca Raton, pp. 281–310 (n.d).
International Conference on Harmonization (ICH), 2014. ICH Guideline M7. http://www.ich.org/fileadmin/Public_Web_Site/ICH_Products/Guidelines/Multidisciplina ry/M7/M7_Step_4.pdf (acessed on 02.11.15).
Jacobs, L.E., Weavers, L.K., Houtz, E.F., Chin, Y.-P., 2012. Photosensitized degradation of caffeine: role of fulvic acids and nitrate. Chemosphere 86, 124–129. http://dx.doi.org/10.1016/j.chemosphere.2011.09.052.
Jarvis, A.L., Bernot, M.J., Bernot, R.J., 2014a. The effects of the psychiatric drug carbamazepine on freshwater invertebrate communities and ecosystem dynamics. Sci. Total Environ. 496, 499–509. http://dx.doi.org/10.1016/j.scitotenv.2014.07.086.
Jarvis, A.L., Bernot, M.J., Bernot, R.J., 2014b. Relationships between the psychiatric drug carbamazepine and freshwater macroinvertebrate community structure. Sci. Total Environ. 496, 499–509. http://dx.doi.org/10.1016/j.scitotenv.2014.07.086.
Jaszczyszyn, A., Gasiorowski, K., ŚwiaTek, P., Malinka, W., Cieślik-Boczula, K., Petrus, J., Czarnik-Matusewicz, B., 2012. Chemical structure of phenothiazines and their biological activity. Pharmacol. Rep. 64, 16–23.
Jha, A.M., Bharti, M.K., 2002. Mutagenic profiles of carbazole in the male germ cells of Swiss albino mice. Mutat. Res. 500, 97–101. http://dx.doi.org/10.1016/S0027-5107(01)00303-7.
Kristiansen, J.E., Dastidar, S.G., Palchoudhuri, S., Roy, D.S., Das, S., Hendricks, O., Christensen, J.B., 2015. Phenothiazines as a solution for multidrug resistant tuberculosis: from the origin to present. Int. Microbiol. 18, 1–12. http://dx.doi.org/10.2436/20.1501.01.229.
Kümmerer, K., 2001. Drugs in the environment: emission of drugs, diagnostic aids and disinfectants into wastewater by hospitals in relation to other sources – a review. Chemosphere 45, 957–969.
Kümmerer, K., 2009. The presence of pharmaceuticals in the environment due to human use – present knowledge and future challenges. J. Environ. Manag. 90, 2354–2366. http://dx.doi.org/10.1016/j.jenvman.2009.01.023.
Laboratory of Mathematical Chemistry B, 2012. OASIS Catalogic Software V. 5.11.6 TB. http://oasis-lmc.org/ (accessed 03.31.15).
Langdon, K.A., Warne, M.S.J., Smernik, R.J., Shareef, A., Kookana, R.S., 2011. Degradation of 4-nonylphenol, 4-t-octylphenol, bisphenol A and triclosan following biosolids addition to soil under laboratory conditions. Chemosphere 84, 1556–1562. http://dx.doi.org/10.1016/j.chemosphere.2011.05.053.
Längin, A., Alexy, R., König, A., Kümmerer, K., 2009. Deactivation and transformation products in biodegradability testing of ß-lactams amoxicillin and piperacillin. Chemosphere 75, 347–354. http://dx.doi.org/10.1016/j.chemosphere.2008.12.032.
Lapworth, D.J., Baran, N., Stuart, M.E., Ward, R.S., 2012. Emerging organic contaminants in groundwater: a review of sources, fate and occurrence. Environ. Pollut. 163, 287–303. http://dx.doi.org/10.1016/j.envpol.2011.12.034.
Latch, D.E., Stender, B.L., Packer, J.L., Arnold, W.A., McNeill, K., 2003. Photochemical fate of pharmaceuticals in the environment: cimetidine and ranitidine. Environ. Sci. Technol. 37, 3342–3350.
Legrini, O., Oliveros, E., Braun, A.M., 1993. Photochemical processes for water treatment. Chem. Rev. 93, 671–698.
Li, Y., Niu, J., Wang, W., 2011. Photolysis of enrofloxacin in aqueous systems under simulated sunlight irradiation: kinetics, mechanism and toxicity of photolysis products. Chemosphere 85, 892–897. http://dx.doi.org/10.1016/j.chemosphere.2011.07.008.
Lin, A.Y.-C., Wang, X.-H., Lee, W.-N., 2013. Phototransformation determines the fate of 5-fluorouracil and cyclophosphamide in natural surface waters. Environ. Sci. Technol. 47, 4104–4112. http://dx.doi.org/10.1021/es304976q.
Mahajan, S., Mahajan, R.K., 2013. Interactions of phenothiazine drugs with surfactants: a detailed physicochemical overview. Adv. Colloid Interface Sci. 199–200, 1–14. http://dx.doi.org/10.1016/j.cis.2013.06.008.
Mahmoud, W.M.M., Toolaram, A.P., Menz, J., Leder, C., Schneider, M., Kümmerer, K., 2014. Identification of phototransformation products of thalidomide and mixture toxicity assessment: an experimental and quantitative structural activity relationships (QSAR) approach. Water Res. 49, 11–22. http://dx.doi.org/10.1016/j.watres.2013.11.014.
Manju, T., Manoj, N., Braun, A.M., Oliveros, E., 2012. Self sensitized photooxidation of N-methyl phenothiazine: acidity control of the competition between electron and energy transfer mechanisms. Photochem. Photobiol. Sci. 1744 http://dx.doi.org/10.1039/c2pp25244a.
Martins, M., Dastidar, S.G., Fanning, S., Kristiansen, J.E., Molnar, J., Pagès, J.M., Schelz, Z., Spengler, G., Viveiros, M., Amaral, L., 2008. Potential role of non-antibiotics (helper compounds) in the treatment of multidrug-resistant Gram-negative infections: mechanisms for their direct and indirect activities. Int. J. Antimicrob. Agents 31, 198–208. http://dx.doi.org/10.1016/j.ijantimicag.2007.10.025.
Martins, R.C., Lopes, R.J.G., Quinta-ferreira, R.M., 2010. Lumped kinetic models for single ozonation of phenolic effluents. Chem. Eng. J. 165, 678–685. http://dx.doi.org/10.1016/j.cej.2010.09.060.
Matter, B.E., Graf, U., Hu, S., Jaeger, I., Racine, R., Suter, W., Wt, F.E., 1983. Mutagenicity evaluation of thioridazine *Salmonella typhimurium*. Mutat. Res. 116, 389–398.
Menz, J., Schneider, M., Kümmerer, K., 2013. Toxicity testing with luminescent bacteria – characterization of an automated method for the combined assessment of acute and chronic effects. Chemosphere 93, 990–996. http://dx.doi.org/10.1016/j.chemosphere.2013.05.067.
Miolo, G., Levorato, L., Gallocchio, F., Caffieri, S., Bastianon, C., Zanoni, R., Reddi, E., 2006. In vitro phototoxicity of phenothiazines: involvement of stable UVA photolysis products formed in aqueous medium. Chem. Res. Toxicol. 19, 156–163. http://dx.doi.org/10.1021/tx0502239.
Nagel, D., Spranger, S., Vincendeau, M., Grau, M., Raffegerst, S., Kloo, B., Lenz, P., Hlahla, D., Neuenschwander, M., Kries, J.P., Von, Hadian, K., Do, B., Lenz, G., Schendel, D.J., Krappmann, D., 2012. Pharmacologic inhibition of MALT1 protease by phenothiazines as a therapeutic approach for the treatment of aggressive ABC-DLBCL. Cancer Cell 825–837. http://dx.doi.org/10.1016/j.ccr.2012.11.002.
Nałecz-Jawecki, G., Hajnas, A., Sawicki, J., 2008. Photodegradation and phototoxicity of thioridazine and chlorpromazine evaluated with chemical analysis and aquatic organisms. Ecotoxicology 17, 13–20. http://dx.doi.org/10.1007/s10646-007-0171-z.
Nyholm, N., 1991. The European system of standardized legal tests for assessing the biodegradability of chemicals. Environ. Toxicol. Chem. 10, 1327–1246.
OECD, 1992. Organisation for Economic Co-operation and Development, 2006. OECD Guideline for Testing of Chemicals 301: Ready Biodegradability. OECD Publishing, Paris.
Rastogi, T., Leder, C., Kümmerer, K., 2014a. Qualitative environmental risk assessment of photolytic transformation products of iodinated X-ray contrast agent diatrizoic acid. Sci. Total Environ. 482–483, 378–388. http://dx.doi.org/10.1016/j.scitotenv.2014.02.139.
Rastogi, T., Leder, C., Kümmerer, K., 2014b. Designing green derivatives of β-blocker metoprolol: a tiered approach for green and sustainable pharmacy and chemistry. Chemosphere 111, 493–499. http://dx.doi.org/10.1016/j.chemosphere.2014.03.119.
Rastogi, T., Leder, C., Kümmerer, K., 2015. A sustainable chemistry solution to the presence of pharmaceuticals and chemicals in the aquatic environment – the example of re-designing beta-blocker Atenolol. RSC Adv. 5, 27–32. http://dx.doi.org/10.1039/C4RA04783D.
Roberts, G., Myatt, G.J., Johnson, W.P., Cross, K.P., Blower, P.E., 2000. LeadScope: software for exploring large sets of screening data. J. Chem. Inf. Comput. Sci. 40, 1302–1314.
Rodil, R., Quintana, J.B., Concha-Graña, E., López-Mahía, P., Muniategui-Lorenzo, S., Prada-Rodríguez, D., 2012. Emerging pollutants in sewage, surface and drinking water in Galicia (NW Spain). Chemosphere 86, 1040–1049. http://dx.doi.org/10.1016/j.chemosphere.2011.11.053.
Ryan, C.C., Tan, D.T., Arnold, W.A., 2010. Direct and indirect photolysis of sulfamethoxazole and trimethoprim in wastewater treatment plant effluent. Water Res. 45, 1280–1286. http://dx.doi.org/10.1016/j.watres.2010.10.005.
Saiakhov, R., Chakravarti, S., Klopman, G., 2013. Effectiveness of case ultra expert system in evaluating adverse effects of drugs. Mol. Inf. 32, 87–97. http://dx.doi.org/10.1002/minf.201200081.
Saiakhov, R., Chakravarti, S., Sedykh, A., 2014. An improved workflow to perform in silico mutagenicity assessment of impurities as per ICH M7 guideline. Toxicol. Lett. 229, S164. http://dx.doi.org/10.1016/j.toxlet.2014.06.563.
Schwabe, U., Paffrath, D., 2014. Arzneiverordnungs-Report 2014: Aktuelle Daten, Kosten, Trends und Kommentare, first ed. Springer-Verlag, Berlin Heidelberg. http://dx.doi.org/10.1007/978-3-540-34370-7.
Sturini, M., Speltini, A., Maraschi, F., Profumo, A., Pretali, L., Fasani, E., Albini, A., 2010. Photochemical degradation of marbofloxacin and enrofloxacin in natural

waters. Environ. Sci. Technol. 44, 4564–4569. http://dx.doi.org/10.1021/es100278n.
Thanacoody, H.K.R., 2007. Thioridazine: resurrection as an antimicrobial agent? Br. J. Pharmacol. 64, 566–574. http://dx.doi.org/10.1111/j.1365-2125.2007.03021.x.
Thanacoody, R.B.H.K., 2011. Thioridazine: the good and the bad. Recent Pat. Anti-infect. Drug Discov. 6, 92–98.
Trautwein, C., Berset, J.D., Wolschke, H., Kümmerer, K., 2014. Occurrence of the antidiabetic drug metformin and its ultimate transformation product guanylurea in several compartments of the aquatic cycle. Environ. Int. 70, 203–212. http://dx.doi.org/10.1016/j.envint.2014.05.008.
Trautwein, C., Kümmerer, K., 2011. Incomplete aerobic degradation of the antidiabetic drug metformin and identification of the bacterial dead-end transformation product guanylurea. Chemosphere 85. http://dx.doi.org/10.1016/j.chemosphere.2011.06.057, 765–763.
Trautwein, C., Kümmerer, K., 2012a. Ready biodegradability of trifluoromethylated phenothiazine drugs, structural elucidation of their aquatic transformation products, and identification of environmental risks studied by LC-MS^n and QSAR. Environ. Sci. Pollut. Res. 19, 3162–3177. http://dx.doi.org/10.1007/s11356-012-1002-1.
Trautwein, C., Kümmerer, K., 2012b. Degradation of the tricyclic antipsychotic drug chlorpromazine under environmental conditions, identification of its main aquatic biotic and abiotic transformation products by LC-MSn and their effects on environmental bacteria. J. Chromatogr. B 889–890, 24–38. http://dx.doi.org/10.1016/j.jchromb.2012.01.022.
U.S. EPA, 2004. United States Environmental Protection Agency. EPA/OPPT/exposure Assessment Tools and Models/estimation Program Interface (EPI) Suite Version 3.12. http://www.epa.gov/oppt/exposure/pubs/episuite.htm (accessed 03.31.15).
Verlicchi, P., Aukidy, M.A., Galletti, A., Petrovic, M., Barceló, D., 2012. Hospital effluent: investigation of the concentrations and distribution of pharmaceuticals and environmental risk assessment. Sci. Total Environ. 430, 109–118. http://dx.doi.org/10.1016/j.scitotenv.2012.04.055.
Wammer, K.H., Korte, A.R., Lundeen, R.A., Sundberg, J.E., McNeill, K., Arnold, W.A., 2013. Direct photochemistry of three fluoroquinolone antibacterials: norfloxacin, ofloxacin, and enrofloxacin. Water Res. 47, 439–448. http://dx.doi.org/10.1016/j.watres.2012.10.025.
Weismana, J.L., Lioub, A.P., Shelatc, A.A., Cohena, F.E., Guya, R.K., DeRisib, J.L., 2006. Searching for new antimalarial therapeutics amongst known drugs. Chem. Biol. Drug Des. 67, 409–416.
West, C.E., Rowland, S.J., 2012. Aqueous phototransformation of diazepam and related human metabolites under simulated sunlight. Environ. Sci. Technol. 46, 4749–4756.
Weyand, E.H., Defauw, J., McQueen, C.A., Meschter, C.L., Meegalla, S.K., LaVoie, E.J., 1993. Bioassay of quinoline, 5-fluoroquinoline, carbazole, 9-methylcarbazole and 9-ethylcarbazole in newborn mice. Fd. Chem. Toxic. 31, 707–715. http://dx.doi.org/10.1016/0278-6915(93)90141-K.
Wójcikowski, J., Maurel, P., Daniel, W.A., 2006. Characterization of human cytochrome p450 enzymes involved in the metabolism of the piperidine-type phenothiazine neuroleptic thioridazine. Drug Metab. Dispos. 34, 471. http://dx.doi.org/10.1124/dmd.105.006445.tion.
Worthington, R.J., Melander, C., 2013. Combination approaches to combat multidrug-resistant bacteria. Trends Biotechnol. 31, 177–184. http://dx.doi.org/10.1016/j.tibtech.2012.12.006.
Zepp, R.G., 1978. Quantum yields for reaction of pollutants in dilute aqueous solution. Environ. Sci. Technol. 12, 1976–1978.
Zepp, R.G., Cline, D.M., 1977. Rates of direct photolysis in aquatic environment. Environ. Sci. Technol. 11, 359–366. http://dx.doi.org/10.1021/es60127a013.

Publikation 6

Hazard screening of photo-transformation products from pharmaceuticals: application to selective β1-blockers Atenolol and Metoprolol

Toolaram, A., Menz, J., Rastogi, T., Leder, C., Schneider, M., Kümmerer, K.

(2017)

Science of The Total Environment 571, 1769-1780

DOI: 10.1016/j.scitotenv.2016.10.242

Science of the Total Environment 579 (2017) 1769–1780

Contents lists available at ScienceDirect

Science of the Total Environment

journal homepage: www.elsevier.com/locate/scitotenv

Hazard screening of photo-transformation products from pharmaceuticals: Application to selective β_1-blockers atenolol and metoprolol

Anju Priya Toolaram, Jakob Menz, Tushar Rastogi, Christoph Leder, Klaus Kümmerer *, Mandy Schneider

Sustainable Chemistry and Material Resources, Institute of Sustainable and Environmental Chemistry, Faculty of Sustainability, Leuphana University of Lüneburg, Germany.

HIGHLIGHTS

- Photolysis led to incomplete mineralization of parent compounds
- Bioassays, chemical analytics together with *in-silico* methods identified hazards
- Photolysis mixtures were more toxic than the β-blockers.
- QSAR analysis of transformation products identified diverse mechanisms of toxicity
- Several photo-TPs predicted to present greater hazards than parent compound

GRAPHICAL ABSTRACT

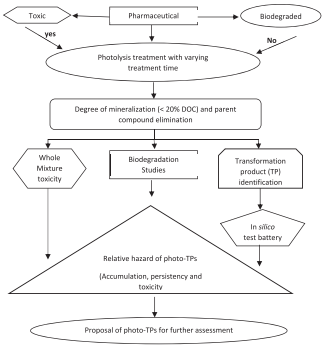

ARTICLE INFO

Article history:
Received 9 September 2016
Received in revised form 13 October 2016
Accepted 13 October 2016
Available online 7 December 2016

Editor: D. Barcelo

Keywords:
Mixture toxicity
Effect based analysis
Quantitative structure-activity relationship (QSAR)

ABSTRACT

The identification of toxic components in cocktail mixtures of pollutants, their metabolites and transformation products (TPs) generated from environmental and treatment processes remains an arduous task. This study expanded in this area by applying a combination of chemical analytics, a battery of *in vitro* bioassays and an *in silico* "testing battery" to UV photolysis mixtures of active pharmaceutical ingredients. The objectives were to understand the toxic nature of the mixtures and to prioritize photo-TPs for risk analysis. The selective β_1-blockers Atenolol (ATL) and Metoprolol (MTL) that are ubiquitous in the aquatic environment were used as an example. The photolysis mixtures were cytotoxic to *Vibrio fischeri* and mammalian cells but not mutagenic in the Ames test or genotoxic in the *in vitro* micronucleus and umu tests. Potentially hazardous TPs were proposed by relating the observed effects to the kinetics of TP occurrence and applying *in silico* toxicity predictions for individual photo-TPs. This model study was done to identify principal mechanisms rather than accurately simulating environmental transformation processes. Several photo-TPs were proposed to present a greater hazard than the

Abbreviations: ATL, Atenolol; ATP(s), transformation product(s) of Atenolol; BCF, bioconcentration factor; *CA*, chromosome aberration; DNA, deoxyribonucleic acid; DOC, dissolved organic carbon; EMA, ethidium monoazide dye (Nuclei acid dye A); HPLC, high performance liquid chromatography; LBT, luminescence bacteria test; LC-MS, liquid chromatography-mass spectrometry; Log Kow, octanol-water partition coefficient; MN, micronucleus; MTL, Metoprolol; MTP(s), Transformation product(s) of Metoprolol; PC, parent compound; QSAR, quantitative structure-activity relationships; TP(s), transformation product(s).

* Corresponding author at: Sustainable Chemistry and Material Resources, Institute of Sustainable and Environmental Chemistry, Faculty of Sustainability, Leuphana University of Lüneburg, Scharnhorststrasse 1/C13, DE-21335 Lüneburg, Germany.

E-mail addresses: toolaram@leuphana.de, anjutoolaram@yahoo.com (A.P. Toolaram), jakob.menz@uni.leuphana.de (J. Menz), tushar.rastogi@leuphana.de (T. Rastogi), cleder@leuphana.de (C. Leder), klaus.kuemmerer@uni.leuphana.de (K. Kümmerer), mschneid@leuphana.de (M. Schneider).

http://dx.doi.org/10.1016/j.scitotenv.2016.10.242

Risk assessment
Emerging contaminants

selected β-blockers and therefore fate and toxicity assessments may be required to determine their environmental relevance.

1. Introduction

Contaminants of emerging concern such as pharmaceuticals are investigated continually to determine their risk to human and ecological health and relevance as environmental micropollutants. Their presence as mixtures with their transformation products (TPs) which are formed during various treatment and/or environmental processes, and other micropollutants have made their environmental risk assessment more challenging. Furthermore, Scientists believed that TPs could add to the overall risks of these contaminants (Escher and Fenner, 2011; La Farré et al., 2008; Richardson and Ternes, 2011) and this warrants further research to identify these potentially hazardous TPs. Such endeavours, usually involved a coupling of analytical and effect based analyses (Escher and Fenner, 2011; Richardson and Ternes, 2011; Toolaram et al., 2014). Sometimes it may be possible to identify TPs of concern in such mixtures by comparing the formation kinetics of TPs and changes in mixture toxicity in lab scale investigations (Escher and Fenner, 2011; Toolaram et al., 2014). However, it remains largely a difficult task to accomplish. Moreover, synthesis or isolation of TPs can be very time- and cost-intensive, which is why a quantitative environmental risk assessment would be only possible for a small number of the identified TPs. In this respect, quantitative structure activity relationship ((Q)SAR) studies as an additional tool would be useful to predict fate and toxicity, and to identify cases for further testing (European Commission, 2003). Additionally, its combination with experimental results can aid in understanding the observed effects and the physicochemical characteristics of the compounds (European Commission, 2003). Given the current state of research, a combination of whole mixture toxicity, chemical analysis and structure activity relationships (quantitative (Q)SAR and ruled based) analyses seemed suitable to ascertain the initial hazards from chemical mixtures.

The selective β1 receptor antagonists Atenolol (ATL) and Metoprolol (MTL) were selected for this study as both have exhibited high hydrolytic stabilities (Liu et al., 2009; Maszkowska et al., 2014) and were not readily biodegradable (Radjenović et al., 2008; Rastogi et al., 2015, 2014b). As a result, they were detected in the ranges of 0.006–25 μg/L in raw effluent with varying degree of removal in wastewater treatment plants (Verlicchi et al., 2012). Fish, algae, amphibians and crustaceans exposed to these β-blockers exhibited specific and non-specific toxicity but at environmentally irrelevant concentrations (Cleuvers, 2005; Contardo-Jara et al., 2010; Escher et al., 2006; Küster et al., 2010; van den Brandhof and Montforts, 2010). However, several β-blockers behaved as baseline toxicants in assays with bacteria (*Vibrio fischeri*), algae (*Desmodesmus subspicatus*) and crustaceans (*Daphnia magna*) and that may be more relevant as contaminants (Cleuvers, 2005; Escher et al., 2006; Küster et al., 2010). Thus far, MTL has not shown evidence of inducing deoxyribonucleic acid (DNA) fragmentation or repair in primary cultures of rat and human hepatocytes but *in vivo* micronucleus (MN) formation in human lymphocytes for ATL was reported (Brambilla and Martelli, 2006; Escher et al., 2006; Okine et al., 1983; Télez et al., 2000). In particular, ATL of average concentration 241 ng/L, similar to the concentration observed in Italian water treatment plants, was reported to cause DNA damage after brief exposure (<14 days) but not after longer term exposure in zebrafish (*Danio rerio*) (Rocco et al., 2012).

Photo-transformation seemed to be the main pathway of β-blockers depletion in the aquatic environment (Liu et al., 2009). In lab–scaled experiments, photo-degradation mimicking sunlight and disinfecting processes resulted in incomplete mineralization leading to the formation of several TPs (Hapeshi et al., 2010; Ji et al., 2012; Rastogi et al., 2015, 2014b; Romero et al., 2011; Šojić et al., 2012). Rastogi et al. (2015, 2014b) described the major pathways for UV photo-degradation of both ATL and MTL as hydroxylation by the attack of electrophilic hydroxyl radical (HO•) at the aromatic ring, dehydration, *i.e.* elimination of water from the isopropyl-amino-propoxy side chain and dealkylation (elimination of propane) from ethanolamine side chain of both beta blockers.

Few studies have indicated that photolytic/photocatalytic mixtures of these β-blockers can exhibit reduced or increased toxicity when compared to the toxicity of the parent compound (PC) in bioassays with algae, crustaceans and bacteria (Hapeshi et al., 2010; Ji et al., 2012; Richard et al., 2014; Romero et al., 2011; Šojić et al., 2012). Šojić et al. (2012) also reported that mixtures derived from several oxidative treatments of MTL were mutagenic in the Ames test and genotoxic in the comet assay. However, the chemical and biological activities of these TPs remained largely unknown both individually and when present in mixtures. As such, our initial hazard assessment of the photolysis mixtures investigated the inherent cytotoxicity and genotoxicity by using a battery of *in vitro* bioassays. Further, the individual photo-TPs previously elucidated in Rastogi et al. (2015, 2014b) were subjected to *in-silico* predictions of fate and toxicity. Therefore, the aims of this study were to characterize the toxicity of the photolysis mixtures and to ascertain photo-TPs for further assessment based on their relative hazard to the PCs. This study is a precursor to an environmental risk assessment used to identify TPs that may be of concern to human and aquatic life.

2. Materials and methods

2.1. UV Photolysis and monitoring of carbon elimination

UV treatment experiments were carried out using a 150 W medium-pressure mercury lamp (TQ 150, UV-Consulting Peschl, Text S1) with an Ilmasil quartz immersion tube. The batch photo reactor was under constant stirring and the temperature (18–20 °C) was maintained by a circulating cooler. The reactor was filled with a solution of the respective β-blocker, Atenolol (CAS-RN: 29122-68-7) and Metoprolol tartrate (CAS-RN: 56392-17-7), dissolved in ultra-pure water (ATL = 100 mg/L, MTL (as a tartrate salt) = 400 mg/L) and irradiation was performed for 256 min. High initial concentrations were selected based on the solubility limits of the β-blockers to ensure that high concentration of the stable TPs can be achieved during photolysis for the analytical and effect based analyses. The degree of mineralization was measured as dissolved organic carbon (DOC) using a Shimadzu TOC-VCPN analyzer. Further information on experimental-setup can be found in Rastogi et al. (2015, 2014b).

2.2. Primary elimination of PC and TP identification

Primary elimination of parent compounds was monitored using a Shimadzu Prominence HPLC system. The formation and identification of the TPs were performed using LC-ESI-IT-MS (HPLC 1100, Agilent Technologies in tandem with Esquire 6000^{Plus}, Bruker Daltonic). All LC instruments, chromatographic parameters and mass spectrometer settings have been detailed elsewhere (Rastogi et al., 2015, 2014b). All TPs identified were previously elucidated using the MetaPC software along with analysing their MS/MS fragmentation pathways and were detailed in Rastogi et al. (2015, 2014b).

2.3. In silico test battery - (Q)SAR predictions

Structure illustrations were performed with MarvinSketch 5.8.0 using the simplified molecular input line entry specification (SMILES) codes. These SMILES codes were introduced into various computer based QSAR models for predicting the effects on a number of toxicity endpoints. QSAR toxicity predictions of ATL, MTL and their elucidated photo-TPs (called ATPs and MTPs respectively) were performed using a set of software each with different algorithms and training sets as an "*in silico* battery". Only the proposed structures of the more stable TPs previously identified in Rastogi et al. (2015, 2014b) were considered in the QSAR analysis. It is a well-known limitation of current QSAR approaches, that these calculations are usually based on the neutral species and do not take into account that the distribution coefficient is highly depending on the ionization of the molecule at different pH. Therefore, the results have to be seen as simplifications and first approximations. Only recently, first attempts are reported to address this limitation, but they are not yet part of the established QSAR platforms (Scherrer and Leo, 2010).

The software used included Case Ultra V.1.5.0.1 (MultiCASE Inc.) (Saiakhov et al., 2013), and Leadscope software V. 3.2.4-1 (Roberts et al., 2000) with training sets from 2012 SAR Genetox Database provided by Leadscope. Oasis Catalogic software from Laboratory of Mathematical Chemistry, University Bourgas, Bulgaria was used to predict bacterial mutagenicity (module mutagenicity v.04) in *Salmonella typhimurium* (Salmonella Catalogic model, SC). Bacterial toxicity was predicted in CASE Ultra V.1.5.0.1 using the environmental bacteria module based on the MICROTOX model for toxicity (MultiCASE Inc.). All the *in silico* models contained validated database and training sets (Chakravarti et al., 2012; Roberts et al., 2000; Saiakhov et al., 2013). Further information on each model can be seen in Supplementary S2. These models also have been applied in other works (Mahmoud et al., 2014; Rastogi et al., 2014a).

Selected physico-chemical and fate parameters including water solubility, octanol-water partition coefficient (Log Kow) and bioconcentration factor (BCF) were predicted using the EPI Suite software KOWWIN v1.68 model (Environmental Protection Agency, US). The results of these predictions were then interpreted based on EPA (2012) recommendations and detailed in Supplementary S3.

2.4. Whole mixture toxicity testing

Photolysis samples were sterile filtered (0.2 μm) and frozen at −150 °C. All tests were performed at least twice with 3 replicates per bacterial test and 2 replicates for *in vitro* MN test. Sample pH was measured and adjusted to pH 7.0 ± 0.2, if needed, prior to performing bioassays. All photolytic mixtures were tested semi-quantitatively for peroxides using Merckoquant Peroxide test strips 0.5–25 ppm (VWR). The peak concentrations of peroxide were detected in the fresh samples of both β-blockers after 256 min irradiation as equivalent to approximately 2 mg/L H_2O_2 in case of MTL and 5 mg/L H_2O_2 in case of ATL. After sample processing and storage up to 2 mg/L H_2O_2 were observed in case of ATL while no peroxides were detected in the stored samples of irradiated MTL. Independent testing showed that the bioassays used in this study were not affected by ≤2 mg/L H_2O_2 nominal concentration in the samples. The results of an independent test with H_2O_2 in the modified luminescent bacteria test can be seen in Supplementary S4.

2.4.1. Modified luminescent bacteria test (modified LBT)

The modified luminescent test using *V. fischeri* NRRL-B-11177 (Hach-Lange GmbH, Düsseldorf) was conducted as described in Menz et al. (2013) and can be found in details in Supplementary S5. The raw data from this test were normalized to percent inhibition in relation to the negative controls. This was conducted for three different endpoints: short-term luminescence inhibition after 30 min ($LI_{30\ min}$), long-term luminescence inhibition after 24 h ($LI_{24\ h}$) and growth inhibition after 14 h ($GI_{14\ h}$). Calculations and data analysis were performed using the recommendation of Menz et al. (2013). A 20% inhibition was considered the threshold value for significant inhibition. Analysis of concentration-response relationships of PCs was performed by plotting the normalized inhibition values against the respective concentrations followed by a non-linear regression using a four-parametric Hill function.

2.4.2. Bacterial mutagenicity - Ames MPF 98/100 aqua

The Ames test was performed using a microplate format that was adapted from the Ames fluctuation assay. It was performed based on the Ames MPF 98/100 Aqua test manual (Xenometrix AG) with *Salmonella typhimurium* TA 98 and TA 100. Further details on the methods are presented in Supplementary S5. Classification as positive for mutagenicity occurred when the response was ≥2 fold increase in the number of revertants over the mean negative control.

2.4.3. Bacterial genotoxicity - umu-test

The umu-test was performed according to ISO 13829 (2000). Further details of the test procedure is given in Supplementary S5. The calculation of growth (G) and induction ratio (IR) were performed according to ISO 13829. Classification as positive for *umuC* induction followed when IR > 1.5 and G ≥ 0.5.

2.4.4. Mammalian genotoxicity and cytotoxicity - in vitro micronucleus assay using flow cytometry

The *in vitro* MN test was performed with Chinese hamster ovary cells (CHO-K1, American Type Culture Collection (ATCC)) and was designed and executed using the guidelines of the *In vitro* MicroFlow Kit (Litron Laboratories) and Bryce et al. (2010). The details of the *in vitro* MN test and the cell staining procedure can be found in Supplementary S5. Flow cytometry analysis was performed using BD Biosciences FACSCalibur with data acquired according to the gatings and settings recommended by the InVitro MicroFlow Kit protocol. 20,000 nucleated cells per samples were analysed for MN formation, cytotoxicity (EMA + and relative survival), and cell cycle perturbation. The validity criteria for the test were defined as suggested by Bryce et al. (2010). Samples were classified as positive when MN frequency ≥3 fold over the mean negative control value. Samples were determined to be cytotoxic if there was ≥50% reduction in relative survival to negative control.

2.5. Statistical analysis

The statistical significance determined by ANOVA (Dunnett method, overall significance level $p \leq 0.05$) using 0 min irradiation as the control group. All statistical analysis and graphs were processed using Microsoft Excel 2010 (Microsoft Corporation) and SigmaPlot 12.0 (Systat Software, Inc.).

3. Results and discussion

3.1. Photo-transformation of ATL and MTL

UV Photolysis achieved a primary elimination of >90% for 100 mg/L ATL and ~60% for 400 mg/L MTL after 256 min of UV irradiation (Figs. 1A, 2A). The difference in the initial concentration could account for the varying rates of primary elimination. Both ATL and MTL resulted in incomplete mineralization and therefore transformed into several TPs (Figs. 1, 2). Detailed description of their photolysis pathway and kinetics were given already in Rastogi et al. (2015, 2014b) and would not be expanded on here. In this study, 12 TPs were detected in MTL (called MTPs) photolytic mixture and >30 TPs were detected in ATL (called ATPs) photolytic mixture (Figs. 1, 2). A list of identified TPs including their respective proposed chemical structures by Rastogi et al. (2015, 2014b) can be found in Supplementary S6. Most of the TPs in the MTL photolysis mixtures begun to steadily rise in abundance at 16 min and peaked at 256 min (Fig. 2B). Most of the ATPs were degraded with

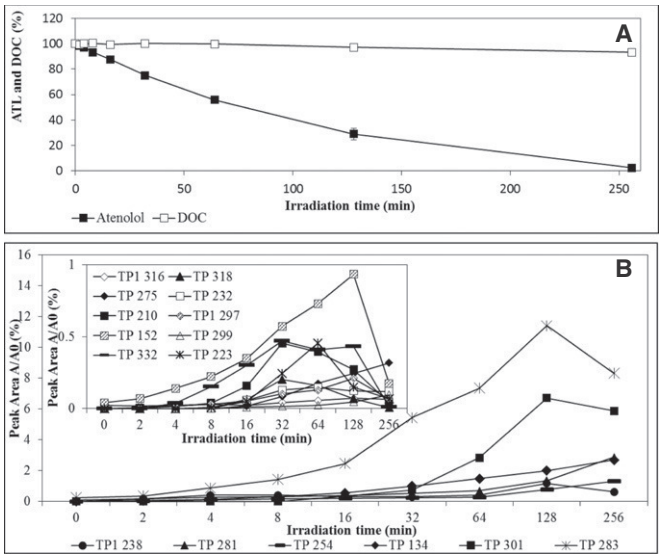

Fig. 1. (a) Percentage 100 mg/L Atenolol (ATL) and dissolved organic carbon (DOC) in photolysis samples. (b) Kinetic of formation of stable photo-transformation products of ATL (ATPs) inset plot: kinetic of formation of ATPs with peak area ratio < 1%.

continuous irradiation and were not present or have reduced in abundance after 256 min of irradiation (Supplementary S7). The more stable ATPs demonstrating an increase in relative abundance over time included ATPs 281, 254, 134, 301, 283, 275, 232, 299 and 316 (Fig. 1B). The proposed structures for TP 134 and TP 210 were found in the photolysis mixtures of both β-blockers.

3.2. Cytotoxic hazards of photolysis mixtures

MTL was the most cytotoxic of the two β-blockers to *V. fischeri* with EC_{50} for $LI_{30\ min}$ > 2000 mg/L, $LI_{24\ h}$ of 526.9 mg/L and $GI_{14\ h}$ of 1258.7 mg/L (Supplementary S8). Exposure of up to 2500 mg/L ATL did not affect *V. fischeri* growth ($GI_{14\ h}$) and luminescence after 30 min ($LI_{30\ min}$) but had an effect of 24% ± 0.74% luminescence inhibition after 24 h exposure ($LI_{24\ h}$) (Supplementary S8). Long term luminescence would account more for the biosynthesis processes of

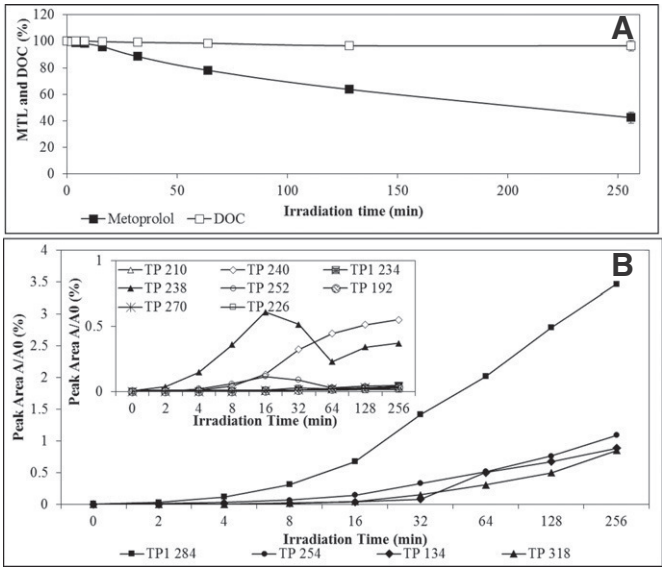

Fig. 2. (a) Percentage of 400 mg/L Metoprolol tartrate (MTL) and dissolved organic carbon (DOC) in photolysis samples. (b) Kinetic of formation of stable photo-transformation products of MTL (MTPs) inset plot: kinetic of formation of MTPs with peak area ratio < 1%.

luminescence than measuring the short term luminescence and further may be relatable to the reproduction inhibition parameter (Backhaus et al., 2000).

More importantly, the photolytic mixtures were more cytotoxic than the β-blockers (Fig. 3). Significant effects on bacterial luminescence was observed in mixtures of ≥16 min irradiation of MTL and ≥32 min irradiation of ATL (Fig. 3). ATL photolytic mixtures exhibited a more pronounced short-term luminescence inhibition ($LI_{30\ min}$) than long-term inhibition ($LI_{24\ h}$), which was contrarily to MTL photolytic mixtures (Fig. 3). MTL was also present in significant amounts in each photolysis mixture (60% after 256 min photolysis) and therefore would have also contributed to the nature and level of toxicity observed. Nevertheless, the presence of luminescence and growth inhibition at the same time suggested that exposure to the photolytic mixtures led to an immediately occurring cytotoxic effect and consequently to a significantly reduced rate of cell multiplication.

Like the concentration of most TPs, bacterial inhibition also increased with irradiation time making it difficult to identify the TPs of concern using kinetics and toxicity data only. As such, QSAR predictions for cytotoxicity were performed using CASE Ultra AUA model as an estimator for short-term bacterial luminescence inhibition. The photo-TPs that had structural alerts for the cytotoxicity to *V. fischeri* included functional groups such as alkenes, ketones, ethers and phenols (Table 1). According to Verhaar et al. (1992), these structural alerts may indicate the mode of actions of narcosis and reactive species contributing to toxicity in the photolytic samples. Generally, the trend in cytotoxicity to bacteria increased with the relative abundance of the photo-TPs (Figs. 1, 2, 3). As such, it can be assumed that the observed toxicity maybe due to the combined exposure to multiple photo-TPs rather than one specifically and therefore, the whole mixture may be more relevant in microbial toxicity.

The applied QSAR model was limited in its application as two parts relating to the aliphatic amine, including the ethanolamine part of the β-blockers molecules were outside of the applicability domain of this model. This occurrence highlighted the limitations of applying QSAR in risk assessments especially for unknown chemicals. Actually, Klopman and Stuart (2003) found that there was no toxicophore for amines that can be connected to the *V. fischeri* Microtox assay and the toxicity of molecules containing them was based on the nature of the chain and other toxicophores in the molecules such as an aromatic ring. Ethanolamine itself was proven also to be toxic to *V. fischeri* in the microtox assay (Libralato et al., 2008). In fact, Šojić et al. (2012) reasoned that TP 134 (called MP1) as well as other aliphatic intermediates formed from oxidative treatment of MTL may have influenced their chronic and acute based test system while Četojević-Simin et al. (2013) suggested that TP 134 (as TP2) was a possible contributor to cytotoxicity of their MTL photocatalytic mixtures to several mammalian cell lines. As a result, these predicted "out of domain" photo-TPs cannot be excluded as possible contributors to bacteria cytotoxicity especially since they were present in the toxic photolytic mixtures and both β-blockers predicted as "out of domain" affected *V. fischeri*.

Exposure to photolysis mixtures of MTL after 16 min and 256 min of photolysis led to a significantly reduced number of healthy and nucleated cells but no significant mammalian cytotoxicity was seen for ATL mixtures (Tables 2, 3). Further the increase of EMA positive events indicated that a significant percentage of cells underwent apoptosis and/or necrosis. This observed toxicity after 16 min–32 min photolysis may be related to the formation kinetics of the MTPs. The relative abundance (A/A0) of the photo-TPs to the PC by means of LC-MS peak area (A/A0 PC) would not be a true indicator of concentration or relevance of that TP in the sample, because ionization rates in the ESI source can be different. The concentration quantification of the individual TPs would require reference standards which were not available in this analysis. The most important feature of the data obtained from this chemical analysis method was the formation kinetics of the TPs and that indicated peak formation of MTPs 238 and MTP 252 at 16–32 min of photolysis.

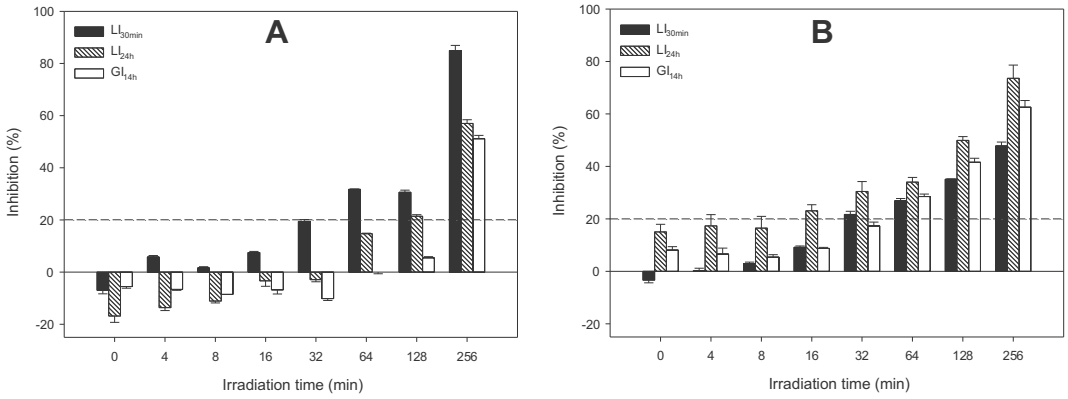

Fig. 3. Growth inhibition ($GI_{14\ h}$) short term luminescence inhibition ($LI_{30\ min}$) and long term luminescence inhibition ($LI_{24\ h}$) in *V. fischeri* caused by exposure to mixtures derived from photolysis of (A) 100 mg/L Atenolol and (B) 400 mg/L Metoprolol tartrate. Samples were twofold diluted in the test media.

As such, these two MTPs may be specifically related to the observed toxicity despite the low relative abundance (A/A0 < 1%) observed in the sample.

3.3. Genotoxic hazard of photolysis mixtures

Investigations of the genotoxic endpoints demonstrated that neither the PCs nor their respective photolytic mixtures can be classified as genotoxic or mutagenic (Tables 2, 3). A statistically significant increase in *umuC* induction was seen in mixtures of both β-blockers after 256 min of irradiation but this was below the threshold to be classified as positive in this test. This may indicate that one or more photo-TPs have potential to be genotoxic but perhaps these TPs did not reach the concentration to exhibit an effect. Interestingly this trend was not observed when using S9-mix for metabolic activation, which would suggest that these transformation products might have undergone biotransformation leading to non-genotoxic metabolites.

The (Q)SAR predictions suggested that a few TPs of both MTL and ATL could present themselves as genotoxic hazards (Table 4, Supplementary S9). ATPs 275, 152, 316, 254, 297, 281, 283, and MTPs 192, 284 were predicted to cause both chromosome aberration (*CA*) *in vitro* and MN formation *in vivo*. In particular, ATP 301 and MTPs 192,

Table 1
Positive alerts for cytotoxicity in *V. fischeri* according to CASE Ultra models prediction for both β-blockers and transformation products.

Case Ultra model	Structural alerts (ID)	Probability of molecules with the alert to be positive (%)	Example structures	TPs
AUA (*V. fischeri* toxicity)	C_2H—C_2H (ID:237)	50	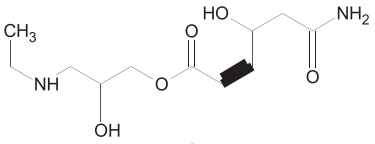	ATP: 275, 232, $301_{a\text{-}f}$ MTP: 318, 192, 234_a
	c:c:cH:c—OH (ID:163)	77.8	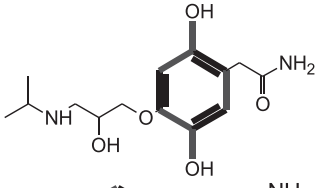	ATP: 299, 316_a
	c:cH:cH:c(:cH)—OH (ID:63)	68.2	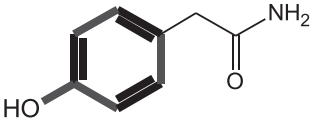	ATP: 152
	c—C_2(—C_2)═O (ID:218)	100	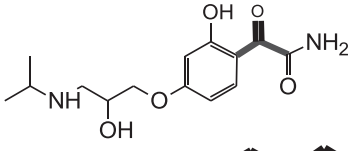	ATP: 297_a
	C_3H_3—C_3H_2—c1:cH:cH:c:cH:cH1 (ID:115)	100	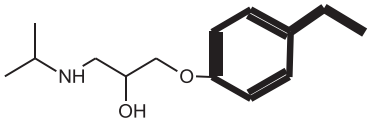	MTP: 238
	C_2—O—C_3H (ID:71)	87.5	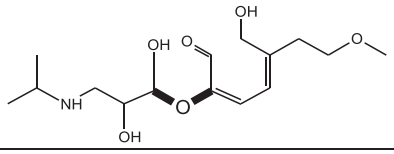	MTP: 318

Table 2
Genotoxicity and cytotoxicity of the mixture derived from the photolysis of 100 mg/L Atenolol (ATL).

Treatment	Dilution factor	Ames				Umu				Mammalian toxicity and *in vitro* micronucleus (MN)			
		Number of revertants				Growth		Induction ratio		Relative survival (%)	EMA + (%)	Hypodiploid (%)	MN (%)
		TA 98		TA 100									
		−S9	+S9	−S9	+S9	−S9	+S9	−S9	+S9				
Millipore water	1.35	2 ± 1	1 ± 1	7 ± 2	3 ± 1								
	1.5					1.00 ± 0.08	0.99 ± 0.04	1.00 ± 0.11	1.00 ± 0.12				
	10									100 ± 7.21	0.34 ± 0.10	0.20 ± 0.02	1.72 ± 0.57
ATL 0 min	1.35	3 ± 2	3 ± 1	5 ± 2	6 ± 6								
	1.5					1.18 ± 0.04	1.07 ± 0.03	0.79 ± 0.08	0.81 ± 0.13				
	10									104.68 ± 0.22	0.33 ± 0.08	0.22 ± 0.07	2.28 ± 1.03
8 min	1.35												
	1.5					1.17 ± 0.07	1.09 ± 0.05	0.83 ± 0.06	0.70 ± 0.05				
	10												
16 min	1.35	1 ± 1	2 ± 2	4 ± 1	1 ± 1								
	1.5					1.09 ± 0.03	1.03 ± 0.01	0.98 ± 0.02	0.78 ± 0.03				
	10									89.30 ± 0.57	0.57 ± 0.03	0.27 ± 0.01	2.21 ± 0.12
32 min	1.35	2 ± 1	1 ± 1	8 ± 3	3 ± 2								
	1.5					1.05 ± 0.04	1.01 ± 0.03	0.97 ± 0.09	0.80 ± 0.09				
	10									69.48 ± 4.53	1.54 ± 0.35	0.38 ± 0.06	1.77 ± 0.04
	20									123.04 ± 6.73	0.22 ± 0.02	0.24 ± 0.07	1.55 ± 0.59
64 min	1.35	3 ± 2	3 ± 1	5 ± 2	3 ± 1								
	1.5					1.06 ± 0.08	1.00 ± 0.05	0.99 ± 0.12	0.73 ± 0.05				
	10									103.15 ± 10.24	0.40 ± 0.25	0.34 ± 0.02	1.99 ± 0.16
128 min	1.35	2 ± 1	2 ± 1	8 ± 1	3 ± 2								
	1.5					0.96 ± 0.09	1.00 ± 0.04	1.05 ± 0.05	0.82 ± 0.16				
	10									103.21 ± 3.26	0.36 ± 0.10	037 ± 0.30	1.48 ± 0.01
256 min	1.35	3 ± 2	1 ± 1	9 ± 2	2 ± 1								
	1.5					0.90 ± 0.05	0.97 ± 0.02	1.37 ± 0.01*	0.99 ± 0.14				
	10									70.51 ± 35.6	5.79 ± 7.5	0.24 ± 0.07	1.93 ± 0.16
	20									116.10 ± 2.67	0.19 ± 0.07	0.28 ± 0.10	1.35 ± 0.01

* $p \leq 0.05$.

318 were predicted to cause both MN induction *in vivo* and bacteria mutagenicity. These genotoxic predictions were based on the presence of several structural alerts.

An α,β-unsaturated aldehyde function in TPs of both β-blockers and the phenylethyl alcohol of MTP 254 served as structural alerts for mutagenic predictions in the Ames test (Table 4). The α,β-unsaturated aldehyde alert contained an electrophilic carbon that can lead to the formation of DNA adducts and is known to cause mutagenicity in Ames test with strain TA 100 and the SOS chromotest (Benigni et al., 2005; Kazius et al., 2005). Although the Leadscope model predicted none of the photo-TPs from either PC to be mutagenic, the Oasis Catalogic model shared similar predictions with the statistical based SALM2013 model for mutagenicity in MTP 192 and MTP 234_a (Table 4, S3). The structural alerts found in the CASE Ultra models were not part of either PC structure, as such, it is possible that some of the TPs from both β-blockers have potential to be mutagenic to one or more of the Ames test strains and should undergo further testing (ICH, 2014).

CA formation was predicted for TPs with an addition of one or more OH groups to the benzene ring (*e.g.* MTP 284_b, ATP 316_b, ATP 281_a) or the inclusion of a carbonyl group (*e.g.* MTP 234_b, ATP 281_a, ATP 254_a) (Table 4). Only the TPs ATP 281_e, ATP 152 and MTP 234_b were predicted to cause *CA* in both Leadscope and CASE Ultra models (Table S2, S3). CASE Ultra model A7S for MN *in vivo* predicted ATL as MN inducing due to the amide structural alert (Table 4). This same structural alert was featured in most of the TPs of ATL predicted as MN inducing and as such may provide enough evidence to consider the TPs of both β-blocker for further testing (Table 4). β-Blockers with their presence of one or more amide group could undergo intragastric nitrosation resulting in genotoxic N-nitroso derivatives (Brambilla and Martelli, 2006; Robbiano et al., 1991). In particular, the *N*-nitroso derivative of

Table 3
Genotoxicity and cytotoxicity of the mixture derived from the photolysis of 400 mg/L Metoprolol tartrate (MTL).

Treatment	Dilution Factor	Ames				Umu				Mammalian toxicity and *in vitro* micronucleus (MN)			
		Number of revertants				Growth		Induction ratio		Relative survival (%)	EMA+ (%)	Hypodiploid (%)	MN (%)
		TA 98		TA 100									
		−S9	+S9	−S9	+S9	−S9	+S9	−S9	+S9				
Millipore water	1.35	1 ± 1	2 ± 2	5 ± 3	4 ± 3								
	1.5					1.00 ± 0.08	0.99 ± 0.04	1.00 ± 0.11	1.00 ± 0.12				
	10									100 ± 7.21	0.34 ± 0.10	0.20 ± 0.02	1.72 ± 0.57
MTL 0 min	1.35	1 ± 1	2 ± 2	4 ± 2	2 ± 2								
	1.5					1.06 ± 0.02	1.05 ± 0.03	0.93 ± 0.09	0.76 ± 0.07				
	40									110.45 ± 0.49	0.34 ± 0.06	0.16 ± 0.01	1.83 ± 0.71
8 min	1.35												
	1.5					1.01 ± 0.05	1.02 ± 0.03	0.95 ± 0.09	0.79 ± 0.07				
	40									109.11 ± 15.067	0.47 ± 0.16	0.18 ± 0.08	1.92 ± 0.80
16 min	1.35	2 ± 2	1 ± 1	7 ± 3	5 ± 3								
	1.5					0.96 ± 0.03	1.02 ± 0.04	1.01 ± 0.02	0.70 ± 0.12				
	40									***46.32 ± 4.02****	***5.25 ± 1.37****	0.28 ± 0.12	4.27 ± 2.00
	80									109.60 ± 3.31	0.18 ± 0.00	0.19 ± 0.01	1.70 ± 0.36
32 min	1.35	1 ± 1	1 ± 1	5 ± 3	5 ± 5								
	1.5					0.97 ± 0.02	1.04 ± 0.03	1.04 ± 0.04	0.85 ± 0.15				
	40									111.04 ± 2.05	0.32 ± 0.02	0.18 ± 0.02	2.30 ± 0.42
64 min	1.35	2 ± 1	1 ± 2	5 ± 2	5 ± 3								
	1.5					0.98 ± 0.01	0.97 ± 0.00	1.10 ± 0.11	0.70 ± 0.10				
	40									116.55 ± 19.82	0.90 ± 0.72	0.15 ± 0.06	1.59 ± 0.14
128 min	1.35	2 ± 1	3 ± 2	5 ± 2	5 ± 2								
	1.5					0.92 ± 0.07	0.99 ± 0.02	1.13 ± 0.02	0.78 ± 0.04				
	40									71.35 ± 13.47	2.50 ± 1.61	0.26 ± 0.07	2.92 ± 0.38
	80									107.06 ± 1.01	0.13 ± 0.02	0.15 ± 0.04	1.12 ± 0.11
256 min	1.35	1 ± 1	1 ± 1	7 ± 2	4 ± 2								
	1.5					0.93 ± 0.09	0.94 ± 0.04	1.25 ± 0.15*	0.91 ± 0.16				
	40									***33.79 ± 3.78****	***12.11 ± 1.86****	0.39 ± 0.19	5.30 ± 2.40
	80									113.95 ± 9.12	0.17 ± 0.05	0.17 ± 0.04	1.42 ± 0.42

* $p \leq 0.05$, *Bold and italic* indicates statistical significant values that can be classified as positive based on test criteria defined in Material and methods.

ATL induced MN formation *in vitro* in rat hepatocytes (Martelli et al., 1994; Robbiano et al., 1991). Other TPs such as ATP 152 and ATP 316_c with more than one OH group added to the benzene ring and the longer side chain of ATP 152 and MTP 284_b were also structural alerts for MN induction *in vivo* in CASE Ultra model A7S

It should be taken into account that (Q)SAR predictions are also not definitive toxicity assessment tools but merely provide an estimate that may or may not be the best for even well evaluated models (European Commission, 2003). Moreover, the QSAR models applied for these unknown chemicals illustrated shortcomings such as the presence of undefined structural parts *e.g.* ethanolamines in the models and the absence of effective concentration predictions. Mixture interferences (such as antagonism), the presence of relevant TPs in non-effective concentrations and the use of only a few test strains (in the Ames test) or cell lines may have contributed to the deviations between the observed and predicted mutagenic or genotoxic activity in the photolysis mixtures. Moreover, no *in vivo* testing was performed to be compared with the *in vivo* prediction models that would account pharmacokinetics in the animals. However, the observed increase in *umuC* induction might indicate that there could be photo-TPs with genotoxic potential

Table 4
Positive alerts for genotoxicity according to CASE Ultra model predictions for both β-blockers and transformation products.

Endpoint	Case Ultra model	Structural alerts (ID)	Probability of molecules with the alert to be positive (%)	Example structures	TPs
CA	A7U	C_2H—C(—O)═O (ID:100)	75	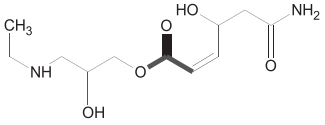	ATP: 275
		C_3H_2—C_2(—C_3H_2)═O (ID:376)	100	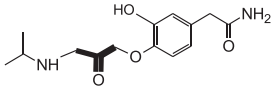	ATP: $281_{a–c}$ MTP: 234_b
		c-C_2H═O (ID:91)	87.5	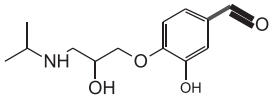	ATP: $254_{a,b}$, 238
		c:cH:cH:c:c—OH (ID:343)	61.5	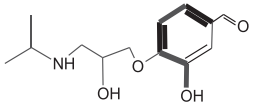	ATP: $254_{a,b}$, $297_{a,b}$, $281_{a,b}$, $283_{a,b}$, 316_b MTP: $284_{a,b}$
		c:cH:c(—OH):c:c (ID:11)	70.6	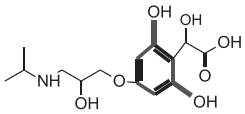	ATP: 316_c
		cH:cH:cH:c—O (ID:113)	71	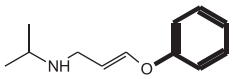	MTP: 192
	A7V	C_2H—C_2═O (ID:20)	70.6	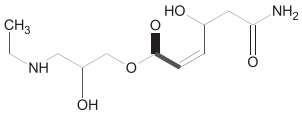	ATP: 275
		cH:cH:c(—OH):cH:cH (ID:128)	75	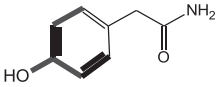	ATP: 152
		c:c:c(:cH)—OH (ID:37)	68.8	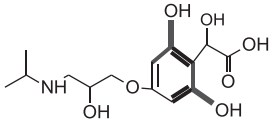	ATP: 316_c
		C_2—C_3H_2—O (ID:32)	83.3	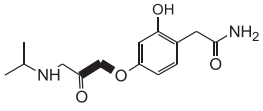	ATP: $281_{a–c,e}$ MTP: 234_b
MN *in vivo*	A7S	C_2—N_3H_2 (ID:4)	72.5	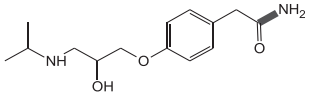	ATL ATP: 275, 299, 223, 152, $297_{a,b}$, $281_{a–e}$, $283_{a–g}$, $301_{a–f}$
		cH:cH:c(—OH):cH:cH (ID:195)	62.5	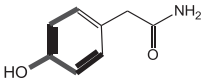	ATP: 152
		cH:cH:c(—O—C_3H_2—C_3H(—OH)—C_3H_2—N_3H—C_3H(—C_3H_3)—C_3H_3):c:cH (ID:240)	100	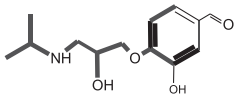	ATP: 254_b, 283_b MTP: 284_b
		c:cH:c:c:c—OH (ID:10)	73.3	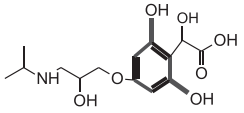	ATP: 316_c
Bacteria mutagenicity	GTI_A7B	C_2—C_2H═O (ID:936)	81.3	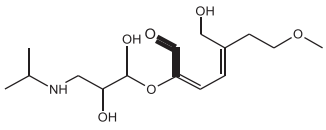	ATP: $301_{a,f}$ MTP: 318
		C_2H—C_2H═O	80		ATP: $301_{b,c,e}$

Table 4 (*continued*)

Endpoint	Case Ultra model	Structural alerts (ID)	Probability of molecules with the alert to be positive (%)	Example structures	TPs
		(ID:886)		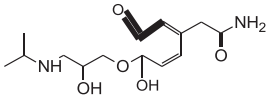	
	SALM2013	C_2H—O (ID:1213)	72.7	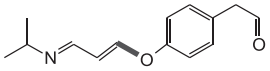	ATP: 232 MTP: 192, 234_a
		C_2—C_2H═O (ID:922)	90.5	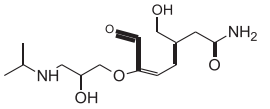	ATP: $301_{a,f}$ MTP: 318
		OH—C_3H_2—C_3H_2—c1:cH:cH:c:cH:cH1 (ID:2542)	100	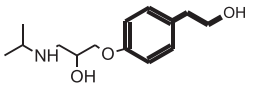	MTP: 254

A7S: MN *in vivo*; A7U: Chromosome aberration composite *in vitro*; A7V: Chromosome aberration in CHO cells; SALM2013: Mutagenicity in *Salmonella* (improved); GT1_A7B: Mutagenicity for 7 major strains of *S. typhimurium*.

in some of the photolysis mixtures for both β-blockers. MTP 284 and MTP 254 were predicted genotoxic and mutagenic, respectively, and were identified also as intermediates found in the genotoxic oxidative samples of Šojić et al. (2012). As such, suspected genotoxic TPs should be further assessed to allow a clear classification especially since QSAR have predicted some toxic structural alerts found in the PC as well as those novel to the TPs. A recommendation for further work on genotoxicity would include subjecting the mixtures to other strains in the Ames test and the use of other cell lines namely, hepatocytes for *CA*/MN analysis.

3.4. Ascertaining photo-TPs of concern for further risk assessment

This study was based on a simplified laboratory simulation of the treatment of a single pharmaceutical. The initial PC concentrations were extremely high for the mixtures to be environmentally relevant but were necessary for identifying hazards using standard *in vitro* bioassays geared at investigating (changes in) the mechanism of toxicity. Moreover, the observed mixture toxicity would be specific to the mixture of photo-TPs generated, the TP concentrations, the type and duration of light exposure, as well as PC concentration. The initial concentration, in particular, can affect both the types of TPs formed and their kinetics of formation. The photolysis mixture of 100 mg/L ATL demonstrated faster primary elimination and led to formation of several intermediate TPs when compared to the photolysis of 400 mg/L MTL. Moreover, photolysis of 10 mg/L MTL led to identification of six more TPs that increased in abundance with irradiation time (Rastogi et al., 2014b). Nevertheless, there can be a greater chance that the same TPs can be generated regardless of the initial concentrations but under same photolysis conditions (Mahmoud et al., 2014; Rastogi et al., 2014a). In fact, Piram et al. (2008) have demonstrated specifically for β-blockers that their photodegradation products can be demonstrated correctly in laboratory setting with higher concentration than environmentally relevant. Further, similar products can be found whether the photolysis was done in pure water or in sewage treatment plant effluent (Piram et al., 2008). Several of the TPs (such as MTP 134, MTP 226, MTP 254, ATP 254, ATP 281) identified here were also proposed in studies under more environmentally relevant conditions using simulated sunlight (Ji et al., 2012; Liu et al., 2009; Romero et al., 2011).

The advantage of this initial hazard screening scheme is the possibility to generate TPs in higher amounts and to demonstrate effects using *in vitro* bioassays without the need to concentrate or alter the mixtures. The inclusion of the QSAR modelling provided an additional tool to understand the toxic properties of these photo-TPs. As a result, some of the photo-TPs were predicted toxic with structural moiety not present in the PC and therefore may present greater hazards. Certainly, the whole mixture toxicity revealed that the mixtures were more cytotoxic. Notably, ATPs 275, 152, 301 and MTP 192 are expected to cause bioluminescence inhibition in *V. fischeri*, bacterial mutagenicity and *CA*/MN induction.

The coupling of the toxicity screening with the expected persistency and bioaccumulation properties of the TPs can further propose those that may be considered for human and/or environmental related risk assessment. All the photo-TPs were expected to be soluble in water and have low bioconcentration potential (Table 5, Supplementary S10). However, there were a few TPs that were expected to behave differently to the PC by having higher Log Kow between 2 and 4 attributed to chemicals that tend to absorb well through the skin (ATP: 275, 232; MTPs: 192, 234, 238) (Table 5, Supplementary S10). Experimentally, Rastogi et al. (2014b, 2015) demonstrated that several of these photo-TPs could undergo bio-transformation and therefore could reduce their concentrations in the aquatic environment. TPs expected to have high bioaccumulation, persistency and toxicity were proposed to be of higher risk to the environment (Belfroid et al., 1998; Escher and Fenner, 2011). As such, a combination of the *in silico* predictions and experiments have led to the proposal of the photo-TPs that in particular did not undergo microbial biotransformation and have the potential to be more toxic than the PC. These photo-TPs, namely ATP: 275, 232 and MTP: 192, 234, 210 should therefore be the priority TPs for further investigations on single substance toxicity (cytotoxicity and genotoxicity) and exposure based analyses (analytical profile, environmental occurrence, partition, persistency) (Table 5). Notwithstanding, the ATPs that would be expected to share similar hazards to ATL need to be investigated as well. As demonstrated by the enhanced toxicity of our photolysis mixture, in depth mixture cytotoxicity assessment with aquatic organisms would be advocated.

4. Conclusions

Our findings clearly showed that photolysis of the β-blockers ATL and MTL can principally lead to the formation of mixtures with increased cytotoxicity. Moreover there was some first predictions that genotoxic TPs also might be formed during photolysis of the two β-

Table 5
Relative hazard of photo-TPs to their parent compound.

Chemical	Physico-chemical properties[a]			Bio-transformation potential[b]	Toxicity predictions[c]					Relative Hazard	Interpretation
	Solubility in Water	Hydrophilicity	Bio-concentration potential		Cytotoxicity[d]	Genotoxicity		Mutagenicity			
					V. fischeri	Chromosome aberration	MN *in vivo*	Bacteria	Mammalian		
Atenolol											
ATL	Very soluble	Hydrophillic	low	No	OD	−	+	−	−		
ATP 275	=	<	=	=	+ (class 3)	+	+	−	+	>	More mobile in the aquatic system greater ability to absorb through the skin and may cause cytotoxicity and genotoxic to bacteria and mammalian cells
ATP 254	=	=	=	=	OD	+	+	−	−	=	
ATP 232	<	<	=	=	+ (class 3)	OD	OD	+	−	>	Greater risk for cytotoxicity and mutagenicity with and greater ability to absorb through the skin and no bio-transformation potential
ATP 316	=	=	=	N.D.	−/OD	+	+	−	−	=/<	
ATP 297	<	=	=	=	+ (class 3)	+	+	−	−	=	
ATP 210	=	=	=	=	−	+	OD	−	−	=	
ATP 152	=	=	=	>	+ (class 3)	+	+	−	+	<	Can be biotransformed in the environment
ATP 301	=	=	=	>	+ (class 3)	−	+	+	−	<	
ATP 299	<	=	=	>	−	+	+	−	−	<	
ATP 281	<	=	=	>	OD	+	+	−	+	<	
ATP 283	<	=	=	>	OD	−	+	−	−	<	
Metoprolol											
MTL	Soluble	Less hydrophillic with potential to absorb through the skin	Low	No	OD	−	−	−	−		
MTP 192	>	=	=	=	+ (class 1/3)	+	OD	−	−	>	Greater risk for cytotoxicity and mutagenicity with no bio-transformation potential
MTP 234	<	=	=	=	+ (class 1/3)	+	−	+	+	>	Greater risk for cytotoxicity and mutagenicity with no bio-transformation potential
MTP 270	>	>	=	=	OD	−	−	−	−	<	
MTP 210	>	>	=	=	−	+	OD	−	−	>	More mobile in the aquatic system with no bio-transformation potential and slight evidence of Chromosome aberration in mammalian cells.
MTP 254	>	=	=	>	OD	−	−	+	−	<	Can be biotransformed in the environment
MTP 318	>	>	=	>	+ (class 1/3)	−	OD	+	−	<	
MTP 238	=	=	=	>	+ (class 1)	−	−	−	−	<	

>, =, <: the property of the photo-TP is predicted to be greater, similar or less than respectively to the parent compound.
−:Negative for activity; +: Positive for activity; OD: out of domain of model predictions; N.D.: Not detected.
[a] Physico-chemical properties predicted by EPI Suite software KOWWIN v1.68 model. Property of the parent compound (ATL or MTL) interpreted based on EPA (2012).
[b] Bio-transformation potential derived experimentally using Close bottle test, OECD 301D and Manometric respiratory test, OECD 301F (Rastogi et al., 2014b, 2015).
[c] Summary of toxicity predictions using the battery of *in-silico* software described in Material and methods.
[d] Class of the chemical based on Verhaar et al. (1992). Class 1: Narcosis chemicals Class 3: Reactive chemicals.

blockers. The overarching repercussion from photolysis of β-blockers would be that it can generate toxic mixtures. Because of the limited sensitivity of (bio)analytical methods, the initial identification and characterization of TPs should be conducted at comparatively high concentrations to take all possible TPs into consideration. On the other hand, the high complexity of resulting photolytic mixtures caused some difficulties in identifying specific TPs of concern. (Q)SAR analysis has enabled the postulation of a few TPs that may have contributed to

the observed toxicity but the lack of their analytic standards inhibited their further characterization. The same accounts for the investigation of the environmental relevance of suggested toxic TPs that would demand targeted analytical procedure. The applied scheme described here is useful to characterize mixture toxicity in comparison to the PC and to prioritize the TPs for further risk analysis.

Acknowledgement

The authors are grateful for the financial support from the German Ministry of Education and Research (NanoPharm, Project No. 03X0094C) and the Innovations-Inkubator Lüneburg (Teilmaßnahme 1.4). The authors also acknowledge Multicase Inc. and Leadscope Inc. for kindly providing the CASE Ultra and Leadscope QSAR software, respectively. The authors are thankful for the assistance of Paula Queiroz de Aquino and Stefanie Hinz in the experimental work.

Appendix A. Supplementary data

Supplementary data to this article can be found online at http://dx.doi.org/10.1016/j.scitotenv.2016.10.242.

References

Backhaus, T., Altenburger, R., Boedeker, W., Faust, M., Scholze, M., Grimme, L.H., 2000. Predictability of the toxicity of a multiple mixture of dissimilarly acting chemicals to *Vibrio fischeri*. Environ. Toxicol. Chem. 19 (9), 2348–2356.

Belfroid, A.C., van Drunen, M., Beek, M.A., Schrap, S.M., van Gestel, C.A., van Hattum, B., 1998. Relative risks of transformation products of pesticides for aquatic ecosystems. Sci. Total Environ. 222 (3), 167–183.

Benigni, R., Conti, L., Crebelli, R., Rodomonte, A., Varí, M.R., 2005. Simple and alpha,beta-unsaturated aldehydes: correct prediction of genotoxic activity through structure-activity relationship models. Environ. Mol. Mutagen. 46 (4), 268–280.

Brambilla, G., Martelli, A., 2006. Genotoxicity and carcinogenicity studies of antihypertensive agents. Mutat. Res. 612 (2), 115–149.

Bryce, S.M., Shi, J., Nicolette, J., Diehl, M., Sonders, P., Avlasevich, S., Raja, S., Bemis, J.C., Dertinger, S.D., 2010. High content flow cytometric micronucleus scoring method is applicable to attachment cell lines. Environ. Mol. Mutagen. 51 (3), 260–266.

Četojević-Simin, D.D., Armaković, S.J., Šojić, D.V., Abramović, B.F., 2013. Toxicity assessment of metoprolol and its photodegradation mixtures obtained by using different type of TiO_2 catalysts in the mammalian cell lines. Sci. Total Environ. 463–464, 968–974.

Chakravarti, S.K., Saiakhov, R.D., Klopman, G., 2012. Optimizing predictive performance of CASE Ultra expert system models using the applicability domains of individual toxicity alerts. J. Chem. Inf. Model. 52 (10), 2609–2618.

Cleuvers, M., 2005. Initial risk assessment for three beta-blockers found in the aquatic environment. Chemosphere 59 (2), 199–205.

Contardo-Jara, V., Pflugmacher, S., Nützmann, G., Kloas, W., Wiegand, C., 2010. The beta-receptor blocker metoprolol alters detoxification processes in the non-target organism *Dreissena polymorpha*. Environ. Pollut. 158 (6), 2059–2066.

EPA, 2012. Chapter 5: estimating physical/chemical and environmental fate properties with EPI Suite™. Sustainable Futures/P2 Framework Manual. US Environmental Protection Agency, Office of Chemical Safety and Pollution Prevention EPA-748-B12-001, Washington. https://www.epa.gov/sustainable-futures/sustainable-futures-p2-framework-manual (accessed on 10/2016).

Escher, B.I., Fenner, K., 2011. Recent advances in environmental risk assessment of transformation products. Environ. Sci. Technol. 45 (9), 3835–3847.

Escher, B.I., Bramaz, N., Richter, M., Lienert, J., 2006. Comparative ecotoxicological hazard assessment of beta-blockers and their human metabolites using a mode-of-action-based test battery and a QSAR approach. Environ. Sci. Technol. 40 (23), 7402–7408.

European Commission, 2003. Technical Guidance Document on Risk Assessment Part III: Chapter 4: Use of (Quantitative) Structure Activity Relationships ((Q)SARs), Use Categories, Risk Assessment Report Format. European Commission, Luxembourg. https://echa.europa.eu/documents/10162/16960216/tgdpart3_2ed_en.pdf (accessed on 12/2014).

Hapeshi, E., Achilleos, A., Vasquez, M.I., Michael, C., Xekoukoulotakis, N.P., Mantzavinos, D., Kassinos, D., 2010. Drugs degrading photocatalytically: kinetics and mechanisms of ofloxacin and atenolol removal on titania suspensions. Water Res. 44 (6), 1737–1746.

ICH, 2014. Assessment and control of DNA reactive (mutagenic) impurities in pharmaceuticals to limit potential carcinogenic risk M7. International Conference on Harmonisation of Technical Requirements for Registration of Pharmaceuticals for Human Use (ICH), fourth ed.http://www.ich.org/products/guidelines/multidisciplinary/multidisciplinary-single/article/assessment-and-control-of-dna-reactive-mutagenic-impurities-in-pharmaceuticals-to-limit-potential.html (accessed 08/2014).

ISO, 2000. ISO 13829: Water Quality-determination of the Genotoxicity of Water and Waste Water Using Umu Test. International Organization for Standardization (ISO), Geneva.

Ji, Y., Zeng, C., Ferronato, C., Chovelon, J.-M., Yang, X., 2012. Nitrate-induced photodegradation of atenolol in aqueous solution: kinetics, toxicity and degradation pathways. Chemosphere 88 (5), 644–649.

Kazius, J., McGuire, R., Bursi, R., 2005. Derivation and validation of toxicophores for mutagenicity prediction. J. Med. Chem. 48 (1), 312–320.

Klopman, G., Stuart, S.E., 2003. Multiple computer-automated structure evaluation study of aquatic toxicity. III. *Vibrio fischeri*. Environ. Toxicol. Chem. 22 (3), 466–472.

Küster, A., Alder, A.C., Escher, B.I., Duis, K., Fenner, K., Garric, J., Hutchinson, T.H., Lapen, D.R., Péry, A., Römbke, J., Snape, J., Ternes, T., Topp, E., Wehrhan, A., Knacker, T., 2010. Environmental risk assessment of human pharmaceuticals in the European Union: a case study with the β-blocker atenolol. Integr. Environ. Assess. Manag. (Suppl. 6), 514–523.

La Farré, M., Pérez, S., Kantiani, L., Barceló, D., 2008. Fate and toxicity of emerging pollutants, their metabolites and transformation products in the aquatic environment. TrAC. Trends Anal. Chem. 27 (11), 991–1007.

Libralato, G., Ghirardini, A.V., Avezzù, F., 2008. Evaporation and air-stripping to assess and reduce ethanolamines toxicity in oily wastewater. J. Hazard. Mater. 153 (3), 928–936.

Liu, Q.-T., Cumming, R.I., Sharpe, A.D., 2009. Photo-induced environmental depletion processes of beta-blockers in river waters. Photochem. Photobiol. Sci. 8 (6), 768–777.

Mahmoud, W.M.M., Toolaram, A.P., Menz, J., Leder, C., Schneider, M., Kümmerer, K., 2014. Identification of phototransformation products of thalidomide and mixture toxicity assessment: an experimental and quantitative structural activity relationships (QSAR) approach. Water Res. 49, 11–22.

Martelli, A., Allavena, A., Sottofattori, E., Brambilla, G., 1994. Low clastogenic activity in vivo of the N-nitroso derivatives of 5 beta-adrenergic-blocking drugs proved to be potent genotoxins in vitro. Toxicol. Lett. 73 (3), 185–191.

Maszkowska, J., Stolte, S., Kumirska, J., Łukaszewicz, P., Mioduszewska, K., Puckowski, A., Caban, M., Wagil, M., Stepnowski, P., Białk-Bielińska, A., 2014. Beta-blockers in the environment: part I. Mobility and hydrolysis study. Sci. Total Environ. 493, 1112–1121.

Menz, J., Schneider, M., Kümmerer, K., 2013. Toxicity testing with luminescent bacteria—characterization of an automated method for the combined assessment of acute and chronic effects. Chemosphere 93 (6), 990–996.

Okine, L.K., Ioannides, C., Parke, D.V., 1983. Studies on the possible mutagenicity of beta-adrenergic blocker drugs. Toxicol. Lett. 16 (3–4), 167–174.

Piram, A., Salvador, A., Verne, C., Herbreteau, B., Faure, R., 2008. Photolysis of beta-blockers in environmental waters. Chemosphere 73 (8), 1265–1271.

Radjenović, J., Pérez, S., Petrović, M., Barceló, D., 2008. Identification and structural characterization of biodegradation products of atenolol and glibenclamide by liquid chromatography coupled to hybrid quadrupole time-of-flight and quadrupole ion trap mass spectrometry. J. Chromatogr. A 1210 (2), 142–153.

Rastogi, T., Leder, C., Kümmerer, K., 2014a. Qualitative environmental risk assessment of photolytic transformation products of iodinated X-ray contrast agent diatrizoic acid. Sci. Total Environ. 482–483, 378–388.

Rastogi, T., Leder, C., Kümmerer, K., 2014b. Designing green derivatives of β-blocker metoprolol: a tiered approach for green and sustainable pharmacy and chemistry. Chemosphere 111, 493–499.

Rastogi, T., Leder, C., Kümmerer, K., 2015. A sustainable chemistry solution to the presence of pharmaceuticals and chemicals in the aquatic environment – the example of redesigning β-blocker atenolol. RSC Adv. 5 (1), 27–32.

Richard, J., Boergers, A., Vom Eyser, C., Bester, K., Tuerk, J., 2014. Toxicity of the micropollutants bisphenol A, ciprofloxacin, metoprolol and sulfamethoxazole in water samples before and after the oxidative treatment. Int. J. Hyg. Environ. Health 217 (4–5), 506–514.

Richardson, S.D., Ternes, T.A., 2011. Water analysis: emerging contaminants and current issues. Anal. Chem. 83 (12), 4614–4648.

Robbiano, L., Martelli, A., Allavena, A., Mazzei, M., Gazzaniga, G.M., Brambilla, G., 1991. Formation of the N-nitroso derivatives of six beta-adrenergic-blocking agents and their genotoxic effects in rat and human hepatocytes. Cancer Res. 51 (9), 2273–2279.

Roberts, G., Myatt, G.J., Johnson, W.P., Cross, K.P., Blower, P.E., 2000. LeadScope: software for exploring large sets of screening data. J. Chem. Inf. Model. 40 (6), 1302–1314.

Rocco, L., Frenzilli, G., Zito, G., Archimandritis, A., Peluso, C., Stingo, V., 2012. Genotoxic effects in fish induced by pharmacological agents present in the sewage of some Italian water-treatment plants. Environ. Toxicol. 27 (1), 18–25.

Romero, V., De la Cruz, N., Dantas, R.F., Marco, P., Giménez, J., Esplugas, S., 2011. Photocatalytic treatment of metoprolol and propranolol. Catal. Today 161 (1), 115–120.

Saiakhov, R., Chakravarti, S., Klopman, G., 2013. Effectiveness of CASE Ultra expert system in evaluating adverse effects of drugs. Mol. Inf. 32 (1), 87–97.

Scherrer, R.A., Leo, A.J., 2010. Multi-pH QSAR: a method to differentiate the activity of neutral and ionized species and obtain true correlations when both species are involved. Mol. Inf. 29 (10), 687–693.

Šojić, D., Despotović, V., Orčić, D., Szabó, E., Arany, E., Armaković, S., Illés, E., Gajda-Schrantz, K., Dombi, A., Alapi, T., Sajben-Nagy, E., Palágyi, A., Vágvölgyi, C., Manczinger, L., Bjelica, L., Abramović, B., 2012. Degradation of thiamethoxam and metoprolol by UV, O_3 and UV/O_3 hybrid processes: kinetics, degradation intermediates and toxicity. J. Hydrol. 472–473, 314–327.

Télez, M., Martínez, B., Criado, B., Lostao, C.M., Penagarikano, O., Ortega, B., Flores, P., Ortiz-Lastra, E., Alonso, R.M., Jiménez, R.M., Arrieta, I., 2000. In vitro and in vivo evaluation of the antihypertensive drug atenolol in cultured human lymphocytes: effects of long-term therapy. Mutagenesis 15 (3), 195–202.

Toolaram, A.P., Kümmerer, K., Schneider, M., 2014. Environmental risk assessment of anticancer drugs and their transformation products: a focus on their genotoxicity

characterization-state of knowledge and short comings. Mutat. Res. Rev. Mutat. Res. 760, 18–33.
van den Brandhof, E., Montforts, M., 2010. Fish embryo toxicity of carbamazepine, diclofenac and metoprolol. Ecotoxicol. Environ. Saf. 73 (8), 1862–1866.
Verhaar, H.J., van Leeuwen, C.J., Hermens, J.L., 1992. Classifying environmental pollutants. Chemosphere 25 (4), 471–491.
Verlicchi, P., Al Aukidy, M., Zambello, E., 2012. Occurrence of pharmaceutical compounds in urban wastewater: removal, mass load and environmental risk after a secondary treatment—a review. Sci. Total Environ. 429, 123–155.

Publikation 7

Transformation products in the water cycle and the unsolved problem of their proactive assessment: a combined *in vitro/in silico* approach

Menz, J., Toolaram, A., Leder, C., Olsson, O., Kümmerer, K., Schneider, M.

(2017)

Environment International 98, 171-180

DOI:10.1016/j.envint.2016.11.003

Environment International 98 (2017) 171–180

Contents lists available at ScienceDirect

Environment International

journal homepage: www.elsevier.com/locate/envint

Full length article

Transformation products in the water cycle and the unsolved problem of their proactive assessment: A combined *in vitro*/*in silico* approach

Jakob Menz, Anju Priya Toolaram, Tushar Rastogi, Christoph Leder, Oliver Olsson, Klaus Kümmerer *, Mandy Schneider

Sustainable Chemistry and Material Resources, Institute of Sustainable and Environmental Chemistry, Leuphana University Lüneburg, Scharnhorststr. 1/C13, DE-21335 Lüneburg, Germany

ARTICLE INFO

Article history:
Received 28 July 2016
Received in revised form 19 October 2016
Accepted 3 November 2016
Available online 15 November 2016

Keywords:
Emerging contaminant
Micropollutant
Propranolol
Hazard assessment
Risk assessment
(Q)SAR

ABSTRACT

Transformation products (TPs) emerging from incomplete degradation of micropollutants in aquatic systems can retain the biological activity of the parent compound, or may even possess new unexpected toxic properties. The chemical identities of these substances remain largely unknown, and consequently, the risks caused by their presence in the water cycle cannot be assessed thoroughly. In this study, a combined approach for the proactive identification of hazardous elements in the chemical structures of TPs, comprising analytical, bioanalytical and computational methods, was assessed by the example of the pharmaceutically active micropollutant propranolol (PPL). PPL was photo-transformed using ultraviolet (UV) irradiation and 115 newly formed TPs were monitored in the reaction mixtures by LC-MS analysis. The reaction mixtures were screened for emerging effects using a battery of *in vitro* bioassays and the occurrence of cytotoxic and mutagenic activities in bacteria was found to be significantly correlated with the occurrence of specific TPs during the treatment process. The follow-up analysis of structure-activity-relationships further illustrated that only small chemical transformations, such as the hydroxylation or the oxidative opening of an aromatic ring system, could substantially alter the biological effects of micropollutants in aquatic systems. In conclusion, more efforts should be made to prevent the occurrence and transformation of micropollutants in the water cycle and to identify the principal degradation pathways leading to their toxicological activation. With regard to the latter, the judicious combination of bioanalytical and computational tools represents an appealing approach that should be developed further.

1. Introduction

Due to the ubiquitous presence in the water cycle, micropollutants can undergo different biotic and abiotic transformation processes along their lifecycle that often lead to the formation of uncharacterized transformation products (TPs). In fact, the presence of numerous active pharmaceutical ingredients along with some of their known TPs in surface water and ground water was recently reported (López-Serna et al., 2012, 2013). However, the chemical identities of most TPs in the aquatic cycle remain still unknown, and therefore, the risk due to their presence cannot be assessed thoroughly (Evgenidou et al., 2015; Fatta-Kassinos et al., 2011; Kosjek and Heath, 2008; Zwiener, 2007). In response to this problem, the proactive assessment of TPs, *i.e.* the characterization of degradation products even before the parent compound comes into use, was repeatedly demanded to be more consequently implemented into the existing regulations for marketing authorization of chemical products (*e.g.* Fenner et al., 2002; Schmitt-Jansen et al., 2007).

The transformation of micropollutants in the aquatic environment is triggered by hydrolysis, photochemical reactions and microbial processes (Längin et al., 2008; Kümmerer, 2008; Packer et al., 2003; Arnold and McNeill, 2007). Beyond that, some water treatment processes, such as the treatment of wastewater using advanced oxidation processes (AOPs) or the disinfection of drinking water by chlorination, ozonation or ultraviolet (UV) irradiation, are well-established pathways for the emergence of TPs (Canonica et al., 2008; Kümmerer et al., 2016). It is known that environmental behavior and hazardous properties of TPs can strongly differ from the parent compounds (DellaGreca et al., 2003; Escher and Fenner, 2011; Garcia-Käufer et al., 2012; Li et al., 2016; Schulze et al., 2010). Moreover, there are strong indications that TPs of pharmaceuticals can remain pharmacologically active (Halling-Sørensen et al., 2002; Rastogi et al., 2015). As a consequence, different strategies for the identification of potentially hazardous TPs

Abbreviations: 4-OH PPL, 4-Hydroxypropranolol; 5-OH PPL, 5-Hydroxypropranolol; 7-OH PPL, 7-Hydroxypropranolol; AOP, Advanced oxidation process; ANOVA, Analysis of variance; DAD, Diode array detector; EDA, Effect-directed analysis; ESI-IT-MS, Electrospray ionization ion trap mass spectrometry; IR, Induction ratio; LC-MS, Liquid chromatography-mass spectrometry; LBT, Luminescent bacteria test; NPOC, Non-purgeable organic carbon; PPL, Propranolol; (Q)SAR, (Quantitative) structure-activity-relationships; ThEL, Theoretical exposure level; TP, Transformation product; UV, Ultraviolet.

* Corresponding author.
E-mail addresses: jakob.menz@leuphana.de (J. Menz), anjutoolaram@yahoo.com (A.P. Toolaram), tushar.rastogi@leuphana.de (T. Rastogi), cleder@leuphana.de (C. Leder), oliver.olsson@leuphana.de (O. Olsson), klaus.kuemmerer@leuphana.de (K. Kümmerer), mandy.schneider@leuphana.de (M. Schneider).

http://dx.doi.org/10.1016/j.envint.2016.11.003
0160-4120/

have been suggested and applied in the recent past. These approaches can be broadly categorized as exposure-driven or effect-driven and have already been extensively reviewed elsewhere (*e.g.* Escher and Fenner, 2011; Fatta-Kassinos et al., 2011; Toolaram et al., 2014; Zonja et al., 2014).

The comprehensive risk assessment of TPs is still impeded by the current lack of standardization in the experimental design (Fatta-Kassinos et al., 2011; Toolaram et al., 2014). Moreover, only in a few cases was it possible to clearly attribute the toxicity of treated mixtures to any of the identified TPs (Escher and Fenner, 2011; Fatta-Kassinos et al., 2011). This was mainly achieved by the coupling of laboratory-scale treatment processes with effect-directed analysis (EDA), which is usually based on a combination of biotesting, fractionation procedures and chemical analytical methods (Brack, 2003). As an example, several toxic photoproducts of anthracene were identified using simulated sunlight irradiation in combination with EDA (Brack et al., 2003). In another study, EDA was used to identify a phytotoxic photo-transformation product of diclofenac (Schulze et al., 2010). Moreover, the toxicity of TPs in treated mixtures was assessed by correlating the time course of the relative TP concentration with the observed mixture effect during the experiment. Using this simple screening method, phytotoxic TPs were tentatively identified in an irradiated mixture of diclofenac (Schmitt-Jansen et al., 2007).

Even if a toxic TP can be successfully identified in a treated mixture, additional research is necessary to elucidate the responsible chemical structural elements and reaction pathways. (Quantitative) structure-activity-relationships ((Q)SARs) are increasingly used to identify hazardous structural features *in silico*, especially in cases where chemicals are not experimentally accessible, which holds true for most TPs. Consequently, (Q)SAR methodologies were recently suggested to be used for the risk assessment of pharmaceuticals and their TPs (Rastogi et al., 2014; Toolaram et al., 2014). Moreover, the recently established ICH M7 guidelines for the assessment of DNA reactive impurities in pharmaceuticals represent a significant advancement in the regulatory acceptance of (Q)SAR models (Barber et al., 2015). These recent developments could indicate new ways for the assessment and regulation of TPs in the water cycle.

In the light of the aspects discussed above, a combined approach for the proactive identification of hazardous elements in the chemical structures of TPs, comprising basic analytical, bioanalytical and computational methods, was explored by the example of the pharmaceutically active micropollutant propranolol (PPL). The nonselective beta-adrenergic receptor-blocking agent was chosen as a model compound for the following reasons:

i. PPL was detected at concentrations up to 373 ng L^{-1} in WWTP effluents, up to 590 ng L^{-1} in river water, and at average concentrations of 1.8 ng L^{-1} in ground waters (Kostich et al., 2014; Santos et al., 2010; Ternes, 1998; Vulliet and Cren-Olivé, 2011).
ii. The presence in ground water of 4-hydroxypropranolol (4-OH PPL), a pharmacologically active human metabolite and TP of PPL, was recently reported (López-Serna et al., 2013).
iii. PPL was reportedly susceptible to phototransformation during technical treatment processes using UV light and also at environmentally relevant conditions using sunlight or simulated sunlight (Andreozzi et al., 2003; Dantas et al., 2010; Liu and Williams, 2007; Peng et al., 2014).
iv. The photochemical reactions of PPL have been intensely researched and with that the formation of a large number of TPs with mainly unknown properties was revealed (Liu and Williams, 2007; Rastogi et al., 2015; Santiago-Morales et al., 2013; Sortino et al., 2002).

The few available studies on the biological effects that could emerge from transformation of PPL do not allow a concluding evaluation of the responsible degradation pathways. Liu et al. (2009b) showed a reduction of ecotoxicity during simulated sunlight-driven photolysis of 10 mg L^{-1} PPL using bioassays with algae and rotifers. Similarly, irradiation of 25 mg L^{-1} PPL with simulated sunlight resulted in a moderate reduction of the cytotoxicity in bacteria (Santiago-Morales et al., 2013). In contrast, Peng et al. (2014) found evidence for the occurrence of intermediate products with increased cytotoxicity in bacteria during UV photolysis of PPL, but the chemical identity of these TPs was not further elucidated. Interestingly, an increasing toxicity to bacteria was also reported after ozonation of PPL at 100 mg L^{-1} and this time three intermediate TPs (m/z $[M + H]^+$ 292, 266 and 282) were identified in the reaction mixture (Dantas et al., 2011). Moreover, it was found that PPL had the ability to induce hemolysis of red blood cells and DNA cleavage upon UVA irradiation (Sortino et al., 2002). Consequently, there are strong indications for the emergence of cytotoxic and genotoxic TPs during UV photolysis of PPL, but there is still insufficient knowledge on the underlying structure-activity-relationships. This impedes the deduction of principle transformation pathways for the toxicological activation of PPL and other related compounds.

This study was not designed to accurately simulate the fate of a compound under specific conditions, but rather (i) to obtain new information on the principle reaction pathways possibly leading to the emergence of hazardous TPs in aquatic environments and (ii) to assess the additional value of a combined *in vitro/in silico* toxicity approach to the proactive identification of potentially hazardous TPs. In order to attain these objectives, a synthetic mixture of TPs was generated from PPL using UV irradiation. This reaction mixture was screened for potentially hazardous TPs using liquid chromatography-mass spectrometry (LC-MS) in combination with selected *in vitro* bioassays for cytotoxic and genotoxic activities. Finally, established (Q)SAR models were used for the *in silico* analysis of structure-activity-relationships in order to attribute the observed effects to specific chemical structure elements.

2. Material and methods

2.1. Chemicals

(±)-Propranolol hydrochloride (CAS 318-96-9) was purchased from Sigma-Aldrich (St. Louis, USA). (±)-4-Hydroxypropranolol hydrochloride (CAS 10476-53-6), (±)-5-hydroxypropranolol hydrochloride (CAS 62117-35-5) and (±)-7-hydroxypropranolol (CAS 81907-81-5) were purchased from Santa Cruz Biotechnology, Inc. (Dallas, USA). All solutions were prepared in ultrapure water.

2.2. Photolysis of propranolol

A high initial concentration of 338 μmol L^{-1} (100 mg L^{-1}) PPL hydrochloride was used for the characterization of TPs and the determination of organic carbon removal, taking into account the limited sensitivity of the analytical instruments and the selected bioassays. An additional experiment was conducted with an optically dilute solution (3.4 μmol L^{-1}) to determine the quantum yield (Φ) and to confirm that principal degradation pathways were not altered by the usage of a high initial concentration. The photolysis was conducted with an initial volume of 800 mL using a medium pressure mercury lamp (TQ150, UV Consulting Peschl, Mainz, Germany) in a cylindrical immersion-type batch reactor with an ilmasil quartz immersion tube. The reaction mixture was stirred constantly and the temperature was maintained between 17 and 20 °C. A sampling volume of 20 mL was collected before the treatment (0 min) and after 2, 4, 8, 16, 32, 64, 128 and 256 min of irradiation. The pH and the peroxide concentration in the photolysis mixture were monitored immediately after sampling. Peroxide was determined semi-quantitatively using MQuant™ peroxide test strips (Merck KGaA, Darmstadt, Germany). The non-purgeable organic carbon (NPOC) was measured directly after the treatment process using a Shimadzu TOC-VCPN analyzer. The photolysis samples for chromatographic analysis and *in vitro* testing were initially stored at −20 °C

for a maximum of 14 days, following sterile filtration (PES, 0.22 μm), aliquoting and storage at −150 °C until further usage. The reaction mixtures of two independent treatments were pooled before sterile filtration to obtain a sufficient volume for all genotoxicity and mutagenicity assays. The photon flux and the quantum yield were determined as described in section S1 of the Supporting Information (SI).

2.3. Chromatographic analysis

The elimination of PPL and the relative abundance of newly formed compounds in the photolysis mixture were monitored by liquid chromatography in combination with electrospray ionization ion trap mass spectrometry (ESI-IT-MS) using an Agilent LC 1100 HPLC system with a diode array detector (DAD) coupled to a Bruker Esquire 6000 Plus mass spectrometer. A NUCLEODUR® RP-C18 (CC 125/4 100–5 μm C18 ec) column and mobile phases consisting of 0.1% formic acid (eluent A) and 100% acetonitrile (eluent B) were used for the chromatographic separation. The flow rate, column oven temperature and injection volume were set to 0.5 mL min^{-1}, 25 °C and 50 μL, respectively. The ESI-IT-MS was operated in positive ion mode and MS^n fragmentation patterns were obtained in the autoMS mode. The gradient flow conditions used for chromatographic separation and operating parameters of the ESI-IT-MS detection are summarized in the SI (S2).

2.4. In vitro bioassays

The following section is to provide a brief overview of the applied *in vitro* bioassays. A more detailed description of the experimental techniques is presented in the SI (S3). The applied assays were selected with regard to the biological activities that were previously reported to emerge from transformation of PPL (genotoxicity and cytotoxicity). The number of assessed time points varied according to the capacity of the respective bioassay. The dark control (0 min) and the samples collected after 4, 16, 64, 128 and 256 min were included as base set in all bioassays. These samples were prioritized with regard to the observed removal kinetics of PPL. The photolysis mixtures were partly supplemented with 2 mg L^{-1} catalase from bovine liver on the day of the respective bioassay for the removal of inorganic peroxide. An overview of selected samples and bioassay conditions is presented in the SI (S3, Table S3.1). The expected mixture concentration of PPL and all of its TPs in the bioassay, hereinafter referred to as theoretical exposure level (ThEL), was based on the assumption that each degraded molecule of PPL would result in the formation of a new TP. Hence, the reported ThEL is the product of the initial PPL concentration and the dilution factor of the respective bioassay.

2.4.1. Genotoxicity in bacteria

The umu-test for genotoxic effects was performed with *Salmonella typhimurium* TA1535 psk 1002 (German Collection of Microorganisms and Cell Cultures GmbH, Braunschweig, Germany) according to ISO/FDIS 13829 (1999). The umu-test is based on the colorimetric measurement of the *umuC* gene induction ratio (*IR*), which is upregulated in the applied tester strain as response to genotoxic lesions in the DNA. A threshold of $IR > 1.5$ was used for the classification of positive results.

2.4.2. Mutagenicity in bacteria

The mutagenicity in bacteria was assessed using the Ames fluctuation test, which was performed with *S. typhimurium* TA98 (Xenometrix AG, Allschwil, Switzerland) for the detection of frameshift mutations and *S. typhimurium* TA100 (Xenometrix AG, Allschwil, Switzerland) for the detection of base-pair substitutions according to ISO 11350 (2012). The frequency of reverse mutation events was tested for significance by analysis of variance (ANOVA), following post-hoc multiple comparisons against the negative control using a Dunnett's test. The raw data was arcsine-square-root transformed prior to statistical analysis as recommended by the ISO 11350 (2012) guideline.

2.4.3. Cytotoxicity and in vitro micronucleus formation in mammalian cells

The testing of cytotoxicity and *in vitro* micronucleus formation in mammalian cells was performed with the CHO-K1 cell line (American Type Culture Collection, Manassas, USA) with an exposure time corresponding to 1.5–2 cell doublings. The viability of cell cultures was monitored fluorometrically after exposure to different concentrations of the test article, using the oxidation-reduction indicator resazurin. Moreover, exposed cell cultures were analyzed by flow cytometry for micronucleated cells, apoptotic and necrotic cells, hypodiploid nuclei, relative survival and test article-induced perturbations to the cell cycle using the MicroFlow® kit (Litron Laboratories, Rochester, USA) according to the manufacturers' recommendations. More information about the principle and experimental procedure of this assay can be found elsewhere (Avlasevich et al., 2006; Bryce et al., 2007; Collins et al., 2008). The statistical significance of measured effects was tested by ANOVA, following post-hoc multiple comparisons against the negative control using a Dunnett's test.

2.4.4. Cytotoxicity in bacteria

The cytotoxicity in bacteria was assessed in a modified luminescent bacteria test (LBT) with *Vibrio fischeri* NRRL-B-11177 (Hach-Lange GmbH, Düsseldorf, Germany) according to Menz et al. (2013). This bioassay allows the combined assessment of luminescence inhibition after 30 min and 24 h exposure, respectively. Additionally, the impact on bacterial proliferation was evaluated at the transition from exponential growth to stationary phase after 14 h incubation. A general threshold of 20% inhibition was used for the classification of positive results.

2.5. Identification of TPs for the analysis of structure-activity-relationships

Specific TPs in the reaction mixture were prioritized for the analysis of structure-activity-relationships using a tiered approach. In a first step, all expected minor TPs with a relative LC-MS peak area ($A_{max}/A_{0\ PPL}$) below 0.1% were removed from the candidate list. In a second step, the time course of the relative concentration (A/A_{max}) of each TP in the reaction mixture was compared to the course of measured effects. In cases where a concentration maximum (A_{max}) coincided with a significant peak of the effect intensity, the respective TP was prioritized for further analysis. In addition, a regression analysis between the relative TP concentration (A/A_{max}) in the reaction mixture and the corresponding mixture effect was performed, in order to assess the significance of the hypothesized relationships over the whole course of the treatment process.

A general structural formula was assigned to each prioritized TP on the basis of the detected molecular ion mass and existing knowledge on the photochemical degradation pathways of PPL. The obtained MS/MS spectra were carefully interpreted and compared with available spectra from literature to confirm the initially proposed structures. The MS/MS spectra, the proposed structures and the references used for the structural interpretation are presented in the SI (Table S6.2, Table S7.2). SMILES strings for the following (Q)SAR analysis were generated with JChem for Excel (ChemAxon Ltd.), taking all expected constitutional isomers into account.

2.6. In silico analysis of structure-activity-relationships

In silico analysis of (Q)SARs was performed using different models provided by the CASE Ultra (v. 1.5.2.0, MultiCASE Inc.) expert system for the substructure based prediction of toxicity and bioactivity of chemicals. In case of bacterial mutagenicity, a statistical model (GT1_A7B) and an expert rule-based model (GT_EXPERT) were used in combination as recommended by the ICH M7 guidelines (EMA/CHMP/ICH/83812, 2013). The statistical AUA model was used for the prediction of short-term bacterial luminescence inhibition in the Microtox assay. This assay is comparable to the short-term endpoint ($LI_{30\ min}$) of the modified LBT (Menz et al., 2013). All *in silico* models

used in this study have defined and validated applicability domains. More information about training sets, validity criteria and predictive performance of the CASE Ultra software can be found elsewhere (Chakravarti et al., 2012; Saiakhov et al., 2013, 2014).

2.7. Statistical analysis

The analysis of variance and the modeling of concentration-response relationships were done with the software package SigmaPlot 12 (Systat Software). Non-linear concentration-response curves were analyzed using a four-parameter Hill model. In case of biphasic concentration-response relationships, an additional curve fitting was done using the Dr-Fit software, which automatically generates and ranks dose-response models with varying degrees of multiphasic features using a generalized Hill model (Di Veroli et al., 2015). A linear regression model was used for the analysis of concentration-response relationships in the Ames fluctuation test, since the overwhelming majority of concentration-response curves in the Ames test were reportedly linear in the low dose region (McCann et al., 1984).

3. Results and discussion

3.1. Transformation of propranolol

The kinetic plots, the absolute photon flux of the medium pressure mercury lamp and the molar absorption coefficient of PPL are depicted in Fig. 1. PPL at 3.4 μmol L^{-1} was rapidly eliminated with a pseudo first-order kinetic ($k = 0.272\ min^{-1}, \Phi = 4.03 \times 10^{-3}$). The elimination of 338 μmol L^{-1} PPL was considerably slower and well fitted by a two steps first-order model ($k_1 = 0.151\ min^{-1}$, $k_2 = 0.020\ min^{-1}$). Even though PPL was completely eliminated within the 256 min of irradiation at both investigated concentrations, there was still about 70% of the initial NPOC remaining in the photolysis mixture of 338 μmol L^{-1} PPL. This showed that PPL was primarily photodegraded into TPs and only partially mineralized. Hence, the altered reaction kinetics at 338 μmol L^{-1} can be explained by the light attenuation that resulted from the accumulation of TPs with absorption characteristics similar to PPL.

The LC-MS non-target screening indicated the presence of at least 115 newly formed molecular ions with 23 different masses in the photolysis mixtures of 338 μmol L^{-1} PPL. This implied that PPL disintegrated into a large number of distinct TPs that were in many cases constitutional isomers. In the photolysis samples of 3.4 μmol L^{-1} PPL, 17 of the 23 TP masses that were identified at 338 μmol L^{-1} were still detectable (SI, Table S4.1). The reduced number of detected molecular ion masses in the photolysis mixture of 3.4 μmol L^{-1} PPL was most probably attributed to the detection limit of the analytical method, because the intensities of most TP signals were found to be considerably lower at 3.4 μmol L^{-1}. Moreover, the elimination kinetics at 3.4 μmol L^{-1} were much faster (Fig. 1), but the sampling intervals were kept constant, which could also explain the apparent absence of some TPs. However, the majority of identified TPs occurred in the photolysis mixtures at both investigated concentrations, leading to the assumption that the principal reaction pathways, and consequently the TPs formed, were independent from the initial concentration in the range of 3.4 to 338 μmol L^{-1}.

It should be noted that the applied sampling regime resulted in an incremental reduction of the irradiated volume that may have inversely influenced the rate of the reaction. Moreover, there was an increasing amount of unspecified peroxides detected in the fresh photolysis mixtures of 338 μmol L^{-1} PPL, starting with a concentration equivalent to 0.5 mg L^{-1} H_2O_2 after 4 min of irradiation and ending with a concentration equivalent to 5 mg L^{-1} H_2O_2 after 256 min of irradiation. Interestingly, the photolysis mixtures collected after 128 and 256 min of irradiation were still tested positive for peroxides after treatment with catalase (SI, Table S4.2). It was assumed that this was attributed to the presence of organic peroxides, which could not be utilized as substrate by the applied bovine catalase, since spiked hydrogen peroxide at 20 mg L^{-1} was removed completely in a control experiment. However, since these residues would resemble derivatives of the parent compound, they should be seen as relevant TPs rather than been disqualified as irrelevant byproducts.

3.1.1. Transformation pathways

The UV photolysis of PPL in pure water involves direct photolysis *via* the triplet state ($^3PPL^*$), and self-sensitized photolysis caused by hydroxyl radical (·OH) and singlet oxygen ($^1O_2$) (Peng et al., 2014). The direct photolysis of PPL occurs *via* ring oxidation and the subsequent loss of carbon monoxide (Liu and Williams, 2007). The indirect photolysis of PPL is triggered by a type II photooxidation that involves the irreversible trapping of self-photogenerated singlet molecular oxygen ($^1O_2$) and cleavage of the ether bond (Sortino et al., 2002). Moreover, the attachment of hydroxyl radicals to the aromatic rings, followed by the ring opening and the formation of alcohol and/or aldehyde moieties, was outlined as another important pathway for indirect photolysis (Rastogi et al., 2015; Santiago-Morales et al., 2013).

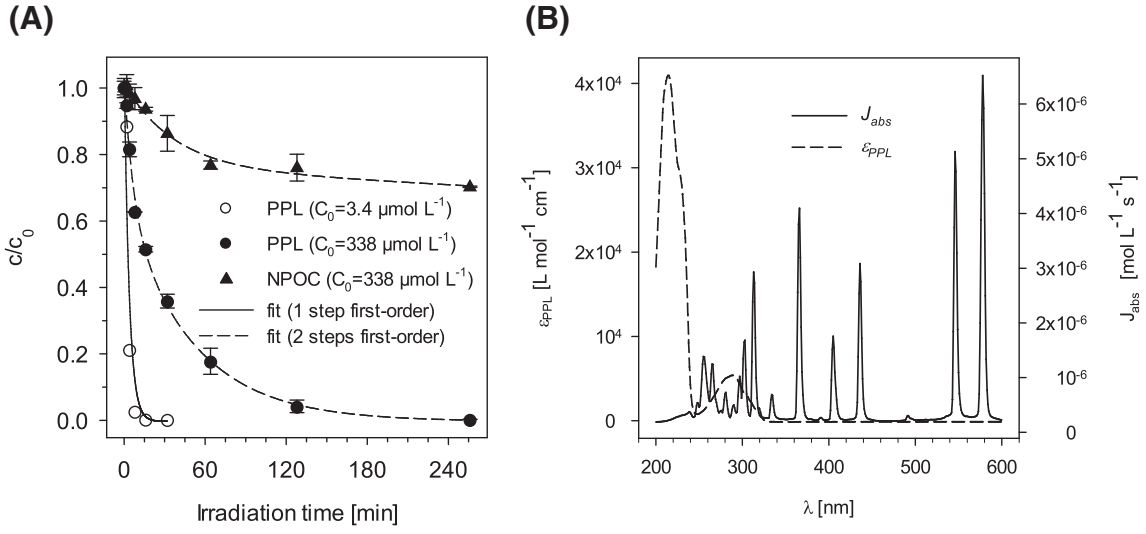

Fig. 1. A: Primary elimination of propranolol (PPL) and mineralization of non-purgeable organic carbon (NPOC) during irradiation with a medium pressure mercury lamp. B: Absolute photon flux (J_{abs}) of the medium pressure mercury lamp and molar absorption coefficient of propranolol (ε_{PPL}).

The obtained LC-MS data was in good agreement with previous studies, since the majority of identified masses have already been described together with the TPs of the abovementioned degradation pathways (SI, Table S4.1). A tentative scheme for the expected degradation of PPL *via* competing direct and indirect photolysis pathways is proposed in Fig. 2. However, it should be noted that this scheme is by far not exhaustive, since it only represents the expected major degradation pathways. The high number of constitutional isomers in the reaction mixture can be explained by the addition of hydroxyl radicals to different positions of the naphthol moiety and a variety of ring-opening reactions. Two newly identified TP masses (*m*/*z* 280 and 298) were tentatively assigned to a previously described degradation pathway, suggesting that *m*/*z* 280 emerged from *m*/*z* 308 by the loss of carbon monoxide and that *m*/*z* 298 was formed by hydroxyl addition to *m*/*z* 282. This hypothesis was in good agreement with observed reaction kinetics (SI, Table S6.1, Table S7.1) and MS/MS fragmentation patterns (SI, Table S6.2).

3.2. In vitro toxicity of the photolysis mixture

Inorganic peroxide (H_2O_2), or reactive oxygen species stemming from H_2O_2, can cause oxidative damage of cellular components, such as DNA, proteins and membrane lipids (Linley et al., 2012). Moreover, H_2O_2 is genotoxic in a variety of bioassay systems and specifically is weakly mutagenic in the Ames test with several *Salmonella typhimurium* test strains (Kensese and Smith, 1989). Therefore, the efficiency of H_2O_2 removal was additionally assessed in a pretest by subjecting the samples collected after 0, 128 and 256 min of irradiation to all the bioassays with and without post-treatment with catalase. This showed that oxidative stress responses to H_2O_2 were efficiently removed by the addition of catalase (SI, Fig. S5.1) or S9-mix, and consequently, these conditions were chosen in the following screening for potentially hazardous TPs.

3.2.1. Genotoxicity and mutagenicity

The umu-test did not show evidence for cytotoxic and genotoxic activity of PPL and the tested photolysis mixtures at the highest investigated ThEL of 225.3 μmol L^{-1} with and without S9-mix (SI, Tables S5.1, S5.2). Moreover, PPL and the assessed photolysis samples of PPL did not significantly impact cellular viability and micronucleus induction in CHO-K1 cells at the highest ThEL of 67.6 and 33.8 μmol L^{-1}, respectively (SI, Tables S5.3, S5.4). Further PPL and the included photolysis mixtures were tested negative for mutagenicity in the Ames fluctuation test using *S. typhimurium* TA98 with and without S9-mix and *S. typhimurium* TA100 with S9-mix (ThEL 270.4 μmol L^{-1}) (SI, Tables S5.5, S5.6). However, there was a significant response observed after 128 min of irradiation in the Ames fluctuation test with *S. typhimurium* TA100 without S9-mix (Fig. 3A). This indicated the presence of TPs at this specific time point of the irradiation process that had the ability to induce base-pair substitutions in the bacterial DNA.

3.2.2. Cytotoxicity in bacteria

PPL before photolysis was only moderately cytotoxic to *V. fischeri* (SI, Fig. S7.1), but there was a strong, transient increase of luminescence and growth inhibition observed in the photolysis mixture at 4 min of irradiation (Fig. 3B). This indicated the formation of intermediate TPs that were much more toxic to *V. fischeri* than the parent compound. Interestingly, similar observations were previously reported for PPL during UV photolysis and ozonation (Dantas et al., 2011; Peng et al., 2014), which showed that the same TPs with bacterial cytotoxicity might have formed under varying treatment conditions. The luminescence inhibition after 30 min ($LI_{30\ min}$) was clearly the most sensitive endpoint, but there was also a significant inhibition of luminescence and growth after 24 and 14 h, respectively. This indicated a rapidly manifesting cytotoxicity as primary effect, which ultimately also resulted in a lowered rate of bacterial cell multiplication. Consequently, $LI_{30\ min}$ was chosen as the most relevant end point for the identification of potentially hazardous TPs.

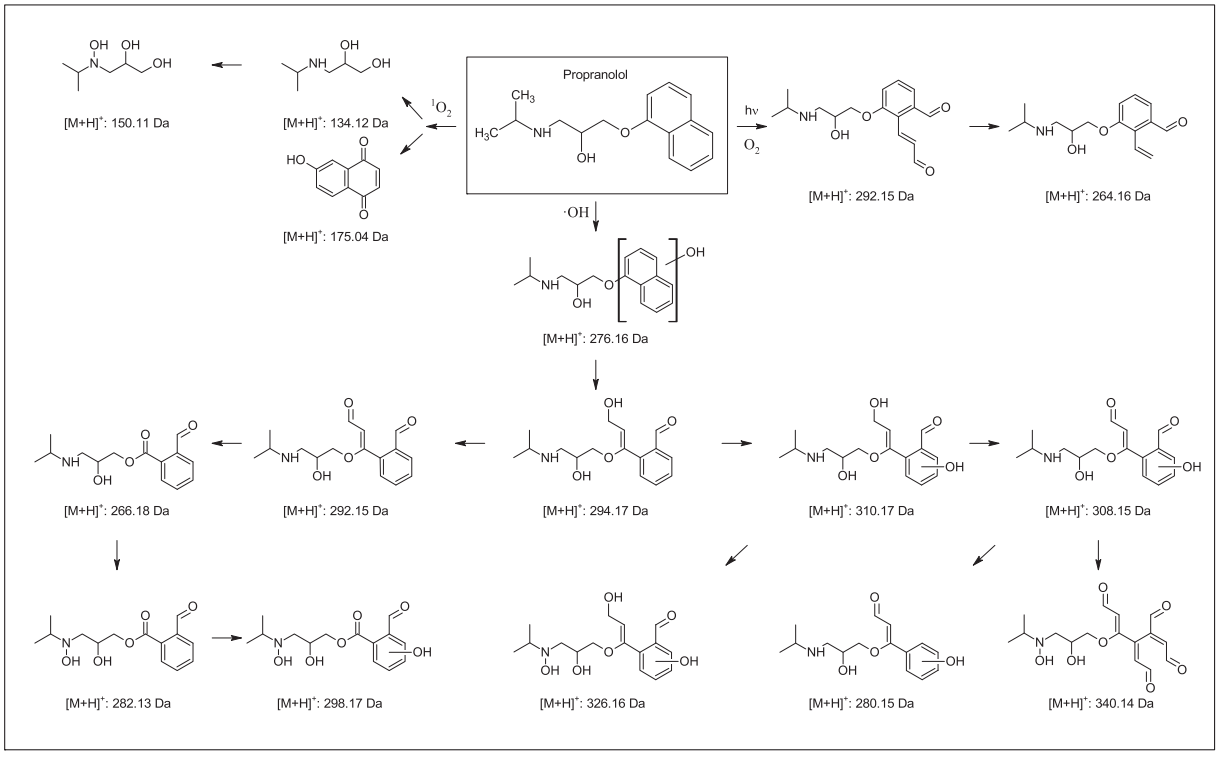

Fig. 2. Possible pathways for the transformation of propranolol initiated by direct photolysis ($h\nu/O_2$) and self-sensitized photolysis involving the hydroxyl radical (·OH) and singlet oxygen ($^1O_2$).

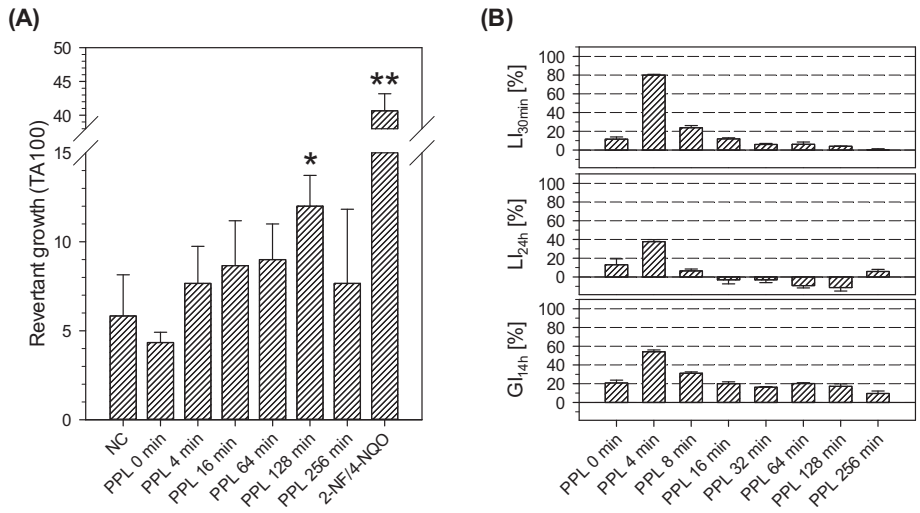

Fig. 3. A: Revertant growth induction of the photolysis mixture of 338 μmol L^{-1} PPL in the Ames-fluctuation test with *S. typhimurium* TA100 w/o S9-mix in comparison to the negative control (NC) (*$p < 0.05$, **$p < 0.01$). The theoretical exposure level (ThEL) was 270.4 μmol L^{-1} and a mixture of 2.4 μmol L^{-1} 2-nitroflourene (2-NF) and 0.13 μmol L^{-1} 4-nitroquinoline 1-oxide (4-NQO) was used as positive control. B: Cytotoxicity in *V. fischeri* of the photolysis mixture of 338 μmol L^{-1} PPL (ThEL 84.5 μmol L^{-1}) by means of luminescence inhibition after 30 min ($LI_{30\ min}$), luminescence inhibition after 24 h ($LI_{24\ h}$) and growth inhibition after 14 h ($GI_{14\ h}$).

3.3. Identification of structural alerts for mutagenicity in bacteria

The reaction mixtures used for the testing of genotoxicity and mutagenicity contained 49 TPs with a peak area ratio ($A_{max}/A_{0\ PPL}$) above 0.1% (Table S6.1). Out of these 49 TPs, the TPs 280(14.3), 282(12.8), 298(10.6) and 326(12.8) reached A_{max} after 128 min of irradiation, which was the reaction mixture that showed the highest mutagenicity (Fig. 4A). Moreover, the relative exposure to the TPs 282(12.8) and 326(12.8) showed a significant linear correlation ($p < 0.05$) with the revertant growth induction over the whole duration of the treatment process, clearly suggesting these TPs as most probable mutagens in the photolysis mixture (Fig. 4B). However, a significant correlation alone does not imply a true causal relationship, which means that further evidence would be necessary to achieve an unambiguous classification.

The proposed chemical structures of suspected mutagenic TPs were analyzed with regard to structure-activity-relationships using a combination of statistical (GT1_A7B) and rule-based (GT_Expert) SAR models for bacterial mutagenicity. An exhaustive list of all included chemical structures and their predicted mutagenic activities is presented in the SI (Table S6.5). Both models concluded negative for PPL, but positive for at least one constitutional variant of the TPs 280(14.3), 282(12.8), 298(10.6), and 326(12.8). This indicated that all the shortlisted TPs may possess new structural features that are linked closely to DNA-reactivity. In particular, GT1_A7B and GT_Expert highlighted both the activated aldehyde functional groups as alerting structures. Moreover, the statistical model (GT1_A7B) identified additional alerting substructures for bacterial mutagenicity, which were not recognized by the rule-based model (Fig. 5). This led to the conclusion that the observed mutagenicity in the photolysis mixture was most probably related to the oxidative opening of the naphthalene moiety, leading to the formation of unsaturated aldehyde functional groups. In fact, alpha-beta unsaturated carbonyl compounds have been reported to interact with DNA by the formation of cyclic deoxyguanosine adducts (Witz et al., 1989). However, the DNA-reactivity of alpha-beta unsaturated carbonyl compounds strongly depends on the length of the carbon chain and their molecular size (Eder et al., 1993). Therefore, further *in vitro* testing of DNA-adduct

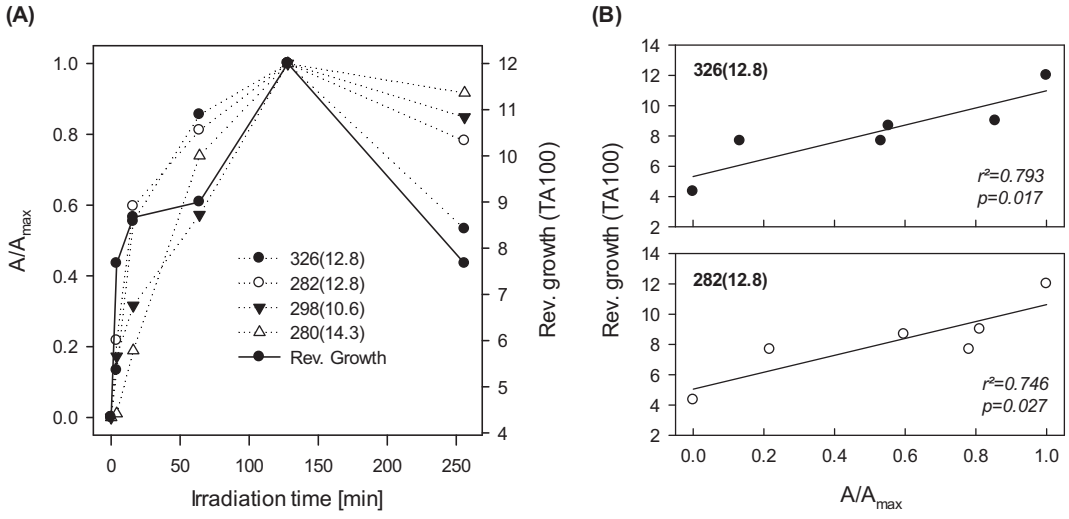

Fig. 4. A: Time course of the relative concentration (A/A_{max}) of prioritized TPs in the photolysis mixture of PPL and the revertant growth induction in the Ames-fluctuation test with *S. typhimurium* TA100 w/o the S9-mix. B: Significant linear relationships between the revertant growth induction and A/A_{max} of suspected mutagenic TPs.

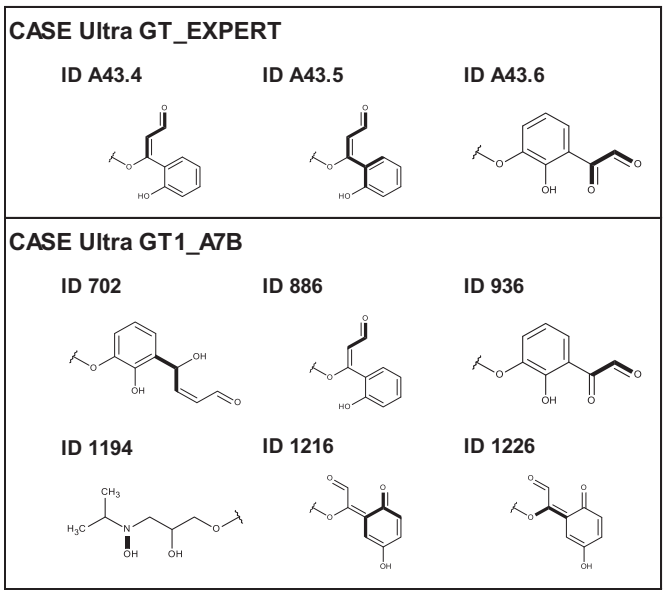

Fig. 5. Structural alerts (in bold) for bacterial mutagenicity identified by the CASE Ultra SAR models GT_EXPERT (expert rules for genotoxicity) and GT1_A7B (*Salmonella* mutagenicity (TA97, 98, 100, 1535–1538)).

formation would be necessary in order to confirm the predicted DNA-reactivity of the aldehyde functional group as part of the whole molecule.

3.4. Identification of structural alerts for cytotoxicity in bacteria

The reaction mixtures used for the testing of bacterial cytotoxicity contained 45 TPs with a peak area ratio ($A_{max}/A_{0\ PPL}$) above 0.1% (SI, Table S7.1). Out of these 45 TPs, only the TPs 276(15.2), 276(16.3), 292(14.9) and 294(10.0) reached A_{max} at 4 min of irradiation, which was the most relevant time point for bacterial cytotoxicity (Fig. 6A). The concentration-response curve of the photolysis mixture at 4 min irradiation was well described by the applied non-linear regression model (SI, Fig. S7.1). Moreover, there was a highly significant non-linear relationship ($p < 0.001$) between the relative concentration of the TPs 292(14.9) and 294(10.0) and the effect of the reaction mixture over the whole duration of the treatment process (Fig. 6B). The modeled concentration-response relationships of the TPs 276(15.2) and 276(16.3) were also statistically significant ($p = 0.0015$), but in both cases the goodness of fit was rather low ($r^2 = 0.925$, AIC = 40.4) (SI, Fig. S7.2). Interestingly, an intermediate TP of PPL with *m/z* 292 was also identified in a reaction mixture with bacterial cytotoxicity by Dantas et al. (2011), which provided additional evidence for the relevance of this degradation product.

The proposed chemical structures of suspected TPs with cytotoxicity in bacteria were analyzed for structure-activity-relationships using the statistical AUA model. An exhaustive list of proposed chemical structures and their predicted activities is presented in the SI (Table S7.3). The QSAR model provided positive predictions not only for PPL, but also for specific constitutional variants of the shortlisted TPs 276(15.2), 276(16.3), 292(14.9) and 294(10.0) (Fig. 7). TP 292(14.9) and TP 294(10.0) were predicted to be active because of the presence of various alkene functional groups and conjugated systems (ID 231 and ID 237). Since these alerting substructures were not present in the parent compound, they might indeed have played a role in the strong increase of bacterial cytotoxicity in the photolysis mixture. In fact, some of the outlined double carbon-carbon bonds contained a polarizable α-substituent, suggesting a Michael type addition of nucleophiles as a mechanism for unspecific reactivity (Verhaar et al., 1992).

Moreover, two structural alerts (ID 5 and ID 241) were identified in the chemical structure of PPL and in some constitutional variants of the hydroxylated TPs 276(15.2) and 276(16.3). The influence of the hydroxyl functional group on the activity of the molecule was further investigated *in vitro* by testing commercially available reference standards. 5-OH PPL and 7-OH PPL showed a similar potency like PPL, but 4-OH PPL was considerably more active (Table 1, SI, Fig. S7.1). In particular, 4-OH PPL was proven to be a 70 times more active inhibitor of bacterial growth than PPL. However, the measured concentration of 4-OH PPL [276(16.3)] in the photolysis mixture was clearly lower than the concentration that would alone cause significant effects in the modified LBT [c(4-OH PPL) < 0.3 μmol L^{-1}, EC_{10} = 1.9 μmol L^{-1}].

3.5. Technical boundaries in hazard assessment of TPs

The vast majority of TPs will never be commercially available and the targeted synthesis of specific TPs can be very laborious, cost-intensive and may be even not possible at the end. As a consequence, the hazard assessment of TPs often starts with the preparation of a synthetic reaction mixture in a laboratory-scale treatment process. This study illustrated that the characterization of a specific TP in such a reaction

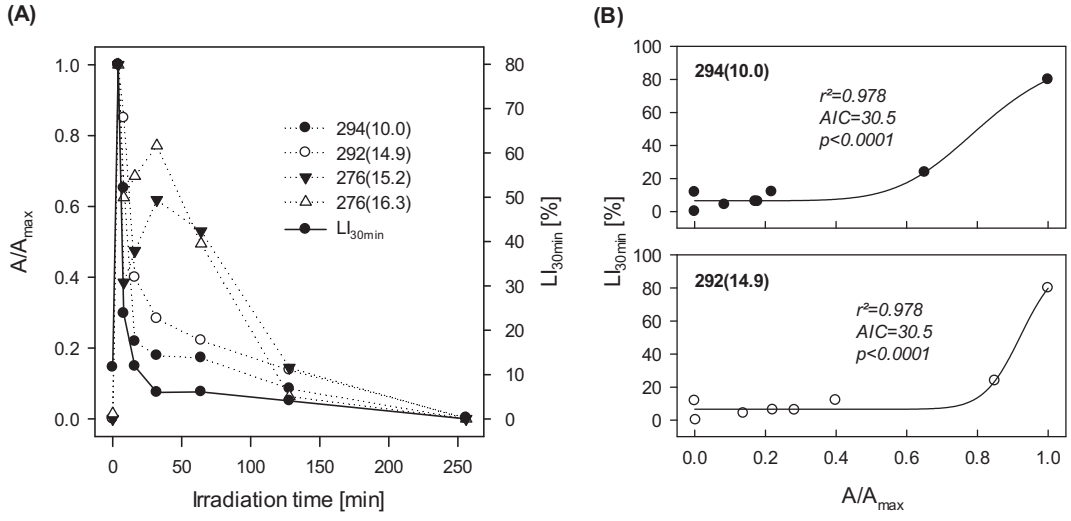

Fig. 6. A: Time course of the relative concentration (A/A_{max}) of prioritized TPs in the photolysis mixture of PPL and the luminescence inhibition after 30 min ($LI_{30\ min}$). B: Non-linear relationships between $LI_{30\ min}$ and A/A_{max} of suspected TPs with bacterial cytotoxicity.

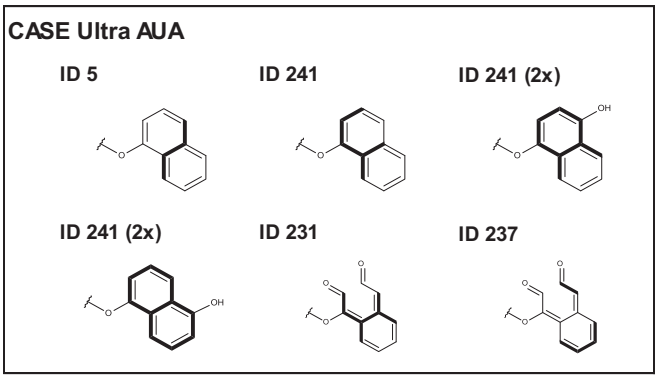

Fig. 7. Structural alerts (in bold) for bacterial cytotoxicity identified by the CASE Ultra QSAR model AUA (toxicity to bacteria).

mixture can be a challenging task, especially when a highly complex mixture of constitutionally isomeric and/or chromatographically not separable compounds is emerging from a transformation process. In such cases, the analysis of time courses to establish a relationship between the exposure to specific TPs and the corresponding mixture effects could represent an efficient alternative to EDA that needs to be developed further. Moreover, there is still room for improvement regarding the environmental significance of effect-oriented studies on TPs, which is mainly attributed to the problem that most standardized bioassays require a preconcentration step to detect trace contaminants at environmentally relevant levels (Hernando et al., 2005). The application of preconcentration techniques to laboratory-scale reaction mixtures is often not compatible with the desired monitoring of multiple endpoints, because the available sample volume usually represents a limiting factor. However, the usage of elevated initial concentrations can only represent an interim solution to this problem, since it will always be at the expense of environmental relevance.

3.6. Environmental significance of synthetic reaction mixtures

The environmental relevance of synthetic reaction mixtures can be verified either by monitoring data or, with regard to the proactive assessment, by fate simulation studies. Following this approach, Piram et al. (2008) compared the photodegradation of PPL and other β-blockers at 10 μg L^{-1} and 10 mg L^{-1} in pure water and in STP effluent. The difference in concentration did not influence degradation pathways and the same photoproducts appeared in both matrices, although environmental waters speeded up the transformation process. This led to the conclusion that photodegradation pathways of β-blockers can be correctly simulated in laboratory scale experiments in pure water and with higher concentrations than those measured in the environment (Piram et al., 2008). Similarly, Liu et al. (2009a,b) found that phototransformation of PPL was much faster in river water than in deionized water, but degradation products were similar in both matrices at two starting concentrations (1 mg L^{-1} and 10 mg L^{-1}). Moreover, it should be noted that 4-OH PPL, a TP that reportedly occurred in ground water of urban aquifers (López-Serna et al., 2013), was confirmed as component in our synthetic reaction mixture [TP 276(16.3)]. These examples showed that treatment processes at high concentrations can be principally used to synthesize TPs for hazard identification, but additional research is advisable in order to confirm the environmental significance of obtained degradation products (Wilde et al., 2016). However, this should not be regarded as a fundamental problem, since it is a common procedure in chemical risk assessment to determine hazards and exposure independently from each other (*e.g.* ECHA, 2011; WHO, 2010).

3.7. Implications for the proactive assessment of transformation products

Over the years numerous studies have been published on a variety of compounds that mainly focused on reaction kinetics and chemical analysis of degradation products with regard to a specific transformation process. Sometimes these studies included a screening-level toxicity assessment in order to evaluate the "safety" of the investigated process. This showed that new biological activities may arise from the transformation of micropollutants, but there is still a fundamental lack in studies that seek to specifically identify the pathways and degradation products that may require a detailed risk analysis. This study illustrated by the example of PPL how small chemical transformations could drastically alter the biological activity of trace contaminants in the water cycle. In particular, the oxidative opening of the naphthalene moiety was identified as a possible mechanism for the emergence of DNA-reactivity and cytotoxicity in bacteria. Moreover, the hydroxylation of PPL at the C4 position of the naphthalene moiety was proven *in vitro* as a transformation pathway for the 70 fold enhancement of cytotoxicity in bacteria. Together with the fact that the concentration of 4-OH PPL in ground water of urban aquifers was reportedly 7 times higher than the concentration of PPL (López-Serna et al., 2013), this example shows that TPs of micropollutants can pose a considerably higher risk than their parent compounds. As a consequence, we need more efficient concepts for the foresighted identification of hazardous TPs.

The follow-up analysis of structure-activity-relationships represents a highly valuable supplement to the effect-driven approach, because this can help to establish a link between the emerging effects during a transformation process and the structural features of the identified TPs. Consequently, the judicious combination of *in vitro* and *in silico* tools could strengthen our understanding of principal pathways for the toxicological activation of micropollutants in the water cycle. This knowledge could be used for the development of exclusively predictive assessment tools that combine the prediction of transformation pathways with the prediction of structure-activity-relationships. With this in mind, it is important (i) to establish frameworks for more harmonized case studies on systematically selected model substances and transformation processes, (ii) to increase the environmental significance of hazard-oriented studies, (iii) to make more use of the advanced bioanalytical tools that have recently been established for the mode-of-action based monitoring of water quality, and (iv) to increase the availability of combined statistical and rule-based *in silico* testing batteries for the same endpoints.

Table 1
Relative activity of propranolol (PPL), 4-OH PPL, 5-OH PPL and 7-OH PPL by means of bacterial luminescence inhibition after 30 min ($LI_{30\ min}$), bacterial luminescence inhibition after 24 h ($LI_{24\ h}$) and bacterial growth inhibition after 14 h ($GI_{14\ h}$).

	$LI_{30\ min}$		$LI_{24\ h}$		$GI_{14\ h}$	
	EC_{50} [μmol L^{-1}]	$EC_{50\ PPL}/EC_{50}$	EC_{50} [μmol L^{-1}]	$EC_{50\ PPL}/EC_{50}$	EC_{50} [μmol L^{-1}]	$EC_{50\ PPL}/EC_{50}$
PPL	768.0	1.0	194.9	1.0	601.0	1.0
4-OH PPL	112.0	6.9	3.5	55.5	8.5	70.7
5-OH PPL	986.3	0.8	225.5	0.9	418.5	1.4
7-OH PPL	751.5	1.0	216.7	0.9	377.1	1.6

4. Conclusion

The contribution of the seemingly limitless number of unknown TPs to the overall impact of micropollutants on human health and the environment is still far from being understood. The coupling of laboratory-scale treatment processes with a combined *in vitro*/*in silico* toxicity approach was proven a useful starting point to tackle this issue. We are convinced that a more comprehensive assessment of TPs can only be achieved with a paradigm shift: away from the isolated and often superficial assessment of individual substances and processes towards a deeper understanding of the principle mechanisms behind the emergence and effects of TPs. Consequently, future hazard-oriented studies should pursue the establishment of a link between the effects of a reaction mixture and the structural properties of the emerging TPs. Finally, it may be necessary to implement the proactive assessment of TPs more consequently into the existing regulations and to prevent the occurrence and transformation of micropollutants in the water cycle. With regard to the latter, it must be questioned whether water treatment technologies that even promote the formation of TPs should still be regarded as a sustainable solution.

Acknowledgement

The authors would like to thank Multicase Inc. for kindly providing the CASE Ultra software, ChemAxon Ltd. for providing the JChem software, Dr. Wolf-Ulrich Palm for the helpful advice and Stefanie Hinz for the great assistance in the experimental work. This work was supported by the German Ministry of Education and Research (NanoPharm, Project No. 03X0094C) and the Innovations-Inkubator Lüneburg (Teilmaßnahme 1.4).

Appendix A. Supplementary data

The online version provides extensive supplementary information which may be necessary to follow this article. The Supporting Information can be found in the online version, at http://dx.doi.org/10.1016/j.envint.2016.11.003.

References

Andreozzi, R., Raffaele, M., Nicklas, P., 2003. Pharmaceuticals in STP effluents and their solar photodegradation in aquatic environment. Chemosphere 50, 1319–1330.
Arnold, W., McNeill, K., 2007. Chapter 3.2 Transformation of pharmaceuticals in the environment: photolysis and other abiotic processes. In: Petrović, M., Barceló, D. (Eds.), Comprehensive Analytical Chemistry vol. 50. Elsevier, Amsterdam.
Avlasevich, S.L., Bryce, S.M., Cairns, S.E., Dertinger, S.D., 2006. In vitro micronucleus scoring by flow cytometry: differential staining of micronuclei versus apoptotic and necrotic chromatin enhances assay reliability. Environ. Mol. Mutagen. 47, 56–66.
Barber, C., Amberg, A., Custer, L., Dobo, K.L., Glowienke, S., van Gompel, J., et al., 2015. Establishing best practise in the application of expert review of mutagenicity under ICH M7. Regul. Toxicol. Pharmacol. 73, 367–377.
Brack, W., 2003. Effect-directed analysis: a promising tool for the identification of organic toxicants in complex mixtures? Anal. Bioanal. Chem. 377, 397–407.
Brack, W., Altenburger, R., Küster, E., Meissner, B., Wenzel, K., Schüürmann, G., 2003. Identification of toxic products of anthracene photomodification in simulated sunlight. Environ. Toxicol. Chem. 22, 2228–2237.
Bryce, S.M., Bemis, J.C., Avlasevich, S.L., Dertinger, S.D., 2007. In vitro micronucleus assay scored by flow cytometry provides a comprehensive evaluation of cytogenetic damage and cytotoxicity. Mutat Res. 630, 78–91.
Canonica, S., Meunier, L., von Gunten, U., 2008. Phototransformation of selected pharmaceuticals during UV treatment of drinking water. Water Res. 42, 121–128.
Chakravarti, S.K., Saiakhov, R.D., Klopman, G., 2012. Optimizing predictive performance of CASE Ultra Expert System models using the applicability domains of individual toxicity alerts. J. Chem. Inf. Model. 52, 2609–2618.
Collins, J.E., Ellis, P.C., White, A.T., Booth, A.E., Moore, C.E., Burman, M., et al., 2008. Evaluation of the Litron In Vitro MicroFlow Kit for the flow cytometric enumeration of micronuclei (MN) in mammalian cells. Mutat. Res. 654, 76–81.
Dantas, R.F., Rossiter, O., Teixeira, A.K.R., Simões, A.S., da Silva, V.L., 2010. Direct UV photolysis of propranolol and metronidazole in aqueous solution. Chem. Eng. J. 158, 143–147.
Dantas, R.F., Sans, C., Esplugas, S., 2011. Ozonation of propranolol: transformation, biodegradability, and toxicity assessment. J. Environ. Eng. 137, 754–759.
DellaGreca, M., Brigante, M., Isidori, M., Nardelli, A., Previtera, L., Rubino, M., Temussi, F., 2003. Phototransformation and ecotoxicity of the drug Naproxen-Na. Environ. Chem. Lett. 1, 237–241.
Di Veroli, G.Y., Fornari, C., Goldlust, I., Mills, G., Koh, S.B., Bramhall, J.L., Richards, F.M., Jodrell, D.I., 2015. An automated fitting procedure and software for dose-response curves with multiphasic features. Sci. Rep. 5, 14701.
ECHA (European Chemicals Agency), 2011. Guidance on Information Requirements and Chemical Safety Assessment: Part A: Introduction to the Guidance Document .
Eder, E., Scheckenbach, S., Deininger, C., Huffman, C., 1993. The possible role of α,β-unsaturated carbonyl compounds in mutagenesis and carcinogenesis. Toxicol. Lett. 67, 87–103.
EMA/CHMP/ICH/83812, 2013. ICH Guideline M7 on Assessment and Control of DNA Reactive (Mutagenic) Impurities in Pharmaceuticals to Limit Potential Carcinogenic Risk. European Medicines Agency, London .
Escher, B.I., Fenner, K., 2011. Recent advances in environmental risk assessment of transformation products. Environ. Sci. Technol. 45, 3835–3847.
Evgenidou, E.N., Konstantinou, I.K., Lambropoulou, D.A., 2015. Occurrence and removal of transformation products of PPCPs and illicit drugs in wastewaters: a review. Sci. Total Environ. 505, 905–926.
Fatta-Kassinos, D., Vasquez, M., Kümmerer, K., 2011. Transformation products of pharmaceuticals in surface waters and wastewater formed during photolysis and advanced oxidation processes — degradation, elucidation of byproducts and assessment of their biological potency. Chemosphere 85, 693–709.
Fenner, K., Kooijman, C., Scheringer, M., Hungerbühler, K., 2002. Including transformation products into the risk assessment for chemicals: the case of nonylphenol ethoxylate usage in Switzerland. Environ. Sci. Technol. 36, 1147–1154.
Garcia-Käufer, M., Haddad, T., Bergheim, M., Gminski, R., Gupta, P., Mathur, N., Kümmerer, K., Mersch-Sundermann, V., 2012. Genotoxic effect of ciprofloxacin during photolytic decomposition monitored by the in vitro micronucleus test (MNvit) in HepG2 cells. Environ. Sci. Pollut. Res. 19, 1719–1727.
Halling-Sørensen, B., Sengeløv, G., Tjørnelund, J., 2002. Toxicity of tetracyclines and tetracycline degradation products to environmentally relevant bacteria, including selected tetracycline-resistant bacteria. Arch. Environ. Contam. Toxicol. 42, 263–271.
Hernando, M.D., Ferrer, I., Agüera, A., Fernandez-Alba, A.R., 2005. Evaluation of pesticides in wastewaters. A combined (chemical and biological) analytical approach. In: Barceló, D. (Ed.), Water Pollution: Emerging Organic Pollution in Waste Waters and Sludge vol. 2. Springer Berlin Heidelberg, Berlin, Heidelberg, pp. 53–77.
ISO 11350, 2012. Water Quality-determination of the Genotoxicity of Water and Waste Water-*Salmonella*/Microsome Fluctuation Test (Ames Fluctuation Test). International Organization for Standardization, Geneva .
ISO/FDIS 13829, 1999. Water Quality-determination of the Genotoxicity of Water and Waste Water Using the Umu-Test: Determination of the Genotoxicity of Water and Waste Water Using the Umu-Test. International Organization for Standardization, Geneva .
Kensese, S.M., Smith, L.L., 1989. Hydrogen peroxide mutagenicity towards *Salmonella typhimurium*. Teratog. Carcinog. Mutagen. 9, 211–218.
Kosjek, T., Heath, E., 2008. Applications of mass spectrometry to identifying pharmaceutical transformation products in water treatment. Trends Anal. Chem. 27, 807–820.
Kostich, M.S., Batt, A.L., Lazorchak, J.M., 2014. Concentrations of prioritized pharmaceuticals in effluents from 50 large wastewater treatment plants in the US and implications for risk estimation. Environ. Pollut. 184, 354–359.
Kümmerer, K., 2008. Pharmaceuticals in the environment — a brief summary. In: Kümmerer, K. (Ed.), Pharmaceuticals in the Environment: Sources, Fate, Effects and Risks. Springer Berlin Heidelberg, Berlin, Heidelberg, pp. 3–21.
Kümmerer, K., Dionysiou, D.D., Fatta-Kassinos, D., 2016. Long-term Strategies for Tackling Micropollutants. In: Fatta-Kassinos, D., Dionysiou, D.D., Kümmerer, K. (Eds.), Advanced Treatment Technologies for Urban Wastewater Reuse. Springer International Publishing, Cham, pp. 291–299.
Längin, A., Schuster, A., Kümmerer, K., 2008. Chemicals in the environment — the need for a clear nomenclature: parent compounds, metabolites, transformation products and their elimination. Clean 36, 349–350.
Li, A.J., Schmitz, O.J., Stephan, S., Lenzen, C., Yue, P.Y.-K., Li, K., Li, H., Leung, K.S.-Y., 2016. Photocatalytic transformation of acesulfame: transformation products identification and embryotoxicity study. Water Res. 89, 68–75.
Linley, E., Denyer, S.P., McDonnell, G., Simons, C., Maillard, J.-Y., 2012. Use of hydrogen peroxide as a biocide: new consideration of its mechanisms of biocidal action. J. Antimicrob. Chemother. 67, 1589–1596.
Liu, Q.-T., Williams, H.E., 2007. Kinetics and degradation products for direct photolysis of β-blockers in water. Environ. Sci. Technol. 41, 803–810.
Liu, Q.-T., Cumming, R.I., Sharpe, A.D., 2009a. Photo-induced environmental depletion processes of β-blockers in river waters. Photochem. Photobiol. Sci. 8, 768.
Liu, Q.-T., Williams, T.D., Cumming, R.I., Holm, G., Hetheridge, M.J., Murray-Smith, R., 2009b. Comparative aquatic toxicitxy of propranolol and its photodegraded mixtures: algae and rotifer screening. Environ. Toxicol. Chem. 28, 2622–2631.
López-Serna, R., Petrović, M., Barceló, D., 2012. Occurrence and distribution of multi-class pharmaceuticals and their active metabolites and transformation products in the Ebro River basin (NE Spain). Sci. Total Environ. 440, 280–289.
López-Serna, R., Jurado, A., Vázquez-Suñé, E., Carrera, J., Petrović, M., Barceló, D., 2013. Occurrence of 95 pharmaceuticals and transformation products in urban groundwaters underlying the metropolis of Barcelona, Spain. Environ. Pollut. 174, 305–315.
McCann, J., Horn, L., Kaldor, J., 1984. An evaluation of *Salmonella* (Ames) test data in the published literature: application of statistical procedures and analysis of mutagenic potency. Mutat. Res. 134, 1–47.
Menz, J., Schneider, M., Kümmerer, K., 2013. Toxicity testing with luminescent bacteria — characterization of an automated method for the combined assessment of acute and chronic effects. Chemosphere 93, 990–996.

Packer, J.L., Werner, J.J., Latch, D.E., McNeill, K., Arnold, W.A., 2003. Photochemical fate of pharmaceuticals in the environment: naproxen, diclofenac, clofibric acid, and ibuprofen. Aquat. Sci. 65, 342–351.

Peng, N., Wang, K.-F., Liu, G.-G., Zeng, L.-Z., Yao, K., Lu, W.-Y., 2014. UV photolysis of propranolol in aqueous solution: mechanism and toxicity of photoproducts [in Chinese]. Huan Jing Ke Xue 35, 3794–3799.

Piram, A., Salvador, A., Verne, C., Herbreteau, B., Faure, R., 2008. Photolysis of β-blockers in environmental waters. Chemosphere 73, 1265–1271.

Rastogi, T., Leder, C., Kümmerer, K., 2014. Qualitative environmental risk assessment of photolytic transformation products of iodinated X-ray contrast agent diatrizoic acid. Sci. Total Environ. 482-483, 378–388.

Rastogi, T., Leder, C., Kümmerer, K., 2015. Re-designing of existing pharmaceuticals for environmental biodegradability: a tiered approach with β-blocker propranolol as an example. Environ. Sci. Technol. 49, 11756–11763.

Saiakhov, R., Chakravarti, S., Klopman, G., 2013. Effectiveness of CASE Ultra Expert System in evaluating adverse effects of drugs. Mol. Inf. 32, 87–97.

Saiakhov, R., Chakravarti, S., Sedykh, A., 2014. An improved workflow to perform in silico mutagenicity assessment of impurities as per ICH M7 guideline. Toxicol. Lett. 229, 164.

Santiago-Morales, J., Agüera, A., Gómez, M.d.M., Fernández-Alba, A.R., Giménez, J., Esplugas, S., Rosal, R., 2013. Transformation products and reaction kinetics in simulated solar light photocatalytic degradation of propranolol using Ce-doped TiO_2. Appl. Catal. B 129, 13–29.

Santos, L.H., Araújo, A., Fachini, A., Pena, A., Delerue-Matos, C., Montenegro, M., 2010. Ecotoxicological aspects related to the presence of pharmaceuticals in the aquatic environment. J. Hazard. Mater. 175, 45–95.

Schmitt-Jansen, M., Bartels, P., Adler, N., Altenburger, R., 2007. Phytotoxicity assessment of diclofenac and its phototransformation products. Anal. Bioanal. Chem. 387, 1389–1396.

Schulze, T., Weiss, S., Schymanski, E., von der Ohe, P., Schmitt-Jansen, M., Altenburger, R., Streck, G., Brack, W., 2010. Identification of a phytotoxic photo-transformation product of diclofenac using effect-directed analysis. Environ. Pollut. 158, 1461–1466.

Sortino, S., Petralia, S., Boscà, F., Miranda, M.A., 2002. Irreversible photo-oxidation of propranolol triggered by self-photogenerated singlet molecular oxygen. Photochem. Photobiol. Sci. 1, 136–140.

Ternes, T.A., 1998. Occurrence of drugs in German sewage treatment plants and rivers. Water Res. 32, 3245–3260.

Toolaram, A.P., Kümmerer, K., Schneider, M., 2014. Environmental risk assessment of anticancer drugs and their transformation products: a focus on their genotoxicity characterization-state of knowledge and short comings. Mutat. Res. Rev. Mutat. Res. 760, 18–35.

Verhaar, H.J., van Leeuwen, C.J., Hermens, J.L., 1992. Classifying environmental pollutants. Chemosphere 25, 471–491.

Vulliet, E., Cren-Olivé, C., 2011. Screening of pharmaceuticals and hormones at the regional scale, in surface and groundwaters intended to human consumption. Environ. Pollut. 159, 2929–2934.

WHO (World Health Organization), 2010. Human Health Risk Assessment Toolkit: Chemical Hazards .

Wilde, M.L., Menz, J., Trautwein, C., Leder, C., Kümmerer, K., 2016. Environmental fate and effect assessment of thioridazine and its transformation products formed by photodegradation. Environ. Pollut. 213, 658–670.

Witz, G., Latriano, L., Goldstein, B.D., 1989. Metabolism and toxicity of trans, trans-muconaldehyde, an open-ring microsomal metabolite of benzene. Environ. Health Perspect. 82, 19–22.

Zonja, B., Aceña, J., Jelic, A., Petrovic, M., Solsona, S.P., Barceló, D., 2014. Transformation products of emerging contaminants: analytical challenges and future needs. In: Lambropoulou, D.A., Nollet, L.M.L. (Eds.), Transformation Products of Emerging Contaminants in the Environment. John Wiley and Sons Ltd, Chichester .

Zwiener, C., 2007. Occurrence and analysis of pharmaceuticals and their transformation products in drinking water treatment. Anal. Bioanal. Chem. 387, 1159–1162.

Supporting Information

for

Transformation products in the water cycle and the unsolved problem of their proactive assessment: a combined *in vitro/in silico* approach

Jakob Menz[a], *Anju Priya Toolaram*[a], *Tushar Rastogi*[a], *Christoph Leder*[a], *Oliver Olsson*[a], *Klaus Kümmerer*[a,*], *Mandy Schneider*[a]

[a]Sustainable Chemistry and Material Resources, Institute of Sustainable and Environmental Chemistry, Leuphana University Lüneburg, Scharnhorststr. 1/C13, DE-21335 Lüneburg, Germany

Table of contents

[*] Corresponding author: klaus.kuemmerer@leuphana.de; tel.: +49 4131 677 2893; fax: +49 4131 677 2848.

S1. Determination of the quantum yield

The absolute photon flux of the radiation source (J_{abs}) was determined by UV-VIS spectroscopy in combination with chemical actinometry. The relative photon flux (J_{rel}) was measured in terms of relative counts from a distance of 5 cm with an integration time of 10 ms using a BlackComet UV-VIS spectrometer (StellartNet Inc., Tampa, USA). Then J_{rel} was converted into J_{abs} by the equations S1.1 and S1.2 according to a method by Palm (2013), using Terbuthylazine (in 1% Acetonitrile) and Metamitron as chemical actinometers.

$$\boldsymbol{FACTOR} = \frac{\frac{\boldsymbol{dc}}{\boldsymbol{dt}}}{\boldsymbol{\Phi} * \sum_{\boldsymbol{200\ nm}}^{\boldsymbol{400\ nm}} \boldsymbol{J_{rel}} * \boldsymbol{2{,}303} * \boldsymbol{c_0} * \boldsymbol{\varepsilon} * \boldsymbol{l}} \qquad \text{(S1.1)}$$

$$\boldsymbol{J_{abs}} = \boldsymbol{FACTOR} * \boldsymbol{J_{rel}} \qquad \text{(S1.2)}$$

where FACTOR is the conversion factor, dc/dt is the initial elimination rate of the actinometer, Φ is the quantum yield of the actinometer, c_0 is the initial concentration of the actinometer, ε is the molar absorption coefficient of the actinometer and l is the path length. The quantum yield of propranolol (Φ_{PPL}) was determined according to equation S1.3.

$$\boldsymbol{\Phi_{PPL}} = \frac{\frac{\boldsymbol{dc}}{\boldsymbol{dt}}}{\boldsymbol{2{,}303} * \sum_{\boldsymbol{200\ nm}}^{\boldsymbol{400\ nm}} \boldsymbol{\varepsilon_{PPL}} * \boldsymbol{J_{abs}} * \boldsymbol{c_0} * \boldsymbol{l}} \qquad \text{(S1.3)}$$

where dc/dt is the initial elimination rate of PPL, ε_{PPL} is the molar absorption coefficient of PPL, J_{abs} is the absolute photon flux, c_0 is the initial concentration of PPL, and l is the path length (1 cm).

Table S1.1. Parameters used for the determination of the absolute photon flux

Parameter	***Terbuthylazine***	***Metamitron***
Φ	0.06[a]	0.017[b]
C_0 [mol L^{-1}]	4.3E-06	4.9E-06
k [s^{-1}]	0.030	0.033
dc/dt [mol L^{-1} s^{-1}]	1.3E-07	1.6E-07
l [cm]	1,0	1,0

[a]Palm and Zetzsch, 1996; [b]Palm et al., 1997

S2. Chromatographic analysis

Table S2.1. Gradient flow conditions used for chromatographic separation

Time (min)	***% Eluent B (Acetonitrile)***
0.01 to 2 min	1
2 to 27 min	1-65
27 to 29 min	65-20
29 to 30 min	20-1
30 to 32 min	1

Table S2.2. Operating parameters of the ESI-IT-MS

Parameters	***Values***
Dry gas temperature	350°C
Nebulizer pressure	30 psi
Dry gas flow	10 L min^{-1}
end plate Offset	-500 Volt
capillary voltage	-3583 Volt
skimmer	40 Volt
capillary exit	110. 5 Volt
octopole one	12.00 Volt
octopole two	1.70 Volt
trap drive	37.7
lens one	-5.0 Volt
lens two	-60 Volt
target mass	260 m/z
maximum accumulation time	200 ms
scan range	40 m/z - 1000 m/z
fragmentation amplitude	1

S3. *In vitro* Bioassays

Table S3.1. Selected samples and bioassay conditions for the in vitro assessment of genotoxicity and cytotoxicity. A: (+) catalase, B: (-) catalase, C: (+) S9-Mix.

Photolysis mixture	***Bioassay***			
	Umu-test	***Ames fluctuation test***	***Cytotoxicity/ micronucleus formation***	***Modified LBT***
PPL 0 min	A, B, C	A, B, C	A, B, C	A, B
PPL 2 min	A, C	-	-	-
PPL 4 min	A, C	A, C	A, C	A
PPL 8 min	A, C	-	-	A
PPL 16 min	A, C	A, C	A, C	A
PPL 32 min	A, C	-	-	A
PPL 64 min	A, C	A, C	A, C	A
PPL 128 min	A, B, C	A, B, C	A, B, C	A, B
PPL 256 min	A, B, C	A, B, C	A, B, C	A, B

Genotoxicity in bacteria

An overnight culture of *Salmonella typhimurium* TA1535 psk 1002 (German Collection of Microorganisms and Cell Cultures GmbH) was prepared in TGA-culture medium and incubated for 16 h at 37°C and 250 rpm. Subsequently, the overnight culture was tenfold diluted with fresh TGA-culture medium and incubated for additional 1.5 h to obtain an exponentially growing culture for inoculation. The exposure cultures were prepared by adding the following components into a 96-well microplate: 180 µL testing material, 20 µL 10x concentrated TGA-culture medium, 70 µL inoculum and optionally 0.8% (v/v) S8 mix for metabolic activation containing Aroclor 1254-induced rat liver homogenate and cofactors (Xenometrix AG). The exposure plate (plate A) was incubated for 2 h at 37°C and 250 rpm. Subsequently, the test cultures of plate A were tenfold diluted with TGA-culture medium in another 96-well plate (plate B) and incubated for additional 2 h at 37°C and 250 rpm. The optical density at 600 nm (OD_{600nm}) of plate B was determined using a Synergy-HT microplate photometer (BioTek Instruments). 30 µl of the contents of plate B were transferred into a new plate (plate C) containing 120 µL B-buffer followed by the addition of 30 µL Ortho-Nitrophenol-ß-d-galactopyranoside (ONPG, Carl Roth GmbH, Germany) solution. Plate C was incubated for 30 min at 28°C, 250 rpm, after which the reaction was stopped using the stop reagent. Finally, the absorbance at 420 nm (A_{420nm}) of plate C was measured to determine the β-galactosidase activity. The growth factor (*G*) and the induction ratio (*IR*) were calculated according to ISO/FDIS 13829 (ISO/FDIS 1999) on the basis of OD_{600nm} and A_{420nm} respectively.

Mutagenicity in bacteria

An overnight culture was prepared from frozen stock cultures of the respective tester strain (TA98 or TA100) by inoculating 20 ml of ampicillin containing growth medium with 20 µl of the stock culture, followed by incubation at 37±1 °C and 250 rpm for 12-16 h. This culture was adjusted with 1x exposure medium to 1800 FTU in case of TA98 and 450 FTU in case of TA100 to be used as inoculum. The exposure plates were prepared by adding the following components into the cavities of a 24-well plate: 400 µL testing material, 50 µL 10x exposure medium, 50 µL inoculum and optionally 15 µL S8 mix for metabolic activation containing Aroclor 1254-induced rat liver homogenate (Xenometrix AG). The exposure plate was incubated in the dark at 37±1 °C and 250 rpm for 80 min, followed by incubation at 20 °C for another 20 min. The optical density at 600 nm (OD_{600nm}) was determined before and after incubation using a microplate photometer (Synergy-HT, BioTek Instruments). Revertants were detected by adding 2.5 ml of reversion indicator medium to the exposed cultures and transferring them in 48 aliquots of 50 µL into 384-well plates. These plates were incubated at 37±1 °C and scored after 48 h for the number of positive (yellow) and negative (purple) wells.

Cytotoxicity and *in vitro* micronucleus formation in mammalian cells

The testing for cytotoxicity and *in vitro* micronucleus formation was performed with the CHO-K1 cell line (ATCC, Manassas, USA). The cells were cultivated at 37°C and 5% CO_2 in HAM's F12 medium (Biochrom GmbH, Berlin, Germany), supplemented with 10% (v/v) FBS superior and 1% (v/v) penicillin/streptomycin (Biochrom GmbH, Berlin, Germany). Before the test, cells were kept in culture for at least two weeks and passaged every 72-96 h in order to maintain subconfluency. Then cells were harvested and diluted with fresh media to a cell count of 12,000 cells ml^{-1}. This cell suspension was seeded into a 24 well plate by adding a volume of 1 ml per well and incubated for 46 h to allow attachment of the cells. The exposure cultures for cytotoxicity testing were prepared by aspirating off the old media and

adding 800 µL of fresh media and 200 µL of the respective sample. After approximately 1.5 doubling times (i.e. 26 h), the exposure media was replaced by fresh media supplemented with 10% (v/v) resazurin solution (440 µmol L^{-1} resazurin sodium salt in PBS), following another incubation step of 4 h. Before and after this final incubation step, the fluorescence emission was determined at 590 nm with 560 nm as excitation wavelength using a Synergy-HT microplate fluorometer (BioTek Instruments). The exposure cultures for the testing of *in vitro* micronucleus formation were prepared by aspirating off the old media and adding 900 µL of fresh media and 100 µL of the respective sample. Then after 26 h incubation a sequential staining procedure was performed, using the MicroFlow® kit (Litron Laboratories, Rochester, USA) according to the manufacturer's recommendations (Litron Laboratories). The first staining was performed with ethidium monoazide (EMA), which crosses the compromised outer membrane of apoptotic and necrotic cells and binds covalently to DNA through photoactivation. Then the cells were lysed and the released chromatin was stained using the SYTOX® Green nucleic acid stain. In this way, differential staining of healthy chromatin versus that of dead/dying cells is achieved. The plate was incubated at room temperature in dark for at least 30 min. Then all the samples were transferred into flow cytometry tubes and 20,000 nucleated cells per sample were analyzed using a FACSCalibur flow cytometer (BD Biosciences). The instrument settings and gatings for the flow cytometric acquisition were adjusted according to the manufacturer's recommendations (Litron Laboratories).

Cytotoxicity in bacteria

An overnight culture of *Vibrio fischeri* NRRL-B-11177 (Hach-Lange GmbH) was prepared in supplemented seawater complete (SSWC) media [0.5% (w/v) Peptone from casein, 0.05% (w/v) Yeast extract, 0.3% (v/v) Glycerol, 3% (w/v) NaCl, 44.2 mM NaH_2PO_4, 12.1 mM K_2HPO_4, $MgSO_4$, 0.8 mM 7 H_2O, 3.8 mM $(NH_4)_2HPO_4$; pH 7]. After overnight incubation at 20 °C for 22±2 h, the culture was diluted with fresh SSWC media to an initial cell density of 20 formazine turbidity units (FTU) and subsequently transferred into a 96-well microplate by adding 100 µL to each well. After 30 min of preincubation at 15 °C, an initial measurement of luminescence emission and optical density (578 nm) was conducted, using a Thermo Varioskan Flash multimode reader. Subsequently, the test cultures were exposed in triplicates to 100 µL of the respective sample and a continuous measurement of luminescence and optical density, respectively, was carried out for 24 h at 15 °C. Prior to testing, all samples were supplemented with NaCl to a final salinity of 2% (w/v).

S4. Transformation of propranolol

Table S4.1. Molecular ion masses of transformation products detected by LC-ESI-MS (●) after photolysis of PPL under varying conditions. The number of identified isomers in the photolysis mixture of 338 µmol L^{-1} PPL for each identified mass is given in parentheses.

***m/z* $[M+H]^+$**	***UV lamp*[a] *338 µmol L^{-1}***	***UV lamp*[a] *3.4 µmol L^{-1}***	***UV lamp*[b] *338 µmol L^{-1}***	***Xenon lamp*[c] *3.4 µmol L^{-1}***	***Xenon lamp*[d] *96.4 µmol L^{-1}***
134	● (1)	●	●		●
149	● (5)	●			
150	● (1)	●			
164					●
175	● (1)	●	●		
192	● (2)		●		
206	● (1)				
218	● (2)	●	●		
220	● (2)	●			
258	● (2)	●		●	
264	● (5)	●	●	●	
266	● (5)	●	●		●
276	● (9)	●	●	●	●
278	● (8)		●		
280	● (8)				
282	● (5)	●	●		●
292	● (5)	●	●	●	●
294	● (7)	●	●		●
298	● (6)	●			
308	● (7)	●	●	●	●
310	● (8)	●	●	●	●
326	● (15)	●	●		
328	● (6)		●		
340	● (4)		●		

[a]Present study; [b]Rastogi et al., 2015; [c]Liu et al., 2009, [d]Santiago-Morales et al., 2013

Table S4.2. Peroxide residues in the photolysis mixtures of 338 µmol L^{-1} propranolol (PPL) determined semi-quantitatively using MQuantTM peroxide test strips.

Photolysis mixture	***Peroxide [mg L^{-1} H_2O_2]***			
	Fresh sample	***Stored sample***	***Stored sample (+) catalase***	***Stored sample (+) S9-Mix***
PPL 0 min	0	0	0	0
PPL 4 min	0.5	0	0	0
PPL 8 min	2	0.5	0	0
PPL 16 min	2	0.5	0	0
PPL 32 min	0.5	0	0	0
PPL 64 min	2	0.5	0	0
PPL 128 min	2	2	0.5	0
PPL 256 min	5	5	2	0

S5. *In vitro* toxicity of the photolysis mixture

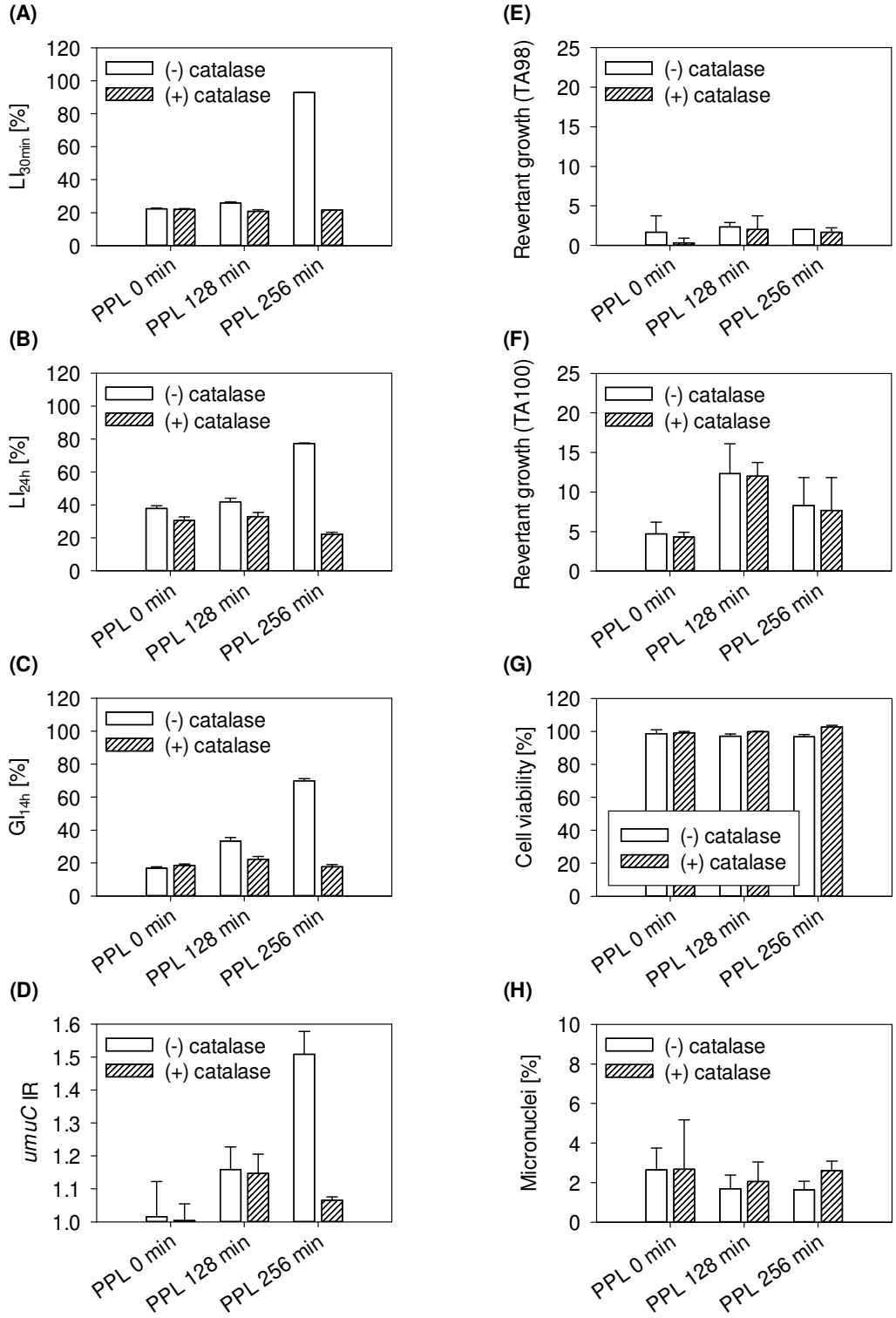

Figure S5.1. Effect of catalase post-treatment by means of bacterial luminescence inhibition after 30 min (A), bacterial luminescence inhibition after 24 h (B), inhibition of bacterial growth after 14h (C), umuC gene induction ratio (D), revertant growth in S. typhimurium TA98 (E), revertant growth in S. typhimurium TA100 (F), viability in CHO-K1 cells (G) and in vitro micronucleus formation in CHO-K1 cells (H).

*Table S5.1. Genotoxicity in Salmonella typhimurium TA1535 psk 1002 of the catalase-treated photolysis mixture of 338 µmol L^{-1} PPL by means of umuC gene induction ratio (IR) w/o S9-mix (ThEL 225.3 µmol L^{-1}, n=3,*IR>1.5). 4-nitroquinoline 1-oxide (4-NQO) was used as positive control.*

Sample	***Growth***			***IR***		
Control (n=9)	1.00	±	0.04	1.00	±	0.06
PPL 0 min	0.96	±	0.02	1.00	±	0.05
PPL 2 min	0.95	±	0.01	0.99	±	0.04
PPL 4 min	0.97	±	0.01	1.07	±	0.06
PPL 8 min	0.97	±	0.02	1.15	±	0.03
PPL 16 min	1.03	±	0.05	1.12	±	0.02
PPL 32 min	1.04	±	0.04	1.07	±	0.03
PPL 64 min	1.01	±	0.05	1.13	±	0.02
PPL 128 min	0.94	±	0.04	1.15	±	0.06
PPL 256 min	0.94	±	0.05	1.07	±	0.01
4-NQO (0.26 µmol L^{-1})	0.97	±	0.03	**4.02***	±	0.08
4-NQO (0.13 µmol L^{-1})	0.97	±	0.01	**2.53***	±	0.14
4-NQO (0.065 µmol L^{-1})	0.98	±	0.04	**1.88***	±	0.06

*Table S5.2. Genotoxicity in Salmonella typhimurium TA1535 psk 1002 of the photolysis mixture of 338 µmol L^{-1} PPL by means of umuC gene induction ratio (IR) with S9-mix (ThEL 225.3 µmol L^{-1}, n=3,*IR>1.5). 2-aminoanthracene (2-AA) was used as positive control.*

Sample	***Growth***			***IR***		
Control (n=9)	1.00	±	0.04	1.00	±	0.05
PPL 0 min	0.82	±	0.03	1.00	±	0.04
PPL 2 min	0.83	±	0.03	0.93	±	0.08
PPL 4 min	0.84	±	0.02	1.14	±	0.00
PPL 8 min	0.81	±	0.01	1.13	±	0.08
PPL 16 min	0.94	±	0.06	1.07	±	0.08
PPL 32 min	0.97	±	0.03	1.09	±	0.04
PPL 64 min	0.97	±	0.01	1.05	±	0.03
PPL 128 min	0.96	±	0.05	0.95	±	0.06
PPL 256 min	0.92	±	0.03	1.09	±	0.06
2-AA (2.1 µmol L^{-1})	0.94	±	0.04	**3.27***	±	0.09
2-AA (1.05 µmol L^{-1})	0.97	±	0.01	**2.10***	±	0.16
2-AA (0.51 µmol L^{-1})	0.99	±	0.02	**1.61***	±	0.07

Table S5.3. Cytotoxicity in CHO-K1 cells of the catalase-treated photolysis mixture of 338 µmol L^{-1} PPL (ThEL 67.6 µmol L^{-1}, n=3). Dimethyl sulfoxide (DMSO) was used as positive control.

Sample	***Cytotoxicity [%]***		
PPL 0 min	0.9	±	0.8
PPL 4 min	7.1	±	1.8
PPL 16 min	8.6	±	1.2
PPL 64 min	2.7	±	4.1
PPL 128 min	0.1	±	0.3
PPL 256 min	-2.7	±	1.0
DMSO (5%, n=6)	51.6	±	1.8

*Table S5.4. Relative survival, EMA-positives, hypodiploid formation and in vitro micronucleus induction in CHO-K1 cells after exposure to the catalase-treated photolysis mixture of 338 µmol L^{-1} PPL (ThEL 33.8 µmol L^{-1}, n=5, **p<0.01).Vinblastine (VB) and mitomycin C (MMC) were used as positive control.*

Sample	***Survival [%]***			***EMA+ [%]***			***Micronucleated [%]***			***Hypodiploid [%]***		
Control (n=10)	100.0	±	50.5	1.0	±	0.5	1.8	±	0.6	0.3	±	0.1
PPL 0 min	77.7	±	17.0	0.8	±	0.4	2.7	±	2.5	0.7	±	0.9
PPL 2 min	108.1	±	31.2	0.6	±	0.1	2.8	±	1.1	0.4	±	0.3
PPL 4 min	96.6	±	18.3	0.7	±	0.1	2.1	±	1.6	0.4	±	0.3
PPL 8 min	107.8	±	29.1	0.6	±	0.1	1.9	±	0.6	0.3	±	0.2
PPL 16 min	105.1	±	10.8	0.7	±	0.2	2.1	±	1.0	0.3	±	0.1
PPL 32 min	85.7	±	21.9	0.9	±	0.3	2.6	±	0.5	0.3	±	0.1
PPL 64 min	55.8	±	17.5	1.1	±	0.4	2.7	±	1.1	0.4	±	0.3
PPL 128 min	88.2	±	31.4	1.0	±	0.6	1.7	±	0.7	0.5	±	0.3
PPL 256 min	104.0	±	21.9	0.8	±	0.2	1.6	±	0.4	0.6	±	0.6
VB (0.02 µmol L^{-1}, n=7)	85.9	±	26.6	1.4	±	0.3	3.4	±	0.3	**2.9****	±	0.2
MMC (0.3 µmol L^{-1}, n=7)	59.2	±	16.6	1.1	±	0.3	**6.0****	±	1.1	0.3	±	0.1

*Table S5.5 Revertant growth induction of the catalase-treated photolysis mixture of 338 µmol L^{-1} PPL in the Ames-fluctuation test with S. typhimurium TA 98 and TA100 w/o S9-mix (ThEL 270.4 µmol L^{-1}, n=3, *p<0.05, **p<0.01). A mixture of 2-nitrofluorene (2-NF) and 4-nitroquinoline 1-oxide (4-NQO) was used as positive control.*

Sample	***Revertants TA98***			***Revertants TA100***		
Control (n=6)	0.3	±	0.8	5.8	±	2.3
PPL 0 min	0.3	±	0.6	4.3	±	0.6
PPL 4 min	2.0	±	0.0	7.7	±	2.1
PPL 16 min	1.3	±	0.6	8.7	±	2.5
PPL 64 min	1.7	±	1.2	9.0	±	2.0
PPL 128 min	2.0	±	1.7	**12.0***	±	1.7
PPL 256 min	1.7	±	0.6	7.7	±	4.2
2-NF (2.4 µmol L^{-1}) 4-NQO (0.13 µmol L^{-1})	**44.0****	±	3.5	**40.7****	±	2.5

*Table S5.6. Revertant growth induction of the photolysis mixture of 338 µmol L^{-1} PPL in the Ames-fluctuation test with S. typhimurium TA 98 and TA100 with S9-mix (ThEL 270.4 µmol L^{-1}, n=3, **p<0.01). 2-aminoanthracene (2-AA) was used as positive control.*

Sample	***Revertants TA98***			***Revertants TA100***		
Control (n=3)	1.3	±	0.6	4.3	±	1.2
PPL 0 min	2.0	±	1.0	3.3	±	1.5
PPL 4 min	1.7	±	1.2	4.3	±	1.2
PPL 16 min	1.0	±	1.0	6.0	±	2.0
PPL 64 min	2.0	±	1.7	7.3	±	2.9
PPL 128 min	2.0	±	1.0	9.0	±	3.5
PPL 256 min	3.0	±	1.0	5.0	±	3.6
2-AA (5.2 µmol L^{-1})	**48.0****	±	0.0	**47.7****	±	0.6

Table S5.7. Cytotoxicity in V. fischeri of the catalase-treated photolysis mixture of 338 µmol L^{-1} PPL (ThEL 84.5 µmol L^{-1}, n=3). 3,5-dichlorophenol (3,5-DCP) and chloramphenicol (CAM) *were used as positive controls.*

Sample	***LI_{30min}***			***LI_{24h}***			***GI_{14h}***		
PPL 0 min	11.7	±	2.3	13.1	±	6.2	20.8	±	3
PPL 4 min	79.9	±	0.9	37.7	±	2.1	54.1	±	1.9
PPL 8 min	23.8	±	2.4	6.5	±	2	31.1	±	1.5
PPL 16 min	11.9	±	1.2	-3.1	±	4.4	20	±	2
PPL 32 min	6	±	1	-3.1	±	2.9	16.2	±	0.7
PPL 64 min	6.1	±	2.5	-9.2	±	2.5	20.1	±	1
PPL 128 min	4.1	±	0.2	-11.3	±	3.7	17.2	±	2.7
PPL 256 min	0	±	1.4	5.8	±	2.3	9.5	±	2.7
3,5-DCP (27.6 µmol L^{-1})	27.1	±	1.6	99.9	±	0	95.3	±	5
CAM (0.15 µmol L^{-1})	8.3	±	2.2	63.5	±	2.6	38.9	±	0.2

S6. Identification of structural alerts for mutagenicity in bacteria

Table S6.1. Occurrence of TPs with a peak area ratio ($A/A_{0\ PPL}$) above 0.1% in the photolysis mixture used for the testing of mutagenicity.

Compound	***Peak Area ratio ($A/A_{0\ PPL}$) [%]***								
ID	***0 min***	***2 min***	***4 min***	***8 min***	***16 min***	***32 min***	***64 min***	***128 min***	***256 min***
PPL	100.00	97.93	91.36	74.62	65.48	51.60	33.76	12.60	0.72
134(1.6)	0.02	0.21	0.70	1.20	1.27	1.43	1.64	1.91	1.96
149(15.7)	0.04	0.04	0.03	0.06	0.05	0.04	0.06	0.10	0.11
150(1.5)	0.01	0.00	0.02	0.05	0.07	0.10	0.15	0.27	0.50
206(2.7)	0.00	0.00	0.01	0.05	0.05	0.06	0.07	0.15	0.30
218(17.2)	0.01	0.12	0.30	0.44	0.50	0.49	0.45	0.21	0.01
220(2.9)	0.00	0.00	0.00	0.01	0.01	0.01	0.02	0.06	0.16
264(17.4)	0.00	0.00	0.02	0.08	0.18	0.20	0.13	0.10	0.07
266(13.1)	0.00	0.01	0.18	0.54	0.67	0.65	0.62	0.37	0.07
266(13.5)	0.00	0.01	0.09	0.33	0.42	0.37	0.32	0.19	0.04
276(15.2)	0.00	0.16	0.14	0.06	0.03	0.02	0.02	0.01	0.00
276(15.7)	0.00	0.12	0.15	0.26	0.23	0.16	0.12	0.06	0.00
276(16.3)	0.00	0.03	0.20	0.16	0.14	0.22	0.17	0.05	0.00
276(17.3)	0.00	0.01	0.04	0.17	0.31	0.21	0.13	0.05	0.00
276(17.7)	0.00	0.06	0.14	0.38	0.34	0.19	0.15	0.13	0.02
278(15.0)	0.00	0.01	0.07	0.10	0.08	0.06	0.04	0.02	0.00
278(15.5)	0.00	0.03	0.13	0.17	0.13	0.10	0.06	0.03	0.00
278(15.7)	0.00	0.01	0.08	0.13	0.10	0.07	0.05	0.03	0.01
278(16.0)	0.00	0.01	0.07	0.14	0.15	0.14	0.10	0.05	0.01
278(16.5)	0.00	0.03	0.28	0.42	0.40	0.35	0.28	0.14	0.02
280(14.3)	0.00	0.00	0.00	0.02	0.05	0.11	0.20	0.27	0.25
280(14.7)	0.00	0.00	0.00	0.02	0.06	0.10	0.13	0.07	0.01
282(11.5)	0.00	0.00	0.05	0.14	0.13	0.09	0.09	0.07	0.03
282(11.8)	0.00	0.01	0.09	0.22	0.23	0.23	0.26	0.24	0.11
282(12.8)	0.00	0.03	0.19	0.50	0.52	0.57	0.71	0.88	0.69
292(10.7)	0.00	0.02	0.08	0.11	0.10	0.07	0.05	0.03	0.01
292(12.7)	0.00	0.04	0.11	0.12	0.10	0.05	0.03	0.02	0.00
292(14.9)	0.00	0.13	0.40	0.42	0.20	0.12	0.09	0.06	0.02
292(15.5)	0.00	0.16	1.05	1.91	1.48	0.81	0.68	0.52	0.22
292(16.0)	0.00	0.60	2.35	2.89	2.21	1.61	1.17	0.86	0.28
294(10.0)	0.00	0.02	0.10	0.11	0.02	0.02	0.01	0.01	0.00
294(10.7)	0.00	0.01	0.10	0.12	0.09	0.08	0.05	0.02	0.00
294(11.0)	0.00	0.14	0.71	0.81	0.62	0.50	0.41	0.21	0.03
294(11.7)	0.00	0.04	0.35	0.48	0.62	0.77	0.64	0.34	0.05
294(12.2)	0.00	0.04	0.25	0.36	0.29	0.21	0.15	0.07	0.01
294(12.4)	0.00	0.01	0.09	0.16	0.16	0.14	0.12	0.08	0.01
294(14.5)	0.00	0.00	0.05	0.15	0.17	0.16	0.16	0.10	0.02
298(10.6)	0.00	0.00	0.04	0.07	0.07	0.08	0.12	0.21	0.18
308(13.7)	0.00	0.03	0.09	0.16	0.11	0.07	0.06	0.05	0.02
308(16.0)	0.00	0.08	0.36	0.55	0.43	0.29	0.21	0.19	0.09

Table S6.1. Occurrence of TPs with a peak area ratio ($A/A_{0\ PPL}$) above 0.1% in the photolysis mixture used for the testing of mutagenicity (continued).

Compound	***Peak Area ratio ($A/A_{0\ PPL}$) [%]***								
ID	***0 min***	***2 min***	***4 min***	***8 min***	***16 min***	***32 min***	***64 min***	***128 min***	***256 min***
310(11.1)	0.00	0.01	0.09	0.18	0.15	0.09	0.07	0.06	0.01
310(11.3)	0.00	0.02	0.17	0.35	0.26	0.18	0.18	0.11	0.02
310(11.7)	0.00	0.03	0.18	0.34	0.22	0.15	0.17	0.12	0.02
310(13.4)	0.00	0.00	0.02	0.04	0.09	0.11	0.12	0.11	0.04
310(8.2)	0.00	0.01	0.07	0.14	0.11	0.07	0.05	0.04	0.01
310(9.0)	0.00	0.01	0.06	0.13	0.14	0.11	0.07	0.05	0.01
326(10.4)	0.00	0.01	0.08	0.12	0.07	0.05	0.03	0.02	0.01
326(11.0)	0.00	0.01	0.06	0.16	0.11	0.07	0.05	0.03	0.01
326(11.3)	0.00	0.01	0.04	0.10	0.06	0.05	0.04	0.04	0.02
326(12.8)	0.00	0.00	0.02	0.11	0.10	0.12	0.16	0.19	0.10

Table S6.2. MS^2 fragmentation patterns and proposed chemical structures of the transformation products prioritized for the analysis of structure-activity relationships.

Compound ID	***Rt (min)***	***m/z $[M+H]^+$ Precursor ion***	***m/z $[M+H]^+$ MS^2 Product ions (% rel. intensity)***	***Proposed Sructure***	***References***
PPL	18.5	260.1	183.0 (100), 116.1 (66), 157.0 (34), 184.0 (14), 218.0 (13)	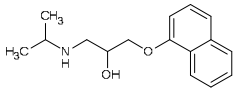	f
280(14.3)	14.3	280.1	146.9 (100), 262.0 (84), 134.0 (61), 116.1 (37)	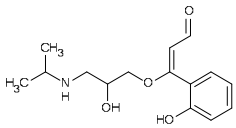 (exemplary structure)	table S6.3
282(12.8)	12.8	282.1	116.1 (100), 264.0 (71), 134.1 (51), 149.0 (17), 98.1 (14)	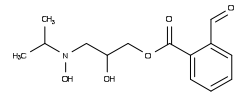 (exemplary structure)	a, b, c, d, e
298(10.6)	10.6	298.1	292.1 (100), 116.1 (24), 294.1 (22), 176.9 (14), 293.1 (13), 250.0 (7), 290.0 (6), 98.2 (5)	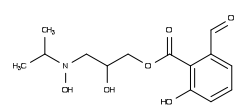 (exemplary structure)	table S6.4
326(12.8)	12.8	326.1	308.1 (100), 290.0 (60), 187.0 (22), 248.0 (10)	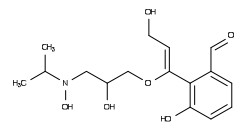 (exemplary structure)	c

[a]Benner and Ternes, 2009; [b]Dantas et al., 2011; [c]Rastogi et al., 2015; [d]Romero et al., 2011; [e]Santiago-Morales et al., 2013; [f]confirmed by reference standard

Table S6.3. Extracted Ion Chromatogram (EIC), MS^2 spectrum and proposed structure of TP 280(14.3) and the product ions formed during the MS^2 fragmentation.

TP 280(14.3)

Extracted Ion Chromatogram (EIC)

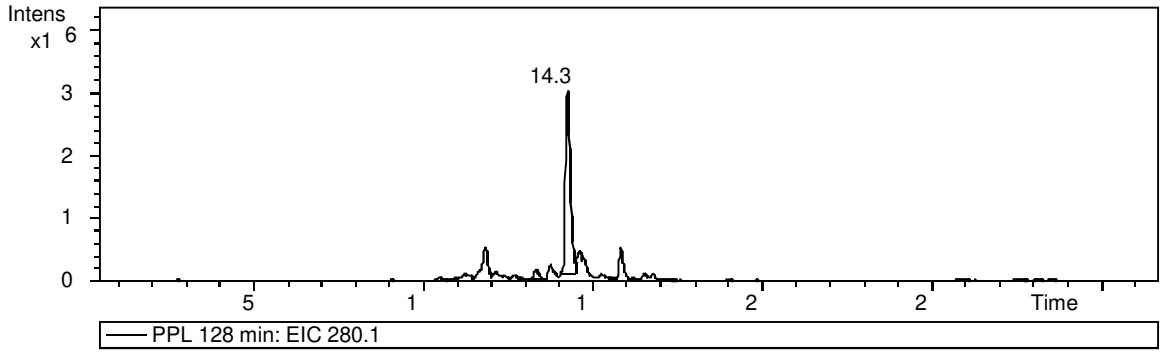

MS^2 Spectrum

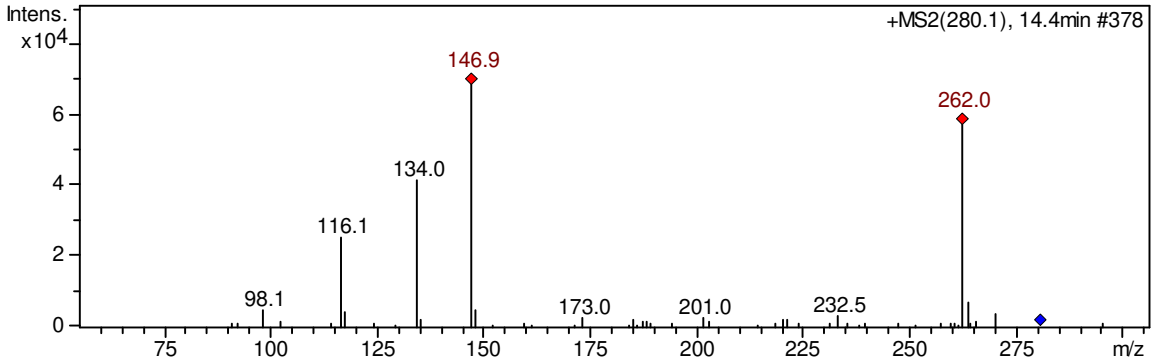

Precursor ion	**m/z**	**Proposed Structure**	**Formula**	**Exact Mass**
$[M+H]^+$	280.1	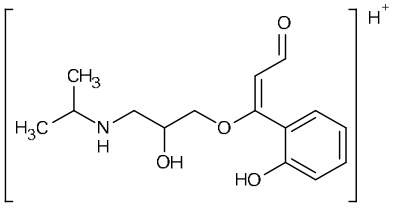	$C_{15}H_{22}NO_4^+$	280.154
Product ions	**m/z**	**Proposed Structure**	**Formula**	**Exact Mass**
$[M+H-H_2O]^+$	262.0	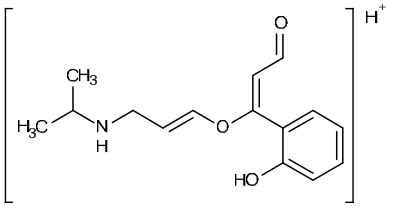	$C_{15}H_{20}NO_3^+$	262.144

$[M+H-C_6H_{15}NO_2]^+$	146.9	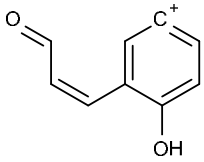	$C_9H_7O_2^+$	147.044
$[M+H-C_9H_8O_2]^+$	134.0	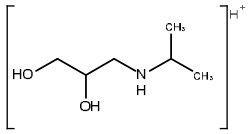	$C_6H_{16}NO_2^+$	134.118
$[M+H-C_9H_8O_2-H_2O]^+$	116.1	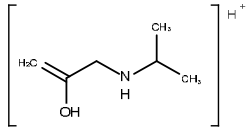	$C_6H_{14}NO^+$	116.107
$[M+H-C_9H_8O_2-H_2O-H_2O]^+$	98.1	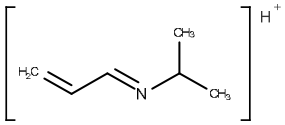	$C_6H_{12}N^+$	98.096

Table S6.4. Extracted Ion Chromatogram (EIC), MS^2 spectrum and proposed structure of TP 298(10.6) and the product ions formed during the MS^2 fragmentation.

TP 298(10.6)

Extracted Ion Chromatogram (EIC)

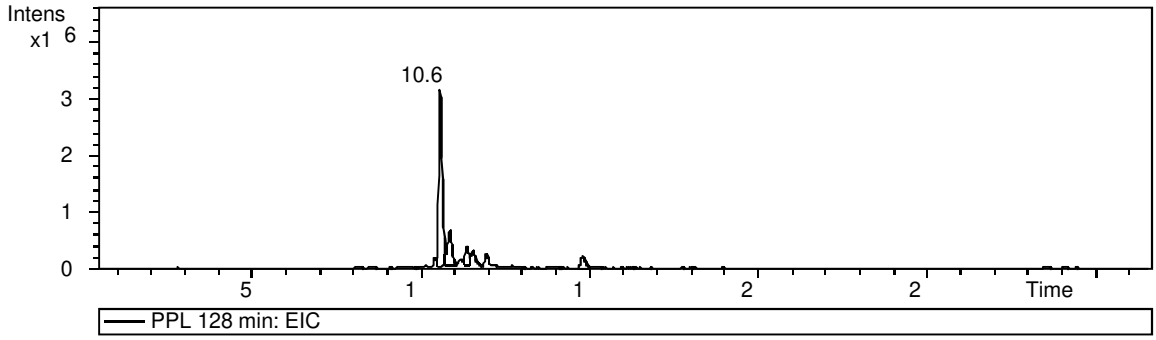

MS^2 Spectrum

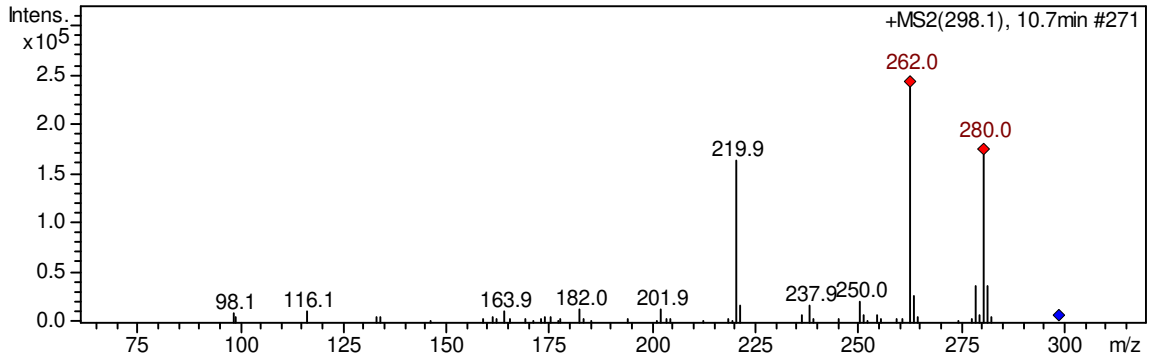

Precursor ion	**m/z**	**Proposed Structure**	**Formula**	**Exact Mass**
$[M+H]^+$	298.1	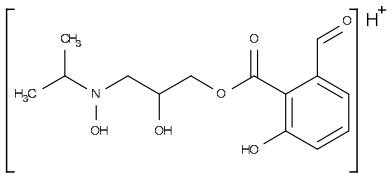	$C_{14}H_{20}NO_6^+$	298.129
Product ions	**m/z**	**Proposed Structure**	**Formula**	**Exact Mass**
$[M+H-H_2O]^+$	280.0	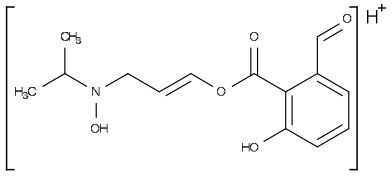	$C_{14}H_{18}NO_5^+$	280.118

$[M+H-H_2O-H_2]^+$	278.0	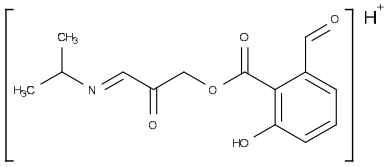	$C_{14}H_{16}NO_5^+$	278.102
$[M+H-2H_2O]^+$	262.0	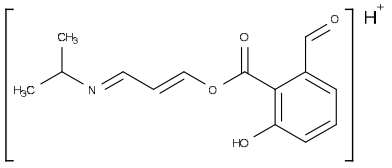	$C_{14}H_{16}NO_4^+$	262.107
$[M+H-2H_2O-CH_2(CH_3)_2]^+$	219.9	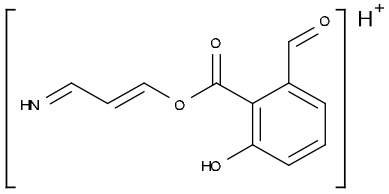	$C_{11}H_{10}NO_4^+$	220.060
$[M+H-H_2O-C_8H_6O_4]^+$	116.1	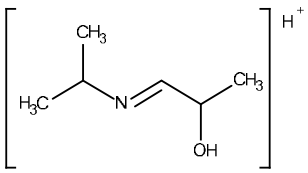	$C_6H_{14}NO^+$	116.107

Table S6.4. Prediction with CASE Ultra models GT_EXPERT (Expert rules for genotoxicity, Model Version 1.5.2.0.10777.500) and GT1_A7B (Salmonella mutagenicity (TA97,98,100,1535-1538), Model Version 1.5.2.0.3979.450).

Structure ID	***Structure***	***SMILES***	***CASE Ultra***[a]	
			GT_ EXPERT	***GT1_A7B***
PPL	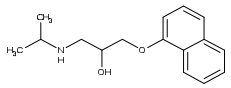	CC(C)NCC(O)COC1=CC=CC2=CC=CC=C12	- (known)	- (known)
280 a	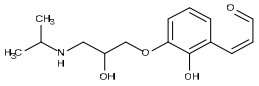	CC(C)NCC(O)COC1=CC=CC(\C=C/C=O)=C1O	+	+
280 b	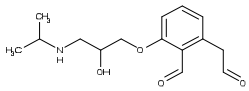	CC(C)NCC(O)COC1=CC=CC(CC=O)=C1C=O	-	-
280 c	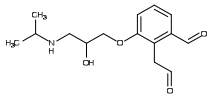	CC(C)NCC(O)COC1=CC=CC(C=O)=C1CC=O	-	-
280 d	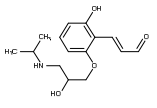	CC(C)NCC(O)COC1=CC=CC(O)=C1\C=C\C=O	+	+
280 e	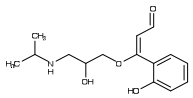	CC(C)NCC(O)CO\C(=C\C=O)C1=CC=CC=C1O	+	+
280 f	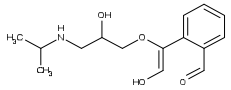	CC(C)NCC(O)CO\C(=C/O)C1=CC=CC=C1C=O	-	-
280 g	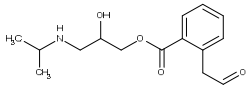	CC(C)NCC(O)COC(=O)C1=CC=CC=C1CC=O	-	-
282 a	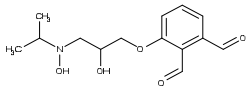	CC(C)N(O)CC(O)COC1=CC=CC(C=O)=C1C=O	+	IN
282 b	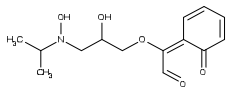	CC(C)N(O)CC(O)CO\C(C=O)=C1/C=CC=CC1=O	+	+
282 c	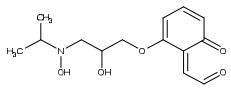	CC(C)N(O)CC(O)COC1=CC=CC(=O)\C1=C/C=O	+	+
282 d	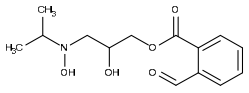	CC(C)N(O)CC(O)COC(=O)C1=CC=CC=C1C=O	+	IN
282 e	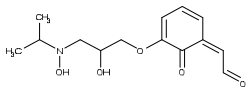	CC(C)N(O)CC(O)COC1=CC=C\C(=C\C=O)C1=O	+	+

298 a	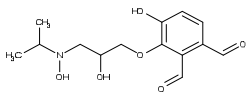	CC(C)N(O)CC(O)COC1=C(O)C=CC(C=O)=C1C=O	+	IN
298 b	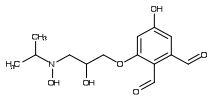	CC(C)N(O)CC(O)COC1=CC(O)=CC(C=O)=C1C=O	+	IN
298 c	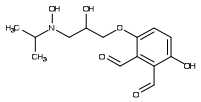	CC(C)N(O)CC(O)COC1=CC=C(O)C(C=O)=C1C=O	+	IN
298 d	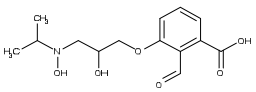	CC(C)N(O)CC(O)COC1=CC=CC(C(O)=O)=C1C=O	+	IN
298 e	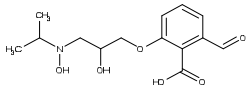	CC(C)N(O)CC(O)COC1=CC=CC(C=O)=C1C(O)=O	+	IN
298 f	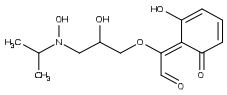	CC(C)N(O)CC(O)CO\C(C=O)=C1/C(O)=CC=CC1=O	+	+
298 g	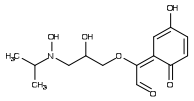	CC(C)N(O)CC(O)CO\C(C=O)=C1/C=C(O)C=CC1=O	+	+
298 h	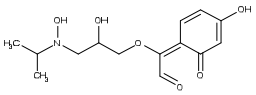	CC(C)N(O)CC(O)CO\C(C=O)=C1/C=CC(O)=CC1=O	+	+
298 i	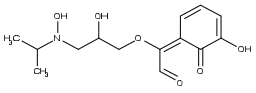	CC(C)N(O)CC(O)CO\C(C=O)=C1/C=CC=C(O)C1=O	+	+
298 j	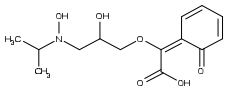	CC(C)N(O)CC(O)CO\C(C(O)=O)=C1/C=CC=CC1=O	-	+
298 k	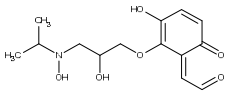	CC(C)N(O)CC(O)COC1=C(O)C=CC(=O)\C1=C/C=O	+	+
298 l	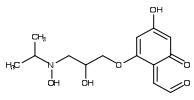	CC(C)N(O)CC(O)COC1=CC(O)=CC(=O)\C1=C/C=O	+	+
298 m	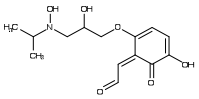	CC(C)N(O)CC(O)COC1=CC=C(O)C(=O)\C1=C/C=O	+	+
298 n	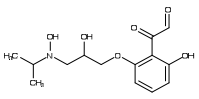	CC(C)N(O)CC(O)COC1=C(C(=O)C=O)C(O)=CC=C1	+	+
298 o	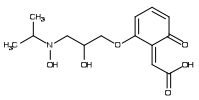	CC(C)N(O)CC(O)COC1=CC=CC(=O)\C1=C/C(O)=O	-	+

298 p	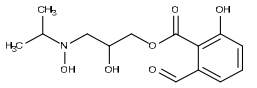	CC(C)N(O)CC(O)COC(=O)C1=C(O)C=CC=C1C=O	+	IN
298 q	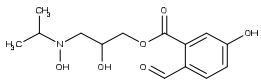	CC(C)N(O)CC(O)COC(=O)C1=CC(O)=CC=C1C=O	+	IN
298 r	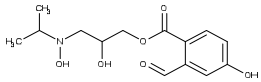	CC(C)N(O)CC(O)COC(=O)C1=CC=C(O)C=C1C=O	+	IN
298 s	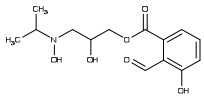	CC(C)N(O)CC(O)COC(=O)C1=CC=CC(O)=C1C=O	+	IN
298 t	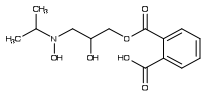	CC(C)N(O)CC(O)COC(=O)C1=CC=CC=C1C(O)=O	-	IN
298 u	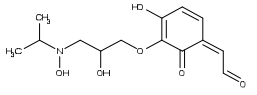	CC(C)N(O)CC(O)COC1=C(O)C=C\C(=C\C=O)C1=O	+	+
298 v	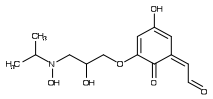	CC(C)N(O)CC(O)COC1=CC(O)=C\C(=C\C=O)C1=O	+	+
298 w	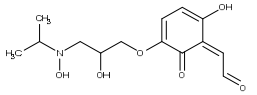	CC(C)N(O)CC(O)COC1=CC=C(O)\C(=C\C=O)C1=O	+	+
298 x	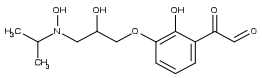	CC(C)N(O)CC(O)COC1=C(O)C(=CC=C1)C(=O)C=O	+	+
298 y	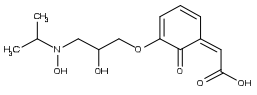	CC(C)N(O)CC(O)COC1=CC=C\C(=C\C(O)=O)C1=O	-	+
326 a	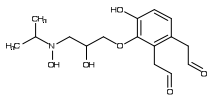	CC(C)N(O)CC(O)COC1=C(O)C=CC(CC=O)=C1CC=O	-	IN
326 b	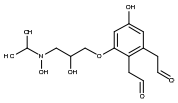	CC(C)N(O)CC(O)COC1=CC(O)=CC(CC=O)=C1CC=O	-	IN
326 c	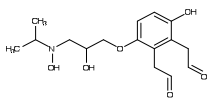	CC(C)N(O)CC(O)COC1=CC=C(O)C(CC=O)=C1CC=O	-	IN
326 d	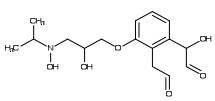	CC(C)N(O)CC(O)COC1=CC=CC(C(O)C=O)=C1CC=O	-	+
326 e	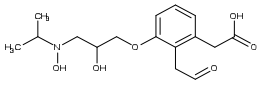	CC(C)N(O)CC(O)COC1=CC=CC(CC(O)=O)=C1CC=O	-	IN

326 f	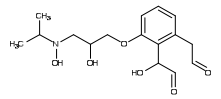	CC(C)N(O)CC(O)COC1=CC=CC(CC=O)=C1C(O)C=O	-	+
326 g	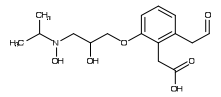	CC(C)N(O)CC(O)COC1=CC=CC(CC=O)=C1CC(O)=O	-	IN
326 h	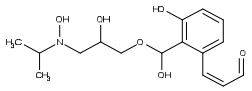	CC(C)N(O)CC(O)COC(O)C1=C(O)C=CC=C1\C=C/C=O	+	+
326 i	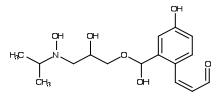	CC(C)N(O)CC(O)COC(O)C1=CC(O)=CC=C1\C=C/C=O	+	+
326 j	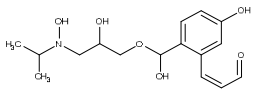	CC(C)N(O)CC(O)COC(O)C1=CC=C(O)C=C1\C=C/C=O	+	+
326 k	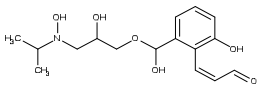	CC(C)N(O)CC(O)COC(O)C1=CC=CC(O)=C1\C=C/C=O	+	+
326 l	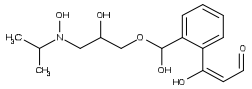	CC(C)N(O)CC(O)COC(O)C1=CC=CC=C1\C(O)=C/C=O	+	+
326 m	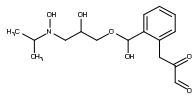	CC(C)N(O)CC(O)COC(O)C1=CC=CC=C1CC(=O)C=O	+	+
326 n	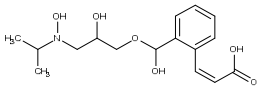	CC(C)N(O)CC(O)COC(O)C1=CC=CC=C1\C=C/C(O)=O	-	IN
326 o	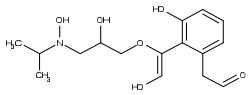	CC(C)N(O)CC(O)CO\C(=C/O)C1=C(O)C=CC=C1CC=O	-	IN
326 p	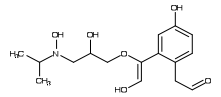	CC(C)N(O)CC(O)CO\C(=C/O)C1=CC(O)=CC=C1CC=O	-	IN
326 q	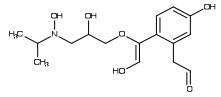	CC(C)N(O)CC(O)CO\C(=C/O)C1=CC=C(O)C=C1CC=O	-	IN
326 r	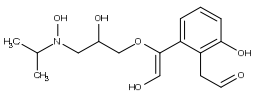	CC(C)N(O)CC(O)CO\C(=C/O)C1=CC=CC(O)=C1CC=O	-	IN
326 s	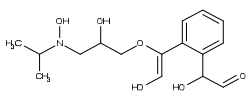	CC(C)N(O)CC(O)CO\C(=C/O)C1=CC=CC=C1C(O)C=O	-	+
326 t	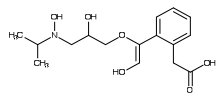	CC(C)N(O)CC(O)CO\C(=C/O)C1=CC=CC=C1CC(O)=O	-	IN

326 u	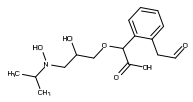	CC(C)N(O)CC(O)COC(C(O)=O)C1=CC=CC=C1CC=O	-	IN
326 v	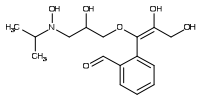	CC(C)N(O)CC(O)CO\C(=C(/O)CO)C1=CC=CC=C1C=O	-	+
326 w	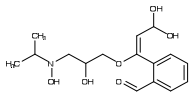	CC(C)N(O)CC(O)CO\C(=C\C(O)O)C1=CC=CC=C1C=O	-	IN
326 x	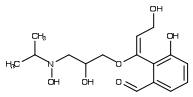	CC(C)N(O)CC(O)CO\C(=C\CO)C1=C(O)C=CC=C1C=O	-	IN
326 y	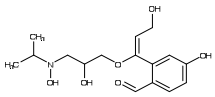	CC(C)N(O)CC(O)CO\C(=C\CO)C1=CC(O)=CC=C1C=O	-	IN
326 z	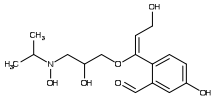	CC(C)N(O)CC(O)CO\C(=C\CO)C1=CC=C(O)C=C1C=O	-	IN
326 aa	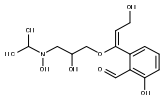	CC(C)N(O)CC(O)CO\C(=C\CO)C1=CC=CC(O)=C1C=O	-	IN
326 ab	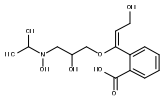	CC(C)N(O)CC(O)CO\C(=C\CO)C1=CC=CC=C1C(O)=O	-	IN
326 ac	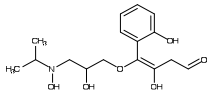	CC(C)N(O)CC(O)CO\C(=C(/O)CC=O)C1=CC=CC=C1O	-	+
326 ae	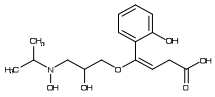	CC(C)N(O)CC(O)CO\C(=C\CC(O)=O)C1=CC=CC=C1O	-	IN
326 af	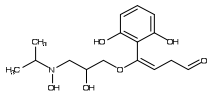	CC(C)N(O)CC(O)CO\C(=C\CC=O)C1=C(O)C=CC=C1O	-	IN
326 ag	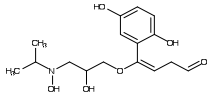	CC(C)N(O)CC(O)CO\C(=C\CC=O)C1=CC(O)=CC=C1O	-	IN
326 ah	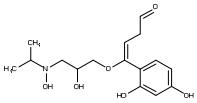	CC(C)N(O)CC(O)CO\C(=C\CC=O)C1=CC=C(O)C=C1O	-	IN
326 ai	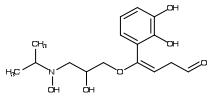	CC(C)N(O)CC(O)CO\C(=C\CC=O)C1=CC=CC(O)=C1O	-	IN
326 aj	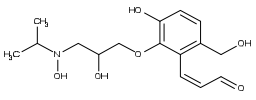	CC(C)N(O)CC(O)COC1=C(O)C=CC(CO)=C1\C=C/C=O	+	+

326 ak	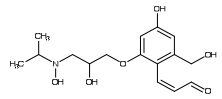	CC(C)N(O)CC(O)COC1=CC(O)=CC(CO)=C1\C=C/C=O	+	+
326 al	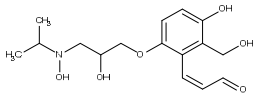	CC(C)N(O)CC(O)COC1=CC=C(O)C(CO)=C1\C=C/C=O	+	+
326 am	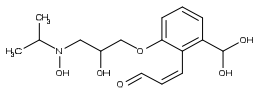	CC(C)N(O)CC(O)COC1=CC=CC(C(O)O)=C1\C=C/C=O	+	+
326 an	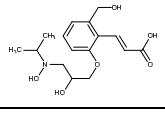	CC(C)N(O)CC(O)COC1=CC=CC(CO)=C1\C=C\C(O)=O	-	IN
326 ao	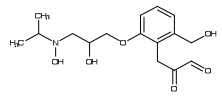	CC(C)N(O)CC(O)COC1=CC=CC(CO)=C1CC(=O)C=O	+	+
326 ap	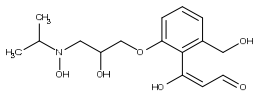	CC(C)N(O)CC(O)COC1=CC=CC(CO)=C1\C(O)=C/C=O	+	+
326 aq	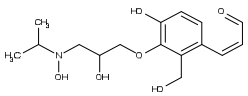	CC(C)N(O)CC(O)COC1=C(O)C=CC(\C=C/C=O)=C1CO	+	+
326 ar	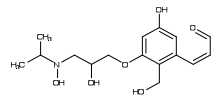	CC(C)N(O)CC(O)COC1=CC(O)=CC(\C=C/C=O)=C1CO	+	+
326 as	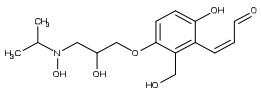	CC(C)N(O)CC(O)COC1=CC=C(O)C(\C=C/C=O)=C1CO	+	+
326 at	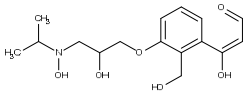	CC(C)N(O)CC(O)COC1=CC=CC(\C(O)=C/C=O)=C1CO	+	+
326 au	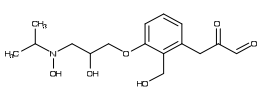	CC(C)N(O)CC(O)COC1=CC=CC(CC(=O)C=O)=C1CO	+	+
326 av	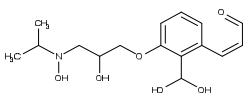	CC(C)N(O)CC(O)COC1=CC=CC(\C=C/C=O)=C1C(O)O	+	+
326 aw	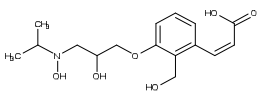	CC(C)N(O)CC(O)COC1=CC=CC(\C=C/C(O)=O)=C1CO	-	IN
326 ax	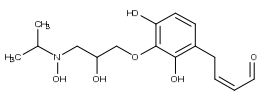	CC(C)N(O)CC(O)COC1=C(O)C=CC(C\C=C/C=O)=C1O	+	+
326 ay	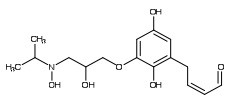	CC(C)N(O)CC(O)COC1=CC(O)=CC(C\C=C/C=O)=C1O	+	+

326 az	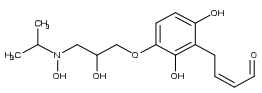	CC(C)N(O)CC(O)COC1=CC=C(O)C(C\C=C/C=O)=C1O	+	+
326 ba	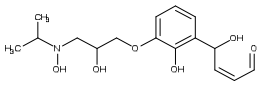	CC(C)N(O)CC(O)COC1=CC=CC(C(O)\C=C/C=O)=C1O	+	+
326 bb	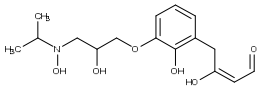	CC(C)N(O)CC(O)COC1=CC=CC(C\C(O)=C/C=O)=C1O	+	+
326 bc	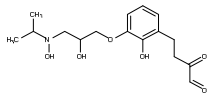	CC(C)N(O)CC(O)COC1=CC=CC(CCC(=O)C=O)=C1O	+	+

[a]Predicted values are shown as + (positive), - (negative), IN (inconclusive) and OD (out of domain). “Inconclusive” means that the calculated probability falls inside the gray zone (40% to 60%) around the model's current classification threshold (50%). “Out of domain” means that the test chemical contains structural features that are not covered by the training set chemicals of the model.

S7. Identification of structural alerts for cytotoxicity in bacteria

Table S7.1. Occurrence of TPs with a peak area ratio ($A/A_{0\ PPL}$) above 0.1% in the photolysis mixture used for the testing of cytotoxicity in bacteria.

Compound	***Peak Area ratio ($A/A_{0\ PPL}$) [%]***								
ID	***0 min***	***2 min***	***4 min***	***8 min***	***16 min***	***32 min***	***64 min***	***128 min***	***256 min***
PPL	100.00	95.04	85.52	71.94	63.22	48.49	26.91	7.06	0.06
134(1.6)	0.00	0.30	0.76	1.11	1.21	1.39	1.71	1.90	1.53
150(1.5)	0.00	0.00	0.02	0.04	0.06	0.10	0.16	0.30	0.70
206(2.7)	0.00	0.00	0.02	0.05	0.05	0.06	0.08	0.16	0.44
218(17.2)	0.00	0.12	0.30	0.37	0.44	0.45	0.36	0.11	0.00
220(2.9)	0.00	0.00	0.00	0.01	0.01	0.01	0.03	0.07	0.28
264(17.4)	0.00	0.00	0.03	0.09	0.17	0.18	0.12	0.11	0.00
266(13.1)	0.00	0.04	0.25	0.63	0.70	0.70	0.65	0.30	0.01
266(13.5)	0.00	0.02	0.14	0.43	0.48	0.42	0.35	0.18	0.00
266(14.0)	0.00	0.00	0.01	0.02	0.04	0.08	0.11	0.05	0.00
276(15.2)	0.00	0.19	0.11	0.04	0.05	0.07	0.06	0.02	0.00
276(15.7)	0.00	0.17	0.17	0.30	0.20	0.16	0.10	0.03	0.00
276(16.3)	0.00	0.10	0.32	0.20	0.22	0.25	0.16	0.02	0.00
276(17.3)	0.00	0.02	0.04	0.24	0.26	0.20	0.13	0.02	0.00
276(17.7)	0.00	0.08	0.16	0.33	0.21	0.17	0.16	0.09	0.00
278(15.5)	0.00	0.07	0.14	0.17	0.13	0.09	0.07	0.02	0.00
278(15.7)	0.00	0.01	0.08	0.11	0.07	0.05	0.04	0.02	0.00
278(16.0)	0.00	0.03	0.09	0.16	0.17	0.15	0.11	0.04	0.00
278(16.5)	0.00	0.08	0.32	0.46	0.46	0.43	0.34	0.11	0.00
280(14.3)	0.00	0.00	0.01	0.02	0.06	0.13	0.25	0.36	0.08
282(11.5)	0.00	0.01	0.06	0.14	0.12	0.10	0.10	0.06	0.00
282(11.8)	0.00	0.02	0.11	0.21	0.20	0.22	0.27	0.21	0.02
282(12.8)	0.00	0.06	0.25	0.45	0.46	0.55	0.74	0.88	0.19
292(12.7)	0.00	0.04	0.10	0.12	0.09	0.05	0.03	0.01	0.00
292(14.9)	0.00	0.22	0.45	0.39	0.18	0.13	0.10	0.06	0.00
292(15.5)	0.00	0.13	1.12	1.46	0.99	0.72	0.59	0.44	0.01
292(16.0)	0.00	0.98	2.20	2.74	2.25	1.73	1.44	0.89	0.03
294(10.0)	0.00	0.03	0.11	0.07	0.02	0.02	0.02	0.01	0.00
294(10.7)	0.00	0.04	0.11	0.12	0.10	0.07	0.04	0.01	0.00
294(11.0)	0.00	0.27	0.77	0.82	0.61	0.50	0.38	0.12	0.00
294(11.7)	0.00	0.12	0.38	0.56	0.68	0.77	0.56	0.15	0.00
294(12.2)	0.00	0.09	0.28	0.34	0.27	0.21	0.13	0.04	0.00
294(12.4)	0.00	0.03	0.11	0.17	0.15	0.13	0.12	0.05	0.00
294(14.5)	0.00	0.01	0.08	0.14	0.15	0.14	0.16	0.08	0.00
298(10.6)	0.00	0.01	0.05	0.08	0.08	0.09	0.16	0.24	0.04
308(13.7)	0.00	0.05	0.11	0.14	0.10	0.07	0.06	0.05	0.00
308(16.0)	0.00	0.16	0.41	0.52	0.40	0.28	0.21	0.17	0.00
310(11.1)	0.00	0.02	0.10	0.16	0.12	0.08	0.08	0.05	0.00
310(11.3)	0.00	0.05	0.21	0.29	0.25	0.19	0.18	0.10	0.00
310(11.7)	0.00	0.05	0.20	0.28	0.20	0.19	0.20	0.11	0.00
310(13.4)	0.00	0.00	0.01	0.04	0.10	0.11	0.13	0.12	0.00
310(8.2)	0.00	0.02	0.09	0.12	0.10	0.06	0.04	0.03	0.00
310(9.0)	0.00	0.02	0.08	0.13	0.13	0.10	0.07	0.05	0.00
326(11.0)	0.00	0.02	0.09	0.14	0.10	0.07	0.04	0.03	0.01
326(12.8)	0.00	0.01	0.04	0.11	0.10	0.15	0.18	0.20	0.02
326(13.8)	0.00	0.04	0.03	0.07	0.07	0.08	0.10	0.10	0.00

Table S7.2. MS^2 fragmentation patterns and proposed chemical structures of the transformation products prioritized for the analysis of structure-activity relationships.

Compound ID	***Rt (min)***	***m/z [M+H]$^+$ Precursor ion***	***m/z [M+H]$^+$ MS^2 Product ions (% rel. intensity)***	***Proposed Sructure***	***References***
PPL	18.5	260.1	183.0 (100), 116.1 (66), 157.0 (34), 184.0 (14), 218.0 (13)	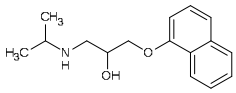	h
276(15.2)	15.2	276.1	134.0 (100), 116.1 (81), 260.0 (77), 258.0 (41), 102.1 (36), 156.9 (32), 231.0 (29), 168.9 (28), 201.0 (27), 198.9 (26)	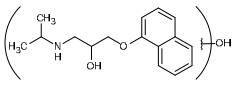	d, f, g
276(16.3)	16.3	276.1	116.2 (100), 199.0 (96), 173.0 (92), 258.2 (47), 98.2 (24), 171.1 (24), 216.0 (20), 86.3 (14), 256.2 (13), 200.1 (13)	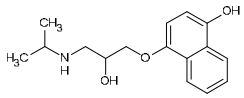	h
292(14.9)	14.9	292.1	116.1 (100), 131.0 (32), 159.0 (16), 232.9 (16), 274.1 (10), 250.0 (10)	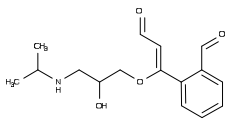 (exemplary structure)	a, b, c, d, e, f, g
294(10.0)	10.0	294.2	276.2 (100), 277.1 (18)	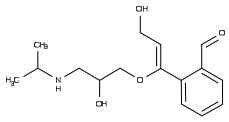 (exemplary structure)	d, f, g

[a]Benner and Ternes, 2009; [b]Dantas et al., 2011; [c]Liu and Williams, 2007; [d]Rastogi et al., 2015; [e]Romero et al., 2011; [f]Santiago-Morales et al., 2013; [g]Wilde et al., 2013; [h]confirmed by reference standard

Table S7.3. Prediction with CASE Ultra model MICROTOX TOXICITY TO ENVIRONMENTAL BACTERIA AUA (toxicity to bacteria, Model Version 1.5.2.0.899.500).

Structure ID	***Structure***	***SMILES***	***CASE Ultra AUA***
PPL	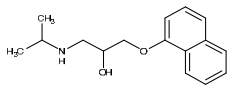	CC(C)NCC(O)COC1=CC=CC2=CC=CC=C12	+
276 a	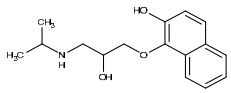	CC(C)NCC(O)COC1=C(O)C=CC2=CC=CC=C12	+
276 b	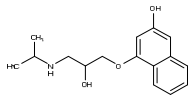	CC(C)NCC(O)COC1=CC(O)=CC2=CC=CC=C12	+
276 c (4-OH PPL)	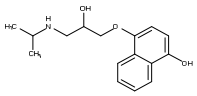	CC(C)NCC(O)COC1=CC=C(O)C2=CC=CC=C12	IN
276 d (5-OH PPL)	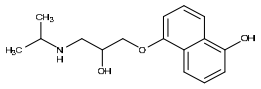	CC(C)NCC(O)COC1=CC=CC2=C(O)C=CC=C12	+
276 e	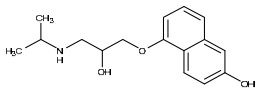	CC(C)NCC(O)COC1=CC=CC2=CC(O)=CC=C12	+
276 f	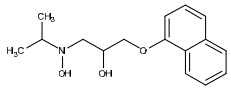	CC(C)N(O)CC(O)COC1=CC=CC2=CC=CC=C12	+
276 g (7-OH PPL)	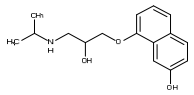	CC(C)NCC(O)COC1=CC=CC2=CC=C(O)C=C12	+
276 h	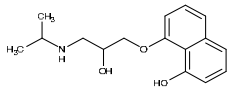	CC(C)NCC(O)COC1=CC=CC2=CC=CC(O)=C12	OD
292 a	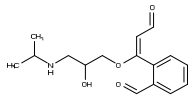	CC(C)NCC(O)CO\C(=C\C=O)C1=CC=CC=C1C=O	IN
292 b	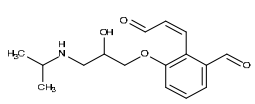	CC(C)NCC(O)COC1=C(\C=C/C=O)C(C=O)=CC=C1	IN
292 c	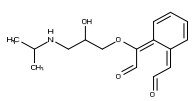	CC(C)NCC(O)CO\C(C=O)=C1/C=CC=C/C/1=C/C=O	+
292 d	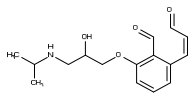	CC(C)NCC(O)COC1=C(C=O)C(\C=C/C=O)=CC=C1	IN
292 e	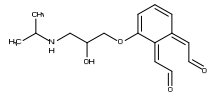	CC(C)NCC(O)COC1=CC=C\C(=C\C=O)\C\1=C/C=O	+

294 a	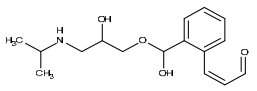	CC(C)NCC(O)COC(O)C1=CC=CC=C1\C=C/C=O	IN
294 b	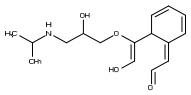	CC(C)NCC(O)CO\C(=C/O)C1C=CC=C\C1=C\C=O	IN
294 c	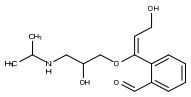	CC(C)NCC(O)CO\C(=C\CO)C1=CC=CC=C1C=O	OD
294 d	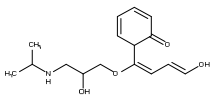	CC(C)NCC(O)CO\C(=C\C=C\O)C1C=CC=CC1=O	IN
294 e	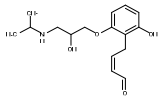	CC(C)NCC(O)COC1=CC=CC(O)=C1C\C=C/C=O	IN
294 f	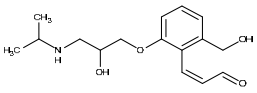	CC(C)NCC(O)COC1=CC=CC(CO)=C1\C=C/C=O	IN
294 g	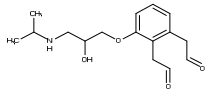	CC(C)NCC(O)COC1=CC=CC(CC=O)=C1CC=O	OD
294 h	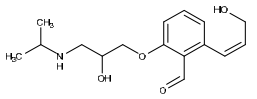	CC(C)NCC(O)COC1=CC=CC(\C=C/CO)=C1C=O	IN
294 i	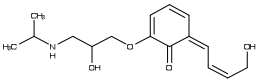	CC(C)NCC(O)COC1=CC=C\C(=C\C=C/CO)C1=O	+

[a]Predicted values are shown as + (positive), - (negative), IN (inconclusive) and OD (out of domain). “Inconclusive” means that the calculated probability falls inside the gray zone (40% to 60%) around the model's current classification threshold (50%). “Out of domain” means that the test chemical contains structural features that are not covered by the training set chemicals of the model.

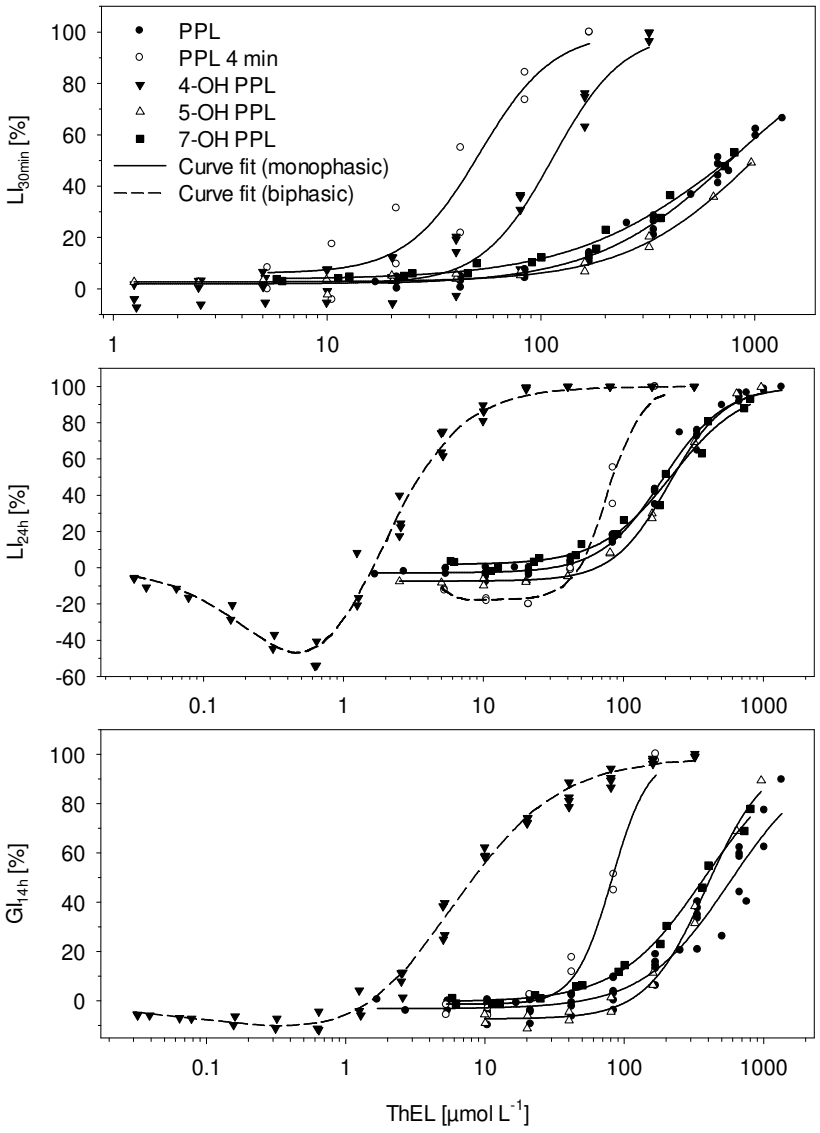

Figure S7.1. Concentration-response relationships in the modified luminescent bacteria test of PPL, the photolysis mixture of 338 µmol L^{-1} PPL after 4 minutes irradiation, 4-OH PPL, 5-OH PPL and 7-OH PPL.

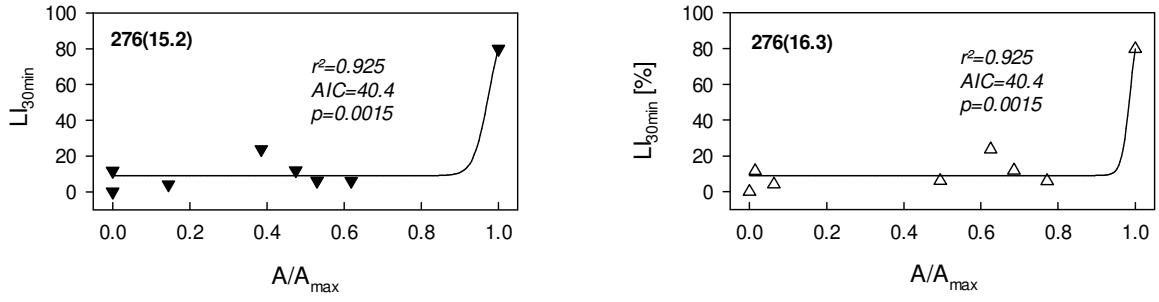

Figure S7.2. Non-linear relationships between LI_{30min} and A/A_{max} of suspected TPs with bacterial cytotoxicity.

S8. References

Benner, J., Ternes, T.A., 2009. Ozonation of Propranolol: Formation of Oxidation Products. Environ. Sci. Technol. 43, 5086–5093.

Dantas, R.F., Sans, C., Esplugas, S., 2011. Ozonation of Propranolol: Transformation, Biodegradability, and Toxicity Assessment. J. Environ. Eng. 137, 754–759.

Liu, Q.-T., Williams, H.E., 2007. Kinetics and Degradation Products for Direct Photolysis of β-Blockers in Water. Environ. Sci. Technol. 41, 803–810.

Liu, Q.-T., Williams, T.D., Cumming, R.I., Holm, G., Hetheridge, M.J., Murray-Smith, R., 2009. Comparative aquatic toxicitxy of propranolol and its photodegraded mixtures: algae and rotifer screening. Environ. Toxicol. Chem. 28, 2622.

Palm, W.U., 2013. Photon flux of the TK150 [in German]. Unpublished manuscript. Leuphana University, Lüneburg.

Palm, W.-U., Millet, M., Zetzsch, C., 1997. Photochemical reactions of metamitron. Chemosphere 35, 1117–1130.

Palm, W.-U., Zetzsch, C., 1996. Investigation of the Photochemistry and Quantum Yields of Triazines Using Polychromatic Irradiation and UV-Spectros Copy as Analytical Tool. Int. J. Environ. Anal. Chem. 65, 313–329.

Rastogi, T., Leder, C., Kümmerer, K., 2015. Re-Designing of Existing Pharmaceuticals for Environmental Biodegradability: A tiered approach with β -Blocker Propranolol as an example. Environ. Sci. Technol. 49, 11756–11763.

Romero, V., La Cruz, N. de, Dantas, R.F., Marco, P., Giménez, J., Esplugas, S., 2011. Photocatalytic treatment of metoprolol and propranolol. Catal. Today 161, 115–120.

Santiago-Morales, J., Agüera, A., Gómez, M.d.M., Fernández-Alba, A.R., Giménez, J., Esplugas, S., Rosal, R., 2013. Transformation products and reaction kinetics in simulated solar light photocatalytic degradation of propranolol using Ce-doped TiO2. Appl. Catal., B .129,13–29.

Wilde, M.L., Mahmoud, Waleed M M, Kümmerer, K., Martins, A.F., 2013. Oxidation-coagulation of β-blockers by K2FeVIO4 in hospital wastewater: assessment of degradation products and biodegradability. Sci. Total Environ. 452-453, 137–147.